WATER USE AND WATER PRODUCTIVITY OF POMEGRANATE ORCHARDS

Report
to the Water Research Commission

by

T Volschenk[1], M Ravuluma[1,2], M Makgato[1], L Sassman[1], K Freitag[1], D Havenga[2], R Kgaphola[3], M van der Rijst[3], S Dzikiti[4], P Tharaga[2,5], S Walker[2,5]

[1] Soil and Water Science Programme, Agricultural Research Council Infruitec-Nietvoorbij
[2] Soil Crop and Climate Sciences, University of the Free State
[3] Biometry, Agricultural Research Council Infruitec-Nietvoorbij
[4] Department of Horticultural Science, Stellenbosch University
[5] Agrometeorology, Agricultural Research Council Natural Resources and Engineering

WRC report no. 3199/1/25
ISBN 978-0-6392-0705-6

May 2025

Obtainable from

Water Research Commission

Private Bag X03

Gezina, 0031

Download from www.wrc.org.za

This is the final report of WRC project no. Project No. C2020/2021-00404

EXECUTIVE SUMMARY

BACKGROUND

The Western Cape has a semi-arid climate and the predictions of climate change are that the province can expect more water stresses with increasing temperatures, increasing evaporation and increasing occurrence of droughts. With increased urbanisation and the perceived impact of climate change, the Western Cape needs to manage rising water demand and increasing climate uncertainty which enhances the risk of water scarcity. Identifying crops that can be grown economically in areas where climate change and population pressure are limiting the amount and quality of water available for agriculture, while also providing for job creation, is a priority. Pomegranate is an alternative crop with climate smart production potential. Besides being sold and exported as whole fruit, pomegranates are also processed to produce punnets of arils or juice, which contributes to value adding and job creation.

A scoping study, co-funded by the Western Cape Department of Agriculture Alternative Crop Fund through the Pomegranate Producers Association of South Africa (POMASA) and the Water Research Commission (WRC), showed that pomegranate yield and fruit quality, as well as water use productivity (yield per unit water used or economic income per unit water used) could potentially be increased through improved irrigation scheduling. This required research on water use of pomegranate orchards under local conditions, including the determination of local crop coefficients and the development of a model to estimate individual orchard water use. The proposed research of this four-year-project aimed to determine the water use, yield and fruit quality, orchard level water use efficiency and biophysical and economic water productivity of selected cultivar 'Wonderful' pomegranate orchards under irrigation in the Western Cape, the main pomegranate production region in South Africa. The cultivar 'Wonderful' is the most widely planted and makes out the bulk of exported fruit. The research also intended to develop a method for practical estimation of crop coefficients for application in a water use model to enable calculation of individual orchard water requirements.

Seasonal evapotranspiration information of pomegranate orchards and potentially a means to determine orchard specific crop coefficients/ basal crop coefficients for pomegranate trees can be used for water management planning purposes at the farm level to achieve maximum water use efficiency and/ or water use productivity. This information can also be used in catchment-wide water management by the Breede-Olifants Catchment Management Agency as the catchment is already considered water stressed. Information regarding income earned relative to volumes of water used can inform national government policy and decision making in the water sector (i.e. economic water productivity). A model for deriving orchard crop coefficients is a potential product to optimize irrigation scheduling in the sector, thereby improving the management of scarce water resources and promoting sustainable farming.

AIMS

The current research project intended to determine the water use, yield and fruit quality of selected pomegranate orchards in Western Cape production areas by pursuing the following aims:

Aim 1: To measure pomegranate orchard water use for orchards with a range of canopy sizes.

Aim 2. To determine the tree and fruit growth, yield and fruit quality of selected pomegranate orchards under irrigation.

Aim 3. To determine the orchard level water use efficiency, biophysical and economic water productivity of selected pomegranate orchards under irrigation.

Aim 4. To develop a method for practical estimation of crop coefficients for application in a water use model to enable calculation of individual orchard water requirements.

METHODOLOGY

In the first year (2021/22), in consultation with industry technical advisors, two high performing commercial pomegranate orchards (cv. 'Wonderful') varying in canopy cover were selected for monitoring over two consecutive seasons on commercial farms. A detailed knowledge review was conducted around new methods for determining orchard water use and pomegranate production practices,

capital equipment was purchased and since the sap flow technique has not previously been used to determine transpiration (T) of pomegranate trees, the most appropriate sap flow monitoring technique for this crop was determined. Team members were trained on the methods that would be used for data collection - i.e. soil water balance and sap flow techniques. In the second (2022/23) and third (2023/24) years orchard water use (evapotranspiration (ETc) and transpiration) and related tree variables were measured for the two orchards varying in age/ size/ training system. In the last year (2024/25) limited data were collected to conclude the second season and to close gaps in the orchard water use measurements. The main focus was on production of the final report.

The research was conducted at a young and a full bearing cultivar 'Wonderful' pomegranate orchard at Avontuur (33°07'29.7"S; 18°56'08.8"E) and Welgemoed (33°35'18.3048"S; 18°59'19.302"E), which covers an area of 6.7 and 4.9 hectares, respectively. The tree spacing was 2.5 m x 5 m for the young, and 2 m x 4.5 m for the mature orchard. At the onset of the study, height of the young trees was about 1.8 m and the canopy spread 1.8 m across the tree row, compared to 2.5 m height and 2.8 m canopy spread across the tree row at the full bearing orchard. Tree stem diameters were approximately 45 mm and 80 mm for the two respective orchards. Pomegranate orchard water use was measured over the 2022/23 and 2023/24 seasons using sap flow, soil water balance and micrometeorological methods, while an automatic weather station and two soil water content monitoring systems per site collected weather and soil water content data, respectively. Soil water was monitored hourly at two trees per orchard below a dripper nearest to the tree, midway to the next dripper and in the work row area at three positions in and at the bottom of the rootzone. Logging flow meters monitored irrigation applied. Sap flow equipment to monitor tree transpiration was installed in August 2022 and July 2023 in four trees per orchard, considering stem size distribution for the orchard. To monitor orchard ETc an eddy covariance system was installed from 21-24 September 2022 in the full bearing orchard at Welgemoed and a surface renewal system in the young orchard on 25 November 2022 at Avontuur. Logged data was either downloaded directly to a computer or data transfer device, or via modem communication.

Tree growth indicators, including stem, shoot and fruit growth, tree canopy dimensions, fractional light interception, leaf area index (LAI) and tree shaded area was measured at selected dates throughout each growing season. Plant physiological measurements were conducted at 10h00, 12h00 and 14h00 approximately monthly from October until April in the 2023/24 season, provided weather conditions were suitable. Yield was determined at harvest, fruit classed for quality and marketability and the gross farm income determined. Water use indicators including water use efficiency (T or ETc divided by the total sum of water applied by irrigation and effective rainfall), biophysical water use productivity (ratio of marketable yield to T or ETc) and economic water productivity (ratio between gross farm income and T or ETc), were calculated from available data. Crop coefficients were estimated as the ratio of T or ETc data to reference evapotranspiration (ETo) derived from weather data variables. Simple linear regressions and multiple stepwise regressions were conducted to obtain calibration relationships for equipment and to establish the most important factors affecting T and ETc using various statistical analysis products.

RESULTS AND DISCUSSION

Physiological measurements conducted in 2023/24 indicated that the water status of the trees of both orchards was optimal or near to optimal on the dates that midday stem water potential measurements were conducted. For the majority of the 2023/2024 season though, photosynthesis rates and shoot growth were lower at the full bearing orchard compared to the young orchard. This, in addition to poor flowering and fruit set (in part attributed to poor weather conditions) could partially explain the low yield for the full bearing orchard for this season.

Orchard upscaled daily transpiration rates were low compared to evapotranspiration. Maximum transpiration rates of 1.3 mm d^{-1} for the young and 1.7 mm d^{-1} for the full bearing orchard appeared low compared to that of several temperate fruit tree species including apple, citrus, peach, pistachio, and walnut, but it was more comparable to that of apricot, macadamia, and in some cases olive. Monthly averages over the season ranged between 0.2- and 1-mm d^{-1} for both orchards in the 2022/23 season, reaching maxima of 1.1- and 1.3-mm d^{-1} for the young and full bearing orchards, respectively, in 2023/24. The seasonal total transpiration for the young and full bearing orchards for the period producers normally irrigate (1 October 2022 until 31 May) was estimated to be 1699.9 and 1618.1 m^3 ha^{-1}, respectively, in 2022/23 and 2195.3 and 2500.7 m^3 ha^{-1}, respectively, in 2023/24.

Simple and multiple linear regression results gave a clear indication that environmental conditions are important drivers of pomegranate tree transpiration rates, particularly net radiation (Rn). By combining daily total Rn, minimum temperature (T_{min}), wind speed, maximum relative humidity (RH_{max}) and maximum temperature (T_{max}) though gave a more reliable indication of the transpiration rate than relying

solely on Rn. The effect of the tree canopy size on the variability in transpiration compared to that of Rn and RH_{max} seems to be small - i.e. about 5.5% while the weather variables accounted for about 76% of transpiration differences. When orchard upscaled transpiration though was related to ETo in combination with different tree canopy variables (fractional light interception, tree canopy area based LAI and orchard LAI), ETo accounted for 55% of the variation in transpiration and the tree canopy variables between 19 and 24%.

With regard to water use indicators, transpiration from October until May equalled 26.9% and 56.9% of the sum total of effective rainfall (corrected for evaporative losses) and irrigation applied at the young and full bearing orchards, respectively, in 2023/24. Yield data for calculation of biophysical water productivity was impacted in the first season for the young orchard by theft and in the second for the full bearing orchard as a result of poor flowering and fruit set. Transpiration based biophysical water productivity calculated using transpiration from October until May equalled 12.4 kg m^{-3} for the young orchard in 2023/24. For the full bearing orchard it amounted to and 20.6 kg m^{-3} in 2022/23 and in 2023/24, due to poor flowering and fruit set, with subsequent inferior yield, 6.7 kg m^{-3}. Economic water productivity based on gross farm income and transpiration from October until May amounted in 2022/23 to R 20.32 m^{-3} for Welgemoed and in 2023/24 to R160.17 m^{-3} and R73.19 m^{-3} for Avontuur and Welgemoed, respectively. It is suspected that for purposes of market classification, blemishes were classed too strictly in 2022/23. If the effect of blemishes were omitted from the market classification model, transpiration based economic water productivity increased to R199.22 m^{-3} for the young orchard in 2023/24 and for the full bearing orchard in the 2022/23 and 2023/24 seasons to R146.76 m^{-3} and R92.50 m^{-3}, respectively. Direct comparison of data from 2018 to current conditions is not valid due to volatility of the markets and the rand value. Nonetheless, the transpiration based economic water productivity of pomegranate is potentially high compared to other fruit crops in the region, even taking into account market fluctuations.

The maximum monthly average ETc occurred during summer in the 2022/23 and 2023/24 seasons and amounted to 3.5- and 2.6-mm d^{-1} for the young orchard compared to 5.4- and 5.2-mm d^{-1} for the full bearing orchard. The ETc reduced to values of 1 mm or less during late fall until mid-winter for both orchards. The seasonal water use for the young orchard based on measured and modelled orchard level ETc data from 1 October until 31 May was 596.7 mm and 465.9 mm for the 2022/23 and 2023/24 growing seasons, respectively. The total ETc for the full bearing orchard, measured and modelled for the same period, amounted to 898.5 mm in the 2022/23 growing season and to 888.6 mm during 2023/24. The young orchard had canola mulch on the tree row with almost no weeds present in the tree or work row, whereas the full bearing orchard did not have a mulch, but weeds contributed to the water use especially at the beginning of the growing season. Evaluation of the effect of selected weather and tree canopy variables on ETc indicated that solar radiation was the main factor determining pomegranate orchard water use.

Due to lack of total seasonal irrigation data for 2022/23, water use efficiency data was only available for 2023/24 and ETc amounted for the young orchard to about 59% of the total effective rainfall and irrigation applied. The full bearing orchard, perceived to be underirrigated during the season, made use of winter water supplies in the soil profile to supplement the ETc, as it exceeded the total effective rainfall and irrigation applied. Irrigation water productivity amounted to 3.464 kg m^{-3} and 5.103 kg m^{-3} for the young and full bearing orchards, respectively, in 2023/24. Biophysical water productivity for the young orchard amounted to 5.819 kg m^{-3} in 2023/24, total yield data not being available for the 2022/23 season as a result of theft on the farm. Biophysical water productivity for Welgemoed for 2022/23 amounted to 3.705 kg m^{-3}, but dropped due to poor flowering and fruit set and consequently lower yield in 2023/24 by almost 50% (1.899 kg m^{-3}). Economic water productivity for the two orchards based on gross farm income and ETc from October 2023 until May 2024 amounted to R75.47 m^{-3} for Avontuur and R20.60 m^{-3} for Welgemoed. Due to the effect of blemishes on the gross farm income economic water productivity was only R3.66 m^{-3} for Welgemoed in 2022/23 despite the marketable yield of 33.3 t ha^{-1}. If the effect of blemishes were omitted from the market classification, ETc based economic water productivity increased to R93.87 m^{-3} for the young orchard in 2023/24 and for the full bearing orchard in the 2022/23 and 2023/24 seasons to R26.43 m^{-3} and R26.03 m^{-3}, respectively.

The monthly average T:ETo ratio (transpiration coefficient or K_t) for the young orchard ranged from 0.13 to 0.20 for the 2022/23 season and from 0.11 to 0.14 during the 2023/24 growing season. For the full bearing orchard it ranged from 0.08 to 0.20 for the 2022/23 season and from 0.18 to 0.23 during the 2023/24 growing season. The monthly average T:ETo ratios for this study were very low, but were comparable to that of peaches whereas crops such as citrus and macadamia nuts reported by Gush and Taylor (2014) had higher ratios. The T:ETo ratios for both orchards was higher during 2023/24 compared to 2022/23.

Monthly average soil water balance derived ETc:ETo ratios were based on incomplete datasets per month and gave seasonal trends that were not comparable to the T:ETo ratios and ETc:ETo ratios based on the surface renewal and the eddy covariance systems. The

ETc:ETo ratios based on the micro meteorological systems were higher for the full bearing orchard as compared to the young orchard for both growing seasons. The monthly average ETc:ETo ratio for the young orchard ranged from 0.23 to 0.51 for the 2022/23 season and ranged from 0.31 to 0.53 during the 2023/24 growing season. The monthly average ETc:ETo ratio for the full bearing orchard ranged from 0.4 to 0.91 for the 2022/23 season and ranged from 0.39 to 0.82 during the 2023/24 growing season.

Fortnightly derived K_t values estimated using the Allen and Pereira approach and measured Kt values for the 2023/24 growing season agreed well (R^2 values of 0.99 and p-values < 0.0001) for both the young and full bearing orchards and for data of the two orchards combined (R^2 value of 0.994). However, the method relies heavily on measured transpiration inferred mean leaf resistance, which may vary for different orchards. More research in this regard is required before the method can be recommended to estimate K_t values for orchards for which mean leaf resistance values are not available. Tree canopy properties can be estimated from the tree shaded area manual method making use of demarcated hardboards although the error of the estimate can be considered high, being 0.036, 0.262 and 0.159 for FI, tree canopy area based LAI and orchard LAI, respectively. Although the regression relationship between orchard level Kc and tree shaded area was significant at a 95% confidence level, the coefficients of determination was low (R^2 = 0.42 for linear and 0.57 for non-linear trends) and it seems risky to estimate crop coefficients for irrigation scheduling using this method without further refinement. To estimate reference evapotranspiration to manage irrigation efficiently using remote sensing, the EEFlux model fared better than PYSEBAL, with coefficients of determination of .0.83 and 0.68, respectively. In contrast PYSEBAL estimated ET better than EEFLUX. There was however, not a significant linear regression relationship between Kc values determined from eddy covariance ETc and weather station derived ETo and the ones determined from ETc and ETo calculated using the two remote sensing products, EEFLUX and PYSEBAL, for the full bearing orchard for which this research was conducted.

GENERAL

The aims set for the project were met overall, although it was not possible to achieve that in both seasons for all the aims. The project experienced delays in equipment procurement (logging flow meters, micrometeorological system components) which impacted the data collection especially in the first season. Irrigation data for the full 2022/23 growing season was therefore not available to calculate all the relevant water use indicators. Late installation and vandalization of micrometeorological systems, theft of a solar panel and power supply issues impacted ETc data collection. This was addressed as best as possible by applying a modelling approach using weather data to patch missing data for each season. Total yield data could not be collected for the young orchard in 2022/23 due to theft reported by the farm, whereas the full bearing orchard experienced poor flowering and fruit set in 2023/24, reducing normal yield by about 50%. Despite these setbacks the project managed to supply valuable data that can assist in irrigation scheduling and irrigation water management.

NEW KNOWLEDGE CREATED

New knowledge created included water use (transpiration and evapotranspiration) and water productivity information for local pomegranate orchards varying in canopy cover to provide guidelines to producers for on-farm irrigation management decisions and to support catchment water management and policy making. No local information on evapotranspiration of pomegranate orchards (climate smart crop) was available and a practical means to derive crop coefficients for different orchards for irrigation scheduling purposes and catchment water management required. This research gap was identified in a scoping study regarding pomegranate orchard water use in selected production areas (WRC Report No. 2958/1/20, ISBN 978-0-6392-0163-4, June 2020). The latter study was co-funded by the Western Cape Department of Agriculture, the pomegranate industry (POMASA) and the Water Research Commission.

The current project generated information regarding pomegranate orchard water use efficiency, biophysical and economic water productivity, seasonal water use, transpiration coefficients and crop coefficients. A method to determine crop coefficients from fractional light interception of pomegranate orchards has been tested but proved to need refinement. Local water use information did not exist for pomegranate orchards that range in age/ size. It was determined for a young and a full bearing orchard of an economically important cultivar ('Wonderful') - filling an important information gap. Accurate irrigation scheduling may improve yield and quality and reduce electricity consumption, impacting economic water productivity and export earnings for the country. Water use measured using micrometeorological (evapotranspiration) and sap flow (transpiration) techniques allowed partitioning of orchard water use between beneficial and non-beneficial components, assisting growers to identify means to reduce non-beneficial water losses, important for a water scarce country such as South Africa. Such a dataset is unique and a first-of-its-kind for pomegranate orchards. A manual fractional light interception method to assist in tree water use estimation can supply producers with a means to do irrigation scheduling

for individual orchards more accurately to achieve the maximum biophysical and economic water use productivity possible. Limiting unnecessary leaching through improved irrigation scheduling may also decrease negative impacts on the environment and groundwater resources. Users and beneficiaries of the product(s)/output(s) include producers, the South African Pomegranate Producers' Association, the Water Research Commission, the Western Cape Department of Agriculture and National Department of Agriculture and Science councils.

CAPACITY BUILDING

One PhD and two MSc students registered to complete their studies pertaining to the project in 2025. Mr Muthianzhele Ravuluma registered at the University Free State Doctor of Philosophy in Agriculture, majoring in Agrometeorology (Department of Soil, Crop and Climate) with thesis title "Current and future water use of pomegranate orchards in the Western Cape of South Africa". Mr Ravuluma participated in and presented a poster in Zealand at the ISHS XIIth International Workshop on Sap Flow 2023 (30 October - 3 November 2023). He published a manuscript in the ISHS Acta of which the title is: "Sap flow dynamics of young and mature pomegranate (Punica granatum Ll.) orchards under semi-arid conditions". Mr Ravuluma received the ISHS Young Minds Award for the best poster presentation at the 12th International ISHS workshop for sap flow. Mr Ravuluma attended a UNESCO training workshop (ICT-IAEA) on Open Hardware and Open Software solutions for sustainable development, 13 – 17 May 2024 in Cape Town. South Africa.

Ms. Raesibe Kgaphola registered for an MSc in Agriculture, majoring in Agrometeorology (Department of Soil, Crop and Climate) at the University of the Free State, with thesis title "Determination of water use in a pomegranate orchard using eddy covariance and remote sensing". She delivered an oral presentation at the 2nd International Symposium on Precision Management of Orchards and Vineyards in Tatura, Australia, in December 2023. A manuscript titled "Using remote sensing models to determine evapotranspiration of a pomegranate orchard in a Mediterranean-type climate" was published by the ISHS in the Acta of the conference. Mr Daniel Havenga registered for an MSc in Horticulture at Stellenbosch University. The title of his thesis is "Water use efficiency of pomegranate".

In terms of institutional capacity building, Mr Muthianzhele Ravuluma was appointed as Junior Researcher in the Department of Soil and Water Science at ARC Infruitec-Nietvoorbij. Mr Lester Sassman, Research Technician, attended the 38th South African Society for Agricultural Technologists on the 22-25 October 2024. He presented a poster titled: "An Accurate Method of Measuring Light Interception for Pomegranate Orchards" and won the "Most Applicable Presentation" award.

CONCLUSIONS

- Water use of pomegranate orchards, in terms of monthly average daily crop evapotranspiration, reached maximum values of. 3.5 mm d^{-1} and 5.4 mm d^{-1} for the young and full bearing orchards, respectively, in mid-summer, with values of 1 mm or less presiding during late fall until mid-winter during the 2022/23 and 2023/24 seasons. Orchard upscaled daily transpiration rates were low compared to evapotranspiration and monthly averages from October to May reached a maximum of 1 mm d^{-1} for both orchards in the 2022/23 season, and maxima of 1.1- and 1.3-mm d^{-1} for the young and full bearing orchards, respectively, in 2023/24.

- The seasonal total transpiration and evapotranspiration of the orchards can with proper interpretation be used for water management purposes. It is important to note that canola mulch covering a double drip line may have reduced evaporative losses for the young orchard and water use may have been affected by advective conditions at times after harvesting of surrounding winter wheat fields. There were almost no weeds present during the growing season in the young orchard. The full bearing orchard did not have a mulch, but a dense weed stand at the beginning of the season until end October after which chemical control was applied.

- Seasonal transpiration from 1 October 2022 until 31 May for the two respective seasons amounted to 28.5% and 47% of orchard evapotranspiration for the young, and 18% and 28% of orchard evapotranspiration for the full bearing orchard. This indicates that there is scope to decrease non-productive water losses from these orchards through irrigation and orchard management in support of sustainable water management.

- The maximum seasonal evapotranspiration over the two seasons approached 600 mm for the young orchard and it was against expectations, lower for the second compared to the first season. Seasonal water use may have been affected by rainfall, which was more prevalent in the first summer compared to the second, adding to more evaporative losses.

- Although the perception is that the full bearing orchard was underirrigated, it made extensive use of winter rainfall water supplies in the soil which allowed seasonal evapotranspiration to approach 900 mm during the two seasons. These values can possibly be considered as a lower benchmark for seasonal water use of full bearing pomegranate orchards since the trees were not optimally irrigated. The weed stand though was quite dense at the beginning of the season, but after chemical control soil in the work row remained bare for the majority of the growing season until April. Interestingly, the water use was fairly similar during the two seasons despite vastly different crop loads (i.e. c. 50% lower in the second compared to the first).

- With regard to water use efficiency of the young orchard, transpiration from October until May equalled 26.9% and ETc about 59% of the sum total of effective rainfall and irrigation applied in 2023/24. For the full bearing orchard transpiration amounted to 57.2% of the sum total of effective rainfall and irrigation applied in 2023/24, whereas the ETc exceeded the total effective rainfall and irrigation applied. Water use efficiency can be improved by precision irrigation and timeous weed management.

- Irrigation water productivity amounted to 3.464 kg m^{-3} and 5.103 kg m^{-3} for the young and full bearing orchards, respectively, in 2023/24. For the young orchard it is substantially less (>50%) compared to irrigation water productivity of surface drip-irrigated pomegranate orchards of similar cultivar and age in California. If the good yield of the orchard is taken into account, the irrigation water productivity could be improved by precision irrigation that minimises leaching beyond the major root zone. Irrigation water productivity of the full bearing orchard, which was about 9.3% less compared to that of their counterparts in California, may be increased by applying orchard management practices that could improve yield.

- Biophysical water productivity for the young orchard amounted to 5.819 kg m^{-3} in its fifth year after planting (2023/24) and for the full bearing orchard during a normal bearing year with yield amounting to 33.3 t ha^{-1}, to 3.705 kg m^{-3} (2022/23). The ETc based biophysical water productivity for pomegranate trees fell within the range of that reported for the intermediate bearing apple trees with medium canopy cover (i.e. between 2 and 8.1 kg m^{-3}), and it was lower compared to that modelled for full bearing apples. It should be noted though that the full bearing pomegranate orchard was not irrigated optimally.

- Economic water productivity for the two orchards based on gross farm income and ETc from October 2023 until May 2024 with the effect of blemishes omitted from the market classification amounted to R93.87 m^{-3} for the young orchard in 2023/24 and for the full bearing orchard in the 2022/23 and 2023/24 seasons to R26.43 m^{-3} and R26.03 m^{-3}, respectively. Apart from the effect of total ETc on the indicator, the economic water productivity was sensitive especially to fruit weight, sunburn colour and degree, which determines amongst other factors, the marketable classes for fruit. These quality parameters, can within limits, be improved through precision irrigation management.

- Seasonal transpiration and crop coefficients were determined for two cultivar 'Wonderful' orchards varying in canopy cover, which can aid in irrigation scheduling of the specific orchards. It should though be kept in mind that the full bearing orchard was not optimally irrigated. The Allen and Pereira approach appears to estimate Kt values based on fortnightly input data for both the young and the full bearing orchards well. However, the method relies heavily on measured transpiration inferred mean leaf resistance, which may vary for different orchards. Additional research regarding a practical method to determine mean leaf resistance for orchards is required before the method can be recommended to estimate Kt values for orchards for which mean leaf resistance values are unknown.

- It seems feasible to estimate tree canopy properties such as fractional light interception, tree canopy area based leaf area index and orchard leaf area index from the manually measured tree shaded area, but in contrast to other research published for pomegranate, there was not a highly significant regression relationship between the crop coefficients and the tree shaded area.

- Evaluation of the capability of remote sensing models to estimate reference evapotranspiration and actual evapotranspiration for purposes of irrigation management indicated that EEFlux was the better model to estimate reference evapotranspiration, whereas the PySEBAL model worked better to estimate ET for the full bearing pomegranate orchard. Ground based crop coefficients did not relate significantly to crop coefficients derived using either remote sensing model and more research is required in this regard.

RECOMMENDATIONS

Further research with better populated datasets is necessary to establish how crop coefficients can be estimated reliably for pomegranate orchards with a range of canopy sizes and to explore the full potential of remote sensing to estimate water use. Producers, the South African Pomegranate Producers' Association, the Water Research Commission, the Western Cape Department of Agriculture, National Department of Agriculture and Science councils can make use of the knowledge generated to improve irrigation scheduling, to perform on-farm and catchment water management and to inform decision making regarding water productivity in the agricultural sector, mindful of limitations outlined in the report.

ACKNOWLEDGEMENTS

The project team wishes to thank the following people for their contributions to the project.

Reference Group	Affiliation
Prof NS Mpandeli	: Water Research Commission
Dr L Nhamo	: Water Research Commission
Dr SN Hlophe-Ginindza	: Water Research Commission (Chairperson)
Prof S Midgley	: Western Cape Department of Agriculture
Dr R. Mulidzi	: Agricultural Research Council
Dr N Murovhi	: Agricultural Research Council
Dr S Schoeman	: Agriwiz
Dr N Taylor	: University of Pretoria
Mr M Masevhe	: University of Limpopo
Mr C Nortjé	: Pomegranate Producers Association of South Africa

The financing of the project by the Water Research Commission is acknowledged gratefully.
Additional funding of pomegranate orchard water use research by the National Research Foundation is also acknowledged gratefully.

This project was only possible with the co-operation of many individuals and institutions. The authors therefore wish to record their sincere thanks to the following:

The Pomegranate Producers Association of South Africa for assistance with research plot selection (Mr J Mulder) and for providing funding for international conference registration for Ms R Kgaphola.

Participating producers:
Avontuur (Mr A Pretorius) for the use of their orchard, orchard information and assistance with field work from October 2024.
Avontuur (Mr H Smith) for the use of the orchard, orchard information and assistance with field work until July 2024 (Mr E Baard and Mr A Esterhuysen).
Welgemoed (Mr P Nell) for the use of the orchard, orchard information and assistance with field work (Mr R Botha and Mr M Prins).

Others:
Ms L. Möller, Department of Forestry and Wood Science, Stellenbosch University, for assistance with wood anatomy analysis.
Dr N. Taylor, Department of Plant and Soil Sciences, University of Pretoria, for assistance with the sap flow scoping study.

TABLE OF CONTENTS

LIST OF FIGURES

LIST OF TABLES

ACRONYMS & ABBREVIATIONS

A_n	Net carbon di-oxide assimilation rate
C-MAP	Crop Monitoring and Assessment Platform
CMAs	Catchment Management Agencies
CP-LAI	Accupar LP-80 ceptometer modelled leaf area index
DAB	Days after bud break
EC_w	Electrical conductivity of water
EC	Eddy covariance
ENDVI	Enhanced Normalized Difference Vegetation Index
ET	Evapotranspiration
ETc	Crop evapotranspiration
ETc adj	Crop evapotranspiration under non-standard conditions
ETo	Reference evapotranspiration
fc	Fractional canopy ground cover
FI	Fractional light interception
FVS	Flux-Variance Similarity
GR	Grean Ratio
g_s	Stomatal conductance
HD	Heat dissipation
HFD	Heat field deformation
HPV	Heat pulse velocity
HRM	Heat ratio method
I	Irrigation amount
Kc	Crop coefficient
Kcb	Basal crop coefficient
Ks	Stress coefficient
LAI	Leaf area index
MS	Multispectral camera
NAN	Non-numerical
NDGNI	Normalized Difference Green Near Infrared Index
NDVI	Normalized Difference Infrared Index
NTG	Natural Thermal Gradients
OLAI	Orchard leaf area index
P	Effective precipitation
PMS	Stem water potential
POMASA	Pomegranate Producers Association of South Africa
R	Runoff
R^2	Coefficient of determination
RH_{max}	Maximum relative humidity

RH_{min}	Minimum relative humidity
Rn	Solar radiation
SA	Shaded area
SF	Sap flow
SHB	Stem heat balance
SR	Surface Renewal
SWB	Soil water balance
T_{max}	Maximum temperature
T_{mean}	Mean temperature
T_{min}	Minimum temperature
TA	Titratable acidity
TD	Thermal dissipation
TDP	Thermal dissipation probes
TIR	Thermal infrared camera
Tr-LAI	Tree canopy area based leaf area index
TSS	Total soluble solids
UAVs	Unmanned Aerial Vehicles
USGS	United States Geological Survey
V	Average sap velocity
V_h	Heat pulse velocity
VHR	Very high resolution
VI	Vegetation Indices
Vis	Multispectral vegetation indices
VPD	Vapour pressure deficit
WRC	Water Research Commission
ΔW	The change in soil water content

CHAPTER 1: BACKGROUND

1.1 INTRODUCTION

Global warming-induced climatic changes, limited water resources and water restrictions for agriculture during drought force producers to invest in crops that are more suited to the potential future climate, such as drought-tolerant pomegranate *(Punica granatum*) trees (DEA, 2016; WCDoA, WCDEA and DP, 2016; Botai et al., 2017; Galindo et al., 2018; Otto et al., 2018; Burls et al., 2019). In South Africa, the pomegranate industry is small but expanding. Of the 1167 ha in 2023 under this crop, 79%, 9% and 11% of the plantings are in the Western Cape, Limpopo and Northern Cape provinces, respectively (Viljoen and Hurter, 2024). Production started in the early 2000s and South Africa is presently an international role player in the production and export from the southern hemisphere to various northern hemisphere countries. In 2024 about 8 616 tons of fruit were exported. Hortgro forecasted production of 10 071 tons of fruit for the industry by 2024 of which 36% will be exported and 64% processed. The cultivar 'Wonderful' is important in terms of industry plantings (88%) and important for the export market (88.7%).

Most commercial pomegranate orchards are either drip or micro-sprinkler irrigated. In Western Cape agriculture, water demands are likely to increase in future with the expected increased temperatures and evaporation (DEA, 2016; WCDoA, WCDEA and DP, 2016; Otto et al., 2018) which will result in an increased irrigation demand for orchards. In addition, prolonged droughts of similar severity to those of the 2015-2017 period are likely to recur in the future, with climate change increasing the likelihood thereof (Otto et al., 2018; Burls et al., 2019). The irrigation volume for the agricultural sector is unlikely to increase as the Department of Water and Sanitation (DWS) has capped agricultural allocations to current levels. Furthermore, a significant reduction in streamflow is predicted for the western region of South Africa, where several Western Cape Water management areas are already water stressed. Water demand-and-supply forecasts for the Berg and Olifants-Doorn water management areas, respectively, indicated a severe (-20% to -80%) and moderate (0% to -20%) gap between the existing supply in 2010 and projected demand in 2030 (McKinsey & Company, 2010). Improved agricultural water use efficiency and productivity is considered a necessity to provide the water needed for the projected increased water demand by human consumption and industrial production by 2030. Such limited water resource availability makes maximizing net income per unit water used a prerequisite for sustainable farming. This can be achieved by using the water for high value niche crops such as pomegranate.

A baseline survey on irrigation and pomegranate tree performance was undertaken during 2017/18 and 2018/19 by the Agricultural Research Council (ARC) (co-funded by the Alternative Crop Fund of the Western Cape Department of Agriculture through the Pomegranate Producers Association of South Africa (POMASA) and the Water Research Commission (WRC)). Results of the scoping study (WRC Project K5/2958) confirmed that although pomegranate trees are considered drought-tolerant, irrigation is required during the dry summer to optimise growth, yield and fruit quality for commercial production. Furthermore, there is potential for some production areas to increase yield and fruit quality through improved irrigation scheduling. Skilful management of limited water resources will be a necessity if optimal production and fruit quality is to be retained for a farm.

For efficient in-field water management, correct irrigation system selection, design and maintenance are very important, but efficient irrigation scheduling is the main key to achieving high irrigation water use productivity. Crop water use or evapotranspiration (ETc) of orchards can, amongst other methods, be estimated using crop coefficients (ratio of ETc/ETo) and reference crop evapotranspiration (ETo) using hourly / daily / long-term weather data. Although FAO56 (Allen et al., 1998) contains crop coefficient values for various crops, pomegranate tree data are not listed. Of the crop coefficients available for pomegranate those determined in Israel for young pomegranate trees were based on Class A pan evaporation (Bhantana and Lazarovitch, 2010), whereas crop coefficients from California, USA, were developed for young to full bearing trees using ETo (Ayars et al., 2017; Zhang et al., 2017). Crop coefficients for pomegranate have furthermore been estimated from site specific empirical relationships of crop coefficient versus day of year (Parvizi et al., 2014; Ayars et al., 2017), or from fractional canopy ground cover (Meshram et al., 2011, 2012; Zhang et al., 2017).

Pomegranate-specific crop coefficient estimates were compared to those for peach (Ayars et al., 2003), grapevine (Williams and Ayars, 2005) and the general deciduous fruit equation used by Meshram et al. (2011). Results indicated that the pomegranate cultivar 'Wonderful' tended to have lower crop coefficient values at comparable fractional ground cover (also measured as shaded area cast

on the ground) than these crops. The differences in slopes and intercepts of these relationships are ascribed to differences in methods used to determine crop evapotranspiration and the shaded areas, and dissimilarities in cultivation practices, specifically irrigation amounts and frequencies (Williams and Ayars, 2005). Crop coefficients developed for different irrigation systems and different cultivars in different countries can therefore not necessarily be applied directly elsewhere. Although there are general POMASA guidelines regarding the irrigation of pomegranates, there are no local research results to guide producers on how the actual water use of pomegranate orchards vary under South African conditions to optimize water management for sustainable production.

In view of the above, the following research questions can be formulated for pomegranate orchards in South Africa:
1) How does the water use of pomegranate orchards vary from planting to full-bearing age?
2) Can accurate crop coefficients be modelled from readily available information and what are the factors that drive their variability?
3) What are the factors that affect fruit growth, yield and fruit quality in pomegranate orchards in South Africa?
4) What is the biophysical and economic water productivity of pomegranate orchards in South Africa and how can these be improved?

To address these questions, research is required to quantify the water use (transpiration and evapotranspiration) of a range of young to full bearing pomegranate orchards. Besides being useful for directly deriving crop coefficients to be used to improve irrigation scheduling in the specific study orchards, these data can be used to develop a model for practical estimation of crop coefficients under local conditions. Such a model - covering a range of fractional light interception regimes - could enable extrapolation of the study findings to other orchards in other production areas. Such a model will aid producers to schedule irrigation according to tree water requirements and prevent over- or under-irrigation which impacts the environment (leaching of fertilizers and water losses) and fruit tree performance (yield and quality).

Orchard water use research utilizing sap flow and/ or micrometeorological techniques has been done locally for apple (Volschenk et al., 2003; Dzikiti et al., 2018), avocado (Mazhawu et al., 2020), citrus (Vahrmeijer et al., 2015) and for macadamia and pistachio (Ibraimo, 2018) trees. However, at the time of inception of the project there were to our knowledge no publications on the use of micrometeorological and sap flow techniques in South Africa nor elsewhere in the world to determine water use of pomegranate orchards. Quantifying water use through sap flow, soil water balance and micrometeorological techniques simultaneously for pomegranate orchards has not been attempted before in South Africa.

Seasonal evapotranspiration information of pomegranate orchards ('Wonderful' cultivar) varying in age/ size/ training system in the main pomegranate production region – the Western Cape, South Africa is required to improve irrigation management to support sustainable farming amidst climate change (i.e. higher temperatures; changing rainfall patterns) and increasingly limited water resources. The use of poor-quality irrigation water may be a viable option for pomegranate production in areas where other water resources are not available provided that the correct irrigation management is applied. Knowledge of water efficient production practices (in this case for example accurate irrigation scheduling) will allow producers to use limited water resources more efficiently and to produce a high value niche crop for the local and export markets. High water use productivity and increased income from quality export fruit may improve the economical welfare of the community i.e. producers and their farm workers will benefit.

Seasonal water use information and potentially a means to determine orchard specific crop coefficients/ basal crop coefficients for pomegranate trees can be used for water management planning purposes at the farm level to achieve maximum water use efficiency and/ or water use productivity. This information can also be used in catchment-wide water management by the Breede-Olifants Catchment Management Agency (amalgamated Breede-Gouritz and Berg-Olifants Catchment Management Agencies (CMAs)). Information regarding income earned relative to volumes of water used can inform national government policy and decision making in the water sector (i.e. economic water productivity). The pomegranate is a versatile fruit which can be marketed fresh, or it can be processed to provide ready-to-eat convenience foods and juice, whereas parts of the fruit can be used in pharmaceutical products. Processing plants supported by a large enough industry may create new job opportunities and promote economic development. A model for deriving orchard crop coefficients is a potential product for improving the management of scarce water resources e.g. by optimizing irrigation scheduling in the sector. Training of students and personnel in the use of orchard water use measurement techniques add research capacity to conduct research that can help to address challenges posed by climate change to South Africa.

Successful production of a drought tolerant crop may provide sustainable income and work opportunities in future when crops currently produced become unproductive or fail. Water savings in agriculture will make available more water to other sectors, which is critical during drought. Improved fruit quality can increase export earnings, which may have a positive impact on the economy. Pomegranate

fruit is marketed locally or exported for fresh consumption or processing purposes. Higher production also may lead to more job opportunities. Leaves, bark and roots of the tree as well as fruit are also used for medicinal purposes. Pomegranate juice contains healthy bioactive compounds, mineral nutrients and is high in antioxidant content. Especially the juice and ready-to-eat arils are considered healthy convenience foods for populations with limited time available. Proper irrigation management will promote efficient use of limited water resources and reduce leaching of fertilizers that impacts on the quality of groundwater. Pomegranate trees are relatively tolerant to salinity and careful management will be necessary to ensure sustainable use of soils where saline irrigation water is applied over the long term.

1.2 PROJECT AIMS

The current research project intended to determine the water use, yield and fruit quality of selected pomegranate orchards in Western Cape production areas.by pursuing the following aims:

Aim 1: To measure pomegranate orchard water use for orchards with a range of canopy sizes.

Aim 2. To determine the tree and fruit growth, yield and fruit quality of selected pomegranate orchards under irrigation.

Aim 3. To determine the orchard level water use efficiency, biophysical and economic water productivity of selected pomegranate orchards under irrigation.

Aim 4. To develop a method for practical estimation of crop coefficients for application in a water use model to enable calculation of individual orchard water requirements

1.3 SCOPE AND LIMITATIONS

This project collected data on water use and water productivity of two pomegranate orchards varying in age (young and full bearing) and canopy size over two growing seasons at different locations in the Western Cape (main) pomegranate production region in South Africa. Water use data were collected by using soil water balance, sap flow and micrometeorological techniques while weather stations collected the necessary data to calculate reference evapotranspiration to relate to water use for irrigation scheduling purposes. A modelling approach was used to supplement missing water use data for periods when equipment malfunctioned. Tree physiological, growth and yield data were collected and fruit quality determined to assess gross farm income to calculate water use indicators. Tree dimensions, fractional light interception, leaf area index and tree shade data were collected at selected stages to relate to the water use data. This information was used to evaluate a method for practical estimation of crop coefficients which enables calculation of individual orchard water requirements. The most important environmental factors affecting transpiration and evapotranspiration was identified using multiple stepwise regression.

The research included a literature overview focussing on pomegranate production and selected orchard water use measurement methodologies (Chapter 2). A general methodology section (Chapter 3) includes important background information on the experimental sites and plant material, soil properties, soil water content and irrigation monitoring and methods used pertaining tree related data (plant physiology, growth and yield, fruit quality, market classification, water use indicators). Chapter 4 focusses on transpiration of young and full bearing orchards and factors affecting it. It contains seasonal transpiration values and concludes with transpiration based water use efficiency, biophysical water productivity and economic water productivity data. Chapter 5 discusses the evapotranspiration losses of pomegranate orchards varying in canopy cover and provides seasonal evapotranspiration data for evapotranspiration based water use indicators. Chapter 6 addresses the modelling of water use for pomegranate orchards varying in canopy cover by providing information on measured crop coefficients, relating estimated tree transpiration coefficients from tree properties to measured transpiration coefficients. Tree shaded area is related to fractional light interception, canopy area based leaf area index, orchard leaf area index and crop coefficients. The use of remote sensing to estimate water use for pomegranate orchards is also investigated.

CHAPTER 2: KNOWLEDGE REVIEW ON POMEGRANATE PRODUCTION AND SELECTED ORCHARD WATER USE MEASUREMENT METHODOLOGIES

2.1 INTRODUCTION

The focus of this literature overview is on pomegranate production and selected orchard water use measurement methodologies. The approach was to first describe the South African pomegranate industry and its production practices, where after methods to determine orchard water use relevant to the proposed project were addressed. The review covers methods available for direct measurement of orchard water use such as sap flow and the soil water balance, as well as indirect methods to estimate evapotranspiration through orchard water use modelling. Newer methods using remote sensing technology to determine orchard water use does not form part of the proposed project, but is also included albeit in less detail.

2.2 SOUTH AFRICAN POMEGRANATE INDUSTRY

The pomegranate plant is an ancient plant that can be related to many cultures around the world. Historical information shows that pomegranate was one of the five wild trees domesticated alongside fig, date palm, grape, and olive trees. The pomegranate (*Punica granatum* L.) is native to Iran, and it is usually grown in arid and semi-arid areas around the world (Sarkhosh et al., 2006). However, the origin of the pomegranate is a controversial matter because it is part of many cultures and has been part of much documented history. The pomegranate can be cultivated in arid and semi-arid areas such as South Africa because of its tolerance to drought and water scarce conditions. The pomegranate can also be planted in Mediterranean, tropical and subtropical regions (Chandra et al., 2010).

The pomegranate fruit has benefits for human beings because of its medicinal application benefits. In South Africa, the pomegranate fruit is produced mainly in the Western Cape for local and global markets. Due to the increasing awareness of healthy lifestyles, the pomegranate fruit is in demand because of its many health benefits (Seeram et al., 2006). South Africa is one of the countries in the southern hemisphere producing pomegranate fruit to supply to the northern hemisphere during the spring and early summer. Recent information from POMASA (Viljoen and Hurter, 2024) indicates that the total area under pomegranate cultivation has increased from less than 800 ha in 2011 to approximately 1167 ha in 2023.

Since pomegranate fruit is one of the oldest cultivated fruits, there are many varieties worldwide. The commercial pomegranate cultivation in South Africa started in the early 2000s, and a few cultivars were selected based on their climate suitability characteristics. However, other features should be considered when selecting a cultivar, such as the fruit's shelf life, size, colour, acidity, and juice content (Pienaar, 2021). The cultivars predominantly grown in South Africa include ‘Wonderful’, ‘Acco’, ‘Hershkovitz’, ‘Kingdom’, ‘Emek’ and ‘Angel Red’. According to Viljoen and Hurter (2024), 88% of the pomegranate fruit trees cultivated in South Africa are the ‘Wonderful’ cultivar, followed by ‘Acco’ and ‘Hershkovitz’, with 3% each (Figure 1). In South Africa, the pomegranate industry was initiated in the Western Cape in the early 2000s, and it then spread to other provinces. Pomegranate production is condensed in the Western Cape, which makes up 79% of the cultivated area, followed by Northern Cape with 11%, Limpopo with 9% and Kwazulu Natal and the Eastern Cape 1% each.

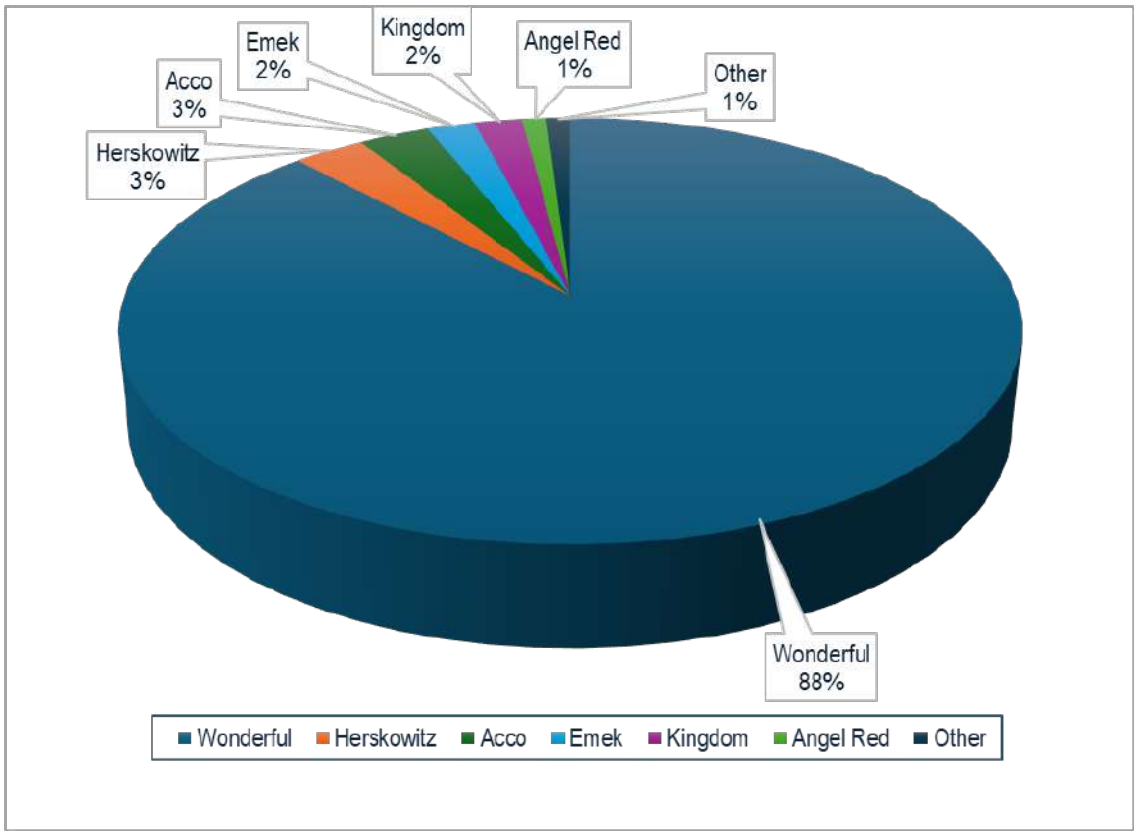

Figure 1. Pomegranate cultivars planted in South Africa (POMASA,2024)

Since there is a lack of adequate and readily available information, it is hard to track the global supply of pomegranate production in terms of cultivated areas and tons of fruits produced. However, there is some scattered information about the production of different countries. According to Pienaar (2021) the pomegranate industry is estimated to have 835 950 hectares and 8.1 million tons in fruit production on a global scale. Moreover, in South Africa, the cultivated area was estimated to be 1032 hectares in 2020 (Viljoen, 2020a), whereas the overall fruit production amounted to 12 984 tons in 2019 (Pienaar, 2021). The South African pomegranate market is relatively new as it was only introduced in early 2000. The market comprises trading with both the local and international market with 51% of the overall yield produced in South Africa being exported, helping to generate foreign income (Pienaar, 2021). In 2024 the South African pomegranate industry exported c. 8616 tons of fruit (i.e., 2 267 368 equivalent cartons of 3.8 kg) (Viljoen and Hurter, 2024). The cultivar 'Wonderful' contributed 88.7%, Acco and Hershkovitz each 3.8% and other cultivars combined, 3.6% to the exported fruit volumes. The local fresh market is relatively new, and the fruit is not well known amongst South African customers. According to a packhouse information survey done in 2024, fruit destined for the local market included 1% of fruit for fresh fruit consumption, 27% of fruit for processing and 6% of fruit for juice. Of the 62% of fruit exported, 16% of fruit were intended for the fresh market and 46% for processing purposes.

The pomegranate market in South Africa has been shown to be growing very quickly. According to the estimation done by Pienaar (2021), there was a 63 % growth in pomegranate production for the years 2015 to 2019, with a further 25% growth in the area planted from 2019 to 2023 (Viljoen and Hurter, 2024). It is expected that an orchard containing a 1000 trees per hectare at a 5 m x 2 m spacing would have an estimated yield of 28 tons at the full bearing stage during the 5th year after establishment (Viljoen, 2020b). According to Viljoen (2020b), the ability for the investment of farmers to break even depends on the cultivar. It was estimated in 2020 that when the most popular cultivars such as 'Wonderful', 'Hershkovitz' and 'Acco' are planted, it will take six, eight and seven years, respectively, for the investment to break even if orchard yield reaches 35 t/ha from year four onwards and 90% pack-out is achieved. This was based on the assumption that the cultivars 'Wonderful', 'Hershkovitz' and 'Acco' earned a net farm income of R111 223, R58 157 and R46 028 per hectare per year, respectively, from year four from establishment. The establishment cost of one hectare of pomegranate trees amounted in 2022 to R196 630 (including trellis system, R268 330), while the production cost for a pomegranate orchard of full-bearing trees was assumed to be R371 928 per hectare per year (Viljoen, 2022). The biggest expenditure incurred with regard to production costs relates to packing material which comprises 58% of the expenditure, while the cost of spraying and labour amounts to about 9% (c. R35 000 per hectare) and 7% (c. R26 714 per hectare), respectively.

2.3 POMEGRANATE PRODUCTION PRACTICES

2.3.1 Pomegranate phenology

Pomegranate buds are small, brownish-green and located in the top part of spurs and vegetative sprouts (Levin, 2006). Pomegranate trees have two types of buds namely large and narrow (Rajaei & Yazdanpanah, 2015). Large buds develop reproductive or vegetative shoots, while narrow buds only develop vegetative shoots (Rajaei & Yazdanpanah, 2015). The vegetative bud swells and produces greenish flowers between leaves. Flowers usually have both male and female parts (Kahramanoglu et al., 2018). However, the pomegranate tree can have three types of flowers, namely, hermaphrodite, male, and intermediate forms (Fattahi et al., 2020). Fruit is derived from hermaphrodite flowers, which have a discoid stigma covered with copious exudate, an elongated style, and an ovary with many ovules, which on fertilization develop into the hundreds of succulent juice containing arils that make up the edible portion of the fruit (Wetzstein et al., 2011). Shulman et al. (1984) stated that male flowers fail to set fruit and have reduced female parts characterized by shortened pistils containing rudimentary, degenerated ovules.

The pomegranate tree has three flowering periods - the first period occurs in early spring with abundant flowers, of which about 25% set fruit and the rest drop (Kahramanoglu et al., 2018). This first flowering period produces large and marketable fruit. The second period occurs in late spring with small to medium fruits, and a third flowering period appears in the middle of summer with small fruit. It is preferred to thin small fruits to improve fruit quality and meet commercial standards (Kahramanoglu et al., 2018). Thinning increases the size of the large fruit and decreases the size of moderate ones. Fruit growth increases to its final size through cell enlargement. During fruit ripening, the flesh seeds change from white to pinkish-red and the skin of the fruit changes to brownish yellow with reddish patches (Melgarejo et al., 1997). Pomegranate fruit become ready for harvesting in less than 11 months after full blossom depending on the cultivar type (Shulman et al., 1984). General growth stages, development and duration of the pomegranate tree are shown in Table 1.

2.3.2 Thinning

Pomegranate trees tend to produce more fruits than they can carry, leading to fruits competing for carbohydrates, resulting in poor fruit size and quality that the market does not require (Kahramanoglu et al., 2018; Bergh, 1990). Fruit thinning needs to be performed when an excessive number of fruit occurs, to ensure that the remaining fruit reach marketable size and quality (Kahramanoglu et al., 2018). Correct fruit thinning limit competition and allows each fruit to receive enough light, which improves fruit colour and flavour (Kahramanoglu et al., 2018). Pomegranate thinning is the most important and critical practice for improving fruit sizes, fruit quality and the next season's yield. Since too many fruits on a tree competes for water, nutrients and deplete carbohydrates that supposed to be used by next season's fruit (Mashavhathskha, 2014; POMASA, 2013).

Fruit thinning can be done through hand or mechanical thinning. Fattahi et al. (2020) mentioned that hand fruit thinning reduces the crop load and increase quantitative and qualitative attributes of the fruit before harvest. Chemical methods are commercially used to remove fruits on a large-scale using growth regulators (Fattahi et al., 2020). Thinning could be successful when the fruit is thinned 4-5 weeks after flowering (POMASA, 2013). In contrast, fruit thinning is recommended to be done about 3-4 weeks after full bloom when the fruits are about walnut size (Kahramanoglu et al., 2018). As a rule of thumb, small, deformed, damaged and axillary fruits should be thinned while the terminal fruit remain (Kahramanoglu et al., 2018). This reduces competition for nutrients, water, and carbohydrate and indirectly improve fruit size and quality.

Kahramanoglu et al. (2018) found that for the cultivar 'Wonderful', leaving between 90 and 99 fruit after thinning provides the highest yield. Leaving less than 90 fruit ensures good fruit size and quality, but it reduces tree yield significantly. Leaving 100 fruit caused a decline in fruit weight, fruit size, fruit quality and total yield. Fattahi et al. (2020) conducted a study to investigate the impact of different thinning levels (control, removal of 10%, 15%, 20% and 25% of fruit). Hand thinning had a positive effect when 20% of fruit is removed and resulted in better yield and fruit quality than other treatments (Fattahi et al., 2020).

Table 1. Phenological growth stages, development and duration of the pomegranate tree, adapted from Melgarejo et al. (1997)

Growth stage	Development	Duration (days)
Bud in winter dormancy	Bud greyish brown, completely closed, deeply linked to the twig and sharply pointed at its tip	61
Bud swelling	Bud swells, becomes paler and rounder in shape	11
Red tip	Bud opens; new shoot comes up with spear shaped and red tip	6
Sprouting of first leaves	First leaves appear; leaves furled and bright red with a pale midrib green	6
Leaf separation	New leaves separate	4
Leaf growth	Leaves grow in length and width; colour changes from bright red to light green	12
Lengthening of internodes	Rapid shoot growth; internodes lengthen	119
Appearance of the flower buds	Greenish flower buds appear on shoots, buds become red after a few days; sepals visible and close together	3
Swollen calyx	Buds increase in size, become pear-shaped; differences between male and hermaphrodite flowers become apparent in shape and the colour of the calyx; terminal branches bud together with several flowers usually abscises	11
Opening of calyx	Sepals open, folded red petals appear inside; petals unfold, and the pistil anthers become visible at later stage	3
Open flower	Calyx and petals open totally, petals unfold over the sepals. Anthers of the stamen change to deep yellow when the pollen is ripe. Pollination takes place	6
Petals fall	Petals wither and fall; the calyx turns colour from red to orange-red; stamens bend towards the longitudinal axis of the flower, and the anthers become greyish yellow. The terminal part of the style withers	2
Fruit setting	The fertilized ovary grows in size, and the base of the calyx swells; the stamens wither, and the fruit changes from orange red to greenish-brown	10
Young fruit	The fruit increases in size rapidly and the colour turns from greenish brown to green	17
Fruit growth	The fruit enlarges almost to its final size through cell enlargement; the sepals form a crown, the dry stamen being inside	90
Second bud sprouting	Resumption of shoot growth on the tree	45
Fruit ripening	The fleshy seeds change from white to pinkish-red or red; the skin of the fruit changes from green to greenish-yellow, and finally to brownish-yellow with reddish patches (according to cultivar)	35
Leaf fall	Leaves turn yellowish, and fall; and when complete, winter dormancy starts	57

2.3.3 Pruning

Pruning is a complex operation of cutting a tree to regulate the tree's growth, development, and production (Ferrara et al., 2021). The main aim of pruning is to obtain better yield, quality, and aesthetic results for ornamental pomegranates. Pruning of pomegranates can be done in winter and in summer. The winter pruning is necessary to create a strong and robust tree structure, create the right shape, to manage light interception and ensure there is air circulating within the canopy, to stimulate vegetative growth, reduce alternate bearing and balance the aerial and the root systems (LaRue 1980; Ferrara et al., 2021). Water shoots, broken, interfering and bent branches should be removed during winter pruning.

Managing light interception of the tree through correct pruning is essential as tree leaves in the shade are not able to produce the optimal amount of photosynthesis required to sustain shoot and fruit growth and flower bud formation, and fruit ripening is promoted by optimal light availability (Ferrara et al., 2021). The vegetative growth response of the tree can be influenced by the intensity of pruning, as light pruning may increase small shoots while heavy pruning may encourage the strong growth of the shoots, including water shoots (Chakma, 2014). Aggressive pruning might significantly impact yield negatively while lighter annual pruning stimulates growth of new fruit shoots (POMASA, 2013).

The timing of winter pruning is very important as late pruning dates decreased production and delayed harvest time (Ferrara et al., 2021). However, Ghosh et al. (2012) found that trees pruned the earliest had good fruit quality (fruit weight, sugars and acid ratio) while late pruning times improved fruit skin colour. In the southern hemisphere pruning can be done in June, July or August, but it also depends on the climate conditions as for colder winters, the pruning is done later.

Summer pruning is done to maintain the size of the tree, control the vigour, remove water sprouts, regulate the canopy microclimate (leaf removal), increase carbohydrates and improve the fruit quality (Ferrara et al., 2021). Summer pruning helps to keep the tree interior open for the sunlight to penetrate (POMASA, 2013). A successful pruning is done by removing excessive overcrowded growth, suckers and deadwood and retained enough fruit-bearing wood (POMASA, 2013).

2.3.4 Cover crops and weed management

Weeds compete with trees for water, sunlight and nutrients and host pests and insects in pomegranate orchards (POMASA, 2013). Weeds can be controlled through application of chemical weed killer, mowing and planting of cover crops in the inter row space (POMASA, 2013). Under Mediterranean climate, weeds can be controlled through tilling the soil using a disc opener and application of post emergent herbicides such as roundup, oxyfluorfen (goal) on bearing or non-bearing pomegranates, or flumioxazin on non-bearing pomegranates (Day and Wilkins 2011).

Pre-emergence weed killers are applied before the season start while glyphosate should be applied throughout the season to control emerging weeds. Glyphosate should be not applied on windy days and the label for application instructions must be consulted and adhered to. Cover crops minimise weeds through competing with them for water and nutrients. Additionally, cover crops serve as a host for natural enemies of potential pests (POMASA, 2013).

2.3.5 Sunburn protection

Pomegranates are mainly grown in hotter areas where air temperatures may rise above 40°C during summer (POMASA, 2013). Sunburn damage in fruit is caused by heat (over 40°C in summer) and radiation (mainly UV-B), which lead to quality and income losses (Abou El-Wafa 2015). Pomegranate fruit from young trees is easily affected by sunburn as a result of sparse leaf coverage. Pomegranates are sensitive to the sun since they are terminal bearing plants and the branches bend when fruit weight increases (Abou El-Wafa 2015). Sunburn damage can cause a grower to lose more than 30% of the fruit harvest (POMASA, 2013; Abou El-Wafa 2015).

Several approaches can be used to reduce sunburn incidence, such as bagging of fruit (paper bags), adjustment of fertilization and irrigation regimes, and use of orchard netting or application of UV protection agents on fruit (POMASA, 2013). Spraying anti-sunburn compounds containing calcium carbonate, such as Purshade, on pomegranate orchards is effective in reducing the effects of high temperature and UV radiation on both fruit quality and yield (Abou El-Wafa, 2015). Compounds such as Purshade as well that containing kaolin also protect fruit against harmful effects of solar radiation and water stress (Badran, 2015). Abou El-Wafa (2015) conducted a study to identify the effect of some white coating (Purshade, $Ca(OH)_2$ and Kaolin) on reducing sunburn in 'Wonderful' pomegranate fruit. The author found that all three treatments were effective in reducing the percentage of 'Wonderful' pomegranate fruit sunburn. Kaolin was though more effective than Purshade and $Ca(OH)_2$.

2.3.6 Harvest

In the Western Cape, South Africa, picking of pomegranate fruit begins in autumn and it is advisable to pick early maturating orchards first and followed by late maturating orchards (LaRue, 1980). On the study that was conducted by Volschenk and Mulidzi (2020) in the Western Cape, the highest yield of 59.4 t ha^{-1} was obtained from Bonnievale area, followed by Gouda (35 t ha^{-1}), Wellington (26.4 t ha^{-1}) and Wolseley (22.9 t ha^{-1}). Pomegranate harvest time is determined by the fruit colour development, sugar and acid contents (POMASA, 2013). For export purposes the fruit must meet maturity standards for packing and shipping such as meeting minimum colour and acid requirements, and be free from decay, sunburn, bruises and cracks (LaRue, 1980).

For South African pomegranates, the maturity indicator required by Department of Agriculture, Land Reform and Rural Development (previously Department of Agriculture, Forestry and Fisheries) for export is a minimum of 14 degrees Brix (Volschenk and Mulidzi, 2020). According to Volschenk and Mulidzi (2020) study conducted in 2017/18 season, Wellington area had highest °Brix of 18.7, followed by Gouda and Wolseley (17.8 °Brix) and Bonnievale (17.5 °Brix). However, in 2018/19 season, Gouda area had highest °Brix of 18.2, followed by Wellington (18.2 °Brix), Wolseley and Bonnievale (17.1 °Brix). In addition, aril and rind colour should be used in combination with other maturity tests such as sugar: acid ratio since they vary with area and season (POMASA, 2013). LaRue (1980) stated that as the fruit approaches maturity on the tree it may split and rain closer to picking cause fruit splitting. Therefore, it is important for the grower to know weather conditions during harvest period as the fruit are susceptible to splitting if rain falls when fruit are near optimal maturity.

2.3.7 Quality and marketing

The Northern Hemisphere produce nearly 90% of global commercial pomegranate fruit with the main producers being India, Iran, United States, Turkey, Spain and Israel (Arendse et al., 2015). The Southern Hemisphere provide fruits to the international markets during the counter season (March up until July), with South Africa being one of the main producers (Pienaar, 2021; Arendse et al., 2015). Pomegranate fruit is valued for its juice containing arils and is consumed fresh and used for health benefits towards coronary heart disease, cancer and infectious diseases (Wetzstein et al., 2011). Arils are the juicy pulp around the seeds formed from ovules present in the ovary of fertilised fruit (Shulman et al., 1984). Pomegranate fruit is marketed as whole fresh fruit, extracted arils, juice, syrup, wine, teas, seed oil and other products (Wetzstein et al., 2011). The juice is extracted using various methods such as modified wine grape or citrus presses and other machinery developed exclusively for pomegranate juicing that can process a million fruit per day (Day and Wilkins, 2011). The pomegranate cultivar 'Wonderful' can produce a high-quality juice that can be used directly as 100% pomegranate juice or as a 100% juice blend with other distinctive fruit juices (Day and Wilkins, 2011).

Pomegranate fruit is used for decoration purposes mostly and is also eaten fresh (LaRue, 1980). Children enjoy eating the kernels and home cooks use the kernels as a garnish for desserts and salads. Kernels are squeezed to extract juice and large extractors are used for greater amounts of juice (LaRue, 1980). The juice is used in a variety of beverages and foods, such a grenadine. Citrus fruit, pears and apples marinated in pomegranate juice makes attractive salads and fruit cocktails. Most popular use of pomegranate extracted juice is to make jelly. The arils contain several compounds groups that are useful in human diet in preventing disease (Tinebra et al., 2021).

2.3.8 Cold chain

Cold chain maintenance during long term storage is important for the preservation of fresh fruit quality (Arendse et al., 2015). Storing pomegranate fruit after harvest is very important in maintaining a consistent supply of high-quality fruit in the marketplace (Sidhu et al., 2019). Chlorine or any registered South African ant-fungal agent should be used to wash fruit intended for the fresh market (POMASA, 2013). Fruit should be packed into boxes by size, and waxed to improve appearance (LaRue, 1980). This helps fruit to be stored in cold storage for several weeks without losing market quality. Darker fruit skin colour continues to develop if the fruit is stored at room temperatures and may last several weeks in decorative arrangements (LaRue, 1980).

Pomegranate fruit usually packed in 4kg (class 1 and 2) or 15 kg cartons can be stored up to six weeks in normal cold storage and up to five months in controlled atmosphere storage (POMASA, 2013). The lowest temperature used during short term storage (less than three weeks) is 5°C and for long term storage is 7°C for optimum quality (POMASA, 2013). According to Sidhu et al. (2019) fruit stored at temperatures less than 5°C under standard refrigerated conditions for more than 2 months may develop browning in arils, pericarp and seeds. Additionally, Arendse et al. (2015) found that 'Wonderful' pomegranate fruit can be stored for 2 months at 5°C and 92% relative humidity without losing overall flavour and aril colour. However, storing the fruit beyond 2 months led in overall quality reduction and development of off-flavours. If fruit is stored at too low temperatures for long periods, the arils soften up and result in fruit decaying (POMASA, 2013). High rates of fruit weight loss may occur when the fruit is stored under high temperatures or low relative humidity (Sidhu et al., 2019).

2.3.9 Irrigation

The amount of intercepted radiation influences irrigation requirement by the canopy which directly affects tree transpiration rate (Meshram et al., 2011). Pomegranates are very drought tolerant. However, adequate soil moisture is required in order to improve plant vigour and fruit yield (POMASA, 2013). Mashavhathskha (2014) mentioned that pomegranates flourish in heat, however, to reach optimal yield and fruit quality, regular irrigation is required throughout the dry season. Commercial pomegranate orchards can be irrigated using micro sprinklers; however, drip irrigation is normally recommended (POMASA, 2013). Drip irrigation positively affects pomegranates parameters such as tree height, stem diameter, fruit yield and fruit weight (Sulochanamma et al., 2005; Shailendra and Narendra, 2005). Regular water supply via a drip irrigation system is necessary for sustainable pomegranate production and reduces fruit splitting (Prasad et al., 2003).

The irrigation must be managed very well particularly in summer, since excessive moisture can increase vegetative growth with softer fruit, resulting in poor fruit quality after harvest (POMASA, 2013). Fruit produced under high summer rainfall conditions tend to be soft and has poor shipping and storage quality (LaRue, 1980)**.** Correct irrigation scheduling developed according to specific soil and climatic conditions in the orchard is necessary (POMASA, 2013). Irrigation scheduling can be monitored by water budget calculations, soil moisture status, probes and tensiometers (Day and Wilkins, 2011). A general guideline for irrigation water requirements of pomegranate trees is 15 m^3 $ha^{-1}day^{-1}$ in the spring and 50 m^3 ha^{-1} day^{-1} in the summer (POMASA, 2013). The estimated total amount of water per season is about 6000 m^3 ha^{-1}. Volschenk and Mulidzi (2020) conducted a scoping study to understand pomegranate orchard water use in Bonnievale, Wellington, Gouda and Wolseley in Western Cape of South Africa. Irrigation water applied to full bearing 'Wonderful' pomegranate orchards as from the first week of September until the end of May ranged from 237 to 834 mm in 2017/18 and 272 to 867 mm in 2018/19 season. Bonnievale (688 to 775 mm) had on average the highest amount of water applied for both seasons, followed by Gouda (426 to 492 mm), Wolseley (385 to 456 mm) and Wellington (243 to 246 mm). The water use efficiency (yield divided by sum total of irrigation applied and effective rainfall, according to Fernández et al., 2021, irrigation water productivity) was ranging from 36.6 to 85.9 kg ha^{-1} mm^{-1} in 2017/18 and from 22. 4 to 73 kg ha^{-1} mm^{-1} in the 2018/19 season (Volschenk and Mulidzi, 2020). Bonnievale had in the two respective seasons, compared to the group mean, the highest irrigation water productivity and best relative economic irrigation water productivity (90 and 80%), as compared to Wellington (54 and 68%), Gouda (35 and 59%) and Wolseley (56 and 36%). The economic irrigation water productivity was based on gross farm income divided by the sum total of irrigation applied and effective rainfall.

Ayars et al. (2017) found in California (USA) higher water productivity (yield per ha divided by mm applied water) for subsurface compared to surface drip irrigated pomegranate trees and concluded it was due to higher yield and less water applied to the subsurface irrigated trees. The water productivity for four, five and six-year-old trees was for the subsurface drip 60.4, 61 and 59.7 kg ha^{-1} mm^{-1} and for the surface drip irrigated trees 51.5, 53.5 and 55.8 kg ha^{-1} mm^{-1}. According to Intrigliolo et al. (2013), deficit irrigation in Spain increased irrigation water use productivity (fruit yield divided by irrigation applied + rainfall) of 'Mollar de Elche' pomegranate trees in the sustained deficit irrigation treatment (59.6 kg ha^{-1} mm^{-1}) and where regulated deficit irrigation was applied during flowering and fruit set (48.9 kg ha^{-1} mm^{-1}) relative to the control (39.5 kg ha^{-1} mm^{-1}). In Iran, Parvizi et al. (2014) reported water productivity (fruit yield divided by water used) of 4.2 kg m^{-3} (average over two seasons) for cultivar 'Rabab' trees irrigated at 100% ET_c whereas seven-year-old 'Shavar' pomegranate trees (Selahvarzi et al., 2017) had water productivity (fruit yield divided by water applied) of 2.15 and 2.45 kg m^{-3} in two consecutive seasons. In Turkey, water use efficiency (yield divided by evapotranspiration, definition according to Fernández et al., 2020, water use productivity) of several irrigation treatments ranged between 28 and 46 kg ha^{-1} mm^{-1}. Irrigation water use efficiency (yield divided by irrigation applied) ranged between 59.5 and 106.6 kg ha^{-1} mm^{-1} (Dinc et al., 2018).

Pomegranate irrigation requirements can be estimated using the daily crop reference evapotranspiration (ETo), as calculated using the Penman-Monteith equation (FAO method), a crop factor based on the time of the year and the percentage of ground area shaded by the tree canopy (Meshram et al., 2012). Volschenk (2020) mentioned that the 'Wonderful' pomegranate cultivar tends to have lower crop coefficient values than grapevine, peach and other deciduous fruit at comparable canopy cover. However, the difference between these crop coefficients is caused by the following factors: orchard slope, light interception, shaded areas, differences in methods used to measure ET_o, cultivation practices and irrigation scheduling (Williams and Ayars, 2005). Providing sufficient irrigation throughout the season until the harvest is essential to minimising the chances for fruit cracking (POMASA, 2013). According to LaRue (1980) adequate soil moisture must be maintained throughout the growing season to minimise fruit cracking. The cultivar 'Wonderful' is prone to cracking, which cause significant production losses (Chater and Garner, 2018). Fruit cracking is caused by excessive or irregular

irrigation, which lead arils to swell and cause the rind to crack during fruit maturation (Holland et al., 2009). There is little irrigation required for pomegranates trees after harvest (Holland et al., 2009).

The pomegranate tree shows high adaptability to water deficit due to its ability to tolerate drought. However, to reach optimal vegetative growth, yield and fruit size, the tree requires regular irrigation throughout the season (Cano-Lamadrid et al., 2018). Laribi et al. (2013) noted that trees subjected to deficit irrigation with mild water stress during flowering and fruit set and more severe stress during the linear phase of fruit growth and ripening gave a redder peel and juice with a higher level of total soluble solids. For some cultivars, application of water deficit during flowering and fruit set may increase aril red colour without negatively affecting the marketable yield, fruit size and chemical composition (Volschenk, 2020).

2.4 METHODS FOR DETERMINING ORCHARD WATER USE

This section of the knowledge review focussed on methods that can be used to determine transpiration and evapotranspiration directly, or to estimate orchard water use utilizing a modelling approach. Since the sap flow technique has not previously been used to determine transpiration of pomegranate trees, a literature review on research regarding sap flow methods in fruit trees was appropriate. Important background information regarding the soil water balance and crop coefficients available for pomegranate trees applicable to the modelling approach are included as well.

2.4.1 Sap flow

2.4.1.1 Description and comparison of methods

González et al. (2008) compared five methods used to determine sap flow in peach trees: compensation heat pulse (HortScience, New Zealand and Greenspan, Australia), non-compensation heat pulse (Ariel, Israel), Stem heat balance (SHB, Dynamax, USA) and heat dissipation (HD, Granier, France). González et al. (2008) found that - amongst these systems - the New Zealand compensation heat pulse was the most sensitive to determine water stress. González et al. (2008) considered the HD method unreliable to estimate transpiration, since sap flow was only determined in a single point in the radial profile. It determined water stress quite accurately though and gave a similar daily pattern as the other methods. Sap flow rate determined using the non-compensation heat pulse, compensation heat pulse and SHB gave similar patterns on an hourly and daily basis and correlated well to daily ET_O. However, there was large sap flow value differences between the methods. Sap flow registered during the night was low in all methods. González et al. (2008) concluded that the compensation heat pulse system from New Zealand and SHB seemed to be the most reliable. Selected sap flow methods for different stems and sizes are summarized below in Table 2.

Table 2. List of sap flow methods, suitable type of stem and stem size range (Smith and Allen, 1996)

Method	Type of stem	Size range (mm)	Manufacturer	Dedicated data logger
Stem heat balance	Woody or herbaceous	2-125	Dynamax Inc. 10808 Fallstone, Houston, USA	No
Trunk sector heat balance	Woody	>120	Ecological Measuring Systems	Yes
Heat pulse	Woody	>30	HortResearch, New Zealand	Yes
Thermal dissipation	Woody	>40	UP GmbH Germany	No

Stem heat balance (Dynamax, USA) (SHB)

The SHB method can be used to determined sap flow in woody and herbaceous crops (Steinberg et al., 1989). The SHB uses Dynamax gauges (models SGA10, Dynamax inc., Houston, TX, USA) to determine sap mass flow rate (Baker & Van Bavel, 1987). The gauges fit around the stems with diameters ranging between 2-124 mm (Sam, 2016). González et al. (2008) installed eight gauges per peach

tree on a linear portion of branches 8 to 15 mm in diameter. The system was installed on one branch per tree for five stressed trees and a control. Gauges were connected to a data logger (CR7, Campbell Scientific, logan, UT, USA). Sap flow was determined in every 30 minutes per unit stem diameter. Sap flow on a leaf area basis per tree was calculated by measuring total leaf area of each branch containing SHB gauges. González et al. (2008) reported that the accuracy of the SHB method was highly affected by the exposure of the selected branch and size of the stem diameter.

Compensation Heat pulse method

Liu et al. (2015) conducted a study to improve an evapotranspiration model for an apple orchard in North Western China using a heat pulse method. The sap flow, soil water balance and microlysimeter method were used to estimate total evapotranspiration rates for the growing season. Trunk sap flow was monitored every 30 minutes using compensation heat pulse sap flow sensors (Model SF100, Greenspan Technology Pty Ltd, Warwick, Australia) consisting of one heated probe and two unheated probes. Two sets of heat pulse probes were installed on the trunk at depths of 1.5 and 2.0 cm on the east and west sides. Sap flow measurements were taken at random on six trees with stem diameters of between 178 and 235 mm. The transpiration was determined from the measured sap flux using the equation below (Liu et al., 2015):

$$SF=1000X\frac{SF0}{SA}. \quad \text{[Eq.1]}$$

Where S_A is the area of the plot (mm^2), SF ($mm\ d^{-1}$) and SF_0 ($L\ d^{-1}$) are the sap velocity and original sap flux, respectively. Sap flow sensor calculation software (version 2.53, Greenspan Technology) was used to determine SF_0.

Saitta et al. (2020) compared orange orchard evapotranspiration using eddy covariance, sap flow and FAO-56 methods. The heat pulse velocity (HPV) method was used to continuously measure water consumption in two trees per irrigation treatment. The HPV method was also used to measure the temperature change (ΔT) in two probes installed asymmetrically into the tree trunk. Each probe contained one 4 cm sensor with two embedded thermocouples. The probe was wired to a data logger (CR 1000, Campbell Sci., Logan, Utah) for measurement of heat pulse in every 30 minutes sampling intervals. Saitta et al. (2020) reported that the HPV sap flow method detected effects of water deficit at different irrigation levels well. Steppe et al. (2010) compared the accuracy between compensation heat pulse velocity (HPV), heat field deformation (HFD) and thermal dissipation (TD) installed radially into a stem segment (Figure 2). For the HPV system, xd and xu represent the distances between the heater and the downstream and upstream needle of the HPV sensor. According to Green (1998), the distance between upstream needle and the heater position is 0.5 mm while the distance between downstream needle and heater position is 5 cm. Steppe et al. (2010) reported that, after applying a wound correction, HPV was more accurate than the HFD and TD methods.

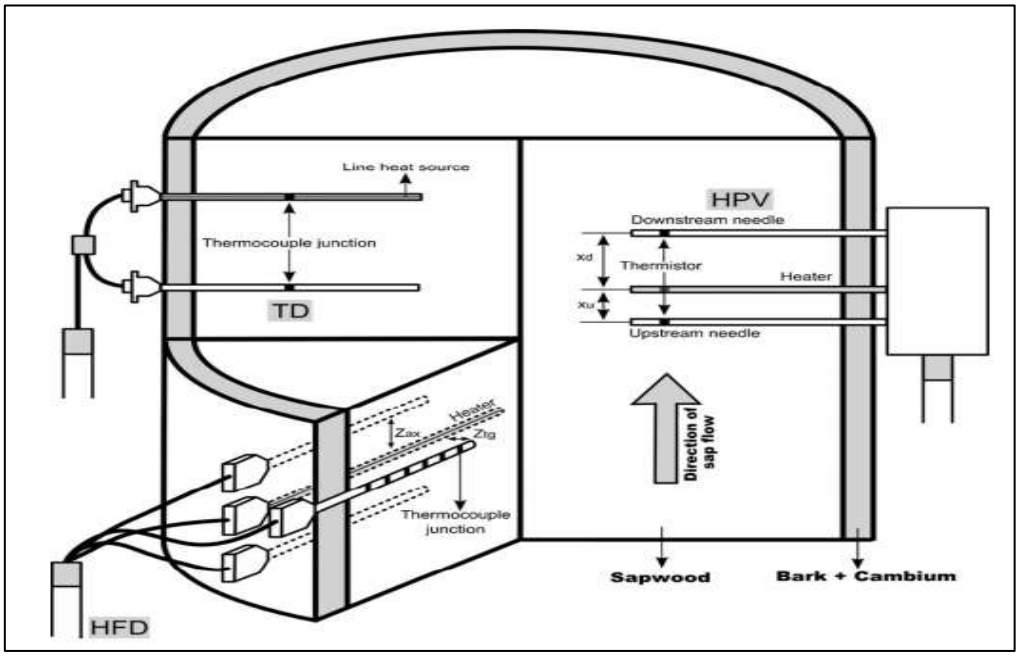

Figure 2. Illustrate heat pulse velocity (HPV) sensor, the thermal dissipation (TD) sensor and the heat field deformation (HFD) sensor, installed radially into a stem segment (Steppe et al., 2010).

Heat Field Deformation method (HFD)

The HFD equipment includes three 1.6 mm diameter needles and a heater as shown at the bottom left in figure 1 (Steppe et al., 2010). Sap flux density at each thermocouple junction position is determined using the following equation:

$$SFD_{HFD}=3600D\frac{K+dTsym-dTasym}{dTasym}\ X\ \frac{Zax}{ZtgLsw}\ (cm^3\ cm^{-2}h^{-1}) \quad [Eq.2]$$

Where D is the fresh wood thermal diffusivity, K is the dT_{sym} – dT_{asym} absolute value under zero sap flow (°C) conditions, dT_{sym} is the difference of temperature between the axial thermocouple junctions (°C), dT_{asym} is the temperature difference between the tangential thermocouple junctions (°C). Zax and Ztg represents the distances between the heater and the upper junction of the axial and tangential thermocouple of the HFD sensor (Fig. 1) and L_{sw} is the depth of sapwood (cm).

Heat ratio method (HRM)

HRM is a heat pulse method that has two equidistant temperature sensor probes set upstream and downstream and a central heater needle as shown in Figure 3 (Burgess et al., 2001). The velocity (V_h) of the heat pulse is determined from the temperature ratio between the two temperature sensor probes, the sapwood thermal diffusivity and the distance as shown in the following equation:

$$V_h=\frac{k}{x}\ln\left(\frac{v1}{v2}\right)3600 \quad [Eq.3]$$

Whereby k is the thermal diffusivity of green wood, x is the distance (cm) between the heater and the sensor probes (Burgess et al., 2001). The $V_1$and V_2 are temperature increases from initial temperatures at in between upstream and downstream needle, from the heater probe. The x is equal to 0.6 cm as probe is positioned at 0,6 cm downstream and upstream from the heater probe. According to Marshall (1958), k has an allocated normal value of 2.5 x 10^{-3} $cm^2\ s^{-1}$. Sap flux density (u) can be obtained by converting heat pulse velocity (V_h) using the following equation:

$$u=\frac{pb}{ps}\left(mc+\frac{cw}{cs}\right).V_h \quad [Eq.4]$$

where p_b is the dry sapwood density (g cm^{-3}), p_s the sap density (assumed to be the density of water), m_c is the fresh sapwood water content, c_w is the dry wood matrix specific heat capacity (1200 J kg^{-1} $°C^{-1}$ at 20 °C) and c_s is the sap specific heat capacity (4.186 J g^{-1} K^{-1}) (Sam, 2016).

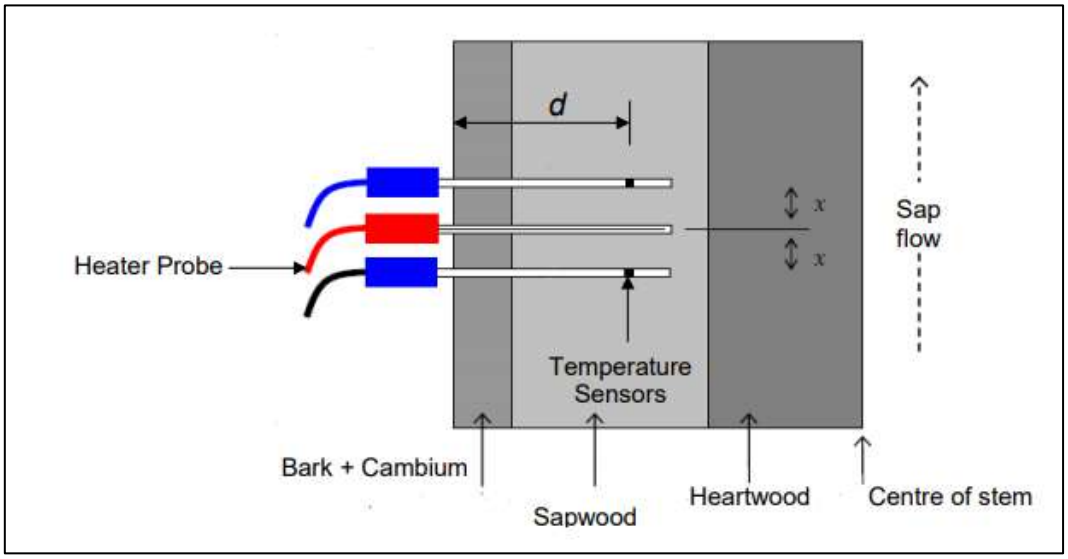

Figure 3 Diagram of a probe set used for HRM sap flow measurements using the heater probe, upper (downstream) and lower (upstream) temperature sensors (Mahohoma, 2016).

Thermal dissipation probes (TDP)

The TDP method was developed to measure sap flow in trees by Granier (1985). The TDP method contained two 2 mm diameter cylindrical probes installed into the trunk about 10 cm apart. Sap flux density can be calculated using the measured temperature difference as follows:

$$u = a\left(\frac{\Delta Tmax - \Delta T}{\Delta T}\right)^b \ (m^3\ m^{-2}\ s^{-1}) \quad \text{[Eq.5]}$$

here ΔT is the measured temperature differences and ΔT_{max} is the maximum temperature difference between the needles recorded at zero flux. a= 118.99 x 10^{-6} ($m^3\ m^{-2}\ s^{-1}$) and b=1.231.

Zhang et al. (2013) conducted a study to characterise water, energy and carbon fluxes of irrigated pear orchards in the North China Plain. Sap flow was determined using TDP (Thermal Dissipation Probe, TDP30-FLGS-TDP XM1000, Dynamax, USA) based on the liquid velocity heat dissipation theory and the data logged using a CR1000 data logger (Campbell Scientific, logan, UT, USA). Sap flow measurements were taken in three randomly selected replicate trees. The sap flow rate (Fs, $cm^3\ h^{-1}$) was calculated as follows:

$$Fs = As \times V \times 3600 \text{ (Granier, 1985)} \quad \text{[Eq.6]}$$

Where *As* is the cross-sectional area of sap conducting wood (cm^2); *V* is the average sap velocity (cm s^{-1}). The sapwood area was calculated by subtracting the heartwood area from the trunk cross sectional area. Trees were cut in the orchard adjacent to the plots and ten trees were selected to measure the cross-sectional area. The average sap velocity was determined as follows:

$$V = 0.0119 \times K^{1231} \text{ and } K = \frac{dTM - dT}{dT} \quad \text{[Eq.7]}$$

where dT (^OC) is the measured temperature difference between that of heated needle and the upstream reference needle. The dT value is determined from the differential voltage measured between the upper and lower thermocouple. The dTM value is the dT value when there is no sap flow. The dTM in this study was equal to 3.23 °C.

Tie et al. (2017) also used thermal dissipation probes (TDP) to measure sap flow. They found that the main factor controlling sap flow was meteorological i.e. photosynthetically active radiation and noticed that sap flow decreased to nearly zero in the middle of November when there were no leaves remaining on the trees. Moreover, Leaf Area Index determined the range and the upper boundary of sap flow, while the environmental factors caused sap flow fluctuations within the upper bound. Rana et al. (2019) used TDP and Flux-Variance Similarity (FVS) method to measure transpiration in vineyards. FVS is a method for separating water fluxes into transpiration and evaporation (Rana et al., 2019). The TDP method largely underestimated hourly transpiration in the central part of the day from 9:00 to 16:00. The TDP values were much lower than the FVS values when evaporative demand of the atmosphere was high. ICT International compared HRM and TDP methods as shown in Tables 3 and 4 below. The advantages and disadvantages of different sap flow methods are shown in Table 5.

2.4.1.2 Calibration requirements

There are several ways of testing sap flow accuracy such as using weighing lysimetry, cut trees methods, micrometeorological methods and stem perfusion (Sam, 2016). The HPV or TDP method sap flux density and actual sap flux density determined gravimetrically can be used for sap flow calibration (Sam, 2016). Fuchs et al. (2017) used sap flux density to calibrate TDP, HRM and HFD methods. Table 4 below summarizes sap flow calibration methods applied to different crops or species. Mahohoma (2016) calibrated the HRM method using eddy covariance measurement of transpiration in a Delta orange orchard. The eddy covariance method was successfully used to calibrate the HRM method for a drip irrigated field, when evaporation was considered to be negligible. This calibration was done twice for a period of nine months and wound width stayed constant. Green et al. (2003) mentioned that wound width is an important physical factor that can affect the accuracy of the heat pulse measurements. Mahohoma (2016) stated that a single virtual wound width gave good correlation between ETc and transpiration and suggested that a single calibration using this method may be enough for long-term transpiration measurements. Virtual wound width is determined by chiselling a piece of wood and cut transverse to measure a wounding width as shown Figure 4 (Mahohoma, 2016). Green et al. (2003) used lysimetry to calibrate T-max heat sap flow measurements and stated that measurements were always in good agreement with the actual transpiration losses.

Table 3 Comparison of the Heat Ratio Method (HRM) and Thermal Dissipation Probe (TDP) sap flow measurement method characteristics (ICT International Pty Ltd, 2014)

Requirement	HRM	TDP
Measurement units	Heat Pulse Velocity cm hr^{-1}, Sap Velocity cm hr^{-1}, Sap Flow g hr^{-1}	Sap Flux Density cm^3 hr^{-1} cm^{-2}
Measurement range and accuracy	-20 to 60 cm hr^{-1} and 0.1 cm hr^{-1} (Corrected Sap Velocity)	4 to 40 cm hr^{-1}
Measurement resolution	0.01 cm hr^{-1} (Corrected sap velocity)	0.1 (MV)
Measures low and high flow	Yes - very accurately between 0 to -20 cm hr^{-1} (at 0.01 cm hr^{-1} resolution) and very accurately between 10 to 60 cm hr^{-1} (at 0.01 cm hr^{-1} resolution	No- just measured minimum velocity of about 4 cm hr^{-1}
Measures reverse flow	Yes - very accurately between 0 to -20 cm hr^{-1} (at 0.01 cm hr^{-1} resolution)	No
Measures multiple radial points	Yes - with two independent measurement points in the same radial profile, spaced 15 mm apart. This can be used to characterise flow in the inner and outer xylem	No
	Application	
Used on large diameter stems	Yes - for trees of any diameter but restricted to those with shallow sapwood (40 mm) or for the outer 40 mm of xylem (sapwood). By using a 35 mm long needle with two measurement points flow can be accurately characterised in both the inner and outer xylem making the measurement more accurate by being able to correct for the radial variation across the sapwood. For species that have a larger sapwood thickness or where an accurate radial profile is required it is recommended to use the Heat Field Deformation (HFD) multipoint sap flow instrument.	Yes - But, only for the outer 20 mm of xylem
Used on small diameter stems	Yes - any woody stem larger than 10 mm diameter is suitable	No - The sensor needle must be fully inserted in sapwood otherwise large errors occur due to Natural Thermal Gradients (NTG) which cannot be measured
Used on roots	Yes - The HRM has facilitated the understanding of phenomenon such as hydraulic lift and hydraulic redistribution in root systems of trees during times of drought	No

Table 4 Comparison of sap flow measurement principles for the Heat Ratio Method (HRM) and Thermal Dissipation Probes Method (TDP) (ICT International Pty Ltd, 2014)

Requirement	HRM	TDP
Is wound response accounted for?	Yes	No
Is wound response relevant?	Yes - all species occlude cells and repair intrusive wounds which causes a non-conductive zone of tissue that affects heat transfer and ultimately measurement sensitivity and accuracy if not taken into account and corrected for processing of raw data	No
Heat Source	Heat Pulse	Continuous
Requires radiation shielding	No - The time required for the heat pulse and the measurement to be completed is so short (100 seconds) no significant changes in ambient air temperature or effects of direct incident radiation will occur that can affect the measurement	Yes - Requires extensive thermal and radiation shielding both around the sensor and distances of between 50 cm to 1 m above and below the sensor to be insulated. Preferably all the way to the ground level and if possible, covering of the surrounding root area on the ground.
Is the technique affected by Natural Thermal Gradients (NTG)?	No	Yes - The use of high energy input can be used in an attempt to overcome this problem but causes other problems like increased wounding and requires needle spacing's to be significantly increased (by a factor of 3) to establish a difference in temperature between the two needles however, this dramatically reduces the sensitivity of the measurement increasing the amount sap velocity is either underestimated or overestimated
Does sensor need to be inserted only in sapwood?	No - multiple measurement points enable measurement of radial gradient and determination of sapwood/heartwood border should the needles extend beyond the sapwood into heartwood.	Yes - it is crucial to the fundamental principle that the entire length of the needle be completely inserted in sapwood and sapwood only. If the needle extends into the heartwood or non-conducting xylem sap velocity will be grossly underestimated anything up to 50 % error. Conversely, if any amount of needle is located in bark or air then the sap velocity can be grossly overestimated by indeterminate amounts rendering the data useless
Can the sensor needle be located in air when used with small diameter stems?	Yes - the end measurement point or inner measurement point can be turned off if sitting in air	No
Do Heat Storage lags affect the measurement?	No - A short heat pulse is generated for each measurement eliminating the effect of ambient thermal conditions.	Yes - Because it is a continuously heated sensor

Table 5 Advantages and disadvantages of sap flow methods as adapted from Sam (2016)

Methods	Advantages	Disadvantages
Heat pulse	*Compensation heat pulse* -Low power requirements -One gauge can be used on plants with widely different stem diameters -The data is produced in electrical signal form suitable for processing or stored on the data logger -Natural temperature gradients in the sapwood does not affect measurement accuracy -Simple and reliable instrumentation	*Compensation heat pulse* -Unable to measure very low and very high densities (< 5 cm^3 cm^{-2} h^{-1} and > 100 m^3 cm^{-2} h^{-1}) -Drilling of holes for sensor installation may cause a damage, which can be accounted by using wounding correction coefficient -Accuracy depends on correctness of sensor spacing during installation -Requires species-specific calibration
	Heat ratio method -The heat ratio method is more successful at measuring low flows -Measures reverse sap flow -Low power requirements and user friendly -The data is produced in electrical signal form suitable for processing or stored on the data logger -Natural temperature gradients in the sapwood does not affect measurement accuracy	*Heat ratio method* -High flow rates affect heat ratio method (> 45 cm^3 cm^{-2} h^{-1}) -Drilling of holes for sensor installation may cause a damage, which can be accounted by using wounding correction coefficient -Accuracy depends on correctness of sensor spacing during installation -Requires species-specific calibration
Thermal dissipation	-User friendly, affordability and predictable power consumption than heater tracer methods -Allows use in large diameter trees -Can be used for low, average and high sap flux densities (-0-80 cm^3 cm^{-2} h^{-1})	-High power requirement -Does not detect reverse flow -Requires species-specific calibration -Drilling of holes for sensor installation may cause damage -Natural temperature gradients in the sapwood negatively affect measurement accuracy

According to Smith and Allen (1996) calibration of heat pulse methods is required for wood species. Aboukhaled et al. (1982) reported that weighing lysimeters are the most accurate and simple method for estimating evapotranspiration. Calibration using the cut tree method requires cutting through the stem of a whole tree (Sam, 2016). After cutting the tree stem, the bottom side of the stem should be shaved to get rid of embolisms and then placed in a container with water, covered with a plastic to avoid evaporation as shown Figure 5. The container can be placed on a weighing balance to record mass loss or to record the volume of water transpired (Knight et al., 1981). According to Sam (2016) one of the advantages of this method is to give direct transpiration measurements for the whole tree and a dye can be added to the water for the sapwood area determination. However, if there is any mistake following the cutting, the tree may only survive for 24-48 hours. Sam (2016) concluded that the stem perfusion method is an accurate technique to calibrate the different sap flow methods for different species and allows measurement of other parameters such as sapwood density and water content, sapwood area, specific heat capacity of the woody matrix and specific heat capacity of the sap. Stem perfusion in a laboratory is a favoured method for sap flow calibration as its advantage is that it permits sap flux density comparison measured by the sap flow technique with that determined gravimetrically. Ferrara. et al (2021) used the heat pulse method to estimate sap flow on a mature pomegranate orchard in Spain. The soil water balance was used to calibrate sap flow determination using capacitance probes. The Heat pulse method give direct plant transpiration estimates which can be easy automated and allows for continuous long term records. It is therefore a method preferred for measuring sap flow in pomegranate orchards.

Table 6 Illustrating sap flow methods and calibration methods that were used in literature for different species (Sam, 2016)

Method	Calibration method	Species	Reference
Thermal dissipation	Weighing lysimeter, stem perfusion	Persimmon, apple, Nectarine	Paudel et al., (2013)
Thermal dissipation	CUT tree/ potometer	Citrus *maxima*	Isarangkool et al., (2010)
Compensation Heat pulse	Stem heat balance	*Populous trichocarpaxdeltiodes*	Hall et al., (1998)
Heat ratio	Weighing lysimeter	*Eucalytus marginata*	Burgess et al., (2001)
Stem heat balance	Weighing lysimeter	Peach	Shackel et al., (1992)
Heat ratio	Eddy covariance	Olive	Williams et al., (2004)
T-max	Stem perfusion	*Populous alba*, Citrus: *Platanus orientalis*	Cohen et al., (1981)

Figure 4 Determining the virtual wound width on a piece of wound cut crosswise from the tree trunk (Mahohoma, 2016)

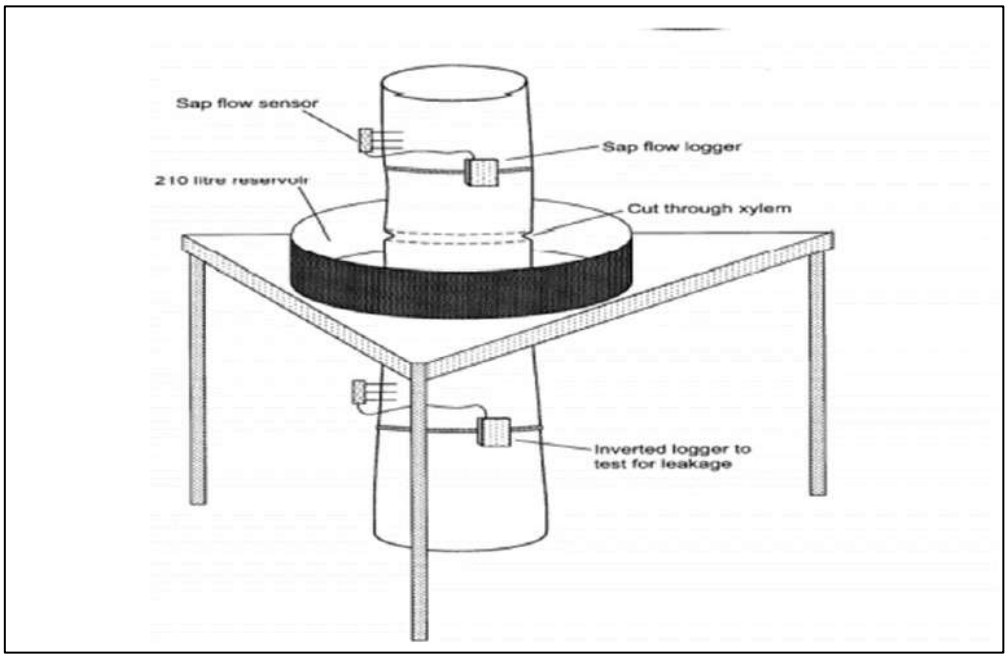

Figure 5 Calibrating sap flow methods using cut tree method (Vertessy et al., 1997)

Sam (2016) calibrated heat ratio, compensation heat pulse and thermal dissipation methods using the stem perfusion method for four different citrus tree species. Calibration using the stem perfusion method was conducted in a laboratory to force water into a stem section where probes are inserted as shown in Figure 6 (Fernández et al., 2001; Steppe al., 2010).

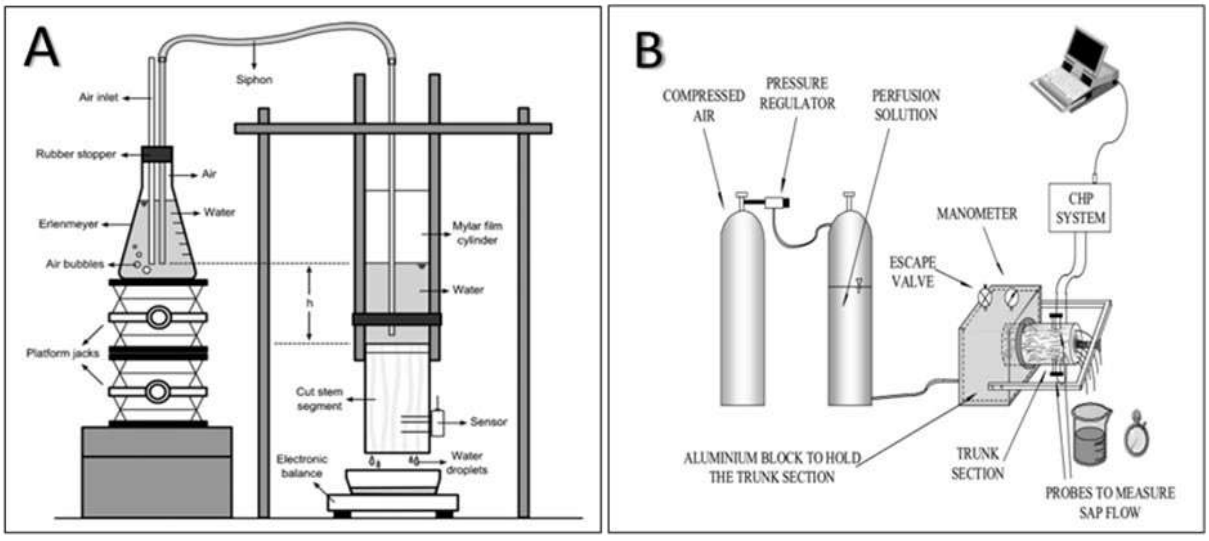

Figure 6. Stem perfusion laboratory setup to calibrate sap flow systems (Fernández et al., 2001). Image A shows a schematic diagram of the Mariotte's principle (Steppe et al., 2010). While image B, shows a special high-pressure device that forces water through stem section (Fernández et al., 2001)

2.4.1.3 Relevance of wood anatomy for measurements

Sam (2016) recommended that xylem anatomy must be taken into account in each new species or orchard where measurement will be made since it has a large influence on measurements. McCulloh et al. (2010) compared hydraulic conductance in branches and trunks of ring porous, coniferous and diffuse porous trees from temperate and tropical forest. The trees varied in their xylem anatomy and ring porous trees showed the highest increase in stem conductivity with stem size (McCulloh et al., 2010). Granier et al. (1994)

studied axial water flow in the trunks of oak trees using sap flowmeters, water absorption from a cut trunk, heat pulse velocity (HPV) and thermo-imaging. It was concluded that sap flow occurs mostly in the outermost ring, where the large early wood vessels are functional. However, inner rings take over if the early wood vessels are disrupted or attacked by factors such as frost, pathogens or mechanical damage (Granier et al., 1994).

Berdanier et al. (2016) used models to predict radial sap flux variation in coniferous, diffuse porous and ring porous temperate trees. The radial sap flux density was dependent on wood type; however, the tree size was independent. The older xylem tends to be less conductive progressively as tree size increase and the newer xylem carry out functions similarly to the former outer xylem (Berdanier et al., 2016). Mahohoma (2016) found during anatomical assessment of citrus wood that the xylem is not thermally homogeneous, therefore, anatomy assessment is required to be done for sap flow measurements. In contrast, the thermal dissipation method parameters do not require wood anatomy or tree characteristics to determine volumetric sap flux density (Granier et al., 1990). However, for methods such as the heat pulse method, wood anatomy measurements are required for species that are not thermal homogeneous (Smith and Allen, 1996).

Smith and Allen (1996) used laboratory method and the excised-branch method on an *Azadirachta indica* A. to validate heat pulse method. The results showed that the heat-pulse method significantly underestimated the flow rates. This inaccuracy was caused by the thermal inhomogeneity from the thickness of interstitial tissue between xylem vessels (Smith and Allen 1996). Mahohoma (2016) noticed damage done by drilling and constant heating in the citrus sap wood as shown in figure 7. Blocked xylem elements in the drilled hole, discolouration of ray cells, vessels blocked with gum and phenols were also observed. The drilling and heating effects ended up extending wound width beyond 2 mm. Barrett et al. (1995) stated that total wound width may extend by 0.3 mm on either side of the drill hole, therefore, a wound correction of 1.8 + 2 X 0.3 mm may be appropriate for a 1.8 mm diameter drill hole.

Figure 7. D**iscolouration due to drilling and constant heating in sap wood (Mahohoma, 2016)**

Lopez-Bernal et al. (2014) performed anatomical observations in the wood to measure thermal properties in order to heat pulse sap flow probes and found differences in anatomical traits, water content and water potential. Lopez-Bernal et al. (2014) stated that the heat pulse sap flow method accuracy is highly affected by sapwood thermal properties and water content variations. Fernández et al. (2006) conducted a study on the relationship between xylem anatomy and sap flow using the compensation heat pulse method in olive, plum and orange trees. The results showed that xylem anatomy differs between these three crops. Plums had greatest total lumen vessel area while oranges had larger and fewer xylem vessels than olive and plum as shown in Table 7 below. The heat pulse velocity (HPV) method gave accurate values of sap flow on a virtual wound width of 2.0 mm for olive and 2.4 mm for plum and orange (Fernández et al., 2006).

Table 7 Xylem vessel anatomy variation of olive, plum and oranges (Fernández et al., 2006)

Crop	Depth (mm)	Lumen diameter(µm)	Distance between groups vessels (µm)
Olive	5	40.3±4.5	102.9±33.1
	25	36.9±4.6	126.9±36.8
Plum	5	45.4±4.9	81.9±21.5
	25	44.8±2.9	80.1±20.3
Oranges	5	83.9±13.6	280.1±60.3
	25	79.5±11.4	340.7±133.8

2.4.1.4 Data processing requirements

The sap flow data for the heat ratio and compensation heat pulse methods are generated via electrical signals suitable for processing and stored on a data logger (Sam, 2016). Table 8 compares data processing requirements for the HRM and TDP method as summarized by ICT International Pty Ltd.

2.4.2 Soil water balance

The soil water balance can be used to determine evapotranspiration through measuring various components of the soil (Allen et al., 1998). This soil water balance method assesses the incoming and outgoing water flux into the root zone over a period of time (Figure 8). Allen et al. (1998) expressed the daily soil water balance as follows:

$$D_{r,i} = D_{r,i-1} - (P\text{-}RO)_i - I_i - CR_i + ET_{c,i} + DP_i \quad \text{[Eq.8]}$$

Where $D_{r,i}$ is a root zone depletion at the end of day i (mm), $D_{r,i-1}$ is the water content in the root zone at the end of the previous day i-I (mm), P_i precipitation on day i (mm), RO_i is the runoff from the soil surface on day i (mm), I_i net irrigation depth on day i that infiltrates the soil (mm), CR_i capillary rise from groundwater Table on day i (mm), $ET_{c,i}$ crop evapotranspiration on day i (mm) and DP_i is the water loss out of the root zone by deep percolation on day i (mm).

Bhantana and Lazarovitch (2010) conducted a study to determine the response of young pomegranate tree growth and evapotranspiration to irrigation with saline water. The study was conducted using lysimeters with the pomegranate cultivars 'Wonderful' and 'SP-2' at the Jacob Blaustein Institutes, Sede Boqer Campus, the Ben-Gurion University of the Negev, Israel. Fifty 0.2 m^3 lysimeters were installed and the 'Wonderful' and 'SP-2' trees were transplanted into the lysimeters in February 2007. Irrigation was automated while drainage water collected manually. A weekly soil water balance, providing evapotranspiration (mm) data for each lysimeter, was determined using the following equation.

$$ET = I - Dr + \Delta\theta D \quad \text{[Eq.9]}$$

Where I is the irrigation (mm), Dr is the drainage, $\Delta\theta D$ is the stored root-zone water change of a root zone depth and D is the depth (mm).

Table 8. Comparison of data processing and analysis and data logging properties for the HRM and TDP Method of Sap Flow Measurement (ICT International Pty Ltd, 2014).

Requirement	HRM	TDP
	Data processing and analysis	
Calibration method	Use of specific wood properties and wound coefficients to convert heat pulse velocity data to corrected sap velocity (cm hr^{-1}) and sap flow (gm hr^{-1})	Utilises an empirical calibration however, detailed data corrections for dTMax are required using extensive modelling of data to achieve approximations of sap flow. These are not accurate direct measurements
Raw data processing required	No - Raw units measured are Heat Pulse Velocity in cm hr^{-1}	Yes - conversion from analogue microvolts to temperatures then apply empirical calibration conversion to sap velocity (cm hr^{-1}).
Software	Yes - 3D graphics software with user interface for entering and adjusting tree specific wood properties	No - Excel Spreadsheet
	Data logging	
Data output	Raw Heat Pulse Velocity (cm hr^{-1}) Corrected Sap Velocity (cm hr^{-1}) Corrected Sap Flow (gm hr^{-1})	Temperature difference (Millivolts or ^{o}C)
Temporal logging resolution	Minimum 10 minutes - This is to ensure all heat input from the previous measurement has been fully dissipated through the xylem within the measurement zone to prevent any compounding on heat which may affect subsequent measurements. Optional resolutions of 15, 20, 30 and 60 minutes for long term deployments	Minimum 1 minute but the large quantity of data becomes cumbersome and exhibits greater "noise". Typical logging resolution is 15 minutes to 60 minutes
Number of sensors per logging system	100	32 (with Multiplexer)
Stand-alone logging capability	Yes	No
USB Communications	Yes	No
Memory capacity	2 GB Standard expandable to 32 GB	None
	Power	
Internal battery	12 V lithium 900 mA Hr	None
Internal voltage regulation	Yes	None
24 Hr Power consumption	0.49 Amps @ 10-minute temporal resolution	1.92 Amps @ 10-minute temporal resolution
Number of days battery back-up without solar charging for 16 sensors on an 85 Ahr 12 V battery	10.75 Days	2.75 Days

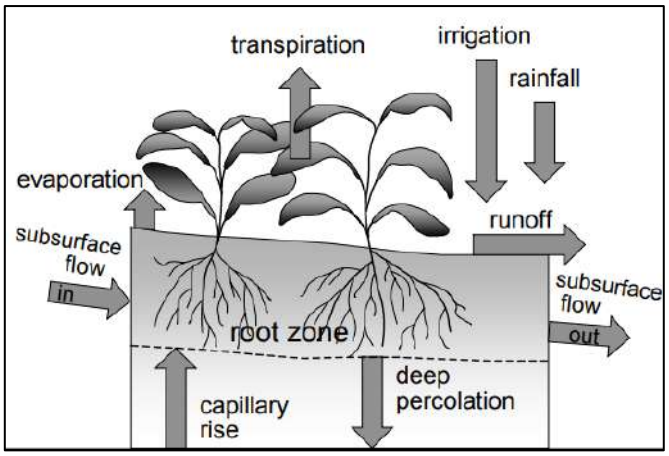

Figure 8 The various components of soil water balance method to measure the evapotranspiration (Allen et al., 1998). The rainfall, irrigation, capillary rise and subsurface flow are the input components (supplying water to the root zone). While transpiration, evaporation, runoff, subsurface and deep percolation are output components (removing water out of the root zone) (Allen et al., 1998)

Liu et al. (2015) used time domain reflectometry (Trime-Pico IPH/T3, IMKO GmbH, Ettlingen, Germany) to measure soil volumetric water content continuously for three randomly chosen apple trees. Four tubes of 180 cm depth were installed at different distances from the tree and the soil water content measured in 10 cm soil layer increments every five days at each tube in the vertical profile. The oven-drying method was used to calibrate the measured soil water content in every month. Three soil samples were collected using a 5 cm diameter soil auger from 50 to 150 cm away from the tubes for the 10 to 180 cm soil profile at 10 cm vertical intervals. The soil samples were weighed and dried for 8 hours. The evapotranspiration (ET) was estimated using soil moisture measurements based on the soil water balance equation. The total ET was calculated between the two measurements as follows:

$$ET = P + I - R - \Delta W \quad \text{[Eq.10]}$$

Where P is the effective precipitation (mm), I is the irrigation amount (mm), and R is water loss through deep seepage and runoff beneath the 2m soil zone (considered negligible in this study) and ΔW is the change in soil water content during the two measurements (mm) (Liu et al., 2015).

2.4.3 Modelling of orchard water use

The modelling approach to estimate ET using reference crop evapotranspiration (ETo) and crop coefficients is explained in detail below.

2.4.3.1 Evapotranspiration

Evapotranspiration (ET) is a process whereby evaporation and transpiration occur simultaneously (Allen et al., 1998). The evapotranspiration is affected by the following factors: crop characteristics, weather parameters, management and environmental aspects. The most prominent evapotranspiration concepts are reference crop evapotranspiration (ET_O), crop evapotranspiration under standard conditions (ET_c) and crop evapotranspiration under non-standard conditions ($ET_{c\ adj}$). The ET_O represent climatic weather parameters as it expresses the evaporating power of the atmosphere and can be calculated from weather data. According to Allen et al. (1998) the FAO Penman Monteith method is the only recommended method to determine ET_o. The ET_c is the evapotranspiration for well managed fields, free from pest and disease, well irrigated and fertilised (Allen et al., 1998). The $ET_{c\ adj}$ is evapotranspiration adjusted for non-uniform fields, sub-optimal crop management and environmental factors.

The ET data can be obtained using a weighing lysimeter (Nolz et al., 2016). Nolz et al. (2016) conducted a study to determine evapotranspiration using an ASCE-EWRI equation and lysimeters in a semiarid area. The results showed that ASCE-EWRI equation (ET_{ref}) little overestimated evapotranspiration as compared to lysimeters. According Jovanovic et al. (2020) the FAO56 approach is the most used and reliable approach to estimate crop evapotranspiration at the field scale through multiplying the grass reference evapotranspiration (ET_O) with a crop coefficient (K_c). Rallo et al. (2021) stated that the FAO56 approach is simple, however, it needs accurate measurements and computations when developing K_c values for a crop using field observations. Rallo et al. (2021) included pomegranate water requirement research of Ayars et al. (2017), Zhang et al. (2017) and Intrigliolo et al. (2011) in their recent update of single and dual crop coefficients for tree and vine fruit crops. Ayars et al. (2017) and Zhang et al. (2017) determined water requirements in drip irrigated orchards in California (USA) using weighing lysimeters, whereas Intrigliolo et al. (2011) used a combined methodology of leaf water potential and leaf gas exchange to estimate crop evapotranspiration for a drip irrigated orchard in Spain.

2.4.3.2 Reference evapotranspiration

Reference evapotranspiration (ET_O) is defined as a local weather function to predict evapotranspiration for a range of vegetation and surface conditions through applying K_c for agricultural areas (Walter et al., 2000). It was developed in the 1970's for determining potential evapotranspiration. Reference evapotranspiration is determined from a uniform dense surface, not short of soil water, actively growing vegetation with specified height and surface resistance, with at least 100 m of the similar vegetation (Walter et al., 2000). The most accurate method to estimate reference evapotranspiration is through using lysimeters and micrometeorological methods, however, these methods are expensive and time consuming (Nolz et al., 2016). Instead, the climatic data can be used to estimate reference evapotranspiration (Gavilan et al., 2007). The Penman-Monteith equation is strongly recommended to estimate reference evapotranspiration over a wide range of climates (Gavilan et al., 2007). The Penman-Monteith equation require the following parameters: temperature, solar radiation, relative humidity, wind speed, net radiation, vapour pressure deficit and soil heat flux (Allen et al., 1998).

Gavilan et al. (2007) used the standardized ASCE Penman- Monteith and FAO56 equation to predict reference evapotranspiration (ET_O) using measured net radiation and soil heat flux, based on hourly and daily meteorological data and evaluated it against lysimeter measurements. The results showed that the predicted values of radiation and soil heat flux can affect the accuracy of the evapotranspiration predictions, particularly when calculated on an hourly basis. Gavilan et al. (2007) found that ASCE equation was more accurate, in measuring radiation and soil heat flux while the FAO56- version was often less accurate. Gavilan et al. (2007) concluded by stating that FA0-56 version performed very well under semiarid conditions during irrigation in predicting daily evapotranspiration. The standardized ASCE equation improved the evapotranspiration accuracy prediction compared to the FA056-equation.

The standardized ASCE Penman- Monteith equation is expressed as follows (Gavilan et al., 2007):

$$ET_0=\frac{0.408\Delta\,(Rn-G)+\gamma\left(\frac{Cn}{Ta+273}\right)U2\,(es-ea)}{\Delta+\gamma\,(1+CdU2)} \qquad \text{[Eq.11]}$$

Whereby ET_o is the reference evapotranspiration (mm h^{-1} or mm day^{-1}), Δ is the saturation vapour pressure slope against air temperature curve (kPa $^{O}C^{-1}$), R_n is the net radiation (MJ m^{-2} h^{-1} or MJ m^{-2} day^{-1} for hourly and daily time step, G is the soil heat flux (MJ m^{-2} h^{-1} or MJ m^{-2} day^{-1} for hourly and daily time step. The γ is the psychrometric constant (kPa $^{O}C^{-1}$), T is the mean daily or hourly temperature (^{O}C), U_2 is the mean daily and hourly wind speed at 2 m height (m s^{-1}), e_s is the saturation pressure deficit (kPa), e_a is the actual pressure deficit (kPa), C_n and C_d are the numerator and denominator constant for a reference type and determination time step. C_n has values of 900 for daily time steps and 37 for hourly time steps. The C_d has a fixed value of 0.34 for daily time step with values of 0. 24 and 0.96 at day and nighttime for hourly time steps. Daytime is identified when the average R_n is bigger than zero during an hourly period. According to Allen et al. (1998) R_n is estimated using the following equation:

$$R_n= R_{ns}- R_{nl} \qquad \text{[Eq.12]}$$

Where R_{ns} is the short- wave irradiance and R_{nl} is the outgoing net long- wave irradiance.
The standardised Penman-Monteith equation for calculating of ET_o is expressed as follows:

$$ET_o = \frac{0.408\Delta\,(Rn-G)+\gamma\left(\frac{Cn}{Ta+273}\right)U2\ VPD}{\Delta+\gamma\,(1+CdU2)} \quad \text{[Eq.13]}$$

Where VPD is saturation vapour pressure deficit (kPa) and other parameters are the same as described under the standardized ASCE Penman- Monteith equation.

2.4.3.3 The single crop coefficient approach

The FAO56 crop coefficient approach can be used to estimate crop evapotranspiration under standard conditions (Allen et al., 1998). Under standard conditions, trees should be well fertilized, free from pests and diseases, no weed infestation, optimum soil water conditions, no limitation on crop growth and evapotranspiration (Allen et al., 1998). The FAO56 defined the crop coefficient (K_c) is the ratio of crop evapotranspiration to the reference evapotranspiration. According to Allen et al. (1998), K_c determination is highly affected by the following factors: crop type, climate, soil evaporation and crop growth stages (initial, mid and late stages). Crop type such as pineapples have very small K_c values since they close the stomata openings during the day. Taller canopies and closely spaced crops such as maize usually have larger K_c values. FAO56 stated that the most arid climatic conditions of greater wind speed give higher K_c values since the K_c for many crops increases as wind speed increases and relative humidity decreases. In addition, most humid climatic conditions of lower wind speed will give lower K_c values.

The K_c combines the soil evaporation with crop transpiration and the reference surface. When the soil is wet, the K_c values may be more than 1, since evaporation from the soil surface will be high. While if soil surface is dry, the K_c values become small and may even be lower than 0.1 (Allen et al., 1998). Due to changes as the crop develops, the K_c values also differ during the growth stages. The K_c values tend to be lower during initial stages of the crop due to less surface cover and green vegetation. At the mid-season stage the K_c values reach their maximum values as the crop is fully developed. The K_c values drop at late season stage as the tree leaves dries out (Allen et., 1998). The single crop coefficient approach combines the effect of crop transpiration and soil evaporation into a single coefficient (Allen et al., 1998). The single coefficient approach (K_c) is used to compute crop evapotranspiration for longer time periods (Allen et al., 1998). According FAO56, evapotranspiration can be determined using K_c for purposes mentioned in Table 9 below.

Table 9. The single coefficient selection approach used to determine evapotranspiration, adapted from FAO56 (Allen et al., 1998)

Single crop coefficient (K_c)	
Calculation purpose	-Irrigation design and planning -Irrigation management -Basic irrigation schedules -Time scheduling of irrigation for non-frequent water applications (surface and sprinkler irrigation)
Time step	-Daily, 10 day, monthly (data and calculation)
Solution method	-Graphical pocket calculator computer

For a single crop coefficient, evapotranspiration is determined as follows (Allen et al., 1998):

$$ET_c = K_c \times ET_0 \quad \text{[Eq.14]}$$

Where ET_c is the crop evapotranspiration (mm d^{-1}), K_c is the crop coefficient and ET_o is the reference crop evapotranspiration.

Single coefficient values under typical irrigation management for selected fruit tree crops are shown in Table 10 (Allen et al., 1998). These values may significantly increase under frequency wettings such as high frequency sprinkle irrigation and daily rainfall (Allen et al., 1998). Although crop coefficients were listed for several crops in FAO56, it contained no data for pomegranate. Rallo et al. (2021) recently published indicative standard values for single crop coefficients relative to the mid- and end-season, under temperate climate, for deciduous fruit tree crops including that for pomegranate (Table 11). The K_c values reported by the pomegranate research were strongly related with the fraction of ground cover (Rallo et al., 2021 and references therein). The cultivar 'Wonderful' pomegranate tends to have lower crop coefficient values as compared to other deciduous fruit at similar canopy cover (Figure 8).

Table 10. Single crop coefficients (time-averaged) (K_c) and mean maximum plant heights for non-stressed and well managed selected fruit trees under sub humid climates (Allen et al., 1998). Ini, mid and end applies to Kc at the beginning of the initial, beginning and end of the mid and end of the late development stages.

Crop	$K_{c\ ini}$	$K_{c\ mid}$	$K_{c\ end}$	Maximum crop height (m)
Apples, cherries and pears				
No ground cover, killing frosts	0.45	0.95	0.70[18]	4
No ground cover and no frosts	0.60	0.95	0.75[18]	4
Active ground cover, killing frost	0.50	1.20	0.95[18]	4
Active ground cover and no frosts	0.80	1.20	0.85[18]	4
Apricots, Peaches and stone fruit				
No ground cover, killing frosts	0.45	0.90	0.65[18]	3
No ground cover and no frosts	0.55	0.90	0.65[18]	3
Active ground cover, killing frost	0.50	1.15	0.90[18]	3
Active ground cover and no frosts	0.80	1.15	0.85[18]	3

Table 11. Updated indicative standard values for single and basal crop coefficients relative to the mid- and end-season, under temperate climate, for deciduous fruit tree crops including reviewed literature and previous tabulated values. Adapted from Rallo et al. (2021).

Density	fc	Plant height (m)	Literature reported Kc		Indicative standard values (±10%) of Kc and Kcb			
			$K_{c\ mid}$	$K_{c\ end}$	$K_{c\ mid}$	$K_{cb\ mid}$	$K_{c\ end}$	$K_{cb\ end}$
Young	0.15-0.25	1.0-2.0	0.36	-	0.35	0.30	0.30	0.20
Low	0.25-0.35	2.5-3.5	0.44	-	0.50	0.45	0.40	0.30
Medium	0.35-0.45	2.5-3.5	0.46-0.56	-	0.60	0.55	0.45	0.40
High	>0.45	2.5-3.5	0.71-1.00	0.40-0.64	0.85	0.80	0.60	0.55

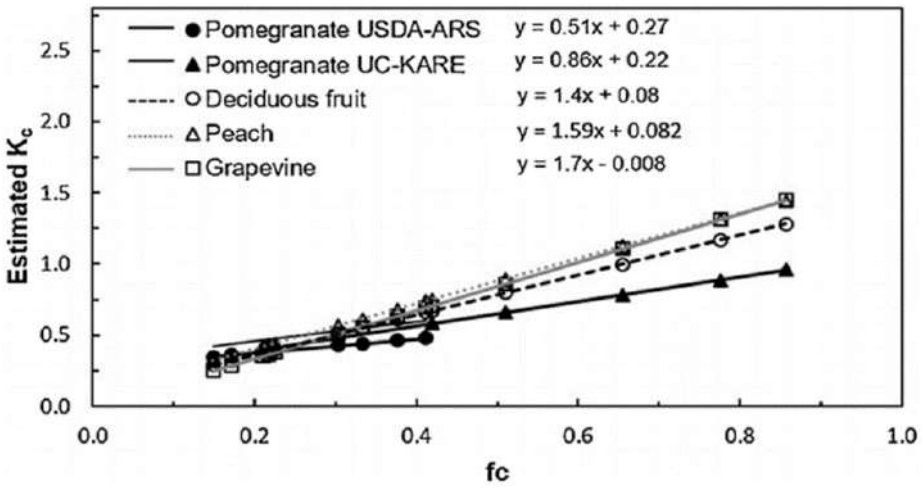

Figure 9. Comparison of the relationship between crop coefficient (Kc) and fractional canopy ground cover (fc) for pomegranate (USDA-ARS and UC-KARE), deciduous fruit, peach and grapevine (Volschenk, 2020)

Bhantana and Lazarovitch (2010) conducted a study to evaluate growth, evapotranspiration, and crop coefficients of pomegranate cultivars under salt stress. The study was conducted on 'Wonderful' and 'SP-2' pomegranate cultivars using drainage lysimeters. These two cultivars were grown in irrigation water with electrical conductivity of 0.8, 1.4, 1.4, 3.3, 4.8 and 8 dS m^{-1} (Table 12). Both cultivars showed a similar response of lower evapotranspiration under salt stress and the crop coefficient values decreased as electrical conductivity increased.

Table 12. Comparison of crop coefficients (K_c) for young 'Wonderful' and 'SP-2' pomegranate trees irrigated with water of different electrical conductivities (EC_w) at different days after bud burst (DAB) (adapted from Bhantana & Lazarovitch, 2010)

DAB	EC_w-0.8 dS m^{-1}		EC_w-1.4 dS m^{-1}		EC_w-3.3 dS m^{-1}		EC_w-4.8 dS m^{-1}		EC_w-8 dS m^{-1}	
	Wonderful	SP-2	Wonderful	SP-2	Wonderful	SP-2	Wonderful	SP-2	Wonderful	SP-2
30	0.16	0.15	0.15	0.15	0.14	0.14	0.12	0.09	0.09	0.09
60	0.19	0.19	0.19	0.19	0.16	0.15	0.13	0.13	0.09	0.09
90	0.49	0.44	0.45	0.41	0.33	0.31	0.23	0.21	0.13	0.13
120	0.64	0.58	0.52	0.53	0.38	0.35	0.25	0.24	0.12	0.11
150	0.53	0.60	0.42	0.54	0.43	0.37	0.29	0.29	0.17	0.17
180	0.39	0.45	0.32	0.44	0.41	0.32	0.30	0.30	0.21	0.17
210	0.22	0.28	0.19	0.27	0.32	0.23	0.25	0.25	0.16	0.12
240	0.20	0.28	0.17	0.23	0.18	0.18	0.28	0.22	0.15	0.15

Meshram et al. (2012) conducted a study to select the best reference crop evapotranspiration model (ET_r), develop crop coefficients (K_c), and actual evapotranspiration of pomegranate for the Pune region of Maharashtra, India. The Radiation-FAO, Pan Evaporation-FAO-PM, Blaney Criddle, Modified Penman-FAO56-PM and Hargreaves Samani approach were used to compare reference crop evapotranspiration (ET_r). The FAO56-PM approach was the most appropriate method for prediction of ET_r. The shaded area approach was used to determine K_c (Equation 14) due to high cost for the experimental set up. The weekly K_c values were developed for different phenological stages from June using the following equation of Williams and Ayars (2005):

$$K_c = 0.014x + 0.08 \quad \text{[Eq.14]}$$

Where x is the percentage of the shaded area (%)

The monthly K_c values developed by Meshram et al. (2012) for 'Mrig Bahar' pomegranate trees at different ages (Table 13) can be used for evapotranspiration estimation if the reference crop evapotranspiration is known. The K_c values increased from 0.22 to 1.10 during the period of leaf initiation to crop development and K_c values were around 1.2 during harvest (Tables 10 & 11, Fig. 10). At late season, the K_C values decreased due to decrease in crop cover as the leaves were dropping, foliage breakdown occurred and fruits were harvested. These findings show that K_c is highly dependent on the crop development stages, canopy cover and architecture as stated by Allen et al. (1998). The K_c is also correlated with the leaf area index and the fractional light interception by the tree canopy (Williams & Ayars, 2005).

Table 13. Monthly shaded area (SA) and crop coefficient (K_c) values from 1st to 5th year 'Mrig Bahar' pomegranate trees (Meshram et al., 2012)

	Age of tree (year)									
	1st		2nd		3rd		4th		5th	
Month	SA	K_C	SA	K_C	SA	K_C	SA	K_C	SA	K_C
July	0.84	0.16	1.68	0.22	1.35	0.13	1.72	0.14	2.07	0.15
August	1.00	0.17	2.43	0.25	4.09	0.21	4.82	0.26	5.26	0.30
September	1.16	0.18	3.30	0.32	7.53	0.48	8.32	0.54	8.46	0.59
October	1.28	0.20	4.05	0.41	9.54	0.83	10.30	0.91	10.55	0.92
November	1.37	0.21	4.13	0.49	9.63	1.06	10.44	1.13	10.60	1.16
December	1.49	0.22	3.44	0.51	8.21	1.08	9.41	1.15	9.73	1.18
January	1.66	0.23	2.65	0.44	7.14	0.94	8.12	1.05	8.91	1.09
February	1.60	0.25	2.01	0.35	6.11	0.78	6.85	0.92	7.73	1.00
March	1.47	0.25	2.01	0.29	5.54	0.68	6.41	0.79	7.25	0.88
April	1.56	0.23	2.16	0.29	5.72	0.65	6.57	0.74	7.58	0.83
May	1.65	0.24	2.34	0.30	5.94	0.67	6.73	0.77	7.77	0.87
June	1.79	0.25	2.50	0.32	6.14	0.69	6.88	0.78	8.02	0.89

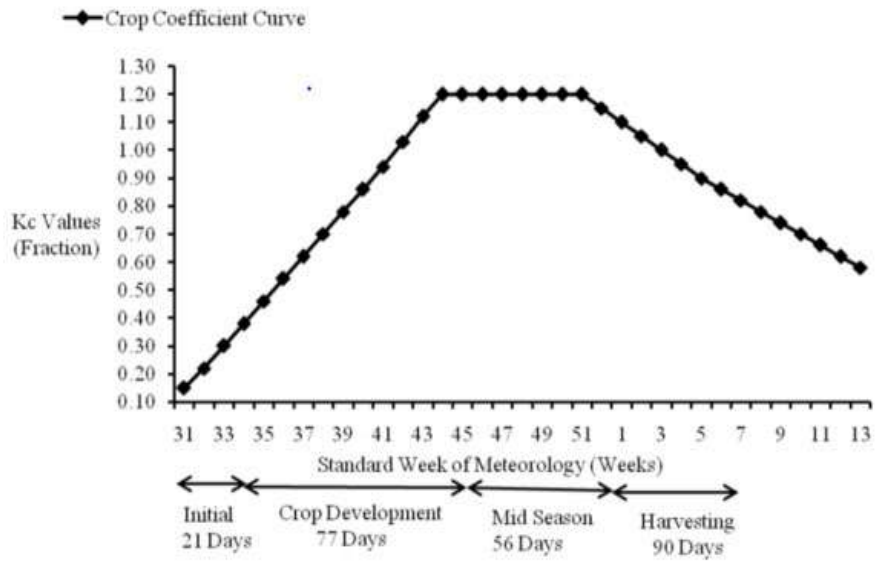

Figure 10. Pomegranate crop coefficient (K_C) curve throughout the season in Maharashtra, India (Meshram et al., 2012)

Table 14. Phenological stages of a mature pomegranate tree in Pune conditions in Mahastra, India (Meshram et al., 2012)

Phenological stages	Periods	Meteorological week
Initial	21 days	31st to 33rd
Crop development	77 days	34th to 44th
Mid-season	57 days	45th to 52nd
Late season	105 days	01st to 15th
Rest period	105 days	16th to 30th

2.4.3.4 The dual crop coefficient approach

The dual crop coefficient method (K_c) was firstly developed by Wright, (1982) to separate evapotranspiration into evaporation and transpiration. The dual crop coefficient approach can be used to split evaporation and transpiration using the following equation (Allen et al., 1998):

$$K_C = (K_{cb} + K_e) \times ET_o \quad \text{[Eq.15]}$$

Where K_{cb} is basal crop coefficient to describe plant transpiration, K_e is the soil water evaporation coefficient to describe evaporation from the soil surface and ET_o, reference crop evapotranspiration.

The basal crop coefficient is the ratio of ET_c to ET_o when the surface of the soil is dry while the average soil water content of the root zone is enough to sustain full plant transpiration (Allen et al., 1998). The basal crop coefficient represents the transpiration component from evapotranspiration; however, it also involves diffusive soil evaporation (Wang et al., 2021). The single and basal crop coefficients under different crop development stages are shown in Figure 10.

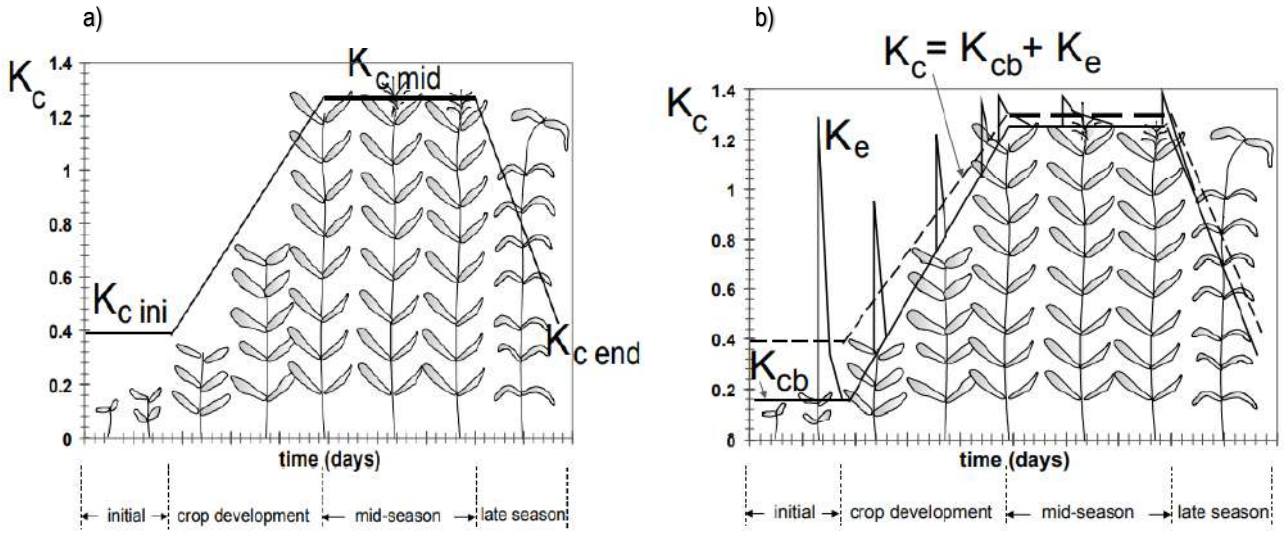

Figure 11. Image a) shows a single crop coefficient curve while image b) shows the crop coefficient curves for the basal K_{cb} (represented by thick line), soil evaporation K_e (indicated by thin line) and the corresponding single curve (indicated by dashed line) $K_c=K_{cb} + K_e$ (Allen et al., 1998). The dashed line indicates the single time averaged crop coefficient K_c. Images from Allen et al. (1998).

Soil evaporation coefficients (K_e) is the evaporation component of evapotranspiration following the rainfall or irrigation of the soil surface (Allen et al., 1998). The K_e tend to be smaller when there is no water left in the soil for evaporation. According to FAO56, soil evaporation occurs at the maximum rate in wet soil, but the crop coefficient never exceeds the maximum value ($K_{c\,max}$). The $K_{c\,max}$ value is calculated from the energy available for evapotranspiration at the surface of the soil:

$$K_{c\,max} \leq K_{cb} + K_e \text{ or } K_e \leq (K_{c\,max} + K_{cb}). \quad \text{[Eq. 16]}$$

The soil evaporation is less when the topsoil dries out, as the evaporation occurs based on the amount of water available in the soil surface and can be calculated as follow (Allen et al., 1998):

$$K_e = K_r (K_{c\,max} - K_{cb}) \leq f_{ew} K_{c\,max} \quad \text{[Eq.17]}$$

Where K_e is the soil evaporation coefficient, K_{cb} is the basal crop coefficient, $K_{c\,max}$ is the maximum value of K_c following rain or irrigation, K_r is a dimensionless evaporation coefficient dependent on the cumulative depth of water evaporated from the topsoil and f_{ew} is the soil fraction that is exposed and wetted (fraction of soil surface from where most of evaporation takes place).
The K_e increases during initial crop developmental stages and towards the end of the season due to less canopy cover (López-Urrea et al., 2020). Zhao et al. (2013) observed a similar trend on a wheat study conduct North China Plain, where the K_e values were high during the initial periods and towards the end of the season but decreased in the middle of the season. Flumignan et al. (2011) conducted a study to determine evapotranspiration components and dual crop coefficients of coffee trees. The K_e was determined using the following equation (Flumignan et al., 2011):

$$K_e = \frac{E}{ETo} \quad \text{[Eq.18]}$$

Where E is the evaporation (mm) and ET_o is reference evapotranspiration (mm).

The E was measured using microlysimeters installed on the lysimeters. The ASCE Penman-Monteith approach was used to determine ET_o hourly values and calculated using a REF-ET program and with inputs from the SIMEPAR's weather station (Flumignan et al., 2011). Results showed that evapotranspiration consisted 35% of evaporation and 65% of transpiration. Flumignan et al. (2011) recommended K_e values of 0.46 for sprinkler irrigated and 0.26 for drip irrigated treatments. Hunsaker et al. (2003) used a daily soil water balance computation of the surface soil evaporation layer subjected to evaporation drying to determine daily K_e. Soil parameters needed in order to determine daily K_e values are field capacity, permanent wilting point of the surface soil layer, depth of surface soil

evaporation layer, readily evaporable water and daily shaded and unshaded fraction by the canopy during rainfall or irrigation events (Hunsaker et al., 2003).

The dual coefficient method works well in irrigation systems that runs under high frequency irrigation and under large day to day variations in soil wetness (Allen et al., 1998). In addition, the dual crop coefficient approach is best used for irrigation scheduling, water balance computations, determining evapotranspiration, soil water profile and deep percolation fluxes and for other purposes shown in Table 14 below (Allen et al., 1998). The dual coefficient approach tends to be more accurate than the single coefficient approach and it is advantageous in orchards that have incomplete cover crops and for drip irrigated crops (Zhao et al., 2013). The crop evaporation can be calculated using the procedure shown in Table 15 (Allen et al., 1998).

Table 15. Dual crop coefficient approach used for determination of evapotranspiration adapted from FAO56 (Allen et al, 1998)

Dual crop coefficient (K_{cb} + K_e)	
Calculation purpose	-Research -Supplemental irrigation -Detailed soil and hydrologic water balance studies -Real time irrigation scheduling for high frequent water applications (micro irrigation and automated sprinkler irrigation)
Time step	-Daily (data and calculation)
Solution method	-Computer

Table 16. The procedure to calculate crop evapotranspiration (ET_C) using a basal crop coefficient (K_{cb}) adapted from Allen et al. (1998)

Crop evapotranspiration calculation (ET_c)	-Lengths of crop growth stages identification and selecting the corresponding K_{cb} coefficients. -The selected K_{cb} coefficients should be adjusted for climatic conditions during the stage. -Create a basal crop coefficient curve. -Daily K_e values should be determined for surface evaporation and determine ET_C as product of ET_o and (K_{cb} + K_e).

According to the FAO56 procedure in Allen et al. (1998) the single or basal crop coefficient for each day during crop growing stages can be obtained as follows: K_c equal to $K_{c\ ini}$ or K_{cb} equal to $K_{cb\ ini}$ at initial growth stage and K_c equal to $K_{c\ mid}$ or K_{cb} equal to $K_{cb\ mid}$ at mid-season stage. While at crop development and late season stage, K_c or K_{cb} differs linearly between the coefficient value of the end of previous stage and the beginning of the next stage as shown in equation below.

$$K_{c\ i} = K_{c\ prev} + \left[\frac{i - \Sigma(Lprev)}{Lstage}\right] (K_{c\ next} - K_{c\ prev}) \quad \text{[Eq.19]}$$

Where i is the number of the day within the growing season, $K_{c\ i}$ is the crop coefficient on day i, L_{stage} is the stage length under consideration (days) and $\Sigma(L_{prev})$ is the lengths sum of all precious stages (days).

2.4.3.5 Stress coefficients

According to FAO56, the stress coefficient is a function of the total available water, readily available water within the root zone, and depletion of root zones. The stress coefficient (K_s) is applied when the soil water content is insufficient and evaporation demand cannot be met (Kokkotos et al, 2020). The crop evapotranspiration ($ET_{c\ adj}$) under soil water stress conditions when basal coefficient (K_{cb}) is used, can be calculated as follow (Allen et al., 1998):

$$ET_{c\ adj} = (K_s\ K_{cb} + K_e)\ ET_o \quad \text{[Eq.20}$$

However, where the single crop coefficient (K_c) is used, the $ET_{c\ adj}$ is expressed as follows:

$$ET_{c\ adj} = K_s\ K_c\ ET_o \quad \text{[Eq.21]}$$

According to Minhas et al. (2020), the water stress coefficient (K_s) is expressed as a linear function of root zone depletion and determined through soil water applied to the root zone as shown on the following equation:

$$K_{s,\,i} = \frac{TAW - Dr,i}{TAW - RAW} = \frac{TWA - Dr,i}{(1-p)TAW} \quad \text{[Eq.22]}$$

Where TAW is the total available water, $D_{r\,i}$ is the depletion of root zone at the end of day (mm), RAW is the readily available water (mm) and p is the depletion fraction for no stress.

According FAO56, the trees are not under water stress if K_s is equal or greater than one and trees are under water stress if K_s is less than one.
The water stress coefficient (K_s) under soil salinity conditions is expressed as follows:

$$K_{s,\,i} = \left(\frac{TAW - Dr,i}{TAW - RAW}\right)\left(1 - \frac{b}{Ky\ 100}(ECe - ECe\ threshold)\right) \quad \text{[Eq.23]}$$

Where K_y is the yield response factor (-) that determine relationship between the relative evapotranspiration deficit and relative yield decrease, $EC_{e\ threshold}$ (dS m^{-1}) is the EC_e value of the soil from where crop production starts to be affected by salinity and b is relative yield decrease percent rate to the excess relative EC_e to $EC_{e\ threshold}$ (%/(dS m^{-1}).

2.4.4 The use of remote sensing to determine orchard water use

Pereira et al. (2021) conducted a study to determine standard single and basal crop coefficients for vegetable crops. The basal crop coefficient (K_{cb}) was used to calculate a single crop coefficient (K_c) value through adding the K_{cb} and K_e values and multiplying with reference evapotranspiration (ET_o) using the Penman Monteith approach (Allen et al., 1998). French et al. (2020) used satellite based vegetation index (VI) pictures to determine evapotranspiration over wheat. The basal crop coefficient (K_{cb}) was modelled using Normalized Difference Vegetation Index (NDVI) time series and ET_o was obtained from the nearest weather station. French et al. (2020) observed that the K_{cb} derived from NDVI accurately predicted crop evaporation and K_c during mid-season. The wheat measured K_c values were similar to those presented in the FAO56 crop coefficient Table (Allen et al., !998) during mid-season and end of the season. However, NDVI was less accurate in estimating evapotranspiration during early season due rainfall and irrigation at low crop cover (French et al., 2020).

Wang et al. (2021) used a weighing lysimeter and a flux station to assess the crop evapotranspiration data from the Satellite Irrigation Management Support (SIMS) framework for sugar beets. The daily crop evapotranspiration from SIMS was 0.55 mm day^{-1} less than the daily crop evapotranspiration from the weighing lysimeter during the initial crop stages. However, there were no significant differences in daily crop evapotranspiration from SIMS and the weighing lysimeter during the crop developmental stages (Wang et al., 2021). Hunsaker et al. (2003) conducted a study in Arizona (USA) to improve irrigation scheduling for cotton using remotely sensed multispectral vegetation indices (Vis). The cotton basal crop coefficient (K_{cb}) was estimated for a full season using NDVI observations. The NDVI-K_{cb} model crop evapotranspiration compared well to actual crop evapotranspiration measurements (Hunsaker et al., 2003). Zhang et al. (2017) used NDVI and Normalized Difference Infrared Index (NDVII) derived from CropScan MRS5 multispectral radiometer (CROPSCAN, Inc., Rochester, MN) to assess the impact of surface and subsurface drip irrigation on a pomegranate orchard. The NDVI and NDVII showed a high correlation with the fraction of ground cover and it can be used by farmers to estimate pomegranate tree water use (Zhang et al., 2017).

According to Allen et al. (2011) satellite imagery can be used to estimate soil evaporation and evapotranspiration using vegetation indices. A common Vegetation Indices (VI) known as Normalized Difference Vegetation Index (NDVI) can be used to estimate crop coefficient (K_c) as expressed in the equation below (Choudhury et al., 1994):

$$K_{co} = 1.25NDVI + 0.2 \quad \text{[Eq.24]}$$

Where K_{co} is the grass crop coefficient.

The Basal K_{cb} vs. NDVI relationship is more reliable than a K_c vs. NDVI relationship since the transpiration is much associated with vegetation than soil evaporation (Allen et al., 2011). The soil evaporation and transpiration are determined separate when K_{cb} vs NDVI relationship and added to give evapotranspiration (Burnett et al., 2008). The advantages and disadvantages of NDVI- basal crop coefficient estimation is expressed in the Table 16 below.

Table 17. Advantages and disadvantages of using NDVI- basal crop coefficient estimation adapted from Allen et al. (2011)

Advantages	Disadvantages
Cover large areas	Relationship tends to overestimate evapotranspiration in conditions of acute water shortage.
Spatial resolution can be high, particular when aerial imagery is used	Struggles to quantify under dense vegetation and multi-storied canopies.
Quick analysis can be done by mid-level technicians	Soil evaporation component estimation is less specific compared to transpiration component.

Balbontín et al. (2017) assessed basal coefficients (K_{cb}) for Table grapes using satellite images from Landsat 8 Operational Land Imager sensor (L8-OLI). The NDVI images were determined using United States Geological Survey (USGS) Global Visualization Viewer. At least two images were used per month, and a minimum of 21 images per growing season (Balbontín et al., 2017). The highest K_{cb} obtained from NDVI was 0.85 which was greater than the K_{cb} proposed for Table grapes in FAO56.
Unmanned Aerial Vehicles (UAVs) in recent years have become essential tools for data collection in large fields which is more advantageous than ground scouting. Delavarpour *et al*. (2021) stated that UAVs platforms are essential for real-time field measurements and observation such as crop monitoring, weed detection, tree classification, pest control, yield estimation, and water stress assessments. Barbedo and Koenigkan (2018) indicated a decline in the prices of drones that can handle agricultural activities. However, several additional costs are linked with the operation of a drone such as insurance, maintenance, image processing software, and navigation software.

The use of UAVs to assess the water stress from high-resolution images is complex, but with the advancement in UAVs technologies, it is possible to analyse one plant from an image obtained from remote sensing images due to the high resolution (Garcia and Barbedo, 2019). Some studies use thermal images for the UAVs to assess the visual changes in the water content. Espinoza *et al.* (2017) indicated that thermal images are applied in the agricultural field to evaluate water stress. The time of day that the thermal images are taken is very important because it affects the quality of the images. Bellvert *et al*. (2014) indicated that the best time to take thermal images is mid-day, especially between 12:00 and 13:30.

Park et al. (2021) determined evapotranspiration for a high density peach orchard with an uneven canopy in Australia using very high resolution (VHR) multispectral and thermal imagery from a single flight of an (UAV). The data for the UAV campaign was collected on a midday hourly average having clear sky, with air temperature of 30.6 ^{0}C, wind speed of 0.6 m s^{-1} and relative humidity of 26.7%. A thermal infrared camera (TIR) and multispectral camera (MS) were connected to a GPS for geo-logging. All the instruments were mounted to an octocopter aircraft (UAV used). Aerial images were collected using TIR and MS images with a single flight within short time period (<15 minutes). The UAV survey was done during midday to capture the period of high evapotranspiration and minimize tree shade. The results showed a strong linear relationship between the estimated evapotranspiration and leaf transpiration measured using a gas exchange sensor. However, NDVI had a limited capability to work under the heterogeneous and complex canopy structure of trees (Park et al., 2021).

Bulanon et al. (2016) evaluated five different irrigation methods (full sprinkler, 50% deficit sprinkler, 50% deficit drip, full drip and 65% drip irrigation) to develop a Crop Monitoring and Assessment Platform (C-MAP) for an apple orchard. C-MAP is a small unmanned aerial monitoring tool with a multispectral camera to assess orchard variation and water input variation. The C-MAP was compared with the following five vegetation indices: ENDVI (Enhanced Normalized Difference Vegetation Index), GR (Grean Ratio), I (Intensity), NDGNI (Normalized Difference Green Near Infrared Index) and SAT (saturation). The ENDVI gave better results than all other vegetation indices and managed to show a significant difference between full drip and the other water deficit methods. Bulanon et al. (2016) found that the C-MAP has very good potential as a monitoring tool, it is inexpensive, efficient and can be mounted on another mobile platform such as tractor.

Gonzalez-Dugo et al. (2013) used high resolution UAV thermal imagery to evaluate the difference in the water status of five fruit tree species. Thermal imagery indicators from an UAV gave accurately spatial variability in crop water status. The thermal imagery gives information for whole orchards, including the mapping on a tree-by-tree basis and it is a valuable tool for managing water and deficit irrigation (Gonzalez-Dugo et al., 2013).

Kangueehi (2018) evaluated the accuracy of Fruitlook spatial data for Table grape growers in Western Cape, South Africa. Fruitlook is an open portal funded by the Western Cape Department of Agriculture to help growers to have access on satellite based information relating to plant, soil and water use status. The Fruitlook data is derived from satellite and ETLook algorithm (Pelgrum et al., 2010). ETLook uses the energy balance to predict evapotranspiration (Kangueehi, 2018). The energy balance equation is expressed as follows:

$$\lambda E = Rn - G - H \quad \text{[Eq.25]}$$

Where λE is latent heat flux density, G is the soil heat flux density and H is the sensible heat flux. Kangueehi (2018) found that FruitLook evapotranspiration can be used for irrigation scheduling as it gave a good indication on water use. ETLook in Stellenbosch provide satellite data for free.

Bastiaanssen et al. (2012) used the ETlook model to determine satellite measurements for surface energy balance and actual evapotranspiration (ET) in a rice-wheat system in Indus Basin, Asia. The highest annual ET values were obtained in alluvial plains as shown in Figure 14, and the average day ET values ranged between 2.3 to 6.3 mm day^{-1}.

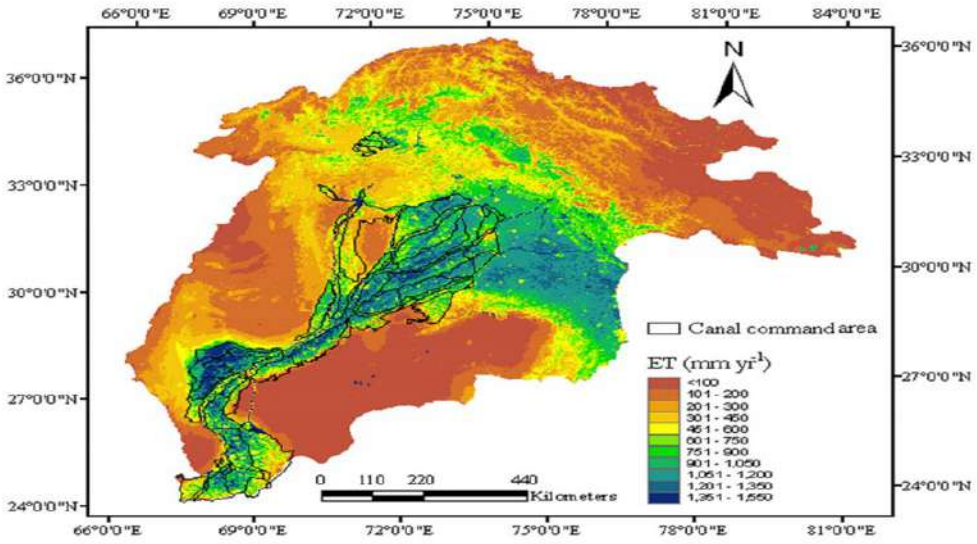

Figure 12. Actual evapotranspiration (ET) for the hydrological year 2007 (January to December) determined using ETLook model. The ET map is superimposed on the irrigation basin areas for irrigated cropland (Bastiaanssen et al., 2012).

2.4.5 Conclusions

The South African pomegranate industry has an opportunity to supply fruit to the Northern hemisphere countries during a period when their own supply of fruit is low. There is therefore scope for the industry to expand and strengthen South Africa's position against other Southern hemisphere countries that also supply pomegranates in the same time frame to the same markets. It will be important though to apply water according to the crop requirements to ensure high production and quality fruit. Selection of a suitable sap flow method to measure transpiration for pomegranate trees is not straightforward, since different types of systems are required for single and multi-stemmed trees and stem size also determines which system should be used. In the case of multi-stemmed trees, affordability may be a determining factor to be taken into account when evaluating the suitability of the method for water use research. Tree stem anatomy should also be assessed to determine if sap flow can be used to determine transpiration successfully. The existing relationships between fractional light interception and crop coefficients derived from other research for pomegranate trees will be compared with results obtained from our own research when it becomes available. The use of new methods such as remote sensing for practical on-farm irrigation scheduling planning and decision-making purposes is important and the cost effectiveness and user-friendliness of these approaches for producers should be assessed.

CHAPTER 3: METHODOLOGY

3.1 INTRODUCTION

This general methodology chapter run through the approach followed regarding plot selection and for a sap flow scoping study, provides experimental site and plant material details and describes methods collecting information relevant to quantification or modelling of fruit tree and orchard water use. The methods focus on monitoring microclimate, establishing soil properties, monitoring soil water content, irrigation, plant physiology, growth, yield and fruit quality. Methods also include assessment of fruit marketability and calculation of appropriate water use indicators.

3.2 PLOT SELECTION

Potential sites for the research were identified with the assistance of a POMASA affiliated pomegranate technical advisor, Mr. Jorrie Mulder. Younger and older orchards were considered for evaluation to supply in the requirement to measure pomegranate orchard water use for orchards with a range of canopy sizes. On 19 and 20 March 2021 project team researchers visited five farms in order to select two orchards to achieve project objectives (Fig. 13). Heavy rainfall prevented a visit to Avontuur on 20 March and the site was visited at a later stage in June 2021 by the project leader and Junior Researcher, and by a larger contingent of the project team on 8 November 2021. An orchard selection process was completed in November 2022.

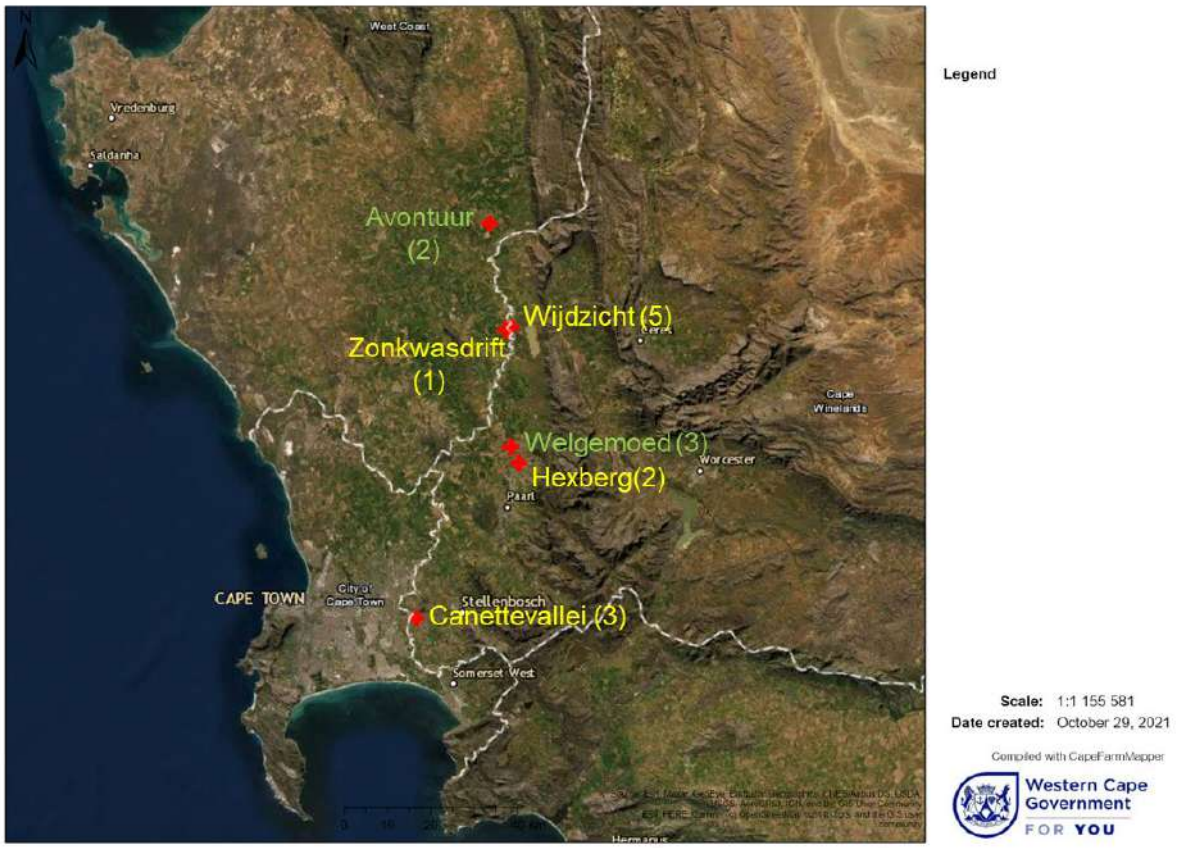

Figure 13. Location of six farms visited and number of blocks evaluated during March, August and November 2022 to select orchards for purposes of pomegranate water use research

The suitability of the orchards was considered for three specific techniques used to determine water use, i.e. sap flow, soil water balance and eddy covariance. Although the use of the eddy covariance technique to determine orchard water use was not included in the original project plan, it was included amongst the techniques for which orchard suitability was scored pending outcome of supplementary funding applications to the NRF and WRC to apply this technique as well. Other factors taken into account in selection of sites were travel distance, farm security, weather station and cell phone reception availability (Table 18). Evaluation for the sap flow method considered the stem nature (single/ multistemmed; stem diameter) of the trees as it determines the type and amount of sap flow equipment needed to determine transpiration. Evaluation of the soil water balance method took into account soil depth, texture and stone/ gravel content, as well as the slope of the block that could result in lateral inflow of water. The type of irrigation scheduling practices applied were also considered. Large stones or high stone/ gravel content can hamper correct installation of the CS650 soil water content sensors and gravimetric soil water sampling for calibration purposes. Evaluation for the eddy covariance method considered amongst others block size relative to canopy height, presence of wind breaks, block slope and prevailing wind direction. Researchers scored the site suitability individually for each technique, the security status of the farm and weather station availability between 0 (Not suitable) and 5 (Highly suitable). A final score was awarded according to consensus between researchers.

Table 18. Suitability scoring of orchards for application of Eddy covariance (EC), soil water balance (SWB) and sap flow techniques. The total score accounts for security of sites and availability of a weather station as well. Not suitable - Score 0, Highly suitable - Score 5.

Farm	Block	EC	SWB	Sap flow	Security	Weather station	Technique score	Total score
Canettevallei	1	0	0	4	1	0	4	5
	2	0	0	2	2	0	2	4
	3	3	1	2	2	0	6	8
Hexberg	2	3	0	3	4	5	6	15
	3	3	0	3	4	5	6	15
Welgemoed	43	5	5	5	5	5	15	25
	42abc	4	3	4	5	5	11	21
Zonquasdrift	1	3	2	2	0	0	7	7
Wijdzicht	1-5	0	0	2	5	0	2	7
Avontuur	Young*	5	5	3	4	0	13	17
	Young**	5	3	5	5	0	13	18
	Mature**	4	4	5	5	0	13	18

*Scored preliminary June 2021 by Dr Volschenk and Dr Dzikiti.

** Scored November 2021 by consensus between Prof Walker, Dr Volschenk and Mr Tharaga.

Only the six orchards having the highest scores are discussed in detail below. In Drakenstein district near Wellington, Welgemoed Blocks 43 and 42abc scored the highest in terms of suitability for the techniques and total score (Table 18, Figure 14). Of the fifteen evaluated blocks only Block 43 at Welgemoed was highly suitable for the soil water balance technique due to sandy soil not containing gravel/ stones. The trees were single stemmed and large enough (c. 80 mm diameter) for sap flow measurements using the heat pulse velocity heat ratio method (Figure 15a). The canopy height of these trees was c. 2.5 m and canopy width c. 2.8 m across the tree row. The orchard was also found highly suitable for the eddy covariance technique. However, in Block 42abc the multi-stemmed trees (four to five stems per tree, c. 43-71 mm diameter) was planted on high ridges, which is not common in the pomegranate industry and the trees are susceptible to water deficits during summer due to irrigation scheduling constraints (Figure 15b). During the previous reference group meeting a concern was raised regarding suspected insufficient irrigation of the Welgemoed orchards. This was discussed recently with the farm manager who indicated that they are willing to adjust their scheduling and apply additional irrigation if the research requires it. At Hexberg, also in Drakenstein district, two blocks each scored 15, but was not suitable for the soil water balance technique due to high gravel content of the soil and slopes of the blocks, which could result in lateral inflow of water (Figure 16). The canopies of the c. 2.8-3 m high trees were c. 2.7 m across the tree row and the trees were multi-stemmed (four to five stems per tree, c. 20-37 mm diameter), which poses challenges for sap flow measurements.

Figure 14. Three sites at Welgemoed farm near Wellington were evaluated for suitability to apply different water use measurement techniques to determine pomegranate orchard water use. This included block W42 and W43, and on the right-hand side of block W42, the location for establishment of a new orchard in August 2021.

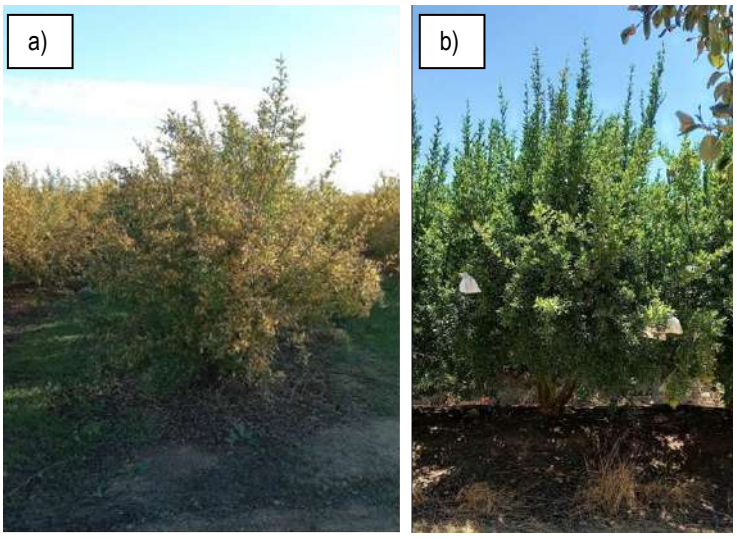

Figure 15. Singled stemmed 'Wonderful' pomegranate trees in block W43 (a) and (b) multi-stemmed trees on ridges in block W42 at Welgemoed farm near Wellington

Figure 16. At Hexberg near Wellington a) three (2 rows on the left-hand side of the picture) and two-year-old (two rows on the right-hand side of the picture) 'Wonderful' pomegranate orchards are located on a downward slope and b) the soil contains a high fraction of gravel

Orchards at Avontuur in Porterville district were visited on 18 June 2020 by the project leader and junior researcher and on 8 November 2021 by a larger contingent of the project team. A preliminary score for the young orchard site was done by the project leader and Dr Dzikiti (Table 18), while Dr Volschenk, Prof Walker and Mr Tharaga scored the young and a mature orchard during the second site visit. The seven-hectare young pomegranate orchard at Avontuur contains two- to three-year-old trees (Figure 17a and b). Large variability between the trees was apparent especially along the outer border of the orchard. The variability may have been caused by drought during establishment or replacement of dead trees. Canopy height of a selection of trees measured between 1.4 and 2.2 m, with canopy width in and across the tree row about 1.8 m. The trees were single-stemmed and stem diameter measured 200 mm from the ground varied between 33 and 57 mm.

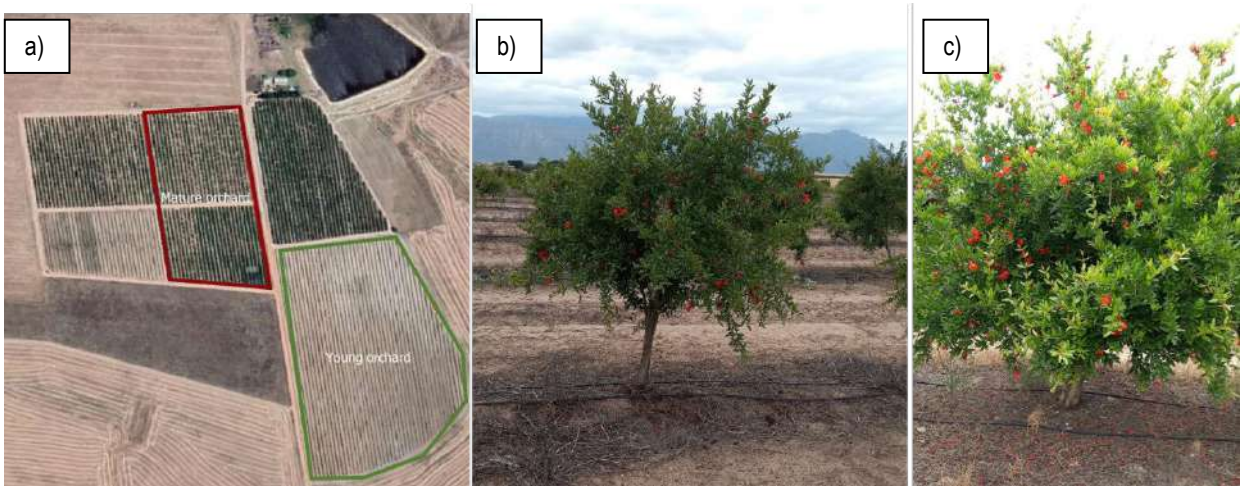

Figure 17. Young and mature pomegranate orchards were scored alongside each other at Avontuur in Porterville district. The young orchard (b) has single stemmed trees, while for the mature orchard (c) tree trunks divide in two stems.

The soil augered was sandy up to a depth of between 0.6 to 0.8 m with hard plinthite below. The orchard has a subtle slope, but it may be possible to do a soil water balance at the highest point of the orchard, which appears to be about in the middle of the block. The irrigation system for the orchard is divided into four irrigation blocks to facilitate separate irrigation for different sections. The orchard is drip-irrigated with a double-line drip irrigation system with 0.6 m spacing and 2.3 $\ell\ h^{-1}$ delivery rate. The cell phone reception was good at the orchard site. Although the tree variability of this orchard is of concern, there is no other suitable site within the 100 km distance range from Stellenbosch supported by the available budget to determine the ETc using a soil water balance.

The mature orchard was on similar soil and located alongside the young orchard (Figure 17a and c). This made it the ideal research setup where the effect of canopy size could be compared for similar climate and soil conditions. The stem of these trees was split in two, but was considered possible to monitor the sap flow by inserting two sets of heat pulse velocity heat ratio probes in each of these stems. The mature orchard was also considered suitable for the use of the eddy covariance technique. However, the producer decided at a late stage that he is going to use drape net on all his mature orchards from the 2022/2023 season onwards. Apparently, the only reason why this orchard was not covered yet was because the supplier of drape net had to close temporarily due to Covid-19 complications. The young orchard at Avontuur and mature Block 43 at Welgemoed covers a range in canopy height and width across the tree row. The largest trees at Avontuur were 2.2 m high and the canopy spread 1.8 m across the tree row, compared to a 2.5 m height and 2.8 m canopy spread across the tree row for Block 43 at Welgemoed. Both orchards are drip irrigated on sandy soil with no/ minimal stone content. Trees in both orchards are single stemmed and both orchards are suitable in size for eddy covariance measurements. Both farm owners agreed that the research can be conducted on their farms over the next two seasons.

3.3 SAP FLOW SCOPING STUDY

The suitability of the sap flow technique to estimate transpiration for pomegranate trees was established by considering the tree structure, tree wood anatomy, field data quality aspects and calibration of the methodology. The tree structure of the pomegranate orchards chosen by the plot selection process were used to assess the suitability for different sap flow systems available. Stem number

per tree, stem height and diameter, stem accessibility and equipment cost aspects were considered. Wood anatomy specialists indicated preference for stem sections rather than wood core samples to do description of the wood anatomy. Since tree stems were not available, wood for anatomy studies were sampled from branches of three trees per orchard for young and mature orchards at Avontuur. Samples where fixed in 10% formalin for a c. 3 weeks and then rinsed with water before sectioning. Samples were sectioned 12 µm thick using a sliding microtome. After sectioning, the samples were placed on a microscope slide, covered in Haupts and left to dry on a warming plate for about 20 minutes. The prepared slides were then left overnight in the fume-hood on a piece of paper towel that has been treated with formalin to allow the samples to set. Samples were stained by submerging the slides in Toluidine blue for 30 seconds and were then rinsed with water to remove excess stain. The wood sections mounted on the glass slides were observed using a Nikon Eclipse E200 binocular light microscope linked to an Olympus EP50 microscope camera. For each branch sampled three slides were prepared with three to five sections (depending on size). For the xylem lumen diameter and distance of xylem vessels from each other a field of view was picked on three sections (in the summer or spring wood) and the xylem vessels and distances were measured between one randomly picked vessel and the next nearest vessel. The distance of the cambium from the bark was measured randomly on each section on a slide for all three slides per branch sample.

Field measurements were conducted to assess if the heat pulse velocity heat ratio sap flow method renders data of acceptable quality for pomegranate trees. Heat pulse velocity heat ratio equipment was installed in a single tree at block W43 on the farm Welgemoed in Drakenstein district during January 2022. Equipment included a logger box with CR1000X logger, tree box and a set of two thermocouples and one heater installed at c. 13-, 23-, 33- and 43-mm depths each in the tree stem (Appendix B3, Figure 79). The sap flow system was powered by a solar panel and/ or 12V batteries. Data was downloaded via Loggernet software by direct connection to a laptop computer. For purposes of calibration of the method, smallish pomegranate trees in 25 ℓ pots were transported in May 2022 from a nursery in the Eastern Cape to University of Pretoria to be grown in a glasshouse, making use of the University of Pretoria's Innovation Africa@UP platform (25° 44‟ 58.66"" S, 28° 15‟ 31.65"" E). Trees were transplanted in August 2023 in 80 ℓ plastic containers in a 1:2 (v/v) mixture of compost to sand to improve growth to obtain stems of suitable size to evaluate the method. A full description of the methodology and results of the experiment conducted to determine if sap flow can be used to determine transpiration for pomegranate trees successfully are included in Appendix B4.

3.4 EXPERIMENTAL SITE AND PLANT MATERIAL

The research was conducted at a young pomegranate orchard at Avontuur (Figures 17a and b) and at a full bearing pomegranate orchard (Figures 14 and 15a) at Welgemoed, which covers an area of 6.7 and 4.9 hectares, respectively (Refer to Chapter 3.2 for details on plot selection). Table 19 summarizes selected properties of the two selected pomegranate water use research sites.

Table 19. Selected properties of the two pomegranate orchard water use research sites during orchard selection in 2021.

Site	Avontuur – Young	Welgemoed - W43
Farm GPS co-ordinates	33°07'29.7"S; 18°56'08.8"E	33°35'18.3048"S; 18°59'19.302"E
Orchard row bearing	172.32° (S7.68°E)	71.06 (N71.06°E)
Year planted	2019	2010
Tree spacing	2.5 m x 5 m	2 m* x 4.5 m
Stem nature	Single stemmed (majority)	Single stemmed (majority)
Stem diameter (mm)	c. 45	c. 80
Tree height (m)	c. 1.8	c. 2.5
Canopy width in tree row (m)	c. 1.8	c. 2.5
Canopy width across tree row (m)	c. 1.8	c. 2.8
Soil texture	Sandy to 0.8 m, plinthite below	Loamy sand
Stone content	None to minimal	None to minimal
Irrigation system	Double line drip, 0.75 m spacing 2.3 ℓ h^{-1} delivery rate	Double line drip, 0.75 m spacing 2.3 ℓ h^{-1} delivery rate
Slope	Level to slight gradient	Level

*Tree spacing according to orchard records and map 2.5 m. Measured between tree spacing equals c. 2 m.

A limited amount of the highly sophisticated and expensive equipment required to measure water use accurately for orchards was available for this project. Selecting representative trees at random for measurement of the soil water balance (two trees), sap flow (five trees) and vegetative growth for such large orchards having large variability may not be appropriate. A survey was therefore done per orchard of tree stem circumferences across the orchard area that is expected to be monitored by micrometeorological methods that represent orchard ET. The measured stem size distribution, based on tree circumference converted to diameter, was analyzed. The anticipated position for the micrometeorological equipment tower was taken into account to select the orchard area to be sampled. For the young orchard at Avontuur the survey covered an area of about 160 m x 200 m (32 rows of c. 80 trees each, spaced 2.5 m x 5 m), which covers two irrigation blocks. Dead and multi-stem trees were denoted as such. For pomegranate plants consisting mainly of watershoots, the stem circumference of one watershoot was denoted. For the full bearing orchard at Welgemoed the surveyed area was about 207 m x 160 m (46 rows of c. 80 trees each, spaced 2 m x 4.5 m). In this case, for multi-stem trees, the sum of stem circumferences was denoted.

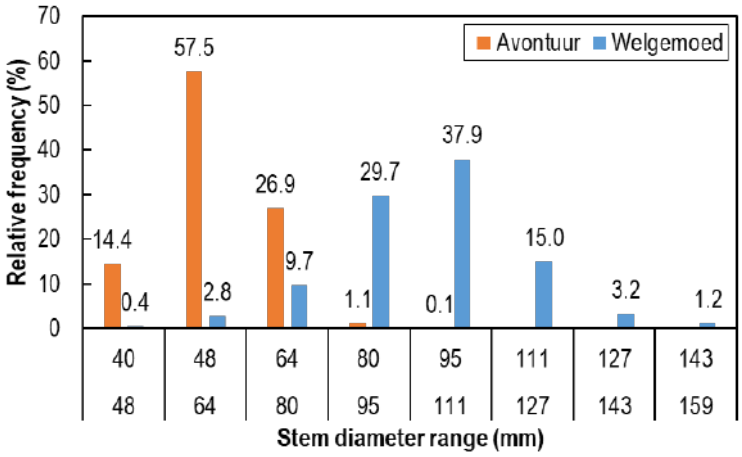

Figure 18. Stem size distribution for the young and full bearing orchards at Avontuur (n = 2121) and Welgemoed (n = 3710) respectively. Trees with stem size between 40 and 159 mm are included in the distribution analysis.

For the young pomegranate orchard, c.4.4% of the 2560 surveyed trees were dead, c. 7% of trees had a stem diameter of less than 40 mm (i.e. not suitable for the heat pulse velocity heat ratio sap flow method) and c.1.4% of the trees were multi-stemmed. Single stemmed trees are preferred for our research since one sap flow system can monitor sap flow for only four trees across four stem depths and there is only one system available per orchard. For the full bearing orchard at Welgemoed of the 3772 trees measured 0.2% were dead, 0.5% had stem diameters less than 40 mm and 0.7% had stem diameters more than 159 mm. The stem size distributions for the orchards excluding trees with diameters smaller than 40 mm and stem diameters exceeding 159 mm are indicated in Figure 18. Stem sizes for the young pomegranate orchard ranged between 40 and 95 mm and for the full bearing orchard between 48 mm and 159 mm. For Avontuur more than half (c. 58%) of the cv. 'Wonderful' trees had stem diameters of between 48 and 64 mm, whereas c. 14%, of trees were smaller (40 - 48 mm) and 28% of the stems were larger (64 - 95 mm). For Welgemoed just more than two thirds of the trees had diameters of between 80-95 mm (c. 30%) and 95 - 111 mm (c. 38%), with 10% of trees being smaller (64 - 80 mm) and 15% larger (111 – 127 mm). Less than 3% of the Welgemoed trees had stem diameters smaller than 64 mm and c. 4.4 % larger than 127 mm. Welgemoed farm management decided to cover several tree rows at the bottom end of block W43 using fixed net for an experiment of their own. The eddy covariance tower was to be set up in the orchard in such a manner that it would avoid monitoring of the netted area.

3.5 ORCHARD MICROCLIMATE

An automatic weather station installed within 50 m from each orchard monitored rainfall and the necessary variables hourly (CR200/ CR300 datalogger: Campbell Scientific Inc., Logan, UT, USA) to calculate reference evapotranspiration (ETo) according to the FAO56 Penman-Monteith modified equation (Allen et al., 1998). At c. 1.2 m above the ground, wind speed and direction were measured using a wind sentry anemometer and vane (Model 03002, R.M. Young Company, Michigan, USA), temperature and humidity using a Hygrovue temperature and relative humidity probe (Campbell Scientific Inc., Logan, UT, USA) installed inside a six plate radiation shield, global solar radiation using a LI-200R M5 pyranometer (Campbell Scientific Inc., Logan, UT, USA), while a Texas Electronics tipping bucket rain gauge (Model# TR-525I 6: Texas Electronics, Campbell Scientific, Dallas, TX, USA) monitored rainfall amounts.

The hourly logged weather data for both stations were downloaded daily via the ARC Agromet services and was made available by email communication to the project manager.

3.6 SOIL PROPERTIES SOIL WATER CONTENT AND IRRIGATION

3.6.1 Soil physical properties

Site selection:
Since the young pomegranate orchard at Avontuur slopes more steeply to the East from row 32, only orchard rows 1-32 were used as the experimental orchard area. Furthermore, it was recommended that the soil water balance equipment should be installed at the highest point of the orchard (irrigation block 3) to prevent lateral inflow of water, which could render the soil water balance invalid. Orchard soil variability prevented selection of two trees in the centre tree row of three representative tree rows as was originally suggested in the proposal methodology. Initially two trees representing the major stem diameter ranges (48-64 mm, 64-80 mm) were identified in row 16 for installation of the soil water balance equipment. Taking tree stem diameter into account, tree 8 in row 8 with stem diameter of 59 mm (from here on referred to as SWB1) and tree 5 in row 7 having a stem diameter of 69 mm (from here on referred to as SWB2) were selected for installation of soil water balance equipment. At Welgemoed orchard rows 1-46 of block W43 were identified as the experimental area and row 23 was selected for installation of soil water balance equipment. In row 23, tree 47 (from here on referred to as SWB3) and tree 67 (from here on referred to as SWB4) having stem diameters of 91.4 mm and 103 mm, respectively, were selected to represent the two dominant stem size groups (Figure 18).

Soil profile description:
At Avontuur profile pits for installation of twelve CS650 soil water content reflectometers (Campbell Scientific Inc., Logan, UT, USA) per site (eight in the tree row, four in the work row) were prepared for two sites and soil profile descriptions were done. The soil form of the loamy to sandy soil was identified as Wasbank (Soil classification workgroup, 1991, Figure 19). The top soil layer for both soil water balance sites was identified as an orthic A horizon that extended c. 190 mm deep in the tree and work rows (Table 20). For SWB1, this was followed by a 560 mm and a 770 mm wide sandy B-horizon for the tree and work row, respectively, which contained small stones (c. 20 mm diameter). The greyish brown colour and texture of the soil profile appeared to be uniform between the 70 mm and 750 mm depths. The stony plinthic layer occurred at 750 mm in the tree row and at 960 mm in the work row area. At the bottom of the soil profile was a hard plinthic layer which could be considered impermeable in places, however, in some places it appeared to be softer and some roots still managed to protrude from crevices in between the stony material. Isolated single roots were observed penetrating this material in the tree row at depths of 900 and 990 mm at different places along the soil profile face, and in the work row up to a depth of 690 mm. The depth at the bottom of the SWB1 soil profile was taken as 1050 mm. For SWB2, the width of the sandy B-horizon in the tree row was c.410 mm and in the work row, 370 mm. This soil horizon therefore was 150 mm and 400 mm narrower in the tree and work row, respectively, compared to that for SWB1. The greyish brown colour was uniform and there was a transition from sand containing few small stones to compacted gravel, with stones of c. 15 to 20 mm diameter becoming more prevalent especially in the bottom 190 mm of the B-horizon. The plinthic layer occurred at 600 mm depth in the tree row soil profile and at 560 mm in the work row. There appears to be accumulation of clay deeper in the soil profile and the soil is more aggregated at 1.2 to 1.3 m depth. Single isolated roots were observed in the tree row down to a depth of 1.2 m, and in the work row up to depth of 540 mm.

Figure 19. A soil profile pit dug in the young orchard at Avontuur indicates a loamy to sandy soil above a plinthic layer. The insertions (left) in the main photo provide a closer look at the materials making up the plinthic layer.

Table 20. Soil profile description for the soil water balance installation sites in irrigation block 3 at Avontuur

Site ID	Location	Orchard area	Soil layer / Depth increment (mm)		
			Orthic A	*B horizon*	*Plinthic layer*
SWB1	Irrigation block 3 Row 8 Tree 8	Tree row	0-190	190-750	750-1050
		Work row	0-190	190-960	960-1050
SWB2	Irrigation block 3 Row 7 Tree 5	Tree row	0-190	190-600	600-1200
		Work row	0-190	190-560	560-1150

For Welgemoed the soil profile was only described in detail for the tree row area. The coarse sandy soil form was identified as a Lamotte (Soil classification workgroup, 1991, Figure 20). The top 130 mm of the lightly coloured sandy soil at both SWB3 and SWB4 was classed as an orthic A (Table 21). For SWB3 this was followed by an E-horizon of 870 mm with iron accumulating in the bottom 240 mm (Table 3). For SWB4 the E-horizon of 1040 mm deep displayed iron accumulation in the bottom 500 mm of soil. A restrictive clay layer at SWB3 occurred at 1.0 m whereas that for SWB4 was deeper i.e. at 1.17 m. The clay at the bottom of both profile pits were unspecified with signs of wetness. Tree roots were observed down to a depth of 1170 mm for SWB3, and 1120 mm for SWB4. In the work row, roots were observed at depths of 220 mm and 380 mm, for SWB3 and SWB4, respectively.

Table 21. Soil profile description for soil water balance installation sites in block W43 at Welgemoed

Site ID	Location	Soil layer / Depth increment (mm)			
		Orthic A	*E horizon - iron insertions*	*E-horizon + iron insertions*	*Clay layer*
SWB3	Row 23 Tree 47	0-130	130-760	760-1000	1000-1140
SWB4	Row 23 Tree 67	0-130	130-670	670-1170	1170-1250

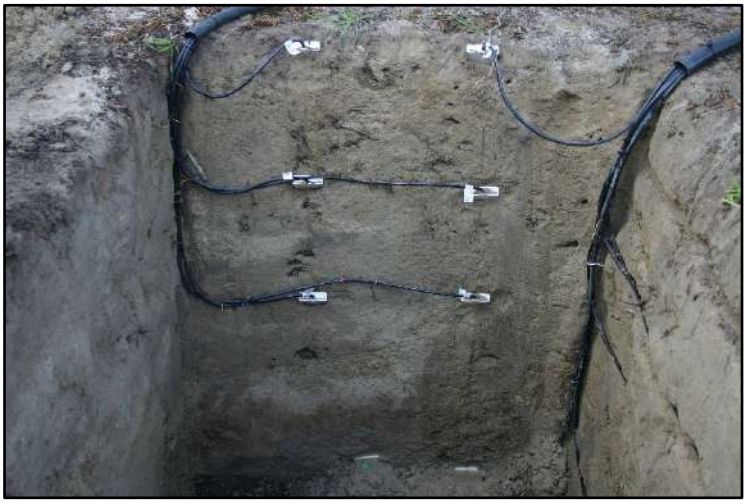

Figure 20. Soil profile pit at Welgemoed indicating a relatively uniform coarse sandy soil

Soil sampling:
During preparation of the profile holes for equipment installation soil samples for texture analysis by a commercial laboratory were taken representatively from the face of the soil profile pit for the different soil layers identified per site. At Avontuur for SWB1, soils were sampled from 0-0.19 m, 0.19-0.5 m, 0.5-0.75 m, 0.75-1.05 m and for SWB2 at 0-0.2 m, 0.0-0.6 m, 0.6-0.9 m, and 0.9-1.2 m according to the identified soil layers. At Welgemoed soils were sampled at SWB3 from 0-0.3 cm, 0.3-0.6 cm, 0.6-0.9 m and 0.9-1.15 m. For SWB4, soils were sampled at 0-0.1 m, 0.1-0.4 m, 0.4-0.7 m, 0.7-1 m and 1-1.25 m. Soil texture was identified from the particle size analysis as sandy for Avontuur and as loamy sand for Welgemoed using a soil texture map (Soil classification workgroup, 1991, Appendix A, Table 38).

Bulk density profile holes for the soil water balance sites at Avontuur were made in comparable positions as the soil water balance profile holes in adjacent rows. Bulk density was determined in the tree and work row using the core method (Blake and Hartge, 1986) in the top soil and an excavation method for the stony soil deeper in the profile (Al-Shammary et al., 2018). At Welgemoed the core method sufficed to determine bulk density in the tree row and work row for the whole profile. Bulk density profile holes for the soil water balance sites at Welgemoed were made in comparable positions as the soil water balance profile holes, but in rows 24 and 21, respectively. Due to the presence of a water table at SWB4 at the 100-125cm soil layer samples, bulk density samples could not be taken for the deepest soil layer. Bulk density at Avontuur ranged in the tree row between 1.39 and 1.547 g cm^{-3} and in the work row between 1.371 and 1.555 g cm^{-3}. At Welgemoed the bulk density ranged between 1.484 and 1.925 in the tree rows and between 1.59 and 1.923 g cm^{-3}. in the work rows (Refer to Appendix A, Table 39).

3.6.2 Soil water content and irrigation

In order to measure tree water use representatively several aspects were taken into account – namely the potential wetted area below the drip irrigation system (drip), volume of soil monitored by and orientation of the CS650 soil water content reflectometer, distinct soil horizons and root distribution patterns. To account for variability in water distribution below the drip irrigation system, CS650 sensors were installed for one dripper line secured at 300 mm from the tree row and at a position directly below the dripper nearest to the tree (c. 30 cm from the tree) as well as midway to the next dripper within the area allocated to the tree (c. 67 cm from the tree) (Figure 21). Spacing between drippers per dripper line was standard 745 mm at both sites.

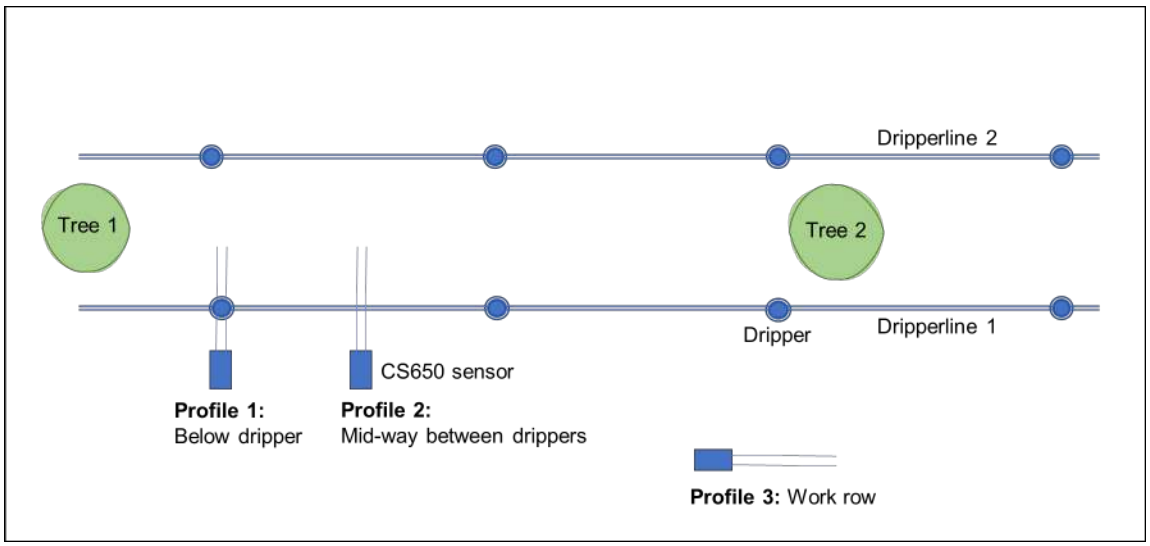

Figure 21. **Diagram indicating installation positions for CS650 soil water content reflectometers below a dripper (Profile 1), midway between two drippers (Profile 2) and in the work row area opposite a dripper and parallel to the drip line**

Another set of sensors were installed in a position representative of the work row (c. 2.25 m from the tree row) with the rods of the sensors parallel to but centred on a dripper positioned next to the tree adjacent to the one which was instrumented in the tree row (Figure 21). A set of four sensors were installed per position in different soil depth increments identified (Table 22) with the goal to measure water use for the tree root zone representatively, and to monitor if leaching of water occurs beyond the root zone.

Table 22. **Soil depth increments for installation of CS650 sensors for purposes of the soil water balance**

Site ID	Soil depth increment (mm)			
SWB1	0-200	200-500	500-900	900-1050
SWB2	0-200	200-600	600-900	900-1200
SWB3	0-300	300-600	600-900	900-1150
SWB4	0-330	330-660	660-1050	1050-1250

In order to measure soil water content as representatively as possible for the area wetted by the dripper, the CS650 sensors were installed perpendicularly to the dripper line and diagonally over the soil depth increment to be instrumented. Care was taken to install rods in the soil profile not less than 80 mm below the soil surface and a distance of at least 200 mm was maintained between rods of sensors in sequential soil layers. The angle of installation for the sensors was dictated by the smallest soil depth increment per profile. The installation depth for each sensor was selected such that the centre of the sensor rods intersected the middle of the soil depth increment. To prevent damage of sensors in the top soil layer in the work row area by orchard traffic these sensors were installed horizontally in the middle of the depth increment. Where a restrictive layer occurred at the bottom of the soil profile, installing sensors horizontally was considered sufficient for the purpose of monitoring excessive leaching.

For Avontuur, the CS650 sensors in the tree row were installed perpendicular to the dripper line and diagonally at a 75° angle relative to the soil surface (Appendix A: Figure 78a, Figure 22). The sensors entered the levelled profile wall at a distance of 226 mm from the dripper line. For the plinthic layer two c. 300 mm holes were drilled in parallel at a 75° angle relative to the soil surface to accommodate the sensor rods in the stony medium, taking into account sensor size specifications. The holes were filled with slurry made from sieved soil originating from the plinthic layer. At Welgemoed, the CS650 sensors in the tree row were installed in a similar manner as at Avontuur, but the larger soil increments between and within soil horizons allowed the sensor to be installed diagonally at a 45° angle relative to the soil surface (Appendix A: Figure 78b, Figure 23). The sensors entered the levelled soil profile wall at a distance of 170 mm from the dripper line. The sensors in the bottom restrictive clay layer and the sensors in the top soil layer of the work rows were installed horizontally. A water table was present at c. 1.25 m depth at SWB4.

Figure 22. **For the young pomegranate orchard at Avontuur CS650 soil water content reflectometers were installed in the tree row directly below the dripper nearest to the tree stem (most left-hand side) and midway to the next dripper (second from left). A set of four sensors were also installed perpendicular to the tree row in the work row (right).**

Figure 23. **For the full bearing pomegranate orchard at Welgemoed CS650 soil water content reflectometers were installed directly below the dripper nearest to the tree stem (most left-hand side) and midway to the next dripper (second from left). A set of four sensors were also installed perpendicular to the tree row in the work row (right).**

At each soil water balance installation a CR1000X logger (Campbell Scientific Inc., Logan, UT, USA) in a weatherproof box was connected to twelve CS650 soil water content reflectometers and two Multi-Jet flow meters (Arad Ltd., Dalia, Israel) to enable hourly logging of soil water content, temperature and electrical conductivity data and to monitor irrigation applied. Delays in the procurement process and calibration of the flow meters allowed installation only by 10 November 2022. Hourly logged data was downloaded on a weekly to bi-weekly basis via modem communication. The loggers for the soil water content monitoring systems at Avontuur ran on solar power, whereas batteries were changed bi-weekly for the Welgemoed site.

In situ calibration for the CS650 sensors via gravimetric sampling was conducted in the two topmost layers at Avontuur, and for all soil layers at Welgemoed. Simple linear regression and non-linear regressions were performed between actual volumetric soil water

content and bulk dielectrical permittivity measured by the sensors to obtain the calibration equations (Refer to Appendix A: Table 40). The factory calibration was used to estimate soil water content for the two deepest soil layers at Avontuur.

3.7 PLANT PHYSIOLOGY, GROWTH AND YIELD

Midday stem water potential (PMS Model 1505D-EXP pressure chamber, PMS Instrument Company, Albany, USA) and leaf level LI6400 XT infrared gas analyzer (LI-COR Inc. Nebraska, USA) measurements (stomatal conductance, net CO_2 assimilation rate and transpiration rate) at 10h00, 12h00 and 14h00 were conducted approximately monthly from October until April during the 2023/24 season on six trees per orchard (two leaves per tree) to obtain additional data on tree water status and performance. Leaves for stem water potential were enclosed in aluminium foil bags at least two hours before measurement. Shoot length (ten shoots per tree) was measured biweekly to monthly on five trees per site from 17 November 2022 until 8 February 2023 and in 2023/24 from 4 October 2023 until 18 January 2024, when shoot growth terminated. Tree stem diameter was measured on selected dates for the five trees on which shoot growth were monitored and for the trees where the soil water balance equipment was installed. In 2022/23 fruit thinning was completed by mid-December, but in 2023/24 thinning at Avontuur was completed only by 8-12 January 2023. Poor flowering and absence of a third flower flush as well as poor fruit set resulted in an abnormally low crop load at the full bearing orchard at Welgemoed and no thinning was done during 2023. After fruit set of the second flower flush, ten fruit per tree of the same trees for which shoot growth were measured, were tagged and fruit diameter measured about monthly. At harvest, all fruit per tree were harvested according to producer norms and the total yield mass per tree determined. In 2023 fruit of eleven trees (2 soil water balance, 4 sap flow, 5 growth, 6 stem water potential) were harvested and in 2024, after adding six stem water potential measurement trees, seventeen trees. Fruit were harvested at Avontuur on 7 March 2023 and on 7 and 14 March 2024. At Welgemoed fruit were harvested on 17 and 27 March 2023 and on 18 March 2024.

Fractional light interception (FI) was measured in 2022/23 at the two soil water balance trees from September 2022, and in addition at the four sap flow trees from December 2022 when a second LP-80 Accupar ceptometer (METER, Pullman, USA) became available. Measurements continued until early July in 2023. In 2023/24, the measurement protocol was adapted to measure fractional light interception at eight trees per site per measurement day using two Accupar LP-80 ceptometers. Measurements were done about monthly at the young and the full bearing orchards from August 2023 until June 2024 on full sun days. Due to weather conditions that turned unfavourable, a complete data set was not collected for Welgemoed on 27 September 2023 (only four sap flow trees measured) and no data was collected at end March 2023. Measurements on both sides of the tree row were conducted about one hour before to one hour after solar noon. Measurements with the 80 cm long probe were done at a constant height from the ground with the probe perpendicular to the tree row. For each side of the tree row, sequential sets of measurements were done in the tree row with the tip of the probe kept at distances of 0 m, 0.8 m and 1.6 m from the centre of the tree row. For Avontuur (tree spacing 2.5 m x 5 m) photosynthetic active radiation levels were measured in the tree row at 0 m, 0.5 m, 1 m, 1.5 m, 2 m and 2.5 m from the edge of the allocated area per tree and for Welgemoed (tree spacing 2 m x 4.5 m) at 0, 0.4 m, 0,8 m, 1.2 m, 1.6 m and 2 m.

Tree canopy dimensions (tree height, width in the tree row and across the tree row at mid-canopy height, bottom width and height) were measured for the sap flow, soil water balance and five growth trees (n=11) on same dates or within three days of the FI measurements. From December 2023 onwards canopy dimensions were also measured for trees on which stem water potential was measured (n=6). Fractional light interception was measured during April 2024 for a range of tree sizes (n=6) at each orchard and leaves were collected during natural leaf fall to calibrate the Accupar LP-80 for actual leaf area index (LAI) estimates. A regression relationship was obtained between Accupar LP-80 ceptometer derived LAI (CP-LAI) and LAI calculated from measured canopy dimensions and actual leaf area. Leaf area index was expressed per tree canopy area (Tr-LAI) and orchard area allocated per tree (OLAI). In 2023/2024, on the same dates that FI was measured, the shaded tree area was determined for three trees per orchard using a manual method that employed 10 cm x 10 cm demarcated hard boards that covered the full surface allocated per tree. Photos were taken of the shaded area and the number of shaded blocks and their degree of shading (25%,50%, 75% or 100%) in the allocated area was determined and averaged. The shaded area was related by linear regression to FI, CP-LAI, Tr-LAI and OLAI.

3.8 FRUIT QUALITY, WATER USE EFFICIENCY AND PRODUCTIVITY

Quality evaluation of all harvested fruit was performed at harvest and individual fruit weight, diameter, colour, sunburn, cracking, blemishes and pest, disease or bird damage ("Other") were classed according to the norms below to compare fruit marketability (Table 23) and to determine gross farm income. Fruit were discarded if damage/ disease extended beyond the integument into the arils. Gross farm income per orchard was determined per marketing class based on the average amounts paid out by a local export company in 2024 for exported fruit and by a local company for juice. Fruit were paid per kg and for purposes of juice, per ton. It was assumed that discarded fruit did not contribute to income. More detailed fruit quality evaluation at harvest (one harvested fruit sampled randomly per tree) included fruit length and diameter, fruit skin colour, colour of the arils and the total soluble solids (TSS), pH, and titratable acidity (TA) of the pomegranate juice. The total soluble solids, total titratable acids and pH (n=3) were determined on juice extracted from pooled samples of fruit.

Table 23. Pomegranate fruit marketing classification norms.

Quality variable	Subdivi-sion	MARKETING CLASS				
		EXTRA CLASS	CLASS 1	PROCESSING	JUICE	DISCARD
Weight (kg)		≥0.25	≥0.25	≥0.19	<0.19	<0.19
Skin colour[1]		1 to 2	3 to 6	7 to 9	Not applicable	Not applicable
Sunburn	Colour	N = none	LB = light brown	LDB = light and dark brown	BL = black	BL = black
	Degree	N = none	L10 = ≤10% surface	M10 = >10% surface	L10 or M10	L10 or M10
Cracking		N = none	N = none	INT = up to integument	INT = up to integument	ARIL = up to arils
Blemishes		N = none	EL10 = 10% surface	EL25 = 25% surface	M25 = >25% surface	M25 = >25% surface
Other		N = none	N = none	N = none	1= up to integument	2=Affecting arils

1 Colour chart

Water use indicators used to quantify pomegranate water use and productivity included orchard water use efficiency, biophysical water productivity in terms or transpiration or evapotranspiration, as well as economic crop water productivity in terms of either transpiration or evapotranspiration. Orchard water use efficiency was calculated either as transpiration or as crop evapotranspiration divided by the sum total of water supplied by irrigation and effective rainfall. Daily rainfall was corrected for evaporative losses by subtracting 0.2ETo (Allen at al., 1998). Biophysical water productivity is the ratio of marketable yield to transpiration or crop evapotranspiration. Economic crop water productivity is the ratio between gross farm income and transpiration or evapotranspiration.

3.9 STATISTICAL ANALYSIS

Simple linear regressions and multiple stepwise regressions were conducted to obtain calibration relationships and to establish the most important factors affecting transpiration and evapotranspiration using STATGRAPHICS Centurion XV, SAS software (Version 9.4, SAS Institute Inc, Cary, USA) and XLStat (Lumivero, 2024, XLSTAT statistical and data analysis solution. https://www.xlstat.com/en).

CHAPTER 4: TRANSPIRATION OF YOUNG AND FULL BEARING POMEGRANATE TREES

4.1 INTRODUCTION

Transpiration is the process by which plants lose water (Ryugo, 1988). Nearly all water taken up by the plant is lost by transpiration and only a small fraction is used within the plant (Allen et al., 1998). About 90% of water absorbed by the roots is removed through stomatal transpiration, whereas the remaining water is lost through cuticular transpiration, lenticels and guttation (Ryugo, 1988). Stomatal transpiration entails the vaporization of liquid water present in plant tissues and removal of the vapour to the atmosphere through stomata embedded in plant leaves (Allen et al., 1998). The rate of transpiration is therefore closely linked to the energy available, vapour pressure deficit and wind and to interpret transpiration dynamics it is important to monitor radiation, air temperature, air humidity and wind. Transpiration rate is also determined by crop characteristics, different crop development stages, the surrounding environment and management practices. This chapter present micrometeorological information for the research sites and details on tree physiology, growth, yield and fruit marketability for the young and full bearing pomegranate orchards where transpiration was monitored. Information on transpiration-based water productivity concludes the chapter.

4.2 METHODOLOGY

4.2.1 Site and general methodology description

The research was conducted at a young pomegranate orchard at Avontuur (33°07'29.7"S; 18°56'08.8"E) and at a full bearing pomegranate orchard at Welgemoed (33°35'18.3048"S; 18°59'19.302"E), which covers an area of 6.7 and 4.9 hectares, respectively (Refer to Chapter 3.4). Orchards were managed by the farm managers according to their respective farm practices. An automatic weather station was installed within 50 m from each orchard to monitor rainfall and the necessary variables hourly to calculate reference evapotranspiration (ETo) and to relate the weather variables to transpiration (Refer to Chapter 3.5). Midday stem water potential (PMS Model 1505D-EXP pressure chamber, PMS Instrument Company, Albany, USA) and leaf level LI6400 XT infrared gas analyzer (LI-COR Inc. Nebraska, USA) measurements (stomatal conductance, net CO_2 assimilation, transpiration rate) at 10h00, 12h00 and 14h00 were conducted approximately monthly during the season on six trees per orchard (two leaves per tree). Tree growth was monitored by measuring stem diameters, shoot and fruit growth at selected times whereas yield, fruit maturity and fruit quality was quantified at harvest (Refer to Chapter 3.7 and 3.8). Gross farm income per orchard was determined per marketing class based on the average amounts paid out by a local export company for exported fruit and local market payments for juice. Transpiration based water use efficiency was calculated as the ratio of transpiration to the sum total of effective rainfall and irrigation applied. Transpiration-based water productivity was calculated as the ratio of marketable yield to crop transpiration, whereas economic crop transpiration water productivity is the ratio between gross farm income and transpiration.

4.2.2 Sap flow

According to the sap flow scoping study (Refer to Chapter 3.3 for details regarding methodology), transpiration of pomegranate trees can be measured using the heat ratio method (HRM) of the heat pulse velocity (HPV) sap flow technique as described by Burgess et al. (2001) (Appendix B). Two heat pulse velocity heat ratio sap flow systems consisting each of one logger box with a CR1000X logger and AM32/16 multiplexer and four custom built tree boxes (Aquamet, Pietermaritzburg) were wired and tested in the laboratory before the equipment was deployed in the orchards. The response of the thermocouples to ice and warmer conditions was tested and heater functionality monitored. Selection of trees for the sap flow measurement per orchard was, as for the soil water balance sites, based on the stem size distribution of stem diameters measured at 200 mm above the ground (Refer to Chapter 3.4). The sap flow system at Avontuur was installed from 15-16 August 2022, and at Welgemoed in the following week (Figure 24). For the young pomegranate orchard one tree in the range of 40-48 mm (45. 3 mm), two trees in the range of 48-64 mm (54.5, 64.5), and one tree in the range of 64-80 mm (67.3) was selected. For the full bearing orchard one tree each was selected for the 64-80 mm (71.7 mm) and 80-96 mm

(90.3 mm) stem diameter ranges. Since there were not trees of the 111-127 mm stem diameter range with stems suitable for the HRM near enough to the other three trees that were selected for monitoring, two trees were selected for the 95-111 mm stem diameter range (94.8 mm, 101.9 mm).

Figure 24. Heat pulse velocity heat ratio method equipment installed during August 2022 to monitor sap flow during the 2022/23 season in a) a young cv. 'Wonderful' pomegranate tree at Avontuur and b) a full bearing tree at Welgemoed. Four sets of thermocouples and heaters were installed in different positions around the stem.

To determine transpiration for the second season, the sap flow systems had to be removed and reinstalled in different trees (Figure 25). In July 2023 stem diameter distribution at 200 mm above the ground was determined for each orchard for a subset of 30 trees and four stem diameter ranges identified for installation of the sap flow equipment in four trees.

Figure 25. Activities during removal and reinstallation of sap flow systems during July 2023 included: a) Dr Dzikiti (collaborator from SU) instructing students and research team, b) sampling to determine wood properties, c) tree core sampling, d) rewiring sap flow system tree boxes, e) installation of thermocouples and heaters in trees, f) testing the system.

Equipment was installed in young pomegranate trees from Avontuur with stem diameters 200 mm above the ground in the range of 50-59 mm (57.3 mm), 59-67 mm (63.6 mm), 67-76 mm (72.9 mm) and 76-84 mm (82.1 mm). For the full-bearing orchard at Welgemoed sap flow equipment was installed for one tree each in the following stem diameter ranges: 72-82 mm (79.9 mm), 82-93 mm (92 mm), 93-104 mm (98.3 mm) and 104-115 mm (108.5 mm). Sap flow was monitored at four stem depths per tree to account for the radial variations in sap velocity, using one set of sensors (an upper and lower thermocouple and one heater element) per stem depth. Heat pulse velocity (cm h^{-1}) for each sensor set was logged hourly per site using a CR1000X logger (Campbell Scientific Inc., Logan, UT, USA) connected to a AM16/32B multiplexer. Data were downloaded via modem communication on a weekly to bi-weekly basis while maintenance of sap flow systems (battery swop, realignment of thermocouples as required) occurred bi-weekly. Sap flow data were collected at Avontuur and Welgemoed from August until May in the 2022/23 and 2023/24 seasons.

Sap velocity data were processed from October until May each season for all instrumented trees (total 8). Non-numerical (NAN) indicators or spikes occurring in recorded data were replaced by interpolating data. Where data of more than one consecutive hour was not usable, a statistical regression equation obtained between the heat pulse velocity of thermocouple sets at adjacent depths were used to estimate and replace the missing data (data not shown). The four heat pulse velocity datasets obtained per tree were corrected for the offset from zero by manually estimating the offset from data graphed for ten-day periods. The approach of Burgess et al. (2001) was followed thereafter to correct the heat pulse velocity data for wounding due to sensor implantation. When wood samples were taken at the end of the 2022/23 season wound width was on average 2.9 mm, wood moisture content 71.8% and wood density 0.656 g cm^{-3}. Wound width determined at the end of 2023/24 season was on average 2.13 mm, wood moisture content 69.56% and wood density 0.93 g cm^{-3}. The hourly total sap flow volume (ℓ $tree^{-1}$) by each tree was calculated as a weighted sum of the products of the sapwood area and the sap flux density (or sap velocity) represented by the specific probe. The weights are the sapwood areas represented by each probe. The sapwood area was determined 2-3 days after injecting methylene blue stain in actively transpiring trees by taking and inspecting stem core samples. The hourly sap flow volume values were accumulated from 01h00 to midnight to obtain a daily sap flow value. The daily sap flow values of the four trees were weighted to obtain orchard level transpiration considering the frequency of the stem size distribution ranges identified for the orchard in July 2023. Orchard level transpiration was calculated for both seasons as:

$$T\_Young\ orchard = (0.367 \times T1) + (0.2 \times T2) + (0.1 \times T3) + (0.333 \times T4) \quad [Eq.\ 26]$$

$$T\_Full\ bearing\ orchard = (0.1 \times T1) + (0.333 \times T2) + (0.133 \times T3) + (0.433 \times T4) \quad [Eq.\ 27]$$

Where T = Transpiration in ℓ d^{-1} or mm d^{-1} and T1-T4 refer to transpiration of the four respective trees.

4.3 RESULTS AND DISCUSSION

The weather conditions prevailing during and tree physiology, growth and yield that may have affected transpiration in the experimental period are presented in Sections 4.3.1 and 4.3.2. The seasonal dynamics of transpiration and summary of total seasonal transpiration (Section 4.3.3.) is followed by an analysis of selected weather and tree factors that affect transpiration (Section 4.3.4). The chapter concludes with relevant information on fruit marketability and transpiration-based water productivity for the young and full bearing pomegranate orchards- (Section 4.3.5).

4.3.1 Micrometeorological data

The monthly mean daily maximum and minimum temperature and maximum and minimum relative humidity for Avontuur and Welgemoed for August 2022 until June 2024 are displayed in Figure 26. The daily maximum temperatures for the two sites were fairly similar (differed by less than 1°C) except for the tendency for it to be higher at Avontuur early in the season (September and October 2022, November 2023, Figure 26a). The daily maximum temperature for both seasons occurred at both sites in January and reached 33.5°C and 33.2°C at Avontuur and Welgemoed, respectively, in 2023, whereas it was similar for both sites in 2024 (34.7°C). The daily minimum temperatures for Avontuur tended to be between 0.6 and 3.7°C higher than that at Welgemoed, except for September 2022, which was 1.1°C lower. The seasonal minimum daily minimum temperature at the young orchard was 7.4°C and 6.4°C for

August 2022 and July 2023, respectively. The minimum daily minimum temperature for Welgemoed for 2022/2023 was 5.6°C (August) and 3.9°C for 2023/2024.

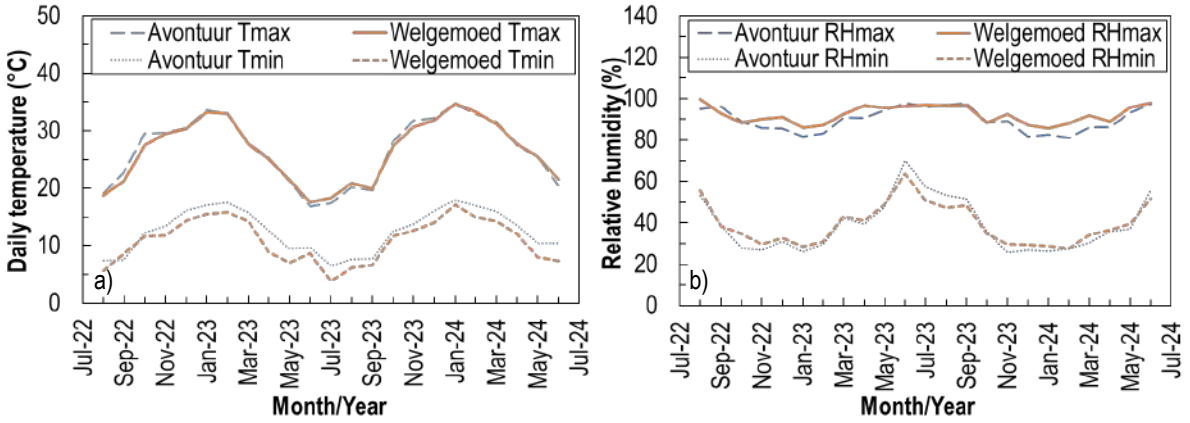

Figure 26. Monthly mean (a) daily maximum (Tmax) and minimum (Tmin) temperature and (b) maximum and minimum relative humidity for Avontuur and Welgemoed for August 2022 until June 2024

The monthly mean of the daily maximum relative humidity ranged for Welgemoed over the two seasons between 85.8% and 99.5% with the lowest values being recorded in January of each season (Figure 26b). During both seasons from about November until May the daily maximum relative humidity tended to be higher at Welgemoed compared to at Avontuur. Daily minimum relative humidity at Welgemoed ranged between 28.5% and 63.6% for 2022/2023 and between 27.7% and 51.6% for 2023/2024. The maximum relative humidity was somewhat lower at Avontuur, ranging from 81% to 97.7%, with the minimum relative humidity being between 25.8% and 70%. The minimum relative humidity was the lowest during January, decreasing in both seasons to about 26% at Avontuur and to 29% at Welgemoed. The minimum relative humidity at Avontuur tended to be lower than that at Welgemoed during both main growing seasons (November - May) but was between 3.1% and 6.6% higher from June until September 2023.

Daily total solar radiation for Avontuur increased from 14.3 MJ m^{-2} d^{-1} in August 2022 to 27.4 MJ m^{-2} d^{-1} in January 2023, decreased to a minimum of 7.1 MJ m^{-2} d^{-1} in June 2023 and increased to a maximum of 30.2 MJ m^{-2} d^{-1} in December 2023 (Figure 27a). For Welgemoed, daily total solar radiation increased from 11.4 MJ m^{-2} d^{-1} in August 2022 to 27.5 MJ m^{-2} d^{-1} in January 2023, it decreased to a minimum of 5.9 MJ m^{-2} d^{-1} in June 2023 and increased in December 2023 to a maximum of 32.6 MJ m^{-2} d^{-1}. The total daily solar radiation for June 2024 was comparable 9.2 and 8.6 MJ m^{-2} d^{-1} for Avontuur and Welgemoed, respectively. For the period March until September 2023 Avontuur received between 8% and 21% more solar radiation than Welgemoed.

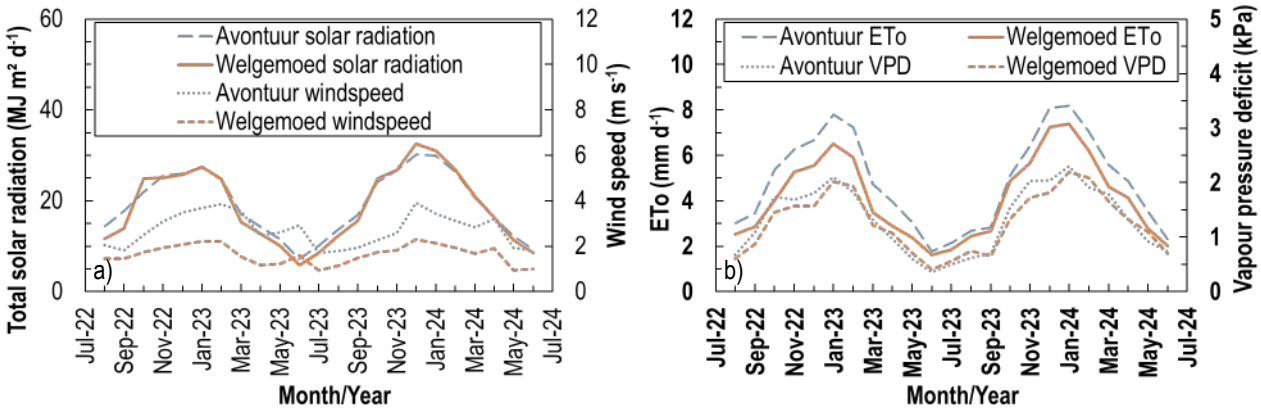

Figure 27. Monthly mean a) daily total solar radiation and average daily windspeed and b) reference evapotranspiration (ETo) and vapour pressure deficit for Avontuur and Welgemoed for August 2022 until June 2024

The daily average wind speed from August 2022 until June 2024 ranged for Avontuur between 1.7 m s^{-1} and 3.9 m s^{-1} and was a bit lower for Welgemoed – i.e. between 0.9 m s^{-1} and 2.3 m s^{-1} (Figure 27a). The maximum daily average wind speed occurred at both sites during February 2023 and December 2023 for the 2022/2023 and 2023/2024 seasons, respectively. The reference evapotranspiration for the two research sites displayed more or less the same trend over the measurement period, with that at Avontuur being consistently higher (between 5% and 36%) than at Welgemoed (Figure 27b). The ETo for Avontuur increased from August 2022 to January 2023 from 3 mm d^{-1} to 7.8 mm d^{-1}, decreased to 7.2 mm d^{-1} in February and more steeply to March (4.8 mm d^{-1}), being 1.8 mm d^{-1} at the end of the season. The ETo for Welgemoed increased from August 2022 to January 2023 from 2.1 mm d^{-1} to 6.5 mm d^{-1}, decreased to 5.9 mm d^{-1} in February and more steeply towards March (3.5 mm d^{-1}), being 1.6 mm d^{-1} at the end of the season (Figure 27b). The reference evapotranspiration for August and September 2023 was lower compared to that of 2022 and increased from about 2.5 mm d^{-1} in September to 8.2- and 7.4 mm d^{-1} in January 2024 for Avontuur and Welgemoed, respectively. The ETo was for most of the experimental period greater at Avontuur compared to Welgemoed reaching a total of 1614.5 mm compared to 1302.6 mm from August 2022 until June 2023 (i.e. c. 24% more). The difference was less for the 2023/2024 season (c. 14%) when the seasonal ETo amounted to 1727.5 mm at Avontuur and 1521.8 mm at Welgemoed.

The average daily vapour pressure deficit at Avontuur ranged between 0.3- and 2.3 kPa compared to between 0.4- and 2.2 kPa at Welgemoed, which seems quite similar (Figure 27b). The vapour pressure deficit was though higher from earlier in the season (August 2022/ September 2023) until January at Avontuur compared to that at Welgemoed. Total rainfall per month during the experimental period ranged for Avontuur between zero (October 2022) and 187 mm (June 2023), and for Welgemoed between 0.8 mm (January 2024) and 171 mm (June 2023) (Figure 28). At Avontuur rainfall totals of less than 20 mm was recorded for September until November 2022, January 2023 and October 2023 until May 2024. Avontuur received more than 20 mm of rainfall during August 2022 (65 mm), December 2022 (81 mm) and from March until October 2023. After a relatively dry summer, 143 mm of rainfall occurred in June 2024. Welgemoed received more than 20 mm of rainfall for most of the experimental period except for October 2022, January and February 2023, October 2023 until February 2024 and April 2024. During the 2022/2023 and 2023/2024 seasons Avontuur received in total 513 mm and 329 mm of rainfall, respectively, compared to 740 mm and 491 mm at Welgemoed during the respective seasons.

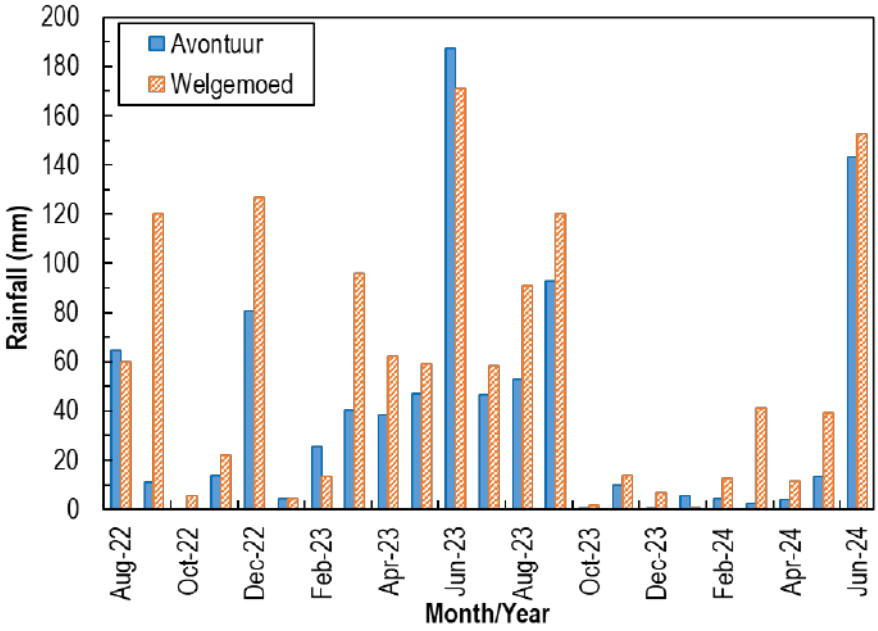

Figure 28. Monthly total rainfall at Avontuur and Welgemoed for August 2022 until June 2024

4.3.2 Tree physiology, growth and yield

Physiological measurements reported on include stem water potential, leaf level g_s, A_n and transpiration rate measured during the course of the 2023/24 season. On selected days between the beginning of October 2023 and end April 2024 the midday stem water potential for the young orchard remained between -0.703 and -0.945 MPa, whereas it fluctuated between. -0.687 and -1.076 MPa for the full bearing orchard (Figure 29). The midday stem water potential tended to decrease from 23 November 2023 until 22 February

2024 shortly before harvest, but it remained below -1 MPa for the young orchard. The midday stem water potential at the full bearing orchard reached -1.038 MPa by about mid-January, but it recovered slightly before harvest to -0.962 MPa. It reached a minimum of -1.076 MPa in about mid-April near the end of the season. Intrigliolo et al. (2023) suggested threshold midday stem water potential values for pomegranate trees of -1 MPa or less during the growing season being indicative of optimum water status under Mediterranean conditions.

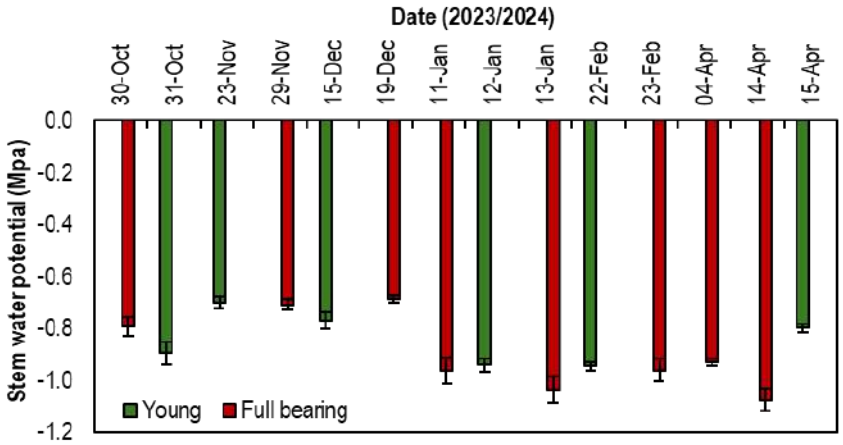

Figure 29. Midday stem water potential (± standard error) for young and full bearing pomegranate trees monitored between October and mid-April during the 2023/2024 season at Avontuur and Welgemoed farms, respectively

For the young orchard there was large variability between g_s of leaves for the measurements conducted at 10h00 (Figure 30a). In general, g_s was the highest at 10h00 and the lowest at 14h00. Over the season the highest g_s occurred at 10h00 during January and February 2024, being 0.395 and 0.369 mol m^{-2} s^{-1}, respectively. In January the g_s at 12h00 and 14h00 decreased by c. 20% and c. 30%, respectively, compared to g_s at 10h00. In February g_s at 10h00 and 12h00 was comparable whereas it decreased at 14h00 by 16% compared to g_s at 10h00. The g_s at 10h00 dropped in April by c. 55% compared to g_s in summer. In April the g_s at 12h00 and 14h00 was 43% and 60% lower, respectively, compared to g_s at 10h00.

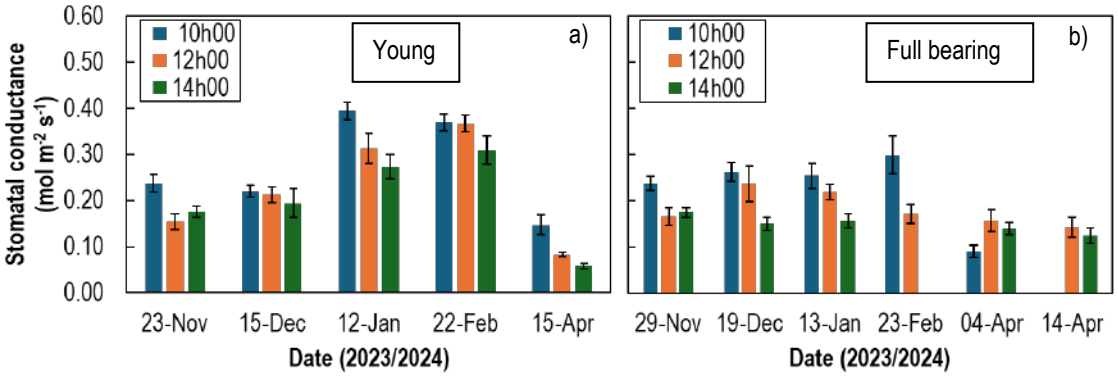

Figure 30. Leaf stomatal conductance at 10h00, 12h00 and 14h00 for a) young and b) full bearing pomegranate trees monitored between November 2023 and April 2024 at the Avontuur and Welgemoed farms, respectively

The g_s at 10h00 at the full bearing orchard was similar to that for the young orchard in November 2023, and it remained more or less at similar levels, even though it increased slightly towards February 2024, reaching a maximum of 0.298 mol m^{-2} s^{-1} for the season (Figure 30b). This was 19% less than the maximum g_s measured in February 2024 for the young orchard. The g_s at 12h00 was comparable to that at 14h00 for November and April, while it was 10% and 14% lower compared to g_s at 10h00 during December and January. In February the g_s at 12h00 decreased by 43% compared to g_s at 10h00. The general trend for g_s at 12h00 was to increase from November to December and to gradually decrease thereafter towards April 2024. The g_s at 14h00 appeared static at about 0.15 mol m^{-2} s^{-1} during December, January and early April but decreased in general from November 2023 towards April 2024 (Figure 30b).

There was no data available for g_s at 14h00 for February, but it was 27%, 43% and 38% lower than g_s at 10h00 in November, December and January, respectively. The g_s in April dropped quite steeply and was unexpectedly lower at 10h00 compared to later in the day. There was no g_s data for 10h00 available for mid-April.

The A_n was in November 2023 at 10h00 c. 13 µmol CO_2 m^{-2} s^{-1} for both the young and full bearing orchards (Figure 31). For the young orchard the A_n at 10h00 ranged between 16.4 and 18.3 µmol CO_2 m^{-2} s^{-1} during summer, values being similar if the standard error is taken into account (Figure 31a). The A_n at 12h00 and 14h00 was lower compared to 10h00, but the difference tended to decrease towards harvest. The A_n at 12h00 increased linearly from 6.1 µmol CO_2 m^{-2} s^{-1} November to 16.1 µmol CO_2 m^{-2} s^{-1} in February, with the difference between A_n at 12h00 and 10h00 decreasing from 52% to 12% towards harvest. The A_n at 14h00 was, compared to A_n at 10h00, 67%, 52%, 43% and 31% lower in November, December, January and February, respectively. The A_n in April 2024 dropped by almost 50% compared to February. The A_n at 10h00 and 12h00 did not differ, but it was at 14h00 21% lower compared to A_n at 10h00.

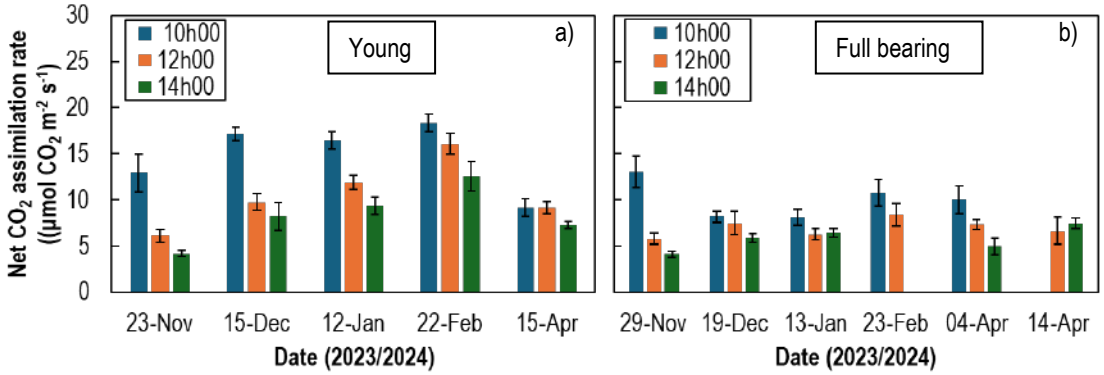

Figure 31. Net CO_2 assimilation rate (µmol CO_2 m^{-2} s^{-1}) at 10h00, 12h00 and 14h00 for a) young and b) full bearing pomegranate trees monitored between November 2023 and April 2024 at the Avontuur and Welgemoed farms, respectively

For the full bearing orchard the A_n at 10h00 decreased in December 2023 and January 2024 by c. 38% to compared to November, reaching only 8.1 µmol CO_2 m^{-2} s^{-1} (Figure 31b). It increased slightly towards February, becoming 10.8 µmol CO_2 m^{-2} s^{-1} and remained at similar levels in April. It was in February still 17% lower compared to A_n at the beginning of the season. The A_n at 12h00 ranged between a minimum of 5.8 µmol CO_2 m^{-2} s^{-1} in November and a maximum of 8.4 µmol CO_2 m^{-2} s^{-1} in February. The A_n at 12h00 was 56%, 9%, 23%, 22% and 27% lower than A_n at 10h00 for November, December, January, February and early in April, respectively. The A_n at 14h00 ranged between 4.1 and 7.5 and was 68%, 29%, 21% and 50% lower compared to A_n at 10h00 in November, December, January and early April.

At the young orchard the highest leaf transpiration rate occurred at 14h00, followed by that at 12h00 and then at 10h00 (Figure 31a). Leaf level transpiration at 10h00 was similar to that at 12h00 for November 2023 as well as for January and April 2024. At the full bearing orchard, with the exception of February 2024, leaf transpiration rate at 12h00 tended to be similar to or higher than at 10h00 (Figure 31b). The transpiration rate at 14h00 was, except for November 2023 when it reached 9.9 mol H_2O m^{-2} s^{-1}, lower than or comparable to the transpiration rate at 12h00.

At the young orchard the transpiration rate at 10h00 was in November and December 2023 similar and on average about 6.3 mol H_2O m^{-2} s^{-1}. It thereafter increased by 41%, reaching a seasonal maximum of 8.9 mol H_2O m^{-2} s^{-1} in January 2024 (Figure 32a). The transpiration rate decreased before harvest and in mid-April by c. 21% and 60%, respectively, compared to January. Transpiration rate at 10h00 compared to that at 12h00, was lower in December 2023 and February 2024. The transpiration rate at 12h00 tended to increase from 6.6 mol H_2O m^{-2} s^{-1} in November to 9.2 mol H_2O m^{-2} s^{-1} in January, with comparable transpiration rate levels for January and February 2024. Transpiration rate at 14h00 followed the same trend as that at 10h00 and was 49%, 26%, 17% and 42% higher compared to the transpiration rate at 10h00 in November, December, January and February, respectively. It reached seasonal maximum values of 10.4 and 10 mol H_2O m^{-2} s^{-1} in January and February, respectively.

For the full bearing orchard leaf transpiration rate at 12h00, with exception or November, tended to be the higher than at 10h00 or 14h00 (Figure 32b). It was 5%, 4% and 11% higher than transpiration rate at 10h00 in November, December and January, respectively, but not significantly different if the standard error is considered. The transpiration rate amounted to 7.2, 10.7 and 9.1 mol H_2O m^{-2} s^{-1} for the respective months. The transpiration rate at 12h00 tended to decrease linearly as the season progressed from December 2023 until April 2024 and was reduced by 62% by the end of the season. Transpiration rate at 10h00 increased in February suddenly to 9.3 mol H_2O m^{-2} s^{-1}, whereas it was unexpectedly low early in April. The transpiration rate at 12h00 was 7.5 mol H_2O m^{-2} s^{-1} in February.

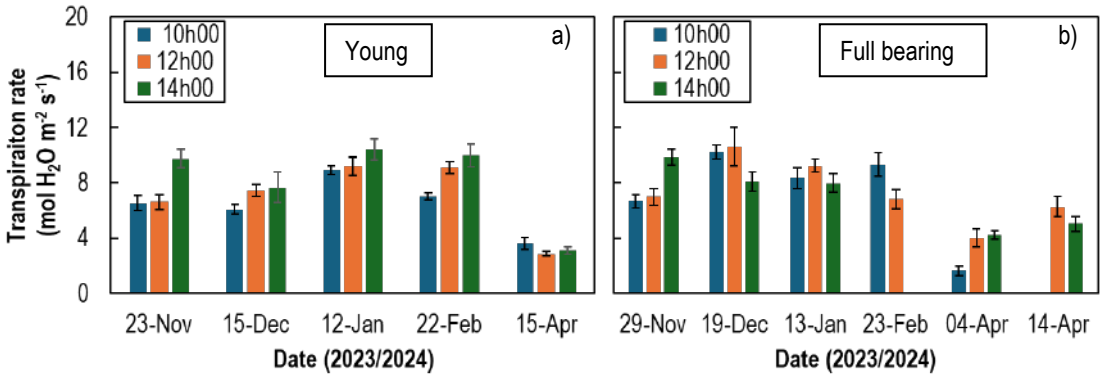

Figure 32. Leaf transpiration rate (mol H_2O m^{-2} s^{-1}) at 10h00, 12h00 and 14h00 for a) young and b) full bearing pomegranate trees monitored between November 2023 and April 2024 at the Avontuur and Welgemoed farms, respectively

Measurement of shoot lengths started in 2022/2023 near the end of the first vegetative growth flush on 17 November 2022 (Figure 33a). From the start of the growth period shoots of the young pomegranate orchard appeared to be longer but did not differ significantly from that of the full bearing orchard (c. 38 cm vs c. 28 cm). Growth over the measurement period for the young orchard (7.7 cm) appeared to be more vigorous compared to that for the full bearing orchard (2.3 cm). Shoot length on 4 October 2023 (Day of season (DOS) 34) was on average slightly more for the young than full bearing orchard, being 18.4 cm and 15.4 cm, respectively (Figure 33b). From 4 -18 October 2023, the shoots of the young orchard had almost double the growth rate (2.4 cm d^{-1}) of the full bearing orchard (1.3 cm d^{-1}). Slower growth at the full bearing orchard may have been due to the very wet conditions followed by high depletion of soil water in an almost rain free October before irrigation commenced (data not shown). Total shoot length for 2023/2024 amounted to 94.5 cm for the young and 72.2 cm for the full bearing orchard, compared to 45.6 cm and 30.5 cm for the 2022/2023 season.

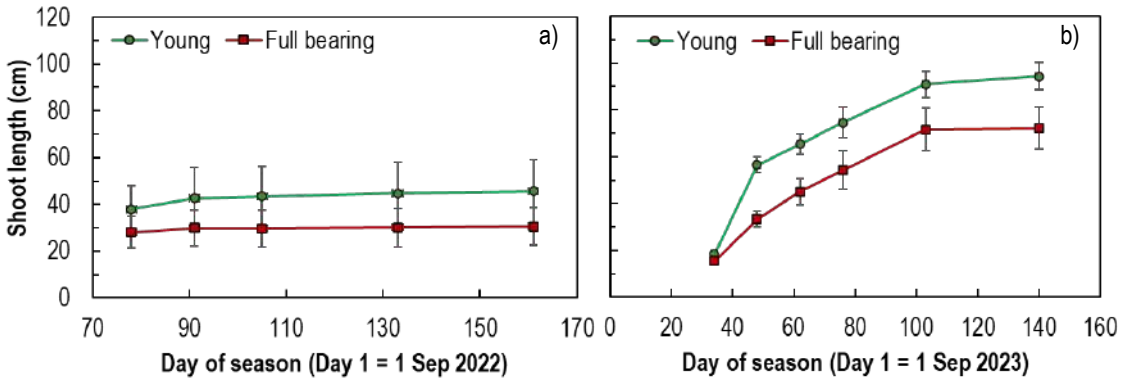

Figure 33. Shoot length (±standard error) for young and full bearing pomegranate trees monitored during the 2022/2023 and 2023/2024 seasons at Avontuur and Welgemoed farms, respectively

The stem diameter of the young orchard was for the 2022/2023 season on average 54.4 mm at the beginning (measured 31 August 2023) and 66.7 mm at the end, increasing to 78.8 mm at the end of the 2023/2024 season (Figure 34). Stem growth amounted to about 11 mm in each season. The stem diameter of the full bearing orchard was on average 94.2 mm and 96.8 mm at the beginning and end of the first season and 102.5 mm at the end of the second. The full bearing orchard stem diameter increased by 2.6 mm in the 2022/2023 season and by 5.6 mm in 2023/2024.

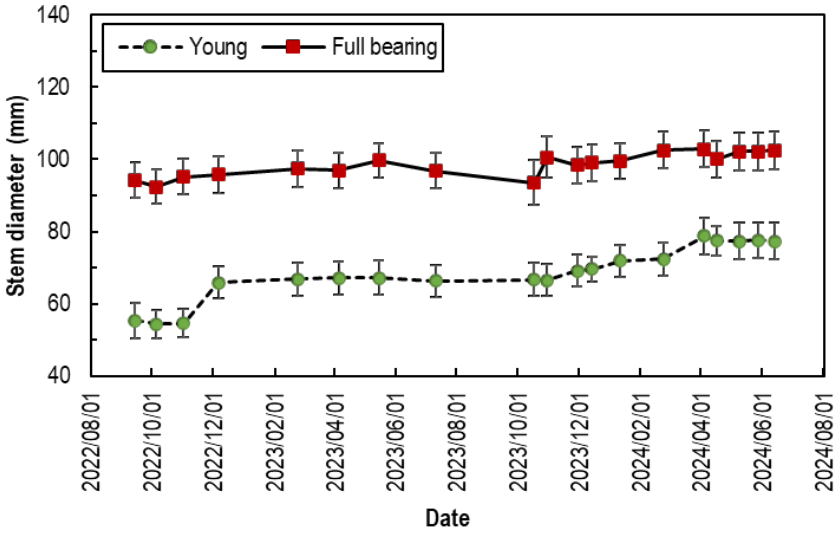

Figure 34. Averaged stem diameter (n=7) for young and full bearing pomegranate trees monitored during the 2022/2023 and 2023/2024 seasons at Avontuur and Welgemoed farms, respectively

During 2022/2023 the fruit diameter was fairly similar at thinning during mid-December for the young and the full bearing trees, being 62 mm and 59 mm, respectively (Figure 35a). By the 8th of March 2023 the fruit diameter of fruit on the young trees increased by 28 mm and for the full bearing trees by 29 mm, resulting in fruit diameters of 90 mm and 88 mm for the two respective orchards. In 2023/2024 fruit size measurements commenced on 1 December 2023 and fruit diameter at the young orchard was on average 54.9 mm, whereas it was 49.5 mm at Welgemoed (Figure 35b). By harvest fruit diameter increased to 98 mm and 93 mm for the two respective orchards. The increase in diameter since measurements started was comparable, i.e. 43 mm for the young and 44 mm for the full bearing orchard. Smaller fruit from December 2023 throughout the season at the full bearing compared to the young orchard may partially be attributed to less assimilates available early in the season due to limited shoot growth (Figure 34b) under extremely wet conditions followed by high levels of soil water depletion during October 2023 (data not shown) and lower net photosynthesis rates from December until harvest at the full bearing compared to the young orchard (Figure 31a and b).

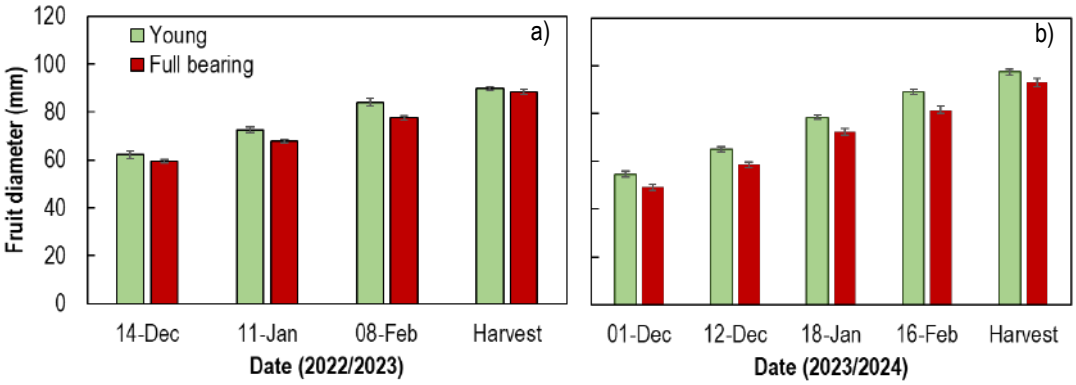

Figure 35. Fruit diameter for five young and full bearing pomegranate trees monitored during the 2022/2023 (a) and 2023/2024 (b) season at Avontuur and Welgemoed farms, respectively. Harvest indicates fruit diameter at harvest in March/April. Diameter data for the young orchard for harvest 2023 was derived from 202 fruit harvested on 7/3/2023.

At the young orchard in 2023, 202 fruit (5.938 t ha^{-1}) were harvested on 7 March, but total yield data was not collected since the second harvest was compromised by theft. For the mature orchard at Welgemoed yield amounted in the 2022/2023 season to 31.5 (±14.3) kg $tree^{-1}$ or 35±15.89 t ha^{-1}, 1058 fruit). This agreed well with the average of 33 t ha^{-1} harvested by the farm for Block W43. In 2023/2024,

both orchards were harvested in March 2024 and the young orchard had almost double the amount of fruit (1495 fruit) compared to that obtained from the full bearing orchard (778 fruit). Total yield (±standard error) for the 2023/2024 season for the orchard at Avontuur amounted to 34.2 (±14.53) kg per tree (27.4 ±11.62 t ha^{-1}). There was no yield data recorded for the block by the farm. For 2023/2024 the yield at Welgemoed varied enormously between trees i.e. by between 3.7 to 35.6 kg tree^{-1}. The trees yielded on average 15.9 (±9.02) kg fruit per tree (17.7±10.02 t ha^{-1}), which is a reduction of more than fifty percent compared to 2022/23. It compared relatively well with the average yield of 14 t ha^{-1} recorded by the farm for the block in 2023/2024. The low yield was attributed to poor and protracted flowering and poor fruit set in 2023. The farm experienced low yield previously also in 2018, when it totalled 15.7 ton ha^{-1}.

4.3.3 Seasonal transpiration dynamics

The sap flow in general varied a lot from October until May during the 2022/2023 and 2023/2024 seasons (Figures 36, 37 and 38), most likely due to changes in canopy cover and atmospheric evaporative demand. For the young trees the maximum individual tree transpiration in 2022/ 2023 during these months was 20.6, 8.3, 8.2 and 17.8 ℓ d^{-1} (1.7, 0.7, 0.7- and 1.4-mm d^{-1}) for T1 to T4 (Figure 36a and b, 37a and b). In 2023/2024 it amounted to 13, 18.7, 21 and 19.6 ℓ d^{-1} (1, 1.5, 1.7- and 1.6-mm d^{-1}). At the full bearing orchard, the seasonal highest individual tree transpiration in 2022/2023 was 8, 18.8, 10.6 and 9.8 ℓ d^{-1} (0.9, 2.1, 1.2- and 1.1-mm d^{-1}) for T1 to T4 (Figure 36c and 37c). In 2023/2024 the maximum individual transpiration reached 19.2, 12.6, 17 and 19.1 ℓ d^{-1} (2.1, 1.4, 1.9- and 2.1-mm d^{-1}) (Figure 36d and 37d). The daily maximum orchard level transpiration for the young orchard occurred in 2022/2023 on 11 February 2023 (14.5 ℓ d^{-1}, 11.6 m^3 ha^{-1} d^{-1} or 1.2 mm d^{-1}) and in 2023/2024 on 15 November 2023 (16.7 ℓ d^{-1}, 13.36 m^3 ha^{-1} d^{-1} or 1.3 mm d^{-1}) (Figure 38). For the full bearing orchard, the daily maximum orchard level transpiration happened on 6 February 2023 (11.5 ℓ d^{-1}, 12.8 m^3 ha^{-1} d^{-1} or 1.3 mm d^{-1}) and 6 December 2023 (15.2 ℓ d^{-1}, 16.9 m^3 ha^{-1} d^{-1} or 1.7 mm d^{-1}) in the two respective seasons. For the young orchard the ETo for the 2022/2023 season ranged between 1.1- and 11.2-mm d^{-1}, whereas it was slightly lower in the 2023/ 24 season, i.e. between 0.9- and 10.4-mm d^{-1} (Figure 38). Reference evapotranspiration for the full-bearing orchard ranged between 0.9- and 8-mm d^{-1} in the first season and 1.2- and 9.4-mm d^{-1} in the second. Monthly averaged orchard upscaled transpiration volume per tree was unexpectedly higher for the young orchard compared to the full bearing orchard for both seasons, although the difference became smaller in 2023/2024 (Figure 39a and b).

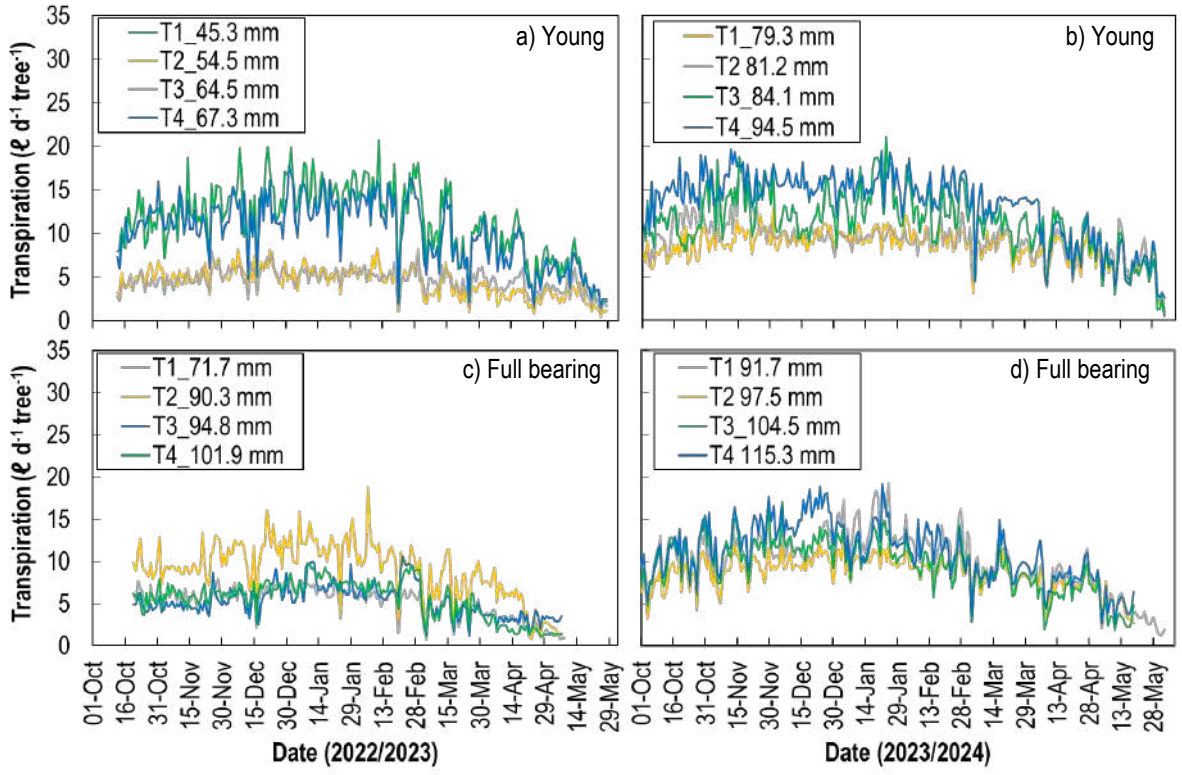

Figure 36. Transpiration trends for four young (a, b) and four full bearing (c, d) pomegranate trees as measured at Avontuur and Welgemoed, respectively, during October until May in the 2022/2023 (a, c) and 2023/2024 (b, d) seasons. The legend indicates tree number and associated stem diameter.

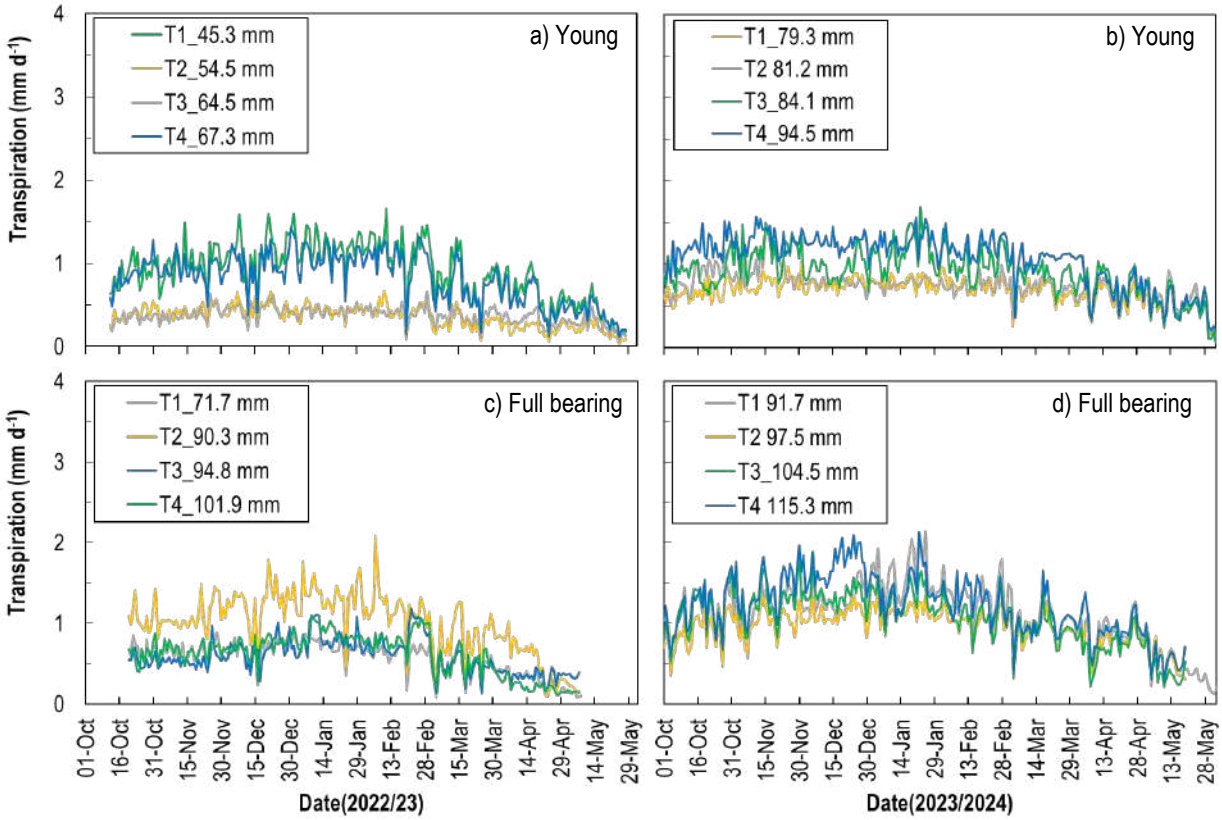

Figure 37. Transpiration trends for four young (a, b) and four full bearing (c, d) pomegranate trees as measured at Avontuur and Welgemoed, respectively, during October until May in the 2022/2023 (a, c) and 2023/2024 (b, d) seasons. The legend indicates tree number and associated stem diameter.

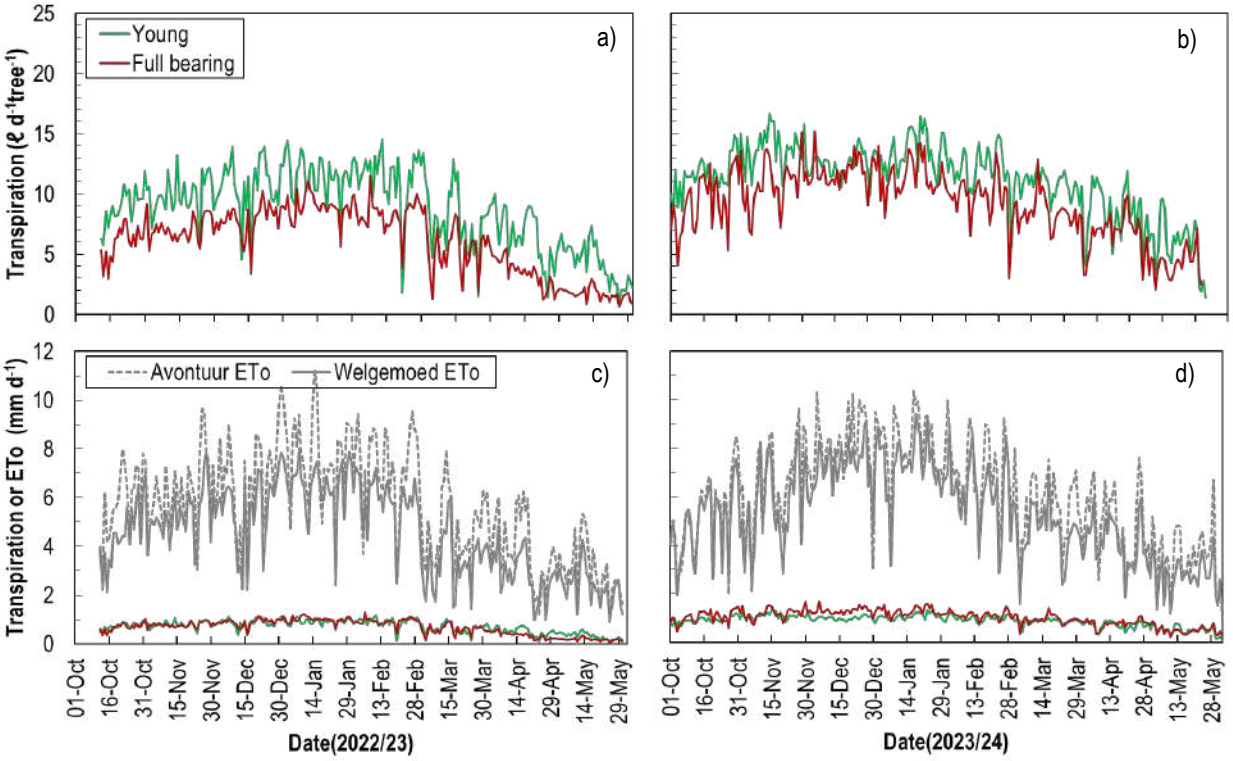

Figure 38. Orchard upscaled transpiration trends in liters per tree per day (a, b) and in mm expressed over the full surface area (c, d) for young and full bearing pomegranate trees as measured at Avontuur and Welgemoed, respectively, during October until May in the 2022/2023 (a, c) and 2023/2024 (b, d) seasons. Reference evapotranspiration (ETo) for the two research sites is also indicated in c) and d).

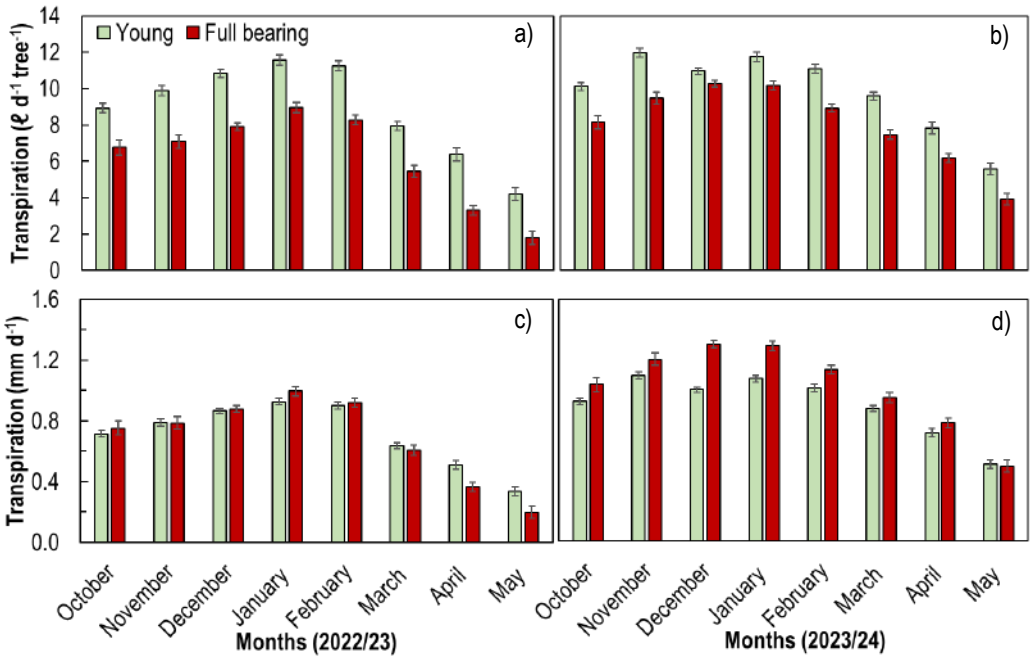

Figure 39. Monthly averaged transpiration of young and full bearing cv. 'Wonderful' pomegranate orchards measured from October until May during the 2022/23 and 2023/24 seasons at Avontuur and Welgemoed. Data was upscaled to orchard level using sap flow data of four trees with varying stem diameters and the orchard stem size distribution. The volume of water transpired (a, b) was also expressed as depth of water in mm over the full surface area allocated per tree (c, d).

For the first season the transpiration of the full bearing trees was between October 2022 and February 2023 24% to 27% lower compared to that of the young orchard, whereas it became 32%, 48% and 57% lower in March, April and May 2023, respectively (Figure 39a). The transpiration difference between orchards was less in the second season (between 6% and 21% from October 2023 until February 2024), and it decreased, compared to the young orchard, by about 21% in March and April and 30% in May (Figure 39b). When monthly averaged orchard upscaled transpiration is considered in terms of water depth over a hectare though, water use was in the first season similar for the two orchards from October until March, with the exception of January, when it was about 8% higher at the full bearing compared to the young orchard (Figure 39c). In April and May though, the full bearing orchard transpiration became 49% and 61% lower compared to that of the young orchard. Leaf senescence of the full bearing orchard started earlier in the seasons compared to at the young orchard, where leaves remained greener for a longer period on the trees at the end of the season.

In the first season, transpiration at the young orchard was in October 2022 and January 2023 slightly lower (0.1 mm d^{-1}) compared to that of the full bearing orchard, but otherwise similar with water use ranging between 0.7- and 1-mm d^{-1} from October 2023 until February 2023 (Figure 39c). The transpiration at the young and full bearing orchard decreased to 0.3- and 0.2-mm d^{-1} in May 2023. In the second season, transpiration tended to be higher than in the first season and for the full bearing compared to the young orchard (Figure 39). Transpiration for the full bearing orchard ranged between 1.1- and 1.3-mm d^{-1} from October until January while being between 0.9- and 1.1-mm d^{-1} at the young orchard (Figure 39d). In February 2024 the transpiration decreased slightly at the young and full bearing orchards, becoming 1- and 1.1-mm d^{-1}, respectively. The transpiration at the full bearing orchard remained about 9% higher compared to that of the young orchard in March and April, whereas it was similar in May at 0.5 mm d^{-1}. The maximum daily transpiration rates of the pomegranate orchards (1.3 mm d^{-1} for the young and 1.7 mm d^{-1} for the full bearing) appeared to be comparable to that of apricot, macadamia, and in some cases olive, but low compared to that of many of the main temperate fruit tree species including apple, citrus, peach, pistachio, and walnut (Bringhenti et al., 2025, Taylor et al., 2015, Villalobos et al., 2013). The monthly average ETo for the2022/2023 and 2023/2024 seasons, respectively, at the young orchard ranged between 3.2- and 7.8-mm d^{-1} and 3.6 to 8.2 mm d^{-1}. For the full bearing orchard, the monthly average ETo reached values of between 2.5- and 6.5-mm d^{-1} for the first season and 2.8- and 7.4-mm d^{-1} for the second.

Transpiration data was not available for September of each season due to technical problems with sap flow system equipment and questionable data quality. Data quality improved later in the season after equipment was shielded from direct sunlight by wrapping it

with foil. The seasonal transpiration was calculated as the sum of daily measured data. Missing data was estimated from the monthly averaged transpiration to ETo ratios and the ETo for the specific dates where data were missing. The total transpiration for the young and full bearing orchards from 1 October 2022 until 31 May 2023 was estimated to be 1699.9 and 1618.1 m^3 ha^{-1}, respectively. For the same period in the 2023/2024 season the total transpiration increased to 2195.3 and 2500.7 m^3 ha^{-1}, respectively. The seasonal transpiration of the young orchard was in the same range of that measured between October and May for young apple orchards with low canopy cover in the Koue Bokkeveld in 2024/15 and in the Elgin/ Grabouw, Villiersdorp and Vyeboom production regions in 2015/16, i.e. between 121-271 mm (Dzikiti et al., 2018). Transpiration of the full bearing orchard was in the first season even lower than that in the young orchard (Table 24), but in the second season comparable to that of a Golden Delicious Reinders' orchard with medium canopy cover in Vyeboom in 2016/2017 (241 mm). In general, transpiration of the full bearing orchard was much lower compared to transpiration of full bearing apple orchards with medium and high canopy cover, which ranged between 357 and 787 mm over the different seasons in the different production regions.

Table 24. Seasonal orchard upscaled transpiration volume per tree and per orchard full surface area as well as depth of water transpired for the 2022/2023 and 2023/2024 seasons (1 October until 31 May) for the young and full bearing cultivar 'Wonderful' pomegranate trees at Avontuur and Welgemoed, respectively

Season	Site	Transpiration water use		
		(ℓ $tree^{-1}$ season)	(m^3 ha^{-1})	(mm)
2022/2023	Young[1]	2124.8	1699.9	170
	Full bearing[2]	1456.3	1618.1	161.8
2023/2024	Young	2744.1	2195.3	219.5
	Full bearing[3]	2250.6	2500.7	250.1

1 Estimated data 29-31 May 2023

2 Estimated data 1-19 October 2022, 8-31 May 2023

3 Estimated data 20-31 May 2024

4.3.4 Factors controlling transpiration

4.3.4.1 Environmental variables

Orchards have variable growth and development of trees; hence, it is essential to measure a range of trees that differs in size and to scale up the results to get a fair representation of the water use of the orchard. The environmental variables are the main drivers of water use, and understanding the relationship between transpiration and different weather conditions can help farmers schedule irrigation accurately. Weather variables such as temperature, VPD, Rn and relative humidity are combined to determine the evaporative demand (Allen et al., 1998). During both the 2022/23 and 2023/24 growing seasons, the linear regression relationships between transpiration of individual trees of both young and full-bearing orchards and selected weather variables were highly significant ($p<0.0001$). The young orchards had during the 2022/23 growing season coefficients of determination (R^2) ranging from 0.092 to 0.735, and for the 2023/24 growing season R^2 values of between 0.015 and 0.612 (Table 25). In 2022/23, the relationship between transpiration and Rn had for all four trees (SF1 – SF4) the highest coefficient of determination amongst all the regression relationships considered. Furthermore, SF4 had the highest coefficient of determination for this relationship during both the growing seasons, being 0.735 and 0.612 in 2022/23 and 2023/24, respectively. However, during the 2023/24 growing season, a better regression relationship was obtained between transpiration and mean daily temperature for SF1 and SF2, and with the minimum relative humidity for SF3, than with solar radiation. For the full-bearing orchard R^2 values for the regression relationships of transpiration with weather variables ranged from 0.083 to 0.739. For both seasons the highest R^2 values amongst all were observed for the relationships between transpiration and solar radiation, with SF1 displaying the best regression relationship in the 2022/23 season (R^2 value of 0.739) and SF4 in 2023/24, having an R^2 value of 0.737. In the case of both orchards, the coefficients of determination for the regression relationships of transpiration to ETo were sometimes better, sometimes worse, and sometimes comparable to that of transpiration with solar radiation. Findings from this study indicate that environmental conditions, particularly solar radiation, are critical factors influencing the transpiration rate of individual pomegranate trees. Mapeto et al. (2018) concluded similar findings where it was modelled that 50% of the uptake rate of water could be linked to environmental conditions.

The individual tree transpiration was upscaled to the orchard level to get a fair representation of the transpiration over the 2022/23 and 2023/24 growing seasons for both young (n=410) and full-bearing (n=368) orchards. As in the case of the individual trees, the relationship between orchard upscaled transpiration and all the selected weather variables was highly significant ($p<0.0001$) for both the young and full-bearing orchards. Figures 40 and 41 show the regression relationships between the daily total transpiration and the most important weather variables. The daily transpiration increased with increasing Rn, T_{max}, T_{min} and VPD (Figure 40a - f, Figure 41e and f). In contrast, transpiration decreased with increasing RH_{max} or RH_{min}, becoming higher as humidity became lower (Figure 41a – d). A non-linear trend described the relationship between transpiration and VPD better than a linear one (Figure 41e and f). The coefficient of determination for the non-linear trend was 7.9% and 6.5% better compared to the linear trend for the young and full bearing orchard, respectively. Transpiration for both orchards initially increased at a fast rate up to VPD of 1 kPa, after which it gradually decreases and tends to level off even more when the VPD becomes 3 kPa. For both orchards the best linear regression relationships were found between orchard upscaled transpiration and Rn (Figure 40a and b) and transpiration and T_{max} (Figure 40c and d). However, poor relationships were observed for both orchards between the transpiration and minimum temperatures (Figures 40 e and f), with an R^2 of 0.1601 for the full-bearing orchard probably being due to large data variability. Orchard upscaled transpiration increased linearly with ETo for both orchards as atmospheric demand increased (Figure 42). A non-linear regression trend fitted the data for the young orchard better compared to linear, indicating that transpiration tended to level off when ETo became higher than c. 8 mm d^{-1}. For the full bearing orchard a non-linear trend for data of both seasons combined did not really improve the coefficient of determination (R^2 value = 0.696), but for the seasons separately the R^2 values for the non-linear trends amounted to 0.766 and 0.755 for the 2022/23 and 2023/24 seasons, respectively (data not shown).

Comparison of the R^2 values of the simple linear regressions of orchard upscaled transpiration and weather variables for data of both seasons combined indicates that it ranged between 0.129 to 0.656 for the young, and between 0.14 and 0.72 for the full-bearing orchard (Table 26). The highest R^2 value observed from the young orchard was from the correlation between transpiration and T_{max}, followed by Rn, ETo and T_{mean}, respectively. The full-bearing orchard had the highest R^2 in the relationship between Rn, followed by ETo, VPD and the Tmax. When examining the relationship between the transpiration and all the weather variables for both sites combined over both seasons, the Rn had the highest coefficient of determination (R^2 = 0.670), whereas ETo rated second best (R^2 = 0.529).

In addition, stepwise regressions were used to assess the effect of each weather variable on the daily orchard upscaled transpiration of the young and full-bearing orchards separately, as well as for data of orchards combined, over the 2022/23 and 2023/24 growing seasons. The adjusted R^2 for the stepwise regression for the young and full-bearing orchard separately, and for the two orchards combined was 73.96%, 76.34% and 72.34, respectively (Table 27). Amongst the weather variables, solar radiation was found to be the most important driver of transpiration in the pomegranate orchards evaluated. The Rn contributed 64.1%, c. 72% and 67% to the variation in transpiration of the young and full-bearing orchards, and of both orchards combined, respectively (Table 24). Studies such as Allen et al. (1998) and Whitley et al. (2007) also indicated that solar radiation is the main driver of tree water use under unstressed conditions.

The stepwise regression results for the young orchard showed that in addition to Rn, T_{max}, T_{min} and RH_{max} accounted for almost 7%, c. 1.8% and less than 1%, respectively, of the variation in transpiration, while wind speed and RH_{min} did not make a significant contribution (Table 27). With the exception of Rn, weather variables played a minor role affecting transpiration at the full bearing orchard – accounting for a mere 4.1% of the variation. At the full bearing orchard, in contrast with the young orchard, RH_{max} affected transpiration slightly more than Tmax, with the effect of RH_{min} being minimal. The effect of T_{min} on transpiration appeared less important at the young and not significant at the full bearing orchard. However, for data of orchards combined for stepwise regression, T_{min} became the most important weather variable, in addition to Rn, to drive transpiration. The contribution of weather variables other than Rn to the variation in transpiration was 5.4%. Interestingly, wind speed, which did not affect transpiration significantly in the stepwise regression for the orchards separately, became significant for data of orchards combined. Based on the stepwise regression for orchards combined over two seasons, T_{min}, wind speed, RH_{max} and T_{max} contributed 3.2%, 1.1% 0.9% and 0.2%, respectively, to the variation in transpiration, while RH_{min} had no significant effect.

Table 25. Summary of the coefficient of determination of statistically significant simple linear regressions (Pearson p values ≤ 0.05) between daily individual tree transpiration and selected weather variables of the young and full-bearing orchards

Site	season	Tree ID	Rn	T_{max}	T_{min}	RH_{max}	RH_{min}	T_{mean}	Wind speed	VPD	ETo
Avontuur	2022/23	SF 1	0.698	0.650	0.344	0.382	0.480	0.630	0.103	0.623	0.745
		SF 2	0.696	0.558	0.259	0.346	0.451	0.519	0.092	0.542	0.682
		SF 3	0.470	0.344	0.191	0.260	0.328	0.338	0.116	0.328	0.488
		SF 4	0.735	0.683	0.358	0.428	0.512	0.659	0.130	0.665	0.804
	2023/24	SF 1	0.483	0.493	0.379	0.248	0.320	0.536	0.028	0.435	0.437
		SF 2	0.544	0.514	0.377	0.322	0.438	0.554	0.085	0.451	0.583
		SF 3	0.142	0.138	0.047	0.105	0.197	0.115	0.015	0.128	0.116
		SF 4	0.612	0.376	0.323	0.139	0.250	0.427	0.038	0.294	0.418
Welgemoed	2022/23	SF 1	0.739	0.479	0.183	0.239	0.454	0.453	0.250	0.477	0.725
		SF 2	0.666	0.457	0.159	0.248	0.430	0.422	0.233	0.455	0.679
		SF 3	0.420	0.308	0.117	0.157	0.267	0.293	0.188	0.310	0.457
		SF 4	0.648	0.483	0.263	0.216	0.321	0.519	0.237	0.448	0.678
	2023/24	SF 1	0.708	0.555	0.410	0.258	0.388	0.645	0.151	0.542	0.747
		SF 2	0.708	0.497	0.207	0.145	0.420	0.492	0.083	0.469	0.693
		SF 3	0.598	0.221	0.089	0.113	0.221	0.213	0.098	0.223	0.497
		SF 4	0.737	0.423	0.194	0.185	0.366	0.425	0.095	0.429	0.679

RH_{max} – Maximum relative humidity, RH_{min} – Minimum relative humidity, Rn – solar radiation, SF 1 – SF 4 – sap flow tree identity, T_{max} - Maximum temperature, T_{mean} – Mean temperature, T_{min} – Minimum temperature, VPD – Vapour pressure deficit, ETo – reference evapotranspiration

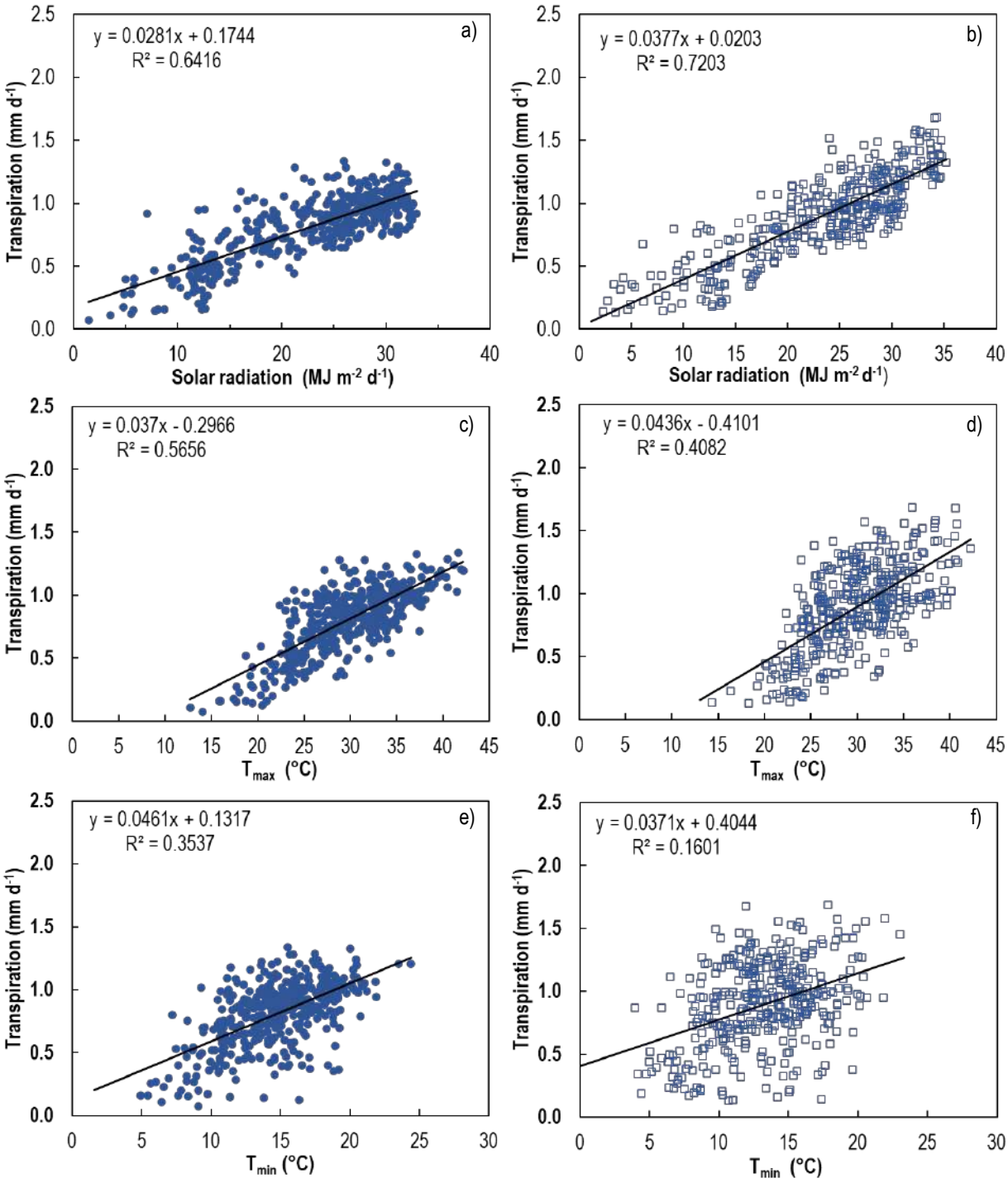

Figure 40. The relationship between orchard upscaled transpiration and weather variables in a young pomegranate orchard (a, c and e) and a full-bearing pomegranate orchard (b, d and f). The weather variables include solar radiation (a and b), maximum temperature (T_{max}) (c and d) and minimum temperature (T_{min}) (e and f).

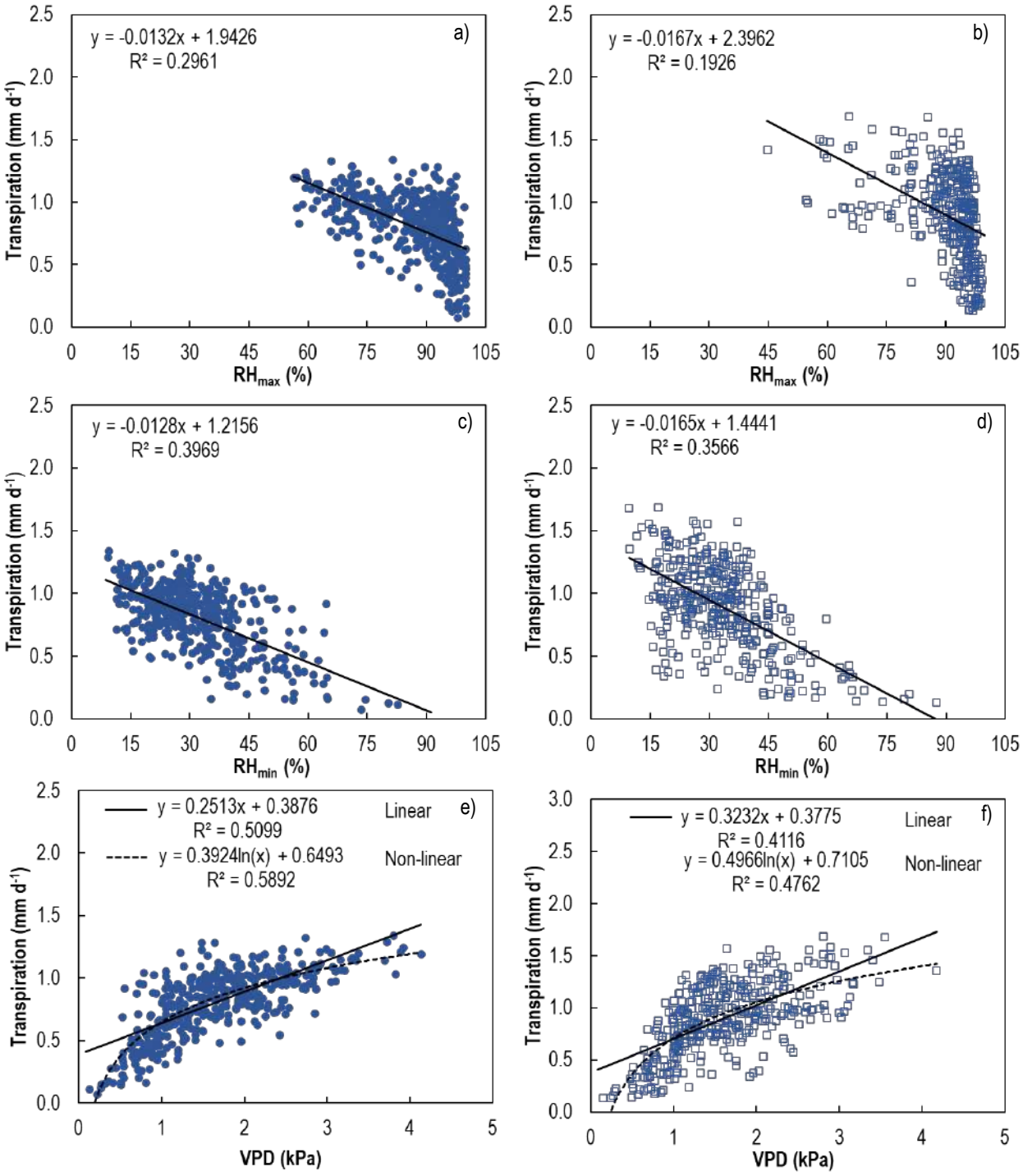

Figure 41. The relationship between orchard upscaled transpiration and selected weather variables in a young (a, c and e) and a full-bearing (b, d and f) pomegranate orchard at Avontuur and Welgemoed, respectively. The weather variables include maximum relative humidity (RH_{max}, a and b), minimum RH (RH_{min}, c and d) and vapour pressure deficit (VPD, e and f) and data are for the 2022/23 and 2023/24 seasons combined.

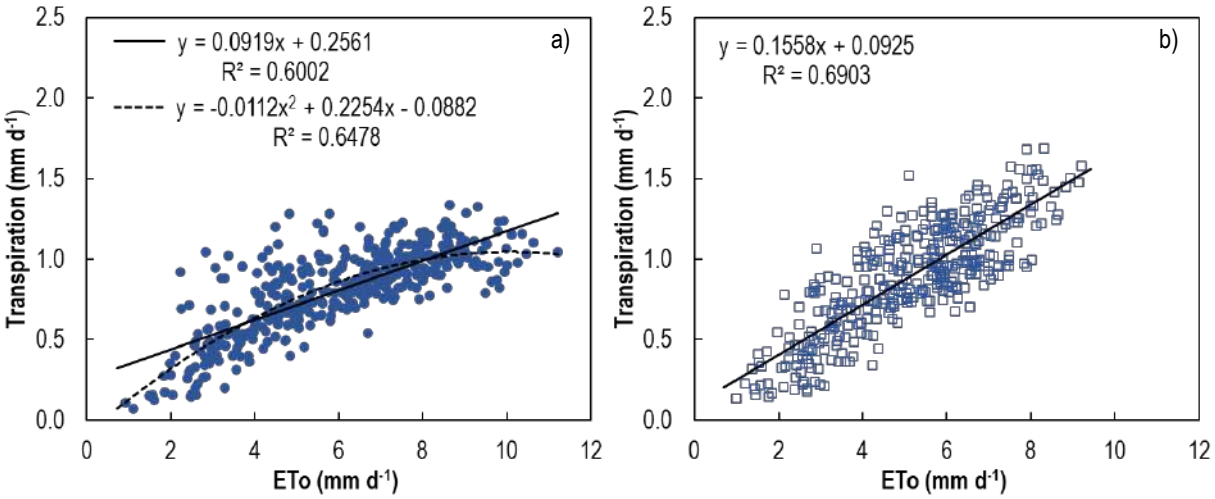

Figure 42. The relationship between orchard upscaled transpiration and reference evapotranspiration (ETo) in a young (a) and full-bearing (b) pomegranate orchard at Avontuur and Welgemoed, respectively, for data of the 2022/23 and 2023/24 seasons combined

Table 26. Coefficient of determination of simple linear regressions between daily orchard upscaled transpiration and selected weather variables or reference evapotranspiration for the young (n = 410) and full bearing (n= 368) cultivar 'Wonderful' pomegranate trees at Avontuur and Welgemoed, respectively, for the 2022/23 and 2023/24 seasons combined

Weather variable	Young	Full bearing	Both orchards
Rn	0.642	0.720	0.670
T_{max}	0.656	0.408	0.458
T_{min}	0.354	0.160	0.191
RH_{max}	0.296	0.193	0.192
RH_{min}	0.397	0.357	0.348
T_{mean}	0.572	0.394	0.430
Wind speed	0.129	0.141	0.020
VPD	0.510	0.412	0.423
ETo	0.600	0.690	0.529

RH_{max} – Maximum relative humidity, RH_{min} – Minimum relative humidity, Rn – solar radiation, T_{max} - Maximum temperature, T_{mean} – Mean temperature, T_{min} – Minimum temperature, VPD – Vapour pressure deficit, ETo – reference evapotranspiration

Table 27. Summary of the multiple stepwise regression results of orchard upscaled transpiration versus selected weather variables for the young and full-bearing cultivar 'Wonderful' pomegranate orchards during the 2022/23 and 2023/24 growing seasons

Variables	Young (n = 410)		Full bearing (n = 368)		Both orchards (n = 778)	
	Adjusted R^2	p-value	Adjusted R^2	p-value	Adjusted R^2	p-value
Rn	64.07	<0.0001	71.96	<0.0001	66.96	<0.0001
T_{min}	1.77	<0.0001	-	-	3.16	<0.0001
Wind speed	-	-	-	-	1.13	<0.0001
RH_{max}	0.94	<0.0001	2.82	0.0243	0.9	<0.0001
T_{max}	6.93	<0.0001	1.03	<0.0001	0.19	0.012
RH_{min}	-	-	0.27	<0.0001	-	-

4.3.4.2 Tree properties

Transpiration is not only affected by the weather variables, but also by tree properties. Fractional light interception measurements were conducted for both the young and full bearing orchards on selected dates during the 2022/23 and 2023/24 growing seasons (Refer to Chapter 3). To assess which effect the tree canopy has on the transpiration, simple linear regressions of daily orchard upscaled transpiration with fractional light interception, ceptometer derived leaf area index, tree canopy area based leaf area index and orchard leaf area index, respectively, was conducted. Although the regression relationships between transpiration and weather variables have already been completed for a more extended dataset, it was also conducted for the data relevant to this smaller dataset (n = 23). The linear regression relationships of transpiration for orchards separately or for orchards combined with fractional light interception, various leaf area index parameters and weather variables were highly significant with p-values of 0.01 or less (Table 28). Amongst the canopy related measurements, fractional light interception seemed to have better regression relationships with transpiration compared to the leaf area index variables for orchards separately or combined. However, for both orchards and seasons combined, tree canopy area based leaf area index or orchard leaf area index had the best coefficients of determination. Overall the regression relationships between transpiration and the canopy related variables were very poor, with maximum R^2 values of about 0.58 for the regressions between transpiration and fractional light interception for the young orchard in both seasons. Very poor correlations between transpiration and the fractional light interception for the full-bearing orchard may partially be due to a lack of variation in transpiration rates of the dataset. Amongst the weather variables Rn still had the best relationship with transpiration at the young orchard in both seasons, whereas RH_{min} also appeared to be important regarding transpiration at the full bearing orchard. Furthermore, the transpiration of the orchards related well to the evaporative demand (ETo) for orchards considered on their own (R^2 values of between 0.668 and 0.88) or combined (R^2 values of 0.513 and 0.824 for the respective seasons). The regression relationships were better during the 2022/23 season than for 2023/2024 for the young, full-bearing, and both orchards combined. The coefficient of determination of the regression relationship between transpiration and ETo for both orchards and seasons combined amounted to 0.78.

As in the case of the extended dataset, multiple stepwise regression was performed to assess the contribution of the canopy related properties and weather variables to the variability in transpiration (Table 29). As previously, Rn was responsible for the majority of variability in transpiration (c. 70%). Differences in fractional light interception, tree canopy area based leaf area index or orchard leaf area index respectively, contributed about 5.5% to the variability in transpiration. In addition, RH_{max} accounted for about 6.5% of the variability in transpiration. This outcome is interesting, since RH_{max} had a lesser albeit significant role compared to T_{min} in the multiple stepwise regression analysis of the larger dataset which did not contain canopy property related data (Table 27). The inclusion of fractional light interception or leaf area index data with weather data improved the coefficient of determination to about 80% (Table 29). However, direct comparison to the multiple regression analysis in Table 27 is not possible since the size of the datasets used differed vastly. Multiple stepwise regressions were also conducted for transpiration with fractional light interception, tree canopy area based LAI or OLAI, respectively, and ETo (data not shown). The adjusted coefficient of determination for the regressions of transpiration with FI, TLAI and OLAI, respectively, and ETo amounted to 74.7%, 78.4% and 79.7% ($p<0.0001$, n = 23). The ETo accounted for 55.3% of the variation in transpiration, whereas FI, TLAI and OLAI was related to 19.4%, 23% and 24.3%, respectively, of the differences in transpiration.

Table 28. Comparison of coefficients of determination (R^2) for simple linear regressions of transpiration to fractional light interception, ceptometer derived leaf area index, orchard leaf area index, tree canopy area based leaf area index and selected weather variables for selected dates during 2022/23 and 2023/24 for data of young, full-bearing and both cultivar 'Wonderful' pomegranate orchards combined (n = 23). Regressions were significant for Pearson p-values ≤0.5.

Weather and Canopy Variables	Young				Full bearing				Both sites				Both sites and seasons	
	2022_23		2023_24		2022_23		2023_24		2022_23		2023_24			
	R^2	p	R^2	p	R^2	P	R^2	p	R^2	p	R^2	p	R^2	p
FI	0.580	0.002	0.585	0.000	0.028	0.008	0.387	0.001	0.012	0.008	0.009	0.007	0.014	0.006
CP_LAI	0.074	0.007	0.022	0.008	0.011	0.008	0.108	0.004	0.111	0.004	0.126	0.002	0.011	0.006
OLAI	0.074	0.007	0.022	0.008	0.011	0.008	0.108	0.004	0.111	0.004	0.129	0.002	0.135	0.001
TLAI	0.074	0.007	0.022	0.008	0.011	0.008	0.108	0.004	0.111	0.004	0.119	0.002	0.138	0.001
Rn	0.839	0.001	0.821	0.000	0.258	0.003	0.924	0.000	0.292	0.002	0.911	0.000	0.809	0.000
T_{max}	0.271	0.005	0.551	0.001	0.313	0.002	0.221	0.002	0.008	0.008	0.238	0.001	0.103	0.001
T_{min}	0.020	0.009	0.542	0.001	0.097	0.005	0.207	0.003	0.031	0.007	0.167	0.001	0.116	0.001
RH_{max}	0.006	0.004	0.297	0.002	0.284	0.003	0.316	0.001	0.029	0.007	0.237	0.001	0.180	0.000
RH_{min}	0.151	0.006	0.012	0.008	0.487	0.001	0.707	0.000	0.101	0.004	0.221	0.001	0.098	0.001
T_{mean}	0.071	0.007	0.619	0.000	0.012	0.008	0.291	0.002	0.002	0.009	0.255	0.001	0.303	0.000
Windspeed	0.023	0.008	0.508	0.001	0.081	0.005	0.176	0.003	0.000	0.010	0.086	0.003	0.024	0.005
VPD	0.197	0.006	0.465	0.001	0.475	0.001	0.590	0.000	0.107	0.004	0.384	0.000	0.261	0.000
ETo	0.668	0.002	0.880	0.000	0.781	0.000	0.847	0.000	0.513	0.000	0.824	0.000	0.779	0.000

CP_LAI – Accupar LP-80 ceptometer derived leaf area index, ETo – reference evapotranspiration, FI – Fractional light interception, OLAI - orchard leaf area index, Tr_LAI - tree canopy area based leaf area index)

Table 29. Summary of multiple stepwise regression statistics relating canopy based and weather variables to variability in orchard level transpiration (n=23). Multiple stepwise regression was conducted between transpiration and fractional light interception, tree canopy based leaf area index and orchard leaf area index, respectively, in combination with various weather variables (solar radiation, minimum and maximum temperature, minimum and maximum relative humidity, windspeed and vapour pressure deficit).

Canopy variable	Statistical description	Model	Rn	Canopy variable	RH_{max}
Fractional light interception	p-value	0.0000	0.0000	0.0042	0.0130
Tree canopy area based leaf area index		0.0000	0.0000	0.0136	0.0365
Orchard leaf area index		0.0000	0.0000	0.0041	0.0130
Fractional light interception	Adjusted R^2 contribution (%)	81.28	69.54	5.64	6.10
Tree canopy area based leaf area index		79.03	69.54	5.23	7.26
Orchard leaf area index		81.35	69.54	5.75	6.06
Fractional light interception	Standard error of estimate	0.113			
Tree canopy area based leaf area index		0.12			
Orchard leaf area index		0.113			

RH_{max} – Maximum relative humidity, Rn – solar radiation

4.3.5 Fruit marketability and transpiration-based water productivity

Suitability of fruit for export purposes depends on the maturity (Section 4.3.5.1) and on external appearance of the fruit (Section 4.3.5.2). Both of these aspects therefore determine income earned and affects the crop economic water productivity (4.2.5.3).

4.3.5.1 Fruit maturity

In 2023, the first harvest and fruit quality evaluation for the young orchard was completed on 7 March, but the second harvest was impacted by theft making it impossible to obtain total yield, complete quality evaluation and calculation of gross farm income earned for the 2022/23 season. Data were though collected for the young orchard for 2023/24 and for the full bearing orchard for both seasons. The fruit maturity analysis data for 2023 for the first harvest for the young orchard, and for both harvests for the full bearing orchard are displayed in Table 30. The ripeness of fruit harvested at the young and full bearing orchard during 2023 conformed to the minimum ripeness requirements for export of the Department of Agriculture, Land Reform and Rural Development (14 °Brix), but only the fruit from Welgemoed met the more stringent requirements of some export companies (16 °Brix).

Table 30. Detailed quality evaluation of fruit from the first (H1) or second harvests (H2) during 2023 for the young (Y) and full bearing (FB) pomegranate orchards at Avontuur and Welgemoed, respectively. Fruit weight (FW), length (FL), diameter (FD), skin colour lightness (L*), red colour (a*), Chroma (C*), Hue°, aril C*, total soluble solids (TSS), total titratable acidity (TTA, g 100 g^{-1} malic acid) and pH are indicated.

Orchard	FW (g)	FL (mm)	FD (mm)	Skin L*	Skin a*	Skin C*	Skin Hue°	Aril C*	TSS (%)	TTA	pH
Y-H1	426	86	91	3	51	40	26	34	15.6	2.1	3.2
FB-H1	471	88	94	4	56	32	31	46	17.7	2.89	3.15
FB-H2	465	88	94	3	53	36	24	36	17.3	2.49	3.17

In 2024 no fruit colour measurements were conducted using a chromameter. Skin colour of fruit evaluated from colour charts indicated that colour from the first harvest at Avontuur was better compared to that of the second harvest or fruit harvested at Welgemoed (Table 31). Skin colour of fruit from both sites complied to that required for Class 1 export. Fruit from both harvests of the young orchard had significantly higher weight, length and diameter compared to fruit from Welgemoed. In 2024, the TSS at both orchards complied to the export company requirements (Table 31) The total soluble solids of fruit for the two orchards were comparable at harvest. Fruit from the young orchard had higher acidity than those from the mature orchard. The pH of fruit juice was slightly lower in fruit of the first

harvest at Avontuur and similar for fruit from the second harvest and those harvested at Welgemoed. Arils colour was poorer for Avontuur compared to Welgemoed, fruit having 57.1% and 60% dark red arils for the first and second harvest, respectively, compared to Welgemoed fruit which contained 76.5% dark red arils. Other than one fruit from the first harvest at Avontuur, no fruit displayed internal decay.

Table 31. Physical characteristics and maturity analysis (mean and standard error) for the young (Avontuur) and full bearing (Welgemoed) cultivar 'Wonderful' pomegranate fruit harvested during March 2024

Variable	Avontuur: Harvest 1		Avontuur: Harvest 2		Welgemoed	
	Mean	SE	Mean	SE	Mean	SE
Skin colour	5.2	0.30	3.9	0.13	4.1	0.38
Weight (g)	557.1	21.68	548.5	46.05	421.5	29.42
Length (mm)	89.1	1.19	86.8	2.58	80.9	1.73
Diameter (mm)	94.7	0.87	92.5	1.62	86.9	1.63
TSS (°Brix)	16.6	0.14	16.6	0.01	16.8	0.03
TTA (g 100g^{-1} malic acid)	2.4	0.06	2.3	0.04	2.0	0.05
pH	3.0	0.03	3.2	0.02	3.2	0.02

4.3.5.2 Fruit quality classification

In 2022/23, for the full bearing orchard, based on fruit weight, 69.2% of fruit was Extra class quality, while 13.4% weighed less than 190 g per fruit and therefore was classed as fruit to be juiced or discarded (Table 32). Taking skin colour into account, 36%, 51.2% and 12.6% of fruit was of Extra class, Class 1 and Processing quality with 0.2% destined for juice. Sunburn appeared to be a large problem with only about 17.8% of fruit which did not have sunburn. Of the total harvest 38.8% of fruit had light brown sunburn (Class 1), 40.9% light and dark brown sunburn (Processing class) and 2.6% black (waste). Of the total harvest, 19.7% of fruit had less than 10% of the fruit surface damaged by sunburn (Class 1), while for 62.4% fruit more than 10% of the fruit surface was affected (Processing class). Cracking appeared not to be a large problem as only 3.5% of fruit had cracks up to the integument, while 5.3% of fruit was cracked to the arils. Blemishes appeared to be a large problem for this orchard or otherwise it was classed too strictly. About 9.6% fruit had blemishes on up to 25% of the fruit surface, whereas 89.4% of the harvested fruit had blemishes covering more than 25% of the fruit surface. This caused the overall classification of fruit for export to class 0.3% of fruit as Class 1, 9.2% as Processing and 85.3% as juice and 5.3 to be discarded (Figure 43). This had dire implications as it reduced gross farm income more than sevenfold compared to where blemishes were omitted from the quality evaluation parameters (data not shown). If blemishes are ignored during the classification process, 2% of fruit becomes Extra class, 16% Class 1, 62.8% processing, 14% juice and 5.3% is discarded.

In 2023/24 both orchards were harvested in March 2024. The fruit distribution of the total harvest indicated that the young orchard had a higher percentage of larger fruit compared to that at Welgemoed in both seasons (Figure 44). For the young orchard 74% of fruit weighed 300 g or more (fruit count for 3.8 kg carton ≤12) in 2023/24 compared to 56% and 60% of fruit in the mature orchard in the first and second season, respectively. Based on quality classification, prospects for fresh fruit export were low (Table 32, Figure 43). Only 0.1% of fruit at Avontuur and none of fruit harvested at Welgemoed were Extra Class, with 7.2% and 3.7% of harvested fruit at Avontuur and Welgemoed, respectively, Class 1. The bulk of the fruit at Avontuur went for purposes of processing (56.3%) with 34.5% destined for juice. At Welgemoed 45.4% of fruit qualified for processing, with more fruit (46.9%) ending up as juice. At Avontuur 1.9% of fruit and at Welgemoed 3.6% had to be discarded due to cracks into the arils or infections such as crown rot. Insufficient colour, degree of sunburn and blemishes and cracking appeared to be factors hindering export of fruit for the fresh market at Avontuur, whereas sunburn colour and degree and degree of blemishes appeared to be more problematic at Welgemoed (Table 32). The impact of not including blemishes in the market classification was not as severe for the 2023/24 season as for 2022/23. In general, the percentage of fruit destined for processing increased whereas that for juicing decreased (Figure 43).

Table 32. Marketing class distribution per fruit quality variable (% of total number of fruit harvested) evaluated during harvest in March 2024 at the young (Avontuur) and full bearing (Welgemoed) orchards

Orchard/ season	Marketing class	Fruit weight	Colour	Sunburn colour	Sunburn degree	Blemishes	Cracking	Other
Avontuur	Extra	83.0	19.8	27.0	27.3	4.9	62.1	96.2
2023/24	Class1	0.0	49.6	44.1	26.8	46.0	-	-
	Processing	10.6	30.6	14.5	45.9	31.1	35.9	-
	Juice	4.5	0.0	14.4	0.0	18.0	0.0	3.8
	Discard	1.9	0.0	0.0	0.0	0.0	1.9	0.0
Welgemoed	Extra	69.2	36	17.8	17.9	0	91.2	100.0
2022/23	Class1	0.0	51.2	38.8	19.7	1.04	-	-
	Processing	17.4	12.6	40.9	62.4	9.55	3.5	-
	Juice	8.1	0.2	2.6	0.0	89.4	-	0.0
	Discard	5.3	0	0.0	0.0	-	5.3	0.0
Welgemoed	Extra	71.2	15.6	3.7	5.3	5.0	84.6	99.5
2023/24	Class1	0.0	59.8	17.5	58.5	33.8	0.0	-
	Processing	14.0	24.7	51.5	36.2	35.3	11.8	-
	Juice	11.2	0.0	27.2	0.0	25.8	0.0	0.5
	Discard	3.6	0.0	0.0	0.0	0.0	3.6	0.0

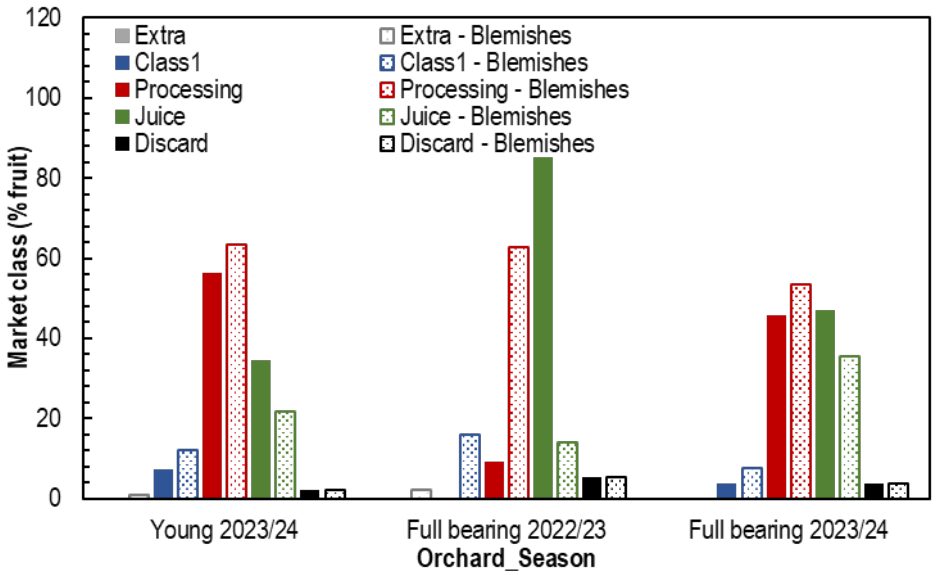

Figure 43. Fruit quality-based market classification of fruit harvested at the young (Avontuur) and full bearing (Welgemoed) orchards in the 2022/23 and 2023/24 seasons. Markets were assigned based on combined evaluation of fruit weight, fruit skin colour, sunburn colour and degree, blemishes, cracking and other factors which determined if it was suitable for juice or to be discarded. Class evaluation omitting blemishes as a factor is indicated by a dotted pattern.

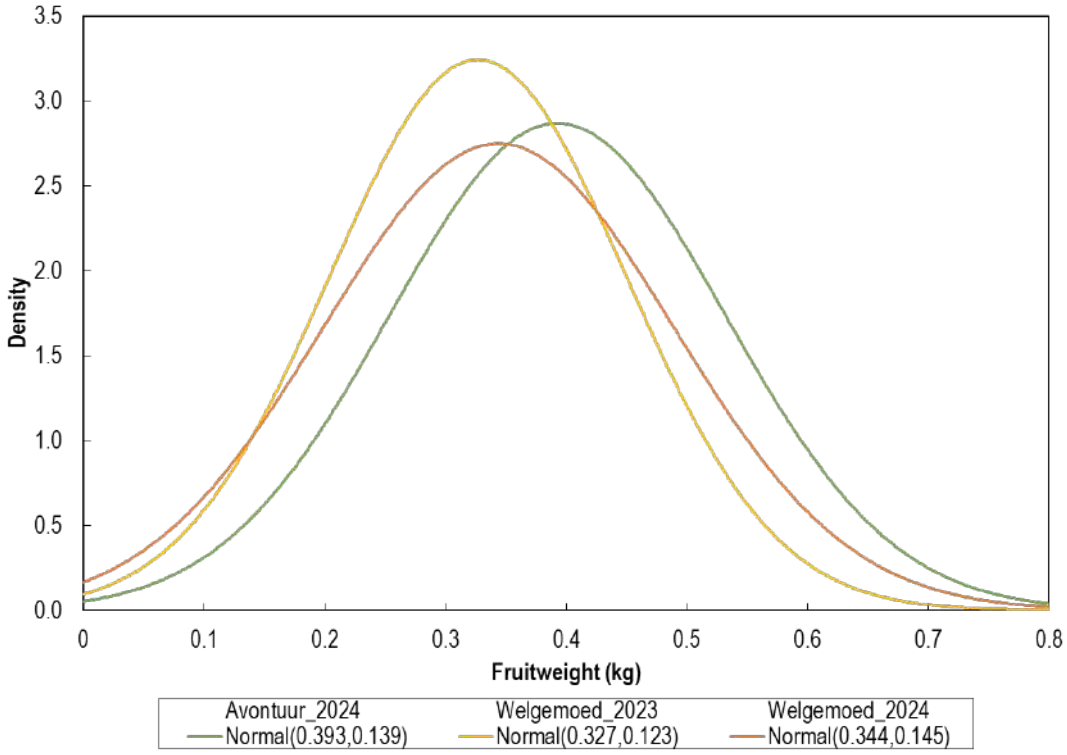

Figure 44. Fruit weight distribution of fruit harvested at the young (Avontuur) and full bearing (Welgemoed) pomegranate orchards in the 2022/23 and 2023/24 seasons. Data are not available for Avontuur for 2022/23. The histogram indicates the fruit weight (kg) normal distribution, average and standard deviation.

4.3.5.3 Water use efficiency and productivity

To calculate water use efficiency and water productivity, irrigation and evapotranspiration data for the full growing season from bud break until leaf fall and total yield data, are required. However, transpiration data was only available from October each season, whereas irrigation data for the whole season and total yield data for the young orchard was not available for 2022/23. In 2023/24, transpiration from October until May equalled 26.9% and 56.9% of the total effective rainfall and irrigation applied at the young and full bearing orchards, respectively. Biophysical water productivity for Avontuur based on 2195.3 m^3 ha^{-1} transpiration for October 2023 until May 2024 and marketable yield of 27.1 t ha^{-1} equalled 12.4 kg m^{-3}. Biophysical water productivity for Welgemoed based on 1618.7 m^3 ha^{-1} transpiration for October 2022 until May 2023 and marketable yield of 33.3 t ha^{-1} equalled 20.6 kg m^{-3}. Due to the lower yield in 2024 though the water productivity based on 2501 m^3 ha^{-1} transpiration for October 2023 until May 2024 and marketable yield of 16.9 t ha^{-1} dropped by almost 69% to 6.7 kg m^{-3}. Economic water productivity for the two orchards based on gross farm income and transpiration from October 2023 until May 2024 amounted to R160.17 m^{-3} for Avontuur and R73.19 m^{-3} for Welgemoed. Due to the effect of blemishes on the gross farm income economic water productivity was only R20.32 m^{-3} for Welgemoed in 2022/23 despite the marketable yield of 33.3 t ha^{-1}. If the effect of blemishes were omitted from the market classification, transpiration based economic water productivity increased to R199.22 m^{-3} for the young orchard in 2023/24 and for the full bearing orchard in the 2022/23 and 2023/24 seasons to R146.76 m^{-3} and R92.50 m^{-3}, respectively.

Transpiration based biophysical water productivity for intermediate bearing apple trees with medium canopy cover in two South African production regions over various seasons ranged between 4.3 and 11.3 kg m^{-3} (Dzikiti et al., 2018), whereas that for full bearing high canopy cover trees varied between 10.8 and 21.5 kg m^{-3}. If the "off season" at Welgemoed in 2023/24 is ignored, the transpiration based biophysical water productivity for pomegranate trees compared well or even slightly exceeded that of the apple trees. The economic water productivity for the apple trees at the time ranged between R20.7 m^{-3} and R66 m^{-3} for the intermediate bearing and between R46.6 and R92.7 m^{-3} for the full bearing apple trees. Direct comparison of data from 2018 to current conditions is not valid

due to volatility of the markets and the rand value. Nonetheless, the economic water productivity of pomegranate is potentially high compared to other fruit crops in the region, even taking into account market fluctuations.

4.3.6 Conclusions

Physiological measurements conducted in 2023/24 indicated that the water status of the trees of both orchards was optimal or near to optimal on the dates that midday stem water potential measurements were conducted. For the majority of the 2023/2024 season though, photosynthesis rates and shoot growth were lower at the full bearing orchard compared to the young orchard. This, in addition to poor flowering and fruit set, could partially explain the low yield for the full bearing orchard for this season.

Orchard upscaled daily transpiration rates were low and monthly averages over the season ranged between 0.2- and 1-mm d^{-1} for both orchards in the 2022/23 season, reaching maxima of 1.1- and 1.3-mm d^{-1} for the young and full bearing orchards, respectively, in 2023/24. The seasonal total transpiration for the young and full bearing orchards from 1 October 2022 until 31 May was estimated to be 1699.9 and 1618.7 m3 ha^{-1}, respectively, in 2022/23 and 2185.8 and 2513.7 m^3 ha^{-1}, respectively, in 2023/24.

Simple and multiple linear regression results gave a clear indication that environmental conditions are important indicators of pomegranate tree transpiration rates, particularly net radiation. By combining Rn, T_{min}, wind speed, RH_{max} and T_{max} though gave a more reliable indication of the transpiration rate than relying solely on Rn. The effect of the tree canopy on the variability in transpiration compared to that of Rn and RH_{max} seems to be small - i.e. about 5.5% while the weather variables accounted for about 76% of transpiration differences. When orchard upscaled transpiration though was related to ETo in combination with different tree canopy variables (fractional light interception, tree canopy area based LAI and OLAI) ETo accounted for 55% of the variation in transpiration and the tree canopy variables between 19 and 24%.

With regard to water use indicators, transpiration from October until May equalled 26.9% and 57.2% of the total effective rainfall and irrigation applied at the young and full bearing orchards, respectively, in 2023/24. Yield data for calculation of biophysical water productivity was impacted in the first season for the young orchard by theft and in the second for the full bearing orchard as a result of poor flowering. Transpiration based biophysical water productivity calculated using transpiration from October until May equalled 12.4 kg m^{-3} for the young orchard in 2023/24. For the full bearing orchard it amounted to and 20.6 kg m^{-3} in 2022/23 and in 2023/24, due to poor flowering and subsequent inferior yield, 6.7 kg m^{-3}.

Economic water productivity based on gross farm income and transpiration from October until May amounted in 2022/23 to R 20.32 m^{-3} for Welgemoed and in 2023/24 to R160.17 m^{-3} and R73.19 m^{-3} for Avontuur and Welgemoed, respectively. It is suspected that for purposes of market classification, blemishes were classed too strictly in 2022/23. If the effect of blemishes were omitted from the market classification model, transpiration based economic water productivity increased to R199.22 m^{-3} for the young orchard in 2023/24 and for the full bearing orchard in the 2022/23 and 2023/24 seasons to R146.76 m^{-3} and R92.50 m^{-3}, respectively. The economic water productivity of pomegranate is considered potentially high compared to other fruit crops in the region.

CHAPTER 5: EVAPOTRANSPIRATION OF POMEGRANATE ORCHARDS VARYING IN CANOPY COVER

5.1 INTRODUCTION

Reliable evapotranspiration information used correctly can contribute considerably to the success of individual farms, water management systems and long term sustainability of irrigated agriculture (Ley, 1994). Peak evapotranspiration rates during the season is used in irrigation systems design, daily or weekly estimates of evapotranspiration rates are used to schedule irrigation, long term average evapotranspiration and rainfall amounts totalled over the season determine net crop irrigation requirements, whereas combined totals of total irrigation requirement for individual fields of farms in a catchment management area or in a region can be used in irrigation water demand management. Soil water content is one of the factors determining the rate of evapotranspiration. This chapter therefore depicts the daily soil water and irrigation dynamics for different soil layers below drippers, between drippers and in the work row area for the different sites over two growing seasons. Daily as well as monthly averaged soil water balance derived crop evapotranspiration (ETc) for individual trees as well as micrometeorological method derived ETc at orchard scale is presented for the young and full bearing orchards varying in canopy cover.

5.2 METHODOLOGY

Evapotranspiration for a young (Avontuur, 33°07'29.7"S; 18°56'08.8"E) and a full bearing (Welgemoed, 33°35'18.3048"S; 18°59'19.302"E) cultivar 'Wonderful' pomegranate orchard differing in canopy cover has been determined over the 2022/23 and 2023/24 seasons using a soil water balance (Section 5.2.1) and micrometeorological methods (Section 5.2.2). A surface renewal system was used at the young, and an eddy covariance system at the full bearing orchard to determine orchard level evapotranspiration (Section 5.2.2), whereas the soil water balance was done in the allocated area of two individual trees per orchard. Details regarding the orchards, soil properties, installation and calibration of the soil water content and irrigation monitoring equipment are described in Chapter 3, Sections 3.4 and 3.6 and Appendix A.

5.2.1 Soil water balance

The soil water balance calculations to obtain evapotranspiration for the full surface for the young orchard (SWB1 and SWB2) and the full bearing orchard (SWB3 and SWB4) were conducted using volumetric soil water content of the CS650 sensors logged at midnight and daily total rainfall and irrigation data.

The full surface evapotranspiration of the orchard was calculated as follows:

$$ET_{FS} = ET_{TR} + ET_{WR} \quad \text{[Eq. 28]}$$

where:

ET_{FS} = full surface evapotranspiration of the orchard (mm)

ET_{TR} = evapotranspiration out of the tree row fraction of the orchard (mm per orchard area)

ET_{WR} = evapotranspiration out of the work row fraction of the orchard (mm per orchard area)

Evapotranspiration from the volume of soil under the tree row was determined as follows:

$$ET_{TR} = \Delta SWC_{TR} + I + P - \Delta SWC_{900} \quad \text{[Eq. 29]}$$

where:

ET_{TR} = evapotranspiration out of the tree row fraction of the orchard (mm)

ΔSWC_{TR} = change in soil water content in the tree row

I = Irrigation applied (mm per tree row area)

P = rainfall (mm)

ΔSWC_{900+} = change in soil water content in the soil layer below the 900 mm depth (1050 mm for SWB4)

The fraction of ET from the work row volume of soil water was calculated according to the following soil water balance equation:

$$ET_{WR} = \Delta SWC_{WR} + P - \Delta SWC_{900+} \quad \text{[Eq. 30]}$$

where:
ET_{WR} = evapotranspiration out of the work row fraction of the orchard (mm)
P = rainfall (mm)
ΔSWC_{900+} = change in soil water content in the soil layer below the 900 mm depth (1050 mm for SWB4)

Daily rainfall was corrected for evaporative losses of 0.2ETo. The evapotranspiration losses from the tree row and work row, respectively, was converted to volume before expressing it as mm per full orchard surface area.

5.2.2 Micrometeorological methods

A surface renewal (SR) system was employed full time in the young orchard at Avontuur and an eddy covariance (EC) system in the full bearing orchard at Welgemoed. The SR system was tested and calibrated at the ARC Infruitec-Nietvoorbij Irrigation laboratory in Stellenbosch before installation on 25 November 2022 at Avontuur. The system was positioned about in the middle of the young pomegranate orchard and took into account the positioning of the soil water balance and sap flow installations. Components of the SR system installed at 1.2 m above the tree canopies includes fine wire temperature sensors (FW 003), a net radiometer (NR Lite-Kipp and Zonen), pyranometer (SR-Apogee) and a 3D Sonic Anemometer (R.M. Young). Two Hukseflux Heat Flux Plates were installed in the tree row 2.5 cm below the ground and two Tcav soil temperature sensors 6 cm below the ground. Data were logged by a CR1000 data logger and downloaded on a bi-weekly to monthly basis using a direct connection to a laptop or other data downloading device.

An EC tower was installed from 21-24 September 2022 at a distance of 75 m from the road in the middle of the Welgemoed orchard and 150 m away from the netted area at the bottom end of the orchard. The height of the instruments was 1 m above the canopy except for the NR Lite radiation sensor (Rn) mounted at c. 8 m above the ground. The instruments installed included the IRGASON (measures H_2O and CO_2 fluxes); pyranometer (solar radiation); EC100 CO_2 and H_2O Processing unit and CR3000 data logger (data processing and programming). A temperature and relative humidity sensor was installed at the canopy level. Equipment installed at ground level in the tree row included a Hukseflux Heat Flux Plate 2.5 cm below the ground, two Tcav soil temperature sensors 6 cm below the ground and a CS616 Soil water content sensor 8 cm below the ground. The system used a solar power system but after theft of the solar panel, batteries were swopped on a weekly basis. The data were collected using direct connections to a laptop or other data downloading devices. The data from both the EC and SR systems were imported and analysed in Excel using the simplified form of the energy balance equation. The evapotranspiration, which is represented by latent heat (LE), was calculated as a residual from net radiation (Rn), sensible heat (H) and the ground heat flux (G). The main difference between the systems is that sensible heat for the SR system was measured using a fine wire thermocouple, and the EC system measured the turbulent fluxes in the atmosphere. Crop coefficients (Kc) for the two research sites were calculated according to Allen et al. (1998) as the ratio of orchard scale measured ETc to ETo.

5.3 RESULTS AND DISCUSSION

5.3.1 Irrigation

Due to delayed installation, calibration and technical problems with flow meters irrigation data became only available for all soil water balance installations by 2 December 2022 (Table 33). High flow data at SWB2 for January 2024 until the end of the season was attributed to a leakage in the irrigation system beyond the soil water balance installation (Figure 45b). The amount of irrigation applied to SWB2 for January until May 2024 was therefore derived from a regression relationship between SWB1 and SWB2 flows measured from November 2022 until December 2023 (data not shown). Furthermore, during the 2023/4 season the flow meters at SWB4 tended to intermittently record lower irrigation compared to SWB3, resulting in a seasonal difference of c. 135 mm. It is not clear if this difference was due to irrigation system pressure issues or due to malfunctioning of the logging water meters. The amount of irrigation applied per day to the young orchard at Avontuur ranged between 0.3 and 5.3 mm, and at Welgemoed between 2.1 and 6.1 mm. The

irrigation interval decreased during mid-summer from the 2022/23 season to the 2023/24 season for both sites. In 2023/24 the irrigation at Avontuur was daily and at Welgemoed, every 1.7 days. The orchard at Welgemoed received compared to Avontuur irrigation less frequently during the harvest period in March of both seasons. For the period from December 2022 until April 2023 the full bearing trees received 22% more irrigation water compared to that applied to the young orchard, but during the 2023/2024 season the young orchard received almost 2.4 times as much water as the full bearing one. The seasonal total irrigation applied to the young orchard was slightly less than the amount of 848 mm applied to five-year-old surface drip irrigated pomegranate trees in California (Ayars et al., 2017). The seasonal irrigation total of the full bearing orchard according to SWB3, was near the bottom end of the range or irrigation amounts applied to the full bearing cultivars 'Mollar de Elche' and 'Wonderful' in Spain on various soil types (392 mm – 776 mm) (Volschenk, 2020). The soil profile at Welgemoed was still at field capacity during middle of October 2023 and only one to two irrigations were applied that month while irrigation was already applied frequently at Avontuur (Table 33, Figures 45 and 46).

Table 33. Monthly averaged irrigation applied and interval for the soil water balance installation sites at Avontuur (SWB1, SWB2) and Welgemoed (SWB3, SWB4) from December 2022 to December 2023

Month	Irrigation applied (mm per full surface area)				Irrigation interval (d)			
	SWB1	SWB2[1]	SWB3	SWB4	SWB1	SWB2	SWB3	SWB4
Dec-22	2.3	2.1	6.1	5.8	2.6	2.6	3.1	3.1
Jan-23	2.3	2.1	5.3	5.4	1.1	1.1	2.1	1.8
Feb-23	2.3	2.0	4.8	4.8	1.3	1.3	2.0	1.8
Mar-23	3.3	2.5	3.8	3.0	1.9	1.9	4.4	4.4
Apr-23	2.3	1.7	3.0	2.1	4.3	3.8	30.0	30.0
May-Jul	No irrigation							
Aug-23	0.6	0.3	0.0	0.0	31.0	31.0	31.0	31.0
Sep-23	2.7	1.8	0.0	0.0	30.0	30.0	30.0	30.0
Oct-23	2.9	2.1	6.0	2.1	1.5	1.5	31.0	15.5
Nov-23	2.3	2.9	4.3	2.7	1.0	1.0	2.3	2.3
Dec -23	2.7	3.3	5.1	4.7	1.0	1.0	1.9	2.1
Jan-24	4.7	4.4	4.5	3.7	1.0	1.0	1.7	1.6
Feb-24	5.1	4.7	5.0	2.8	1.0	1.0	1.8	1.7
Mar-24	5.3	4.9	4.1	1.5	1.0	1.0	2.8	1.9
Apr-24	4.7	4.4	4.7	0.9	1.6	1.6	3.3	3.3
May-24	3.1	2.8	3.0	1.3	2.1	1.9	15.5	15.5
2022/2023[2]	212.9	185.1	236.9	249.3				
2023/2024	793.1	772.353	398.0	263.3				

1 Irrigation volume applied estimated from regression relationship with SWB1 flow for January – May 2024

2 December 2022 – April 2023

5.3.2 Soil water dynamics

Hourly trends in soil water content for SWB1 and 2 are presented in Figure 45 and for SBW3 and 4 in Figure 46. The irrigation applied below the drippers wetted the soil to midway between two drippers for all soil water balance installations (Figure 45a - d, Figure 46a - d). At Avontuur overlap of wetted areas of adjacent drippers may be the cause of the increased soil water content deeper in the soil profile (Figure 45a and b). At Welgemoed the top 300 mm of soil profile was frequently refilled by irrigation, but the 300-600 mm depth tended to dry out especially in November 2022, January until March 2023 and November 2023 until February 2024 (Figure 46a and b). Soil water dynamics in the work row appeared to be affected mainly by rainfall events (Figure 45e and f, Figure 46e and f). The soil profiles for both orchards were refilled at the end of each season by ample rainfall in June until September 2023 and again in June 2024 (Figure 28, Figures 45 and 46).

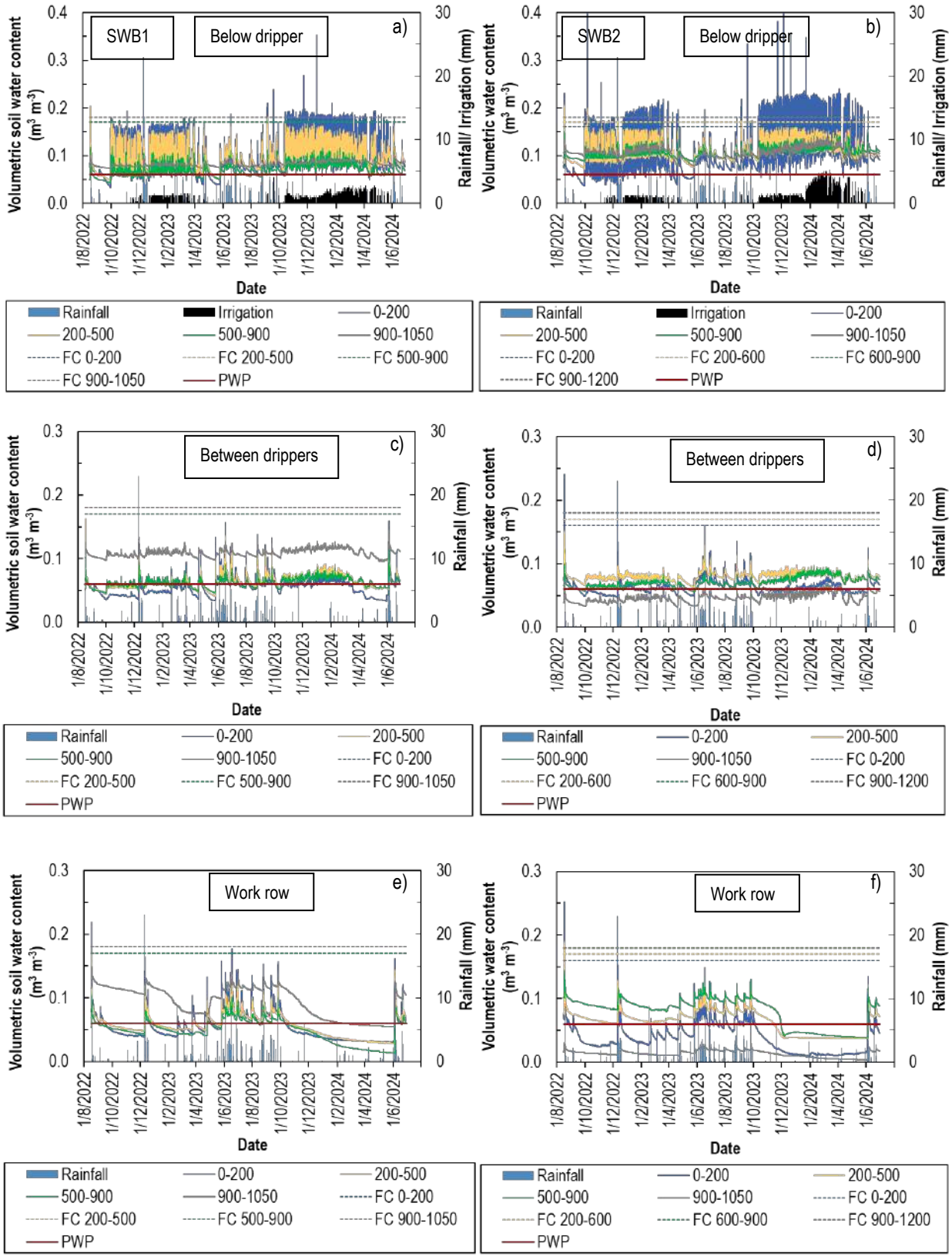

Figure 45. Trends in hourly CS650 volumetric soil water content measured below a dripper (a and b), between two drippers (c and d) and in the work row (e and f) for SWB1 (a, c and e) and SWB2 (b, d and f) in the young pomegranate orchard at Avontuur from August 20022 until June 2024. Soil depth increments are in units of millimetres. Rainfall or irrigation applied is in mm d^{-1} per full surface area.

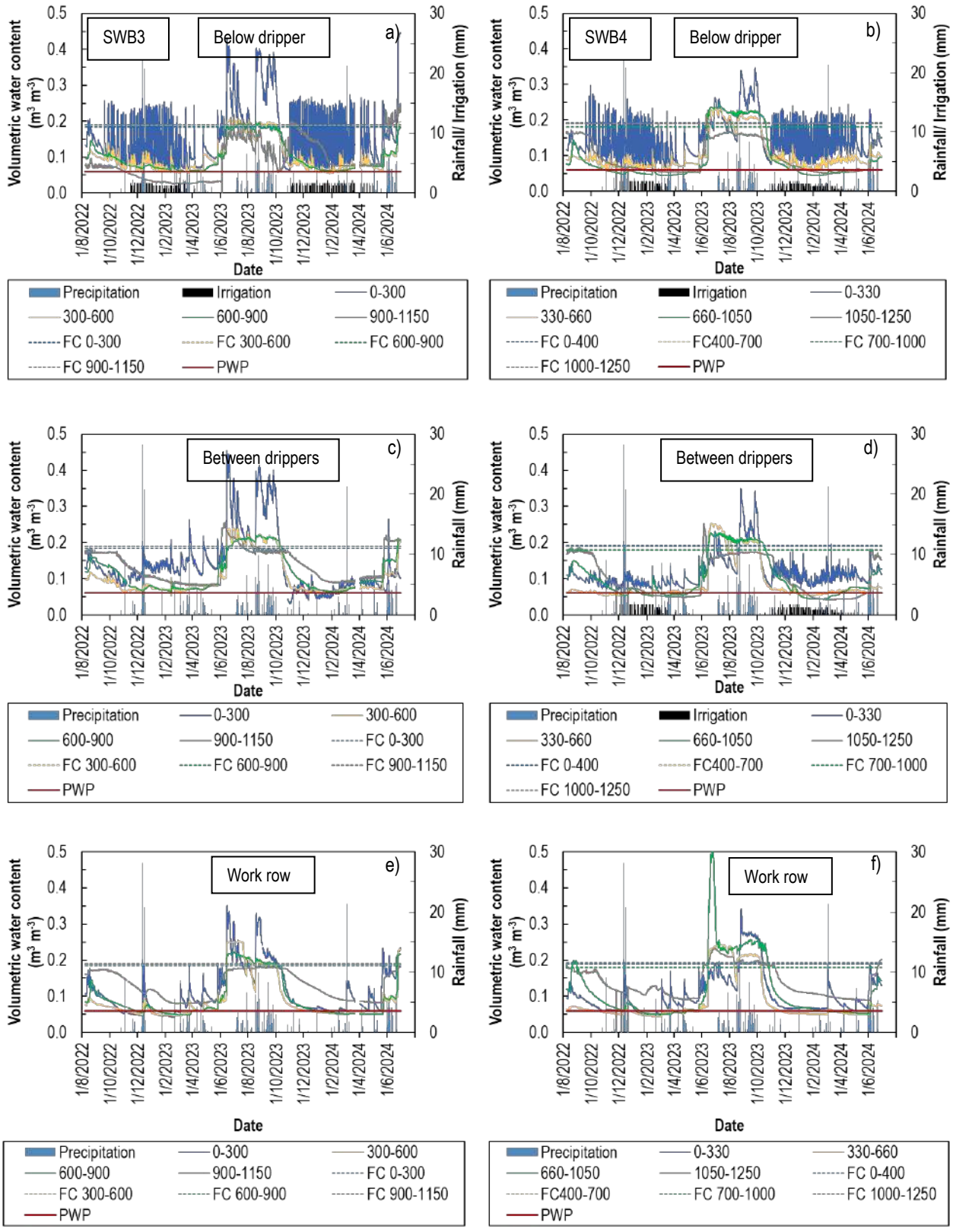

Figure 46. Trends in hourly CS650 volumetric soil water content measured below a dripper (a and b), between two drippers (c and d) and in the work row (e and f) for SWB3 (a, c and e) and SWB4 (b, d and f) in the full bearing pomegranate orchard at Welgemoed from August 20022 until June 2024. Soil depth increments are in units of millimetres. Rainfall or irrigation applied is in mm d^{-1} per full surface area.

Welgemoed is located in the vicinity of the Berg River and flooding saturated the soil profile to the top soil level during winter in 2023. Water remained above field capacity (compared to soil water retention curve estimated values based on texture) in the soil profile in the tree row up to 900 cm depth until about mid-October (Figure 46a - f). The water table below 900 cm depth fully subsided in 2022/2023 by mid-November and in 2023/2024 by January 2024. Soil water in the top three soil layers depleted from field capacity steeply to the end of October 2023. At Avontuur the soil profile below 900 cm depth was above field capacity for six days in 2022/2023 and two days during 2023/2024.

Seasonal trends of the hourly CS650 volumetric soil water content averaged for the two topmost soil layers below the dripper nearest to the tree and mid-way to the next dripper are displayed in Figure 47. Figure 47 gives an indication of the average soil water content for the top two soil layers in which most of the roots were concentrated (field observation during equipment installation). In the young orchard in the first season, the soil water content below the dripper c. 30 cm from the tree at SWB1 tended not to get back to field capacity and the soil wetness fluctuated around the -100 kPa soil water retention level between field capacity and permanent wilting point (Figure 47a). In the second season it more frequently reached field capacity. In SWB2 in the first season and in the second season, field capacity was reached more frequently after irrigation and the soil profile was for the majority of the time above the -100 kPa level (Figure 47c). The soil water content midway to the next dripper was in both the young and full bearing orchards mainly dry and approached at times the permanent wilting point level (Figure 47b, d, f and h).

At the full bearing orchard the average soil water content of the top two soil layers for SWB3 and SWB4 rarely reached field capacity and was, especially for SWB4, for the majority of time below the -100 kPa soil water retention level (Figure 47e and g). It was though multiple times above the -100 kPa soil water retention level, which may explain why the stem water potential measured at selected dates did not reflect extreme stress (Refer Chapter 4, Figure 29). It might also be that the trees managed to maintain their water status adequately making use of the water in the top 300/ 330 mm (Figure 46a and b) and by reducing stomatal conductance (Refer Chapter 4, Figure 30). The low average soil water content in the top soil layers at the full bearing orchard (Figure 47e and g) appears to be due to underirrigation which refilled the top 300/ 330 mm of soil to field capacity at most irrigations, but resulted in depletion of soil water in soil layers beyond that to extremely dry levels (Figure 47a and b). The farm irrigated according to and indicated that soil water content levels was, based on data of their own soil water content monitoring system, adequate.

5.3.3 Soil water balance derived evapotranspiration

Daily and monthly averaged soil water balance determined evapotranspiration (ETc) are displayed for the tree row, work row and fully allocated orchard area for young and the full bearing orchards for the 2022/23 and 2023/24 seasons in Figures 48 and 49. The orchard ETc increased from August 2022 until January 2023 for both orchards (Figure 48e and f; Figure 49a and b). A decrease in ETc during September 2022 at both orchards may be attributed to less rainfall that occurred during this period compared to August 2022 (Figure 28). At the young orchard ETc decreased slightly from January to February and then more steeply toward the end of the season in May 2023 (Figure 48e, Figure 49a). At the full bearing orchard there was a substantial drop in ETc from January to February, decreasing further to March, with the lowest ETc for the season occurring already in April (Figure 48f, Figure 49b). Monthly averaged ETc of the tree and work row was comparable during May, June and July and was slightly higher compared to April, maybe due to the presence of weeds and/ or greater exposure of the tree row soil surface to solar radiation during wintertime (Figure 49).

From September 2023, tree row ETc tended to become higher compared to work row ETc, most likely due to bud break that occurred already in August followed by early canopy development (Figure 48a-d, Figure 49). There was a substantial increase in ETc from October to November for both orchards. This increase can be ascribed to the increase in ETo in addition to the contribution of new shoot growth, which expanded the transpiring canopy area (Refer Chapter 3, Figure 33b). Although the general trend was for ETc to increase from July towards January at the young orchard in both seasons and in the first season for the full bearing orchard, it increased for the latter only up to December in 2023. The ETc of the full bearing orchard decreased slightly in January 2024 compared to in December and then decreased gradually until May 2024. The ETc for the young orchard decreased slightly from January towards March, with a substantial drop of evapotranspiration rate (c. 40%) towards April, most likely triggered by fruit removal during harvest, which occurred on 7 and 14 March 2024. Hereafter it gradually decreased towards June 2024.

There was a lot of variability in the available ETc data with maximum orchard evapotranspiration values being 9.4 mm and 10.7 mm for the young and 8.8 mm and 6.7 mm for the full bearing orchard for the two respective seasons (Figure 48e and f). Water losses from

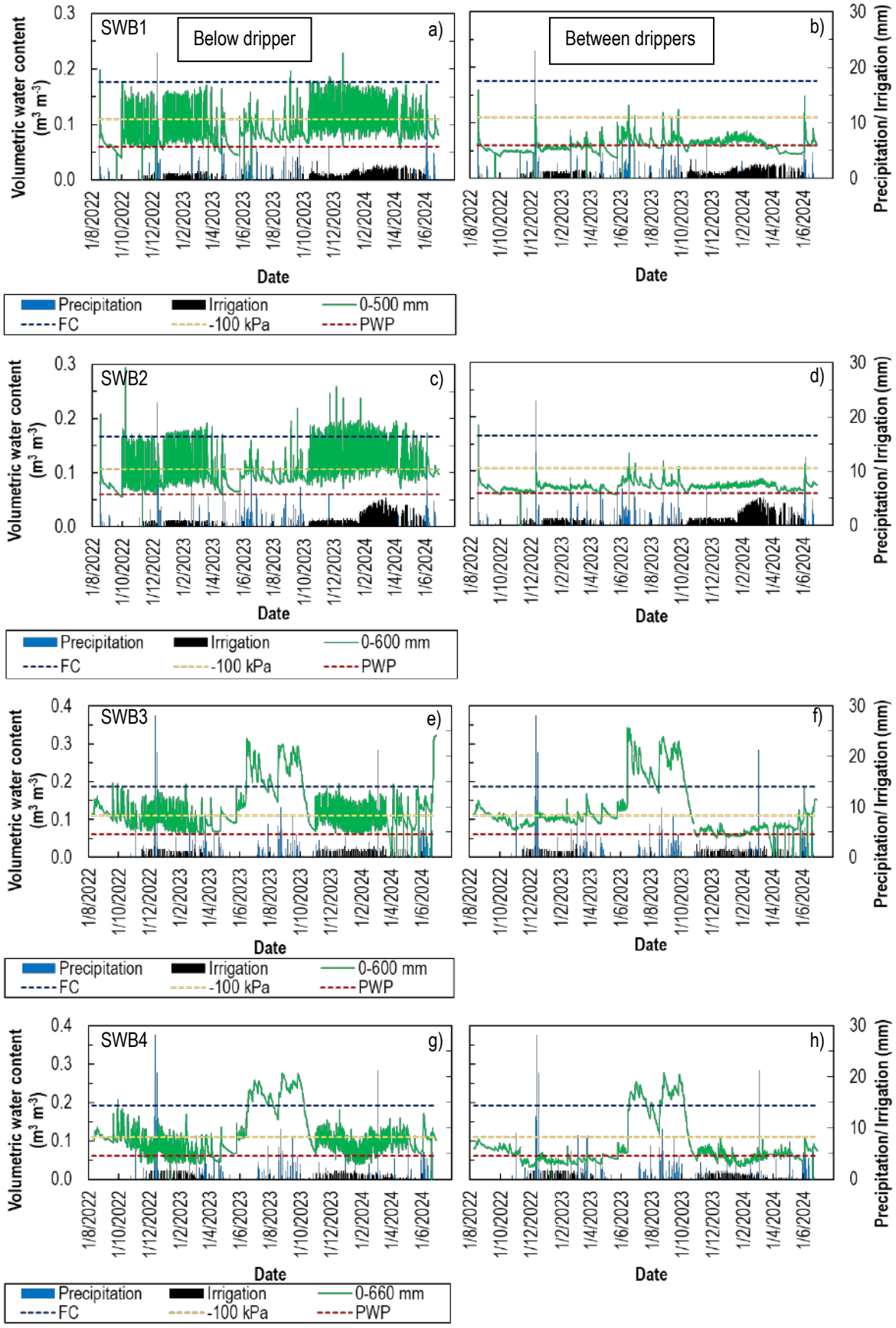

Figure 47. Seasonal trends of hourly CS650 volumetric soil water content for the top soil a) below a dripper (a, c, e and g) between two drippers (b, d, f and h) for the young (SWB1: a and b, SWB2: c and d) and for the full bearing (SWB3: e and f; SWB4: g and h) pomegranate orchard at Avontuur and Welgemoed, respectively, from 8 August 2022 until end June 2024. The Y-axis for rainfall or irrigation applied (mm d^{-1} per full surface area) is indicated in the Below dripper graphs (b, d, f, h)

the work row during the season reached maximum values of 2.5 mm at Avontuur and 3.3 mm at Welgemoed (Figure 48c and d). These maxima were associated with rainfall events at Avontuur and Welgemoed. Since no rainfall occurred in October 2023 at Welgemoed water losses from the work row indicated weed water use of up to 2.1 mm d^{-1}. Water loss in the case of the young orchard (Figure 48c) was mainly due to soil evaporation with minimal, if any, effects from weeds (field observation). Increased water losses from the work row of the full bearing orchard compared to the young orchard, especially during October 2023, were attributed to the presence of weeds in the work row (Figure 48c and d).

At Avontuur, during August and September 2022 when the young orchard was without leaves or had limited leaf coverage, the monthly averaged ETc was comparable for the mulched tree row and bare soil surface in the work row. For August, it was on average 0.82 mm d^{-1}, with an orchard ETc of 1.6 mm d^{-1} (Figure 49a). Less rainfall occurred during September (Refer Chapter 3, Figure 28) and the ETc decreased to 0.26 mm d^{-1} for the tree and work row and 0.5 mm d^{-1} for the orchard (Figure 49a). From October until January the orchard ETc increased from 2.8 mm d^{-1} to 4.95 mm d^{-1}. The ETc from the tree row varied between 2.8 mm d^{-1} and 4.8 mm d^{-1}. The contribution of the work row to the total ETc was minimal (ranged between 0.1 mm d^{-1} and 0.7 mm d^{-1}) and varied, depending on prevalence of rainfall events (Figure 48c). During February, March, April and May water use in the tree row decreased almost linearly, being 4.6 mm d^{-1}, 3.7 mm d^{-1}, 2.1 mm d^{-1} and 0.5 mm d^{-1}, while the soil evaporation losses from the work row varied between from 0.2- and 0.4-mm d^{-1} (Figure 49a). Orchard water use decreased from 4.8 mm d^{-1}.to 2.4 mm d^{-1} during February, March and April and became less than 1 mm d^{-1} in May (Figure 49a).

During June, increased water use compared to May for the orchard (1.3 mm d^{-1}) was attributed to higher evaporation (0.7 mm d^{-1}) associated with 20 rainfall events that occurred as leaf drop was already at an advanced stage (Figure 49a). Water loss from the orchard was similar to June in July 2023, being 0.64 mm d^{-1} for the tree and work row and in total 1.3 mm d^{-1} for the orchard. Orchard water use for the 2023/2024 season increased from 1.7 mm d^{-1} in August 2023 to 6.5 mm d^{-1} in January 2024, after which it decreased slightly to 5.9 mm d^{-1} and 5.4 mm d^{-1} in February and March. The ETc dropped steeply in April to 3.2 mm d^{-1} after which it gradually decreased towards 1.5 mm d^{-1} in June 2024. The maximum orchard water use occurred in January 2024 and it increased by 30% compared to January in the previous season.

At Welgemoed, during August 2022, the monthly averaged ETc for the tree row and work row with some weeds was 0.8 mm d^{-1}, with an orchard ETc of 1.6 mm d^{-1} (Figure 49b). As for the young orchard, the ETc for the orchard decreased during a drier September (Refer Chapter 3, Figure 28; Figure 49b). It decreased to 0.9 mm d^{-1} mainly due to lower water losses from the work row (0.3 mm d^{-1}) (Figure 48d and f). From October until January 2023 the orchard ETc increased from 1.7 mm d^{-1} to 3.6 mm d^{-1}. The ETc from the tree row increased from 1.5 mm d^{-1} in November 2022 to 3.4 mm d^{-1} in January 2023. The contribution of the work row to the total ETc varied and appeared to depend on growth dynamics of the weeds and prevalence of rainfall events that sustain its growth in the non-irrigated work row. The ETc in the work row ranged between 0 mm d^{-1} and c. 0.8 mm d^{-1} during the season, with higher ETc values (except for December 2022 when excessive rainfall occurred, Refer Chapter 3, Figure 28) more prevalent towards the end of the season (Figure 48d). Water use in February decreased by c. 48% compared to that in January. During February and March, water use in the orchard decreased from 1.7 mm d^{-1} and 1.8 mm d^{-1} to 0.7 mm d^{-1} and 1 mm d^{-1} in April and May 2023. Since leaf drop already started near end April and was at an advanced stage, increased water use for the orchard during June (1.3 mm d^{-1}) compared to May was attributed to higher weed transpiration and evaporation associated with 17 rainfall events that occurred during June 2023. For the 2023/2024 season, orchard water use increased from 0.9 mm d^{-1} in July to 3.1 mm d^{-1} in December 2023. It decreased in January and February to 2.9 mm d^{-1} and 2.5 mm d^{-1}, respectively, and thereafter reduced gradually towards May. Maximum water loss from the work row occurred in October 2023 (0.9 mm d^{-1}) when there was a dense stand of weeds present and only 1.5 mm rainfall occurred (Figure 48d and Figure 49b).

The ETc of the individual trees at the young orchard tended to be higher compared to that at the full bearing orchard in both seasons (Figure 49). This can partially be explained by higher atmospheric evaporative demand at Avontuur compared to Welgemoed, more vigorous growth at the young compared to the full bearing orchard (Refer Chapter 3, Figure 33) and in 2023/24 higher stomatal conductance (Refer Chapter 3, Figure 30) and higher crop load. However, the monthly averaged transpiration for the full bearing orchard was comparable to or more than that for the young orchard (Refer Chapter 3, Figure 39c and d). Monthly means were based on available data and the number of data points used in calculations differed between months. Except for June 2023, which had 5 and 2 data points only for Avontuur and Welgemoed, respectively, the number of data points per month ranged between 8 (September 2023) and 27 (September 2022) for Avontuur and between 8 (February 2023) and 28 (October 2023) for Welgemoed.

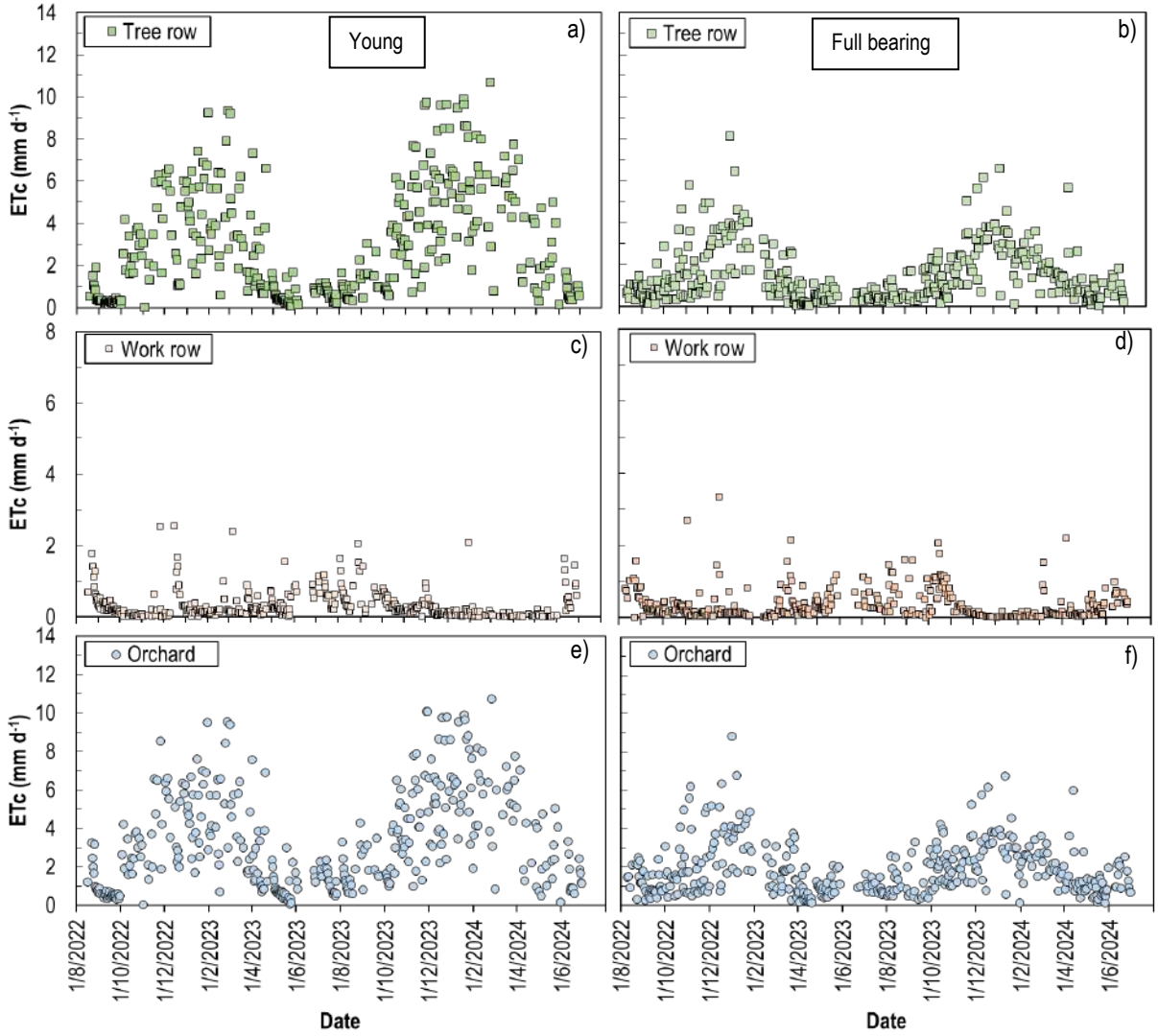

Figure 48. Daily soil water balance derived evapotranspiration (ETc, expressed as mm over the full surface) for the tree row (a, b), work row (c, d) and orchard (e, f) for young (Avontuur, a, c, e) and full bearing (Welgemoed, b, d, f) pomegranate trees for August 2022 until June 2024

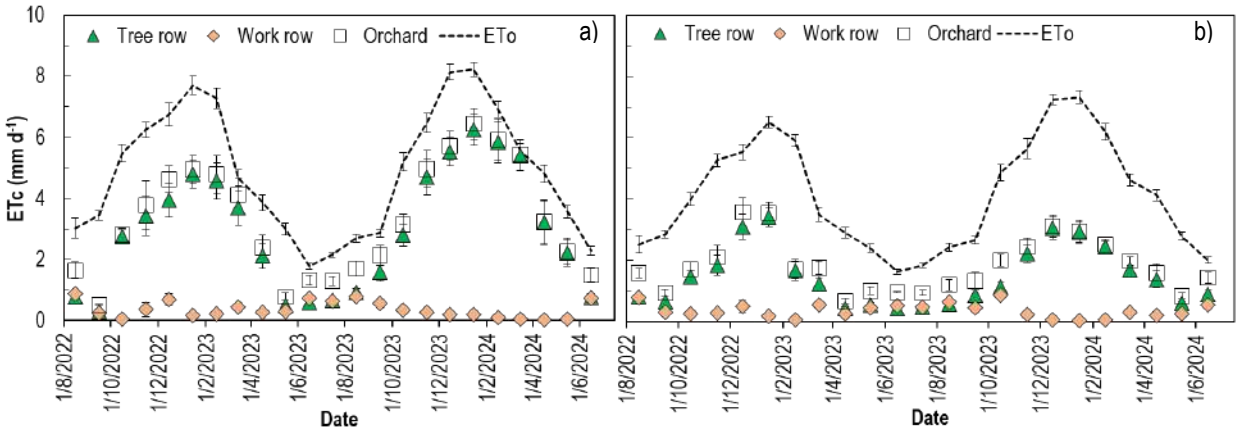

Figure 49. Monthly averaged soil water balance derived evapotranspiration (ETc, expressed as mm over the full surface) for the tree row, work row, and fully allocated area per tree per orchard for young (Avontuur, a) and full bearing (Welgemoed, b) pomegranate trees for August 2022 until June 2023. Means are based on available data and number of data points used in calculations differ between months.

5.3.4 Micrometeorological systems derived evapotranspiration

Figure 50 indicates diurnal patterns of energy balance components, including net radiation (Rn), sensible heat flux(H), latent heat flux (LE) and soil heat flux (G) for the young pomegranate orchard at Avontuur for selected days per season over the 2023/24 growing season. The Rn constitute the equilibrium between short-wave radiation and long-wave radiation. The H represents heat transfer between the surface of the earth and the atmosphere through conduction and convection.The LE represent the heat transfer related to the phase change of liquid water to water vapour. The G represents heat transfer through the soil profile. There is variability in water use within the growing season due to different weather conditions and different crop development stages. There are clear differences in the intensity of weather parameters that drive evapotranspiration, such as the Rn over the growing season. The highest Rn was observed in the summer, reaching a maximum of 637.5 W m^{-2} (Figure 50b). Similar results were observed from a study conducted by Mashabatu et al. (2025) on a Japanese plum orchard where the radiation peaked during the summertime, particularly during January. The maximum Rn during the late autumn was 343.3 W m^{-2}, which is 47% less than what was recorded in the summertime (Figure 50d). The soil heat flux was at its highest during September (Figure 50a). The high G values can be attributed to the exposed soil, as the leaf area index was still low shortly after bud break occurred late in August 2023 (data not shown). The highest maximum LE of 409.7 W m^{-2} was observed during early autumn just before harvest and may be partially due relatively high crop load of the young trees. However, the LE was at its lowest in late autumn, with a maximum of 274 W m^{-2}. This decrease in LE can be due to the combined effects of fruit removal during harvest, the onset of the leaf fall stage and a trend for lower atmospheric evaporative demand from March towards the end of May (Figure 54).

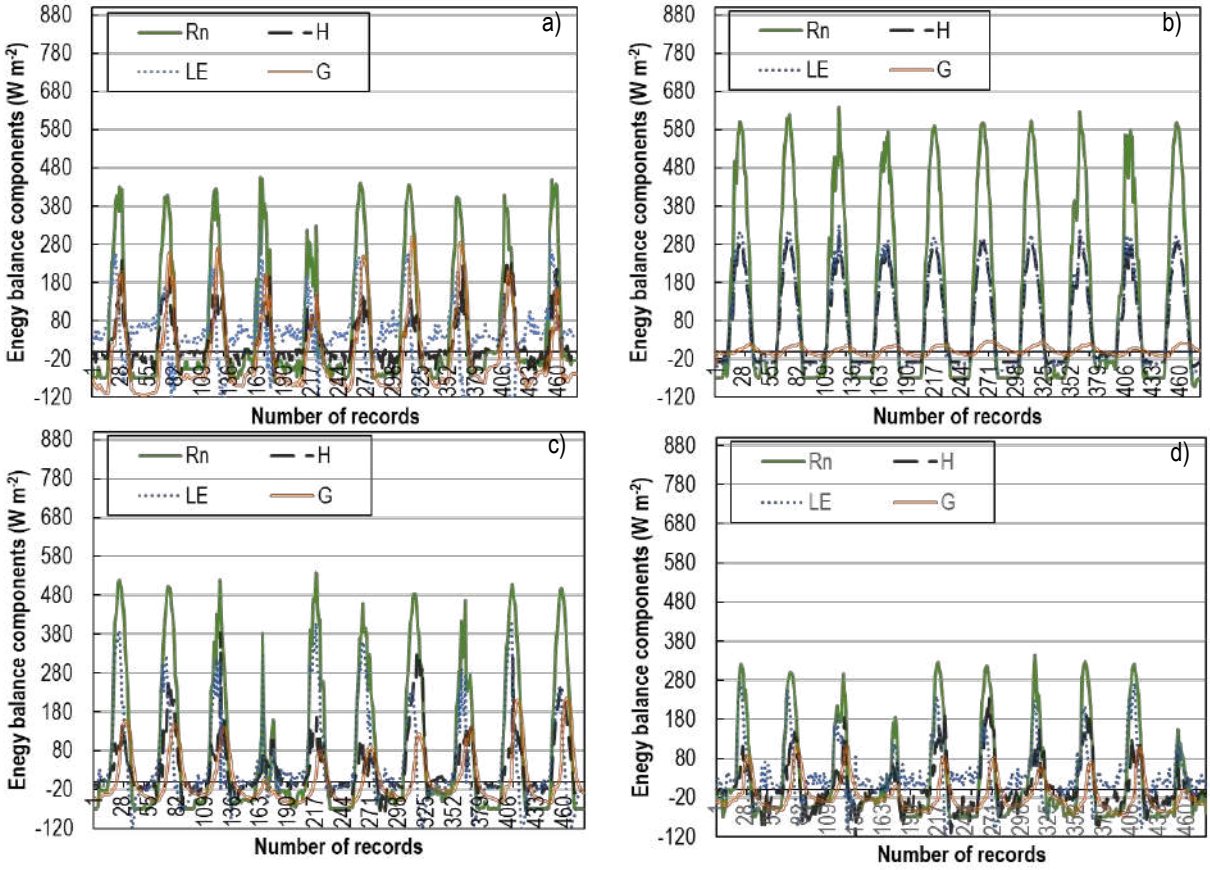

Figure 50. The diurnal patterns of energy balance components measured using the surface renewal method for the young cv. 'Wonderful' pomegranate orchard, including net radiation (Rn), sensible heat flux (H), latent heat flux (LE) and soil heat flux (G) during the 2023/24 growing season at Avontuur. Figure 49a, b, c and d depict the energy balance components during the ten first days of spring (September), summer (December), early autumn (March) and late autumn (May), respectively.

The energy balance components for the full-bearing orchard were measured using the eddy covariance system to estimate crop evapotranspiration and are displayed for selected days during four seasons (Figure 51). There was a lot of variation in the energy balance components during the four seasons, particularly the net radiation and latent heat. The Rn was observed to be at its highest

during the summer season with a maximum of 806.1 W m^{-2}, and the maximum during the winter season was 353.6 W m^{-2}, which shows a 43.9% decline from the summer to the winter season (Figure 51b and d). The western cape of South Africa has a Mediterranean climate that has rain events during the wintertime; hence, it was observed that there are several days with Rn and LE that were lower than 180 W m^{-2}. The latent heat can also be expressed as evapotranspiration (Twine et al., 2000). The highest LE was observed during the summer season with a maximum of 561.97 W m^{-2}. The LE had a 26.3% increase from the spring season to the summer season, and the LE had a 39.8 % decrease from the summer season to the autumn season. Interestingly, LE intensity is closely related to the Rn because Figure 51 shows that the LE will increase with an increase in Rn. For example, when the maximum Rn increased by 21.8% from the spring to the summer season, a similar trend was observed where the LE increased by 26.3% from the spring to the summer season. The H increased from spring to summer and gradually declined from summer to winter, where the lowest maximum H was observed (174.283 W m^{-2}). The soil heat flux (G) had an opposite trend over the four seasons compared to the other three energy balance components. The highest maximum G was observed during the April season (39.71 W m^{-2}). Contrary to what was observed from Rn, H and LE, the lowest maximum G value was observed during the summer season (15.185 W m^{-2}).

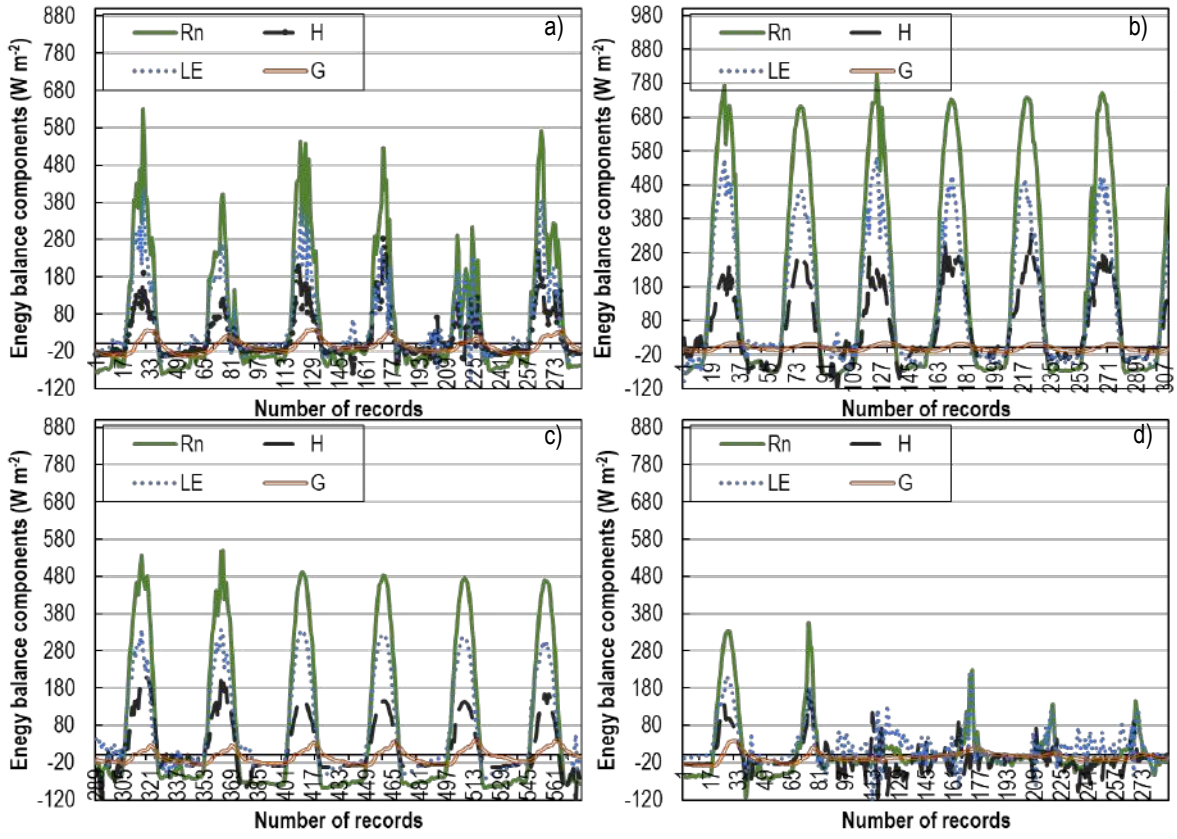

Figure 51. The diurnal patterns of energy balance components measured using the eddy covariance method for the full-bearing cultivar 'Wonderful' pomegranate orchard, including net radiation (Rn), sensible heat flux (H), latent heat flux (LE) and soil heat flux (G) during the 2023/24 growing season at Welgemoed. Figure 50a, b, c and d depict the energy balance components during six days of spring (September), summer (January), autumn (April) and winter (June), respectively.

In this study the energy balance closure was done using the residual-LE closure approach. The sum of the latent heat and sensible heat fluxes were plotted against the available energy for one month of the seasons to show the change in the closure over the growing season. Figure 52a, b, c and d depict the energy balance closure during spring (September), summer (December), early autumn (March) and late autumn (May), respectively for the young orchard. Figure 53a, b, c and d depict the energy balance closure during of spring (September), summer (January), autumn (April) and winter (June), respectively for the full bearing orchard. The R^2 values for the four months ranged from 0.95 to 0.99 (Figure 52). Figure 52c shows that at least 5% of the available energy was not accounted for by the sensible and latent heat fluxes. The R^2 values for the four months for the full bearing orchard ranged from 0.99 to 1 (Figure 53).

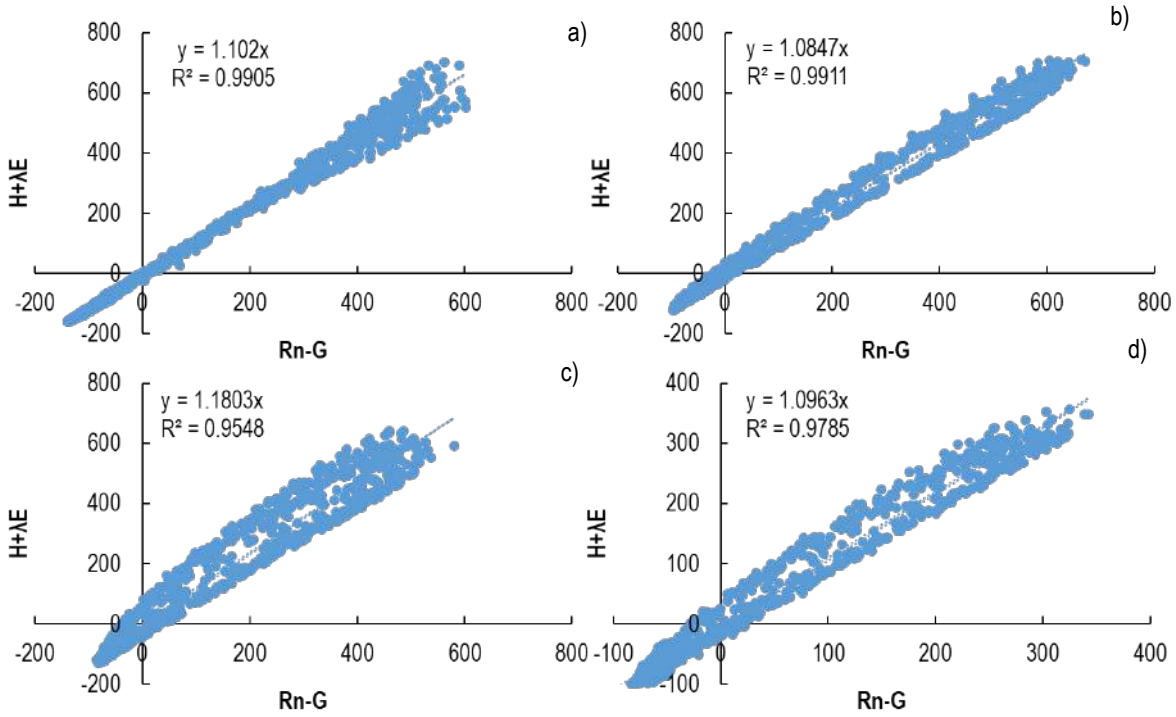

Figure 52. Energy balance closure for young non-bearing orchards measured using the surface renewal method for the cv. 'Wonderful' pomegranate orchard. Figure 52a, b, c and d depict the energy balance closure during spring (September), summer (December), early autumn (March) and late autumn (May), respectively.

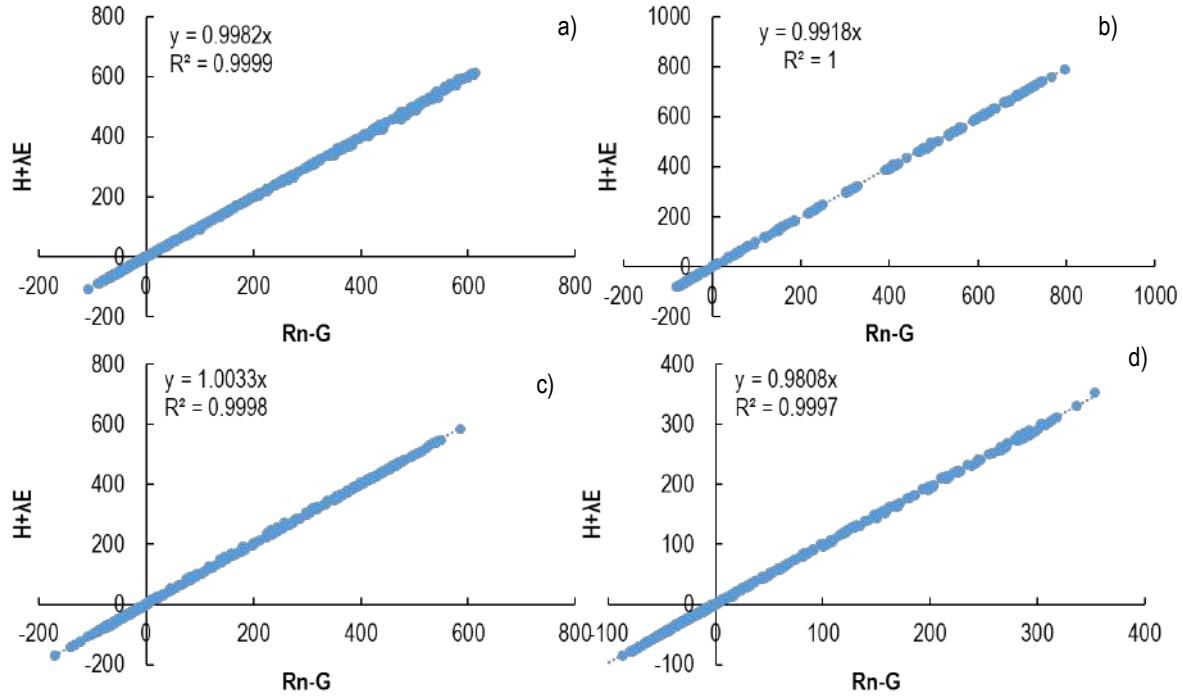

Figure 53. Energy balance closure for full-bearing orchard measured using the eddy covariance method for the cv. 'Wonderful' pomegranate orchard. Figure 53a, b, c and d depict the energy balance closure during spring (September), summer (January), autumn (April) and winter (June), respectively.

Figure 54 shows the seasonal curve of daily orchard level evapotranspiration (ETc) obtained from surface renewal measurements and the Penman-Monteith reference evapotranspiration (ETo) for the young orchard at Avontuur. Missing ETc data was estimated from a multiple regression relationship with daily Rn and T_{mean} (data not shown). This regression relationship was obtained via stepwise

regression conducted using all the weather variables recorded by the automatic weather station (Refer Chapter 3.5, R^2 = 72.86, $p<0.0001$). The ETc followed the same general trend as the evaporative demand (ETo). Figure 54 depicts a sinusoidal curve for the ETc and ETo with a high peak during the summer season. Figure 55 shows the seasonal curve of daily orchard level ETc obtained from the eddy covariance system and the Penman-Monteith ETo for the full bearing orchard at Welgemoed. Similarly, to what was observed in Figure 54, the full bearing orchard ETc followed the ETo general trend that peaked around the summertime and was the lowest during winter.

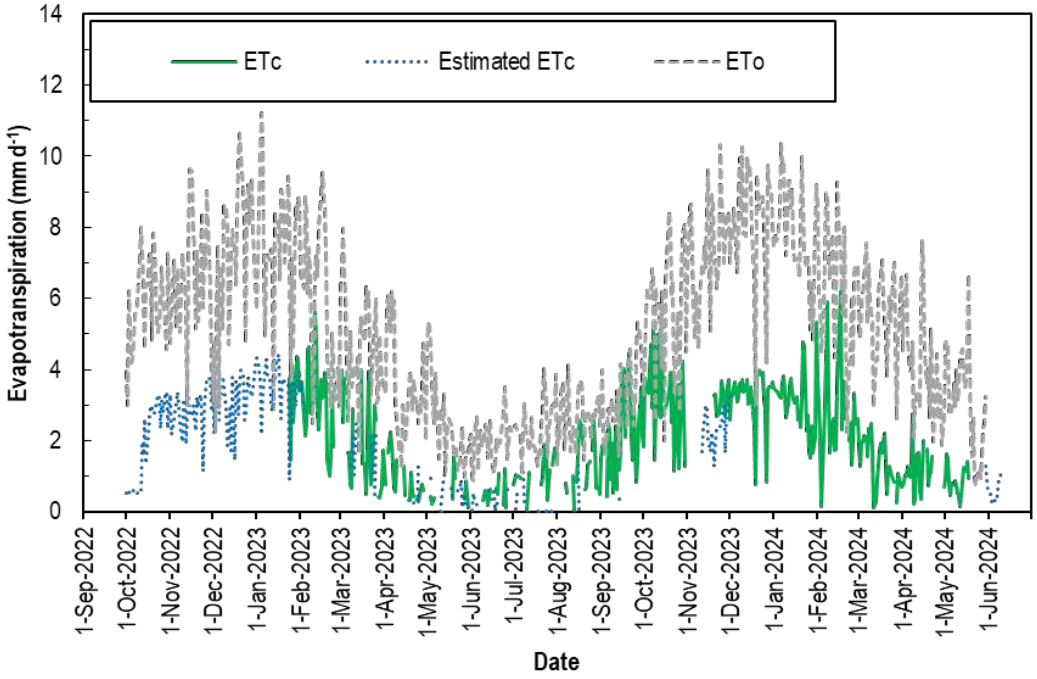

Figure 54. Daily surface renewal estimated crop evapotranspiration (ETc) and Penman-Monteith reference evapotranspiration (ETo) for a young cultivar 'Wonderful' pomegranate orchard at Avontuur from 1 October 2022 until 30 June 2024

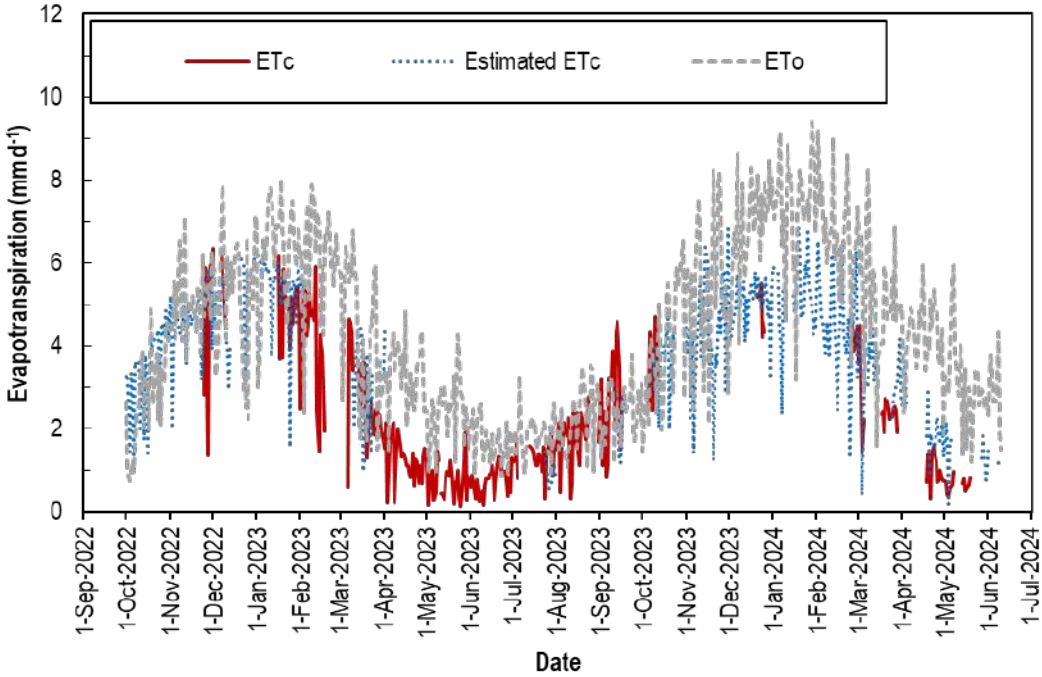

Figure 55. Daily eddy covariance estimated crop evapotranspiration (ETc) and Penman-Monteith reference evapotranspiration (ETo) for a full-bearing cultivar 'Wonderful' pomegranate orchard at Welgemoed from 1 October 2022 until 30 June 2024

Monthly average crop evapotranspiration values for both the young and the full bearing orchard are shown in Figure 56a and b during the 2022/23 and 2023/24 growing seasons, respectively. Figure 56a shows that there was a gradual increase in ETc from October 2022 to January 2023 for both the young (2.5- to 3.5 mm d^{-1}) and the full bearing (4.2- to 5.4 mm d^{-1}) orchard. In a similar fashion, the ETc for both the young and full bearing orchards had a rapid decline from February to June 2023. The ETc dropped by 41% and 35% for the young and the full bearing orchards, respectively, in March compared to February. The ETc became less than 1 mm d^{-1} for both orchards In May and June 2023. Likewise, the ETc was less than 1 mm d^{-1} for the young orchard in July and August 2023, but for the full bearing orchard only in July (Figure 56b). For the young orchard, ETc increased by about 79% from c. 1.4 mm d^{-1} in September and October to 2.5 mm d^{-1} November, there after remaining more or less similar until it reached 2.6 mm d^{-1} in February 2024. It dropped substantially in March (c. 44% compared to February) and decreased gradually towards June. For the full bearing orchard, the ETc increased from c. 1.4 mm d^{-1} in August 2023 to 5.2 mm d^{-1} in January 2024. The increase towards summer was more gradual compared to the abrupt increase for the young orchard from October to November 2023. The ETc for the full bearing orchard increased from September 2023 by 27%, 12%, 15% and 3% in October, November, December and January 2024, respectively. It tended to decrease linearly from January towards May (1.1 mm d^{-1}), flattening off in June at 0.9 mm d^{-1}.

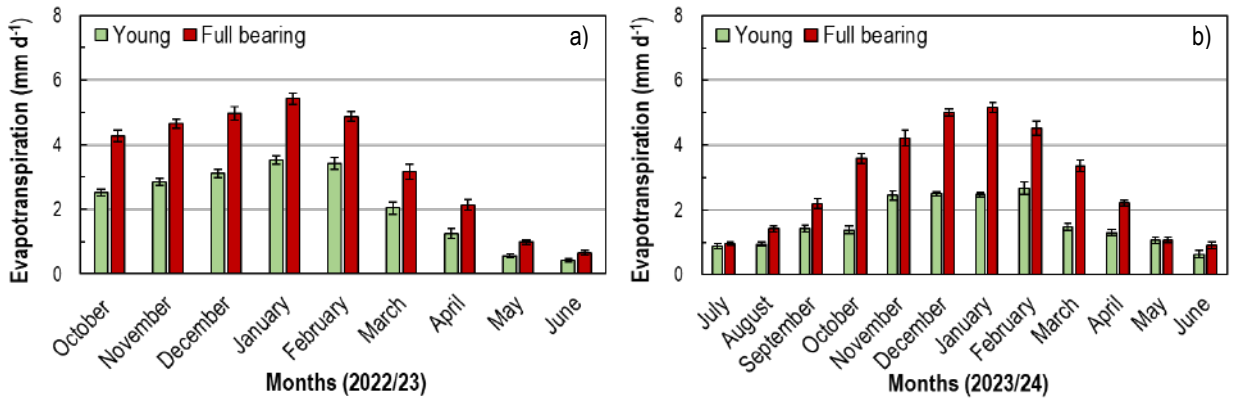

Figure 56. Monthly averaged crop evapotranspiration for the young and full-bearing cultivar 'Wonderful' pomegranate orchards during the 2022/23 (a) and 2023/24 (b) growing seasons

At the young orchard the highest monthly average ETo was observed in January for both the 2022/23 (7.8 mm d^{-1}) and 2023/24 (8.2 mm d^{-1}) seasons (Refer Chapter 3, Figure 27b). The ETc for the young orchard generally followed the trend of ETo over each season (Figure 54, Refer Chapter 3, Figure 27b; Figure 56a and b). However, contrary to what was observed for the ETo, the maximum monthly average ETc were observed in January 2023 (3.5 mm d^{-1}) and February 2024 (2.7 mm d^{-1}) for the 2022/23 and 2023/24 growing seasons, respectively (Figure 56).

The highest monthly average ETo for the full bearing orchard was observed in January for both the 2022/23 (6.5 mm d^{-1}) and 2022/23 (5.2 mm d^{-1}) seasons (Refer Chapter 3, Figure 27b). Similarly maximum monthly average ETo coincided with the maximum monthly averages observed for ETc in January for the 2022/23 (5.4 mm d^{-1}) and 2023/24 (5.2 mm d^{-1}) growing seasons. (Figure 56a and b). The minimum monthly average ETc was observed in the winter during June for both orchards with the average taken over both seasons amounting to 0.53 mm d^{-1} and 0.78 mm d^{-1} for the young and full bearing orchard, respectively.

The pomegranate-growing season in the Western Cape normally begins end August or at the beginning of September just after bud break and ends in autumn (May) after most leaf fall occurred. Unless the season was preceded by a dry winter, frequent irrigation normally commences in October and ends in April after harvest. The total ETc for the young orchard, based on measured and modelled data for the 2022/23 growing season from 1 October 2023 until 31 May 2024, was 596.7 mm whereas 465.9 mm was measured for the 2023/24 growing season. The ETc was c. 28% more in 2022/23 than in 2023/24 although the seasonal ETo at Avontuur was c. 5% lower in the first (1413 mm) compared to the second season (1491 mm). The total ETc for the full bearing orchard, measured and modelled from 1 October 2022 until 31 May 2023 during the 2022/23 growing season, amounted to 898.5 mm and during the 2023/24 growing season to 888.6 mm. The seasonal ETc was a mere 1.1% higher in the first compared to the second season. The seasonal total ETo was though 20% higher in 2023/24 (1307 mm) compared to 2022/23 (1091 mm).

5.3.4.1 Factors controlling evapotranspiration

The daily orchard level ETc estimated by the surface renewal system (SR) for the young orchard and the eddy covariance (EC) system for the full-bearing orchard was related through simple linear regressions to selected weather variables for two growing seasons, namely 2022/23 and 2023/24. Table 34 summarizes the coefficients of determination (R^2) of these highly significant ($p<0.0001$) linear regression relationships for the young and full-bearing orchards separately per season and for data of both orchards for seasons combined. The young orchard had coefficients of determination ranging from 0.097 to 0.652 during the 2022/23 growing season, and the R^2 values for the 2023/24 growing season ranged from 0.036 to 0.688. Based on the R^2, better regression relationships were observed between ETc and the weather variables during the 2022/23 season compared to the 2023/24 season, with the exception of Rn and RH_{min}, which improved slightly in 2023/24. For the full-bearing orchard R^2 values for the regression relationships between ETc and the weather variables for the 2022/23 growing season ranged from 0.085 to 0.884 and for the 2023/24 growing season from 0.096 to 0.798 (Table 34). The highest R^2 values for both seasons were observed for the regression relationship of ETc with solar radiation, with R^2 values of 0.884 and 0.798 for the 2022/23 and 2023/24 growing seasons, respectively. Literature indicates that environmental conditions are the most critical factors influencing the ETc rate of orchards, particularly solar radiation (Allen et al, 1998). It is also important to note that the wind speed, surface roughness and stability of the air above the area where the evaporation occurs influence other weather variables, such as the VPD and air temperature, that play a large role in water use. The VPD and T_{max} had a good relationship with the ETc with R^2 values of 0.682 and 0.723, respectively, for the 2022/23 growing season. However, wind speed correlated poorly to ETc with resultant low R^2 values. Linear regression relationships for ETc data of orchards combined for both the 2022/23 and 2023/24 growing seasons versus weather variables did not improve R^2 values compared to those for the young orchard conducted per season for both seasons, or for the full bearing orchard in the second season. The regression relationships did improve compared to those for the full bearing orchard in the second season, except for Rn and wind speed, which was worse off when data for orchards and seasons were combined.

The correlation between the total daily ETc for the young and full bearing orchards and the most important weather variables for data of both seasons combined is shown in Figure 57 (Rn, T_{max} and T_{min}) and Figure 58 (RH_{min}, RH_{max} and VPD). The daily total ETc is compared to reference evapotranspiration of both the young and full bearing orchards in Figure 59. The regression relationship between ETc and Rn, the temperature variables and VPD, respectively, had for both orchards a positive slope (Figure 57 and 56e - f). Conversely, the graphs with RH_{min} and RH_{max} had a negative slope, meaning that the ETc decreased with an increase in RH_{max} or min (Figure 58a - d). Non-linear trends, compared to the linear, did not notably improve the regression relationship of ETc with RH_{min} (data not shown). The daily ETc increased with increasing Rn, T_{max}, T_{min}, VPD and ETo (Figures 57, 58e - f and 59). The best linear relationships were found between ETc versus solar radiation, Tmax or the VPD, respectively, for both orchards (Figure 57a – d, Figure 58e and f). However, poor relationships were observed between the ETc and maximum relative humidity (Figures 58a and b) for both orchards, giving an R^2 of 0.142 for the full-bearing orchard. Although a non-linear trend improved the regression relationship between transpiration and VPD compared to a linear approach (Refer to Chapter 3, Figure 41e and f), this was not the case for the regression relationship between ETc and VPD, where the linear regression relationship described the data best (Figure 58e and f). The regression analysis shows moderate to good linear relationships between the orchard ETc and daily ETo for data of both seasons combined with R^2 values of 0.548 and 0.767 for the young and full bearing orchards respectively.

Table 35 summarizes stepwise regression results to assess the effect of each weather variable on the daily orchard ETc for both the young and full-bearing orchards during the 2022/23 and 2023/24 growing seasons, and for data of both orchards and seasons combined. The sequence of the weather variables in the table were based on their contribution to the adjusted R^2 where data from both sites and seasons were combined. The adjusted R^2 for the multiple regression for the young orchard for the 2022/23 and 2023/24 seasons was 70.13% and 78.44%, respectively. The Rn contributed 64.9% and 68.7% to the variation in ETc during the two respective seasons). The p-values from the stepwise regression of ETc and weather variables were highly significant for Rn and RH_{max} during 2022/23 and for Rn, wind speed, RH_{min} and VPD for the 2023/24 season. The 2022/23 stepwise regression model included two weather variables (Rn >RH_{max}) and during the 2023/24 season four weather variables were selected for the model (Rn>VPD>Wind speed>RH_{min}). The adjusted R^2 for the multiple regression for the full bearing orchard for the 2022/23 and 2023/24 seasons was 91.2% and 86.2%, respectively. In the case of the full bearing orchard Rn contributed 88.4% to the variation of ETc during the 2022/23 growing season and 76.7% during 2023/24. The 2022/23 stepwise regression model of the full bearing orchard included two weather variables (Rn >T_{min}) and during the 2023/24 season all of the weather variables except for T_{max} were selected for the model (Rn>T_{mean} >T_{min} >RH_{min} >RH_{max}>Wind speed> VPD). The results indicated that solar radiation is the most important weather variable affecting pomegranate orchard water use for both the young and full bearing orchards.

Table 34. Coefficient of determination of simple linear regressions between daily orchard crop evapotranspiration versus selected weather variables for the young and full bearing cultivar 'Wonderful' pomegranate orchards during the 2022/3 and 2023/24 growing seasons

Site	Season	Rn	Tmax	Tmin	RHmax	RHmin	Tmean	Windspd	VPD	ETo	n
Young	2022/23	0.652	0.607	0.482	0.260	0.332	0.647	0.097	0.560	0.591	97
	2023/24	0.688	0.505	0.268	0.235	0.354	0.442	0.036	0.494	0.528	273
Full bearing	2022/23	0.884	0.723	0.357	0.205	0.496	0.721	0.085	0.682	0.850	138
	2023/24	0.798	0.409	0.209	0.125	0.277	0.419	0.096	0.461	0.694	147
Young and full bearing	2022/23 and 2023/24	0.599	0.487	0.242	0.163	0.329	0.440	0.035	0.461	0.457	655

Rn - Net radiation, T_{max} - Maximum temperature, T_{min} - Minimum temperature, RH_{max} - Maximum relative humidity, RH_{min} - Minimum relative humidity, T_{mean} - Mean temperature, VPD - vapour pressure deficit

Table 35. Summary of the stepwise regression results of the crop evapotranspiration versus selected weather variables for the young and full-bearing cultivar 'Wonderful' pomegranate orchards during the 2022/23 and 2023/24 growing seasons. The adjusted coefficient of determination is indicated as percentages.

Variables	Young				Full bearing				Both orchards	
	2022/23		2023/24		2022/23		2023/24			
	Adjusted R^2	p-value	Adjusted R^2	p-value	Adjusted R^2	p-value	Adjusted R^2	p-value	Adjusted R^2	p-value
Rn	64.851	<0.0001	68.658	<0.0001	88.354	<0.0001	79.677	<0.0001	59.810	<0.0001
Wind speed	-	-	3.965	<0.0001	-	-	0.473	0.038	4.727	<0.0001
RH_{min}	-	-	1.108	0.000	-	-	0.601	0.007	1.329	<0.0001
VPD	-	-	4.712	<0.0001	-	-	0.353	<0.0001	0.590	0.001
T_{min}	-	-	-	-	2.857	<0.0001	1.816	<0.0001	0.226	0.036
T_{max}	-	-	-	-	-	-	-	-	-	-
T_{mean}	-	-	-	-	-	-	3.358	<0.0001	-	-
RH_{max}	5.279	<0.0001		-	-	-	0.509	<0.0001	-	-

Rn - Net radiation, T_{max} - Maximum temperature, T_{min} - Minimum temperature, RH_{max} - Maximum relative humidity, RH_{min} - Minimum relative humidity, T_{mean} - Mean temperature VPD - vapour pressure deficit

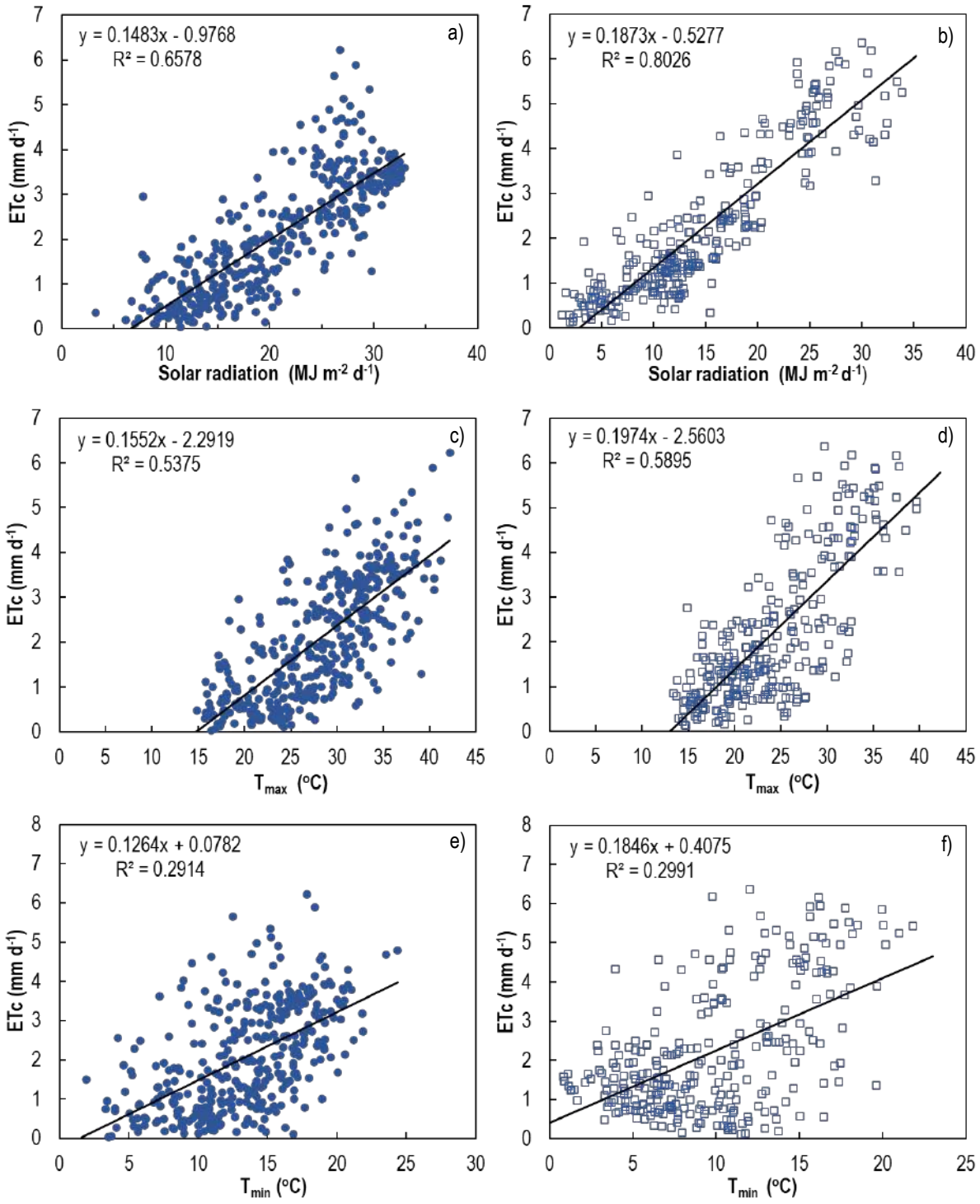

Figure 57. The relationship between crop evapotranspiration (ETc) and selected weather variables in a young (a, c and e) and a full-bearing (b, d and f) cultivar 'Wonderful' pomegranate orchard. The weather variables include solar radiation (a and b), maximum temperature (T_{max},) c and d) and minimum temperature (T_{min}, e and f).

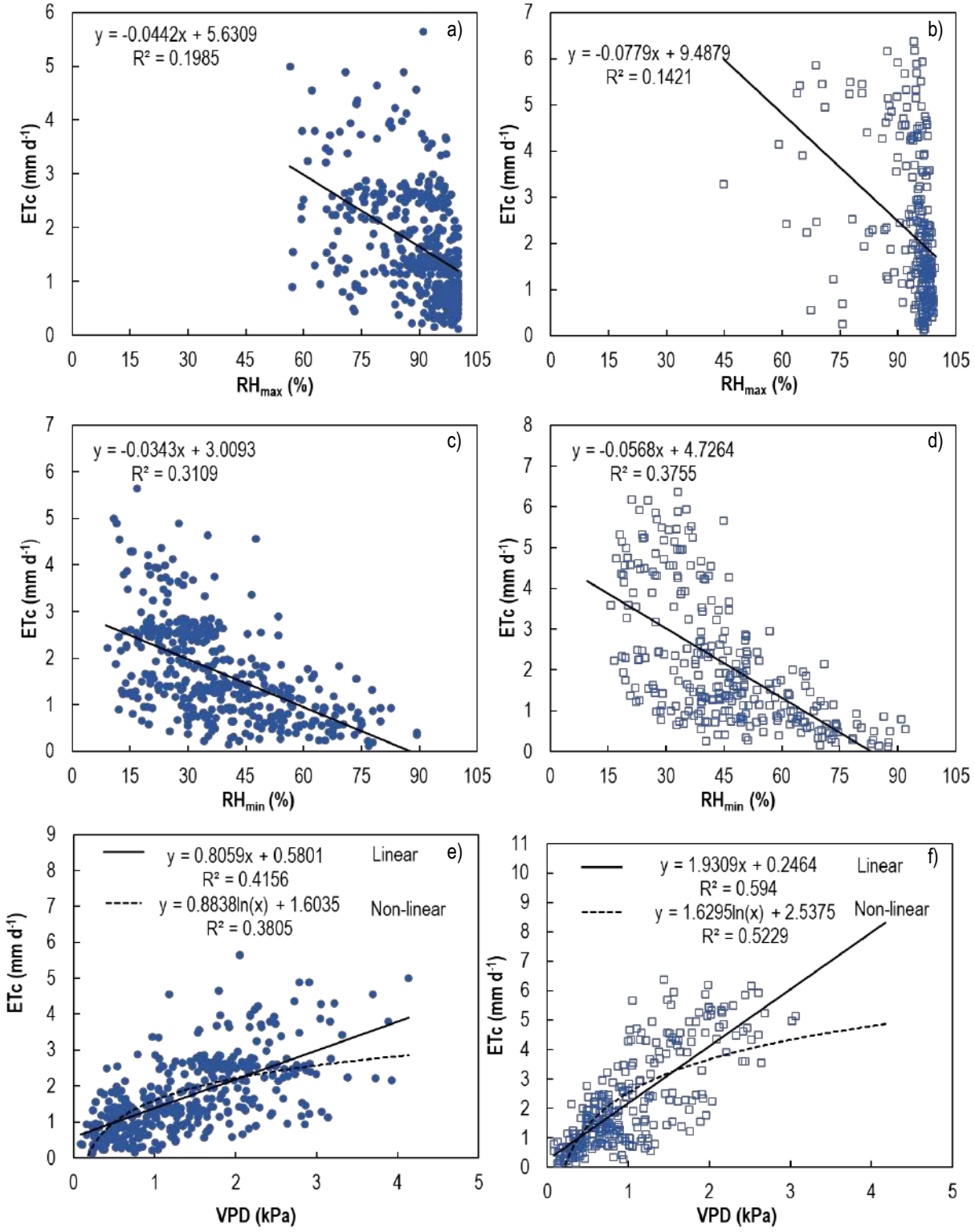

Figure 58.The relationship between crop evapotranspiration (ETc) and weather variables in a young pomegranate orchard (a, c and e) and a full-bearing pomegranate orchard (b, d and f). The weather variables include maximum relative humidity (RH_{max}, a and b) minimum relative humidity (RH_{min}, c and d) and vapour pressure deficit (VPD, e and f).

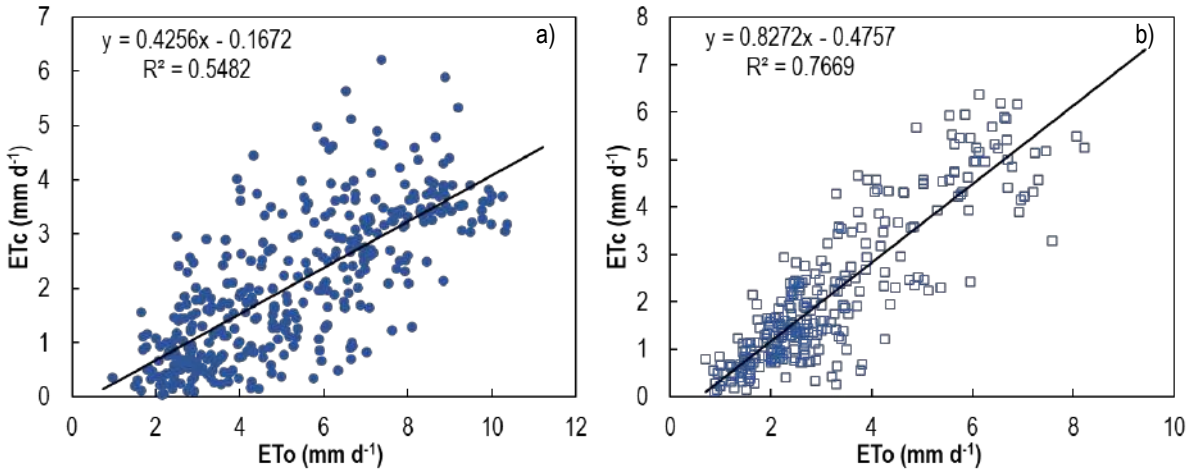

Figure 59 .Comparison of orchard level crop evapotranspiration (ETc) to reference evapotranspiration (ETo) in a young (a) and full-bearing (b) cultivar 'Wonderful' pomegranate orchard at Avontuur and Welgemoed respectively, for two growing seasons (2022/23 and 2023/24) combined

The stepwise regression model based on data of the young and full bearing orchards for both seasons combined had an adjusted R^2 value of 66.7%, with the sequence of weather variables contributing significantly to variation in ETo being Rn>wind speed>RH_{min}>VPD>Tmin. The Rn contributed 59.8% to the variation in ETc of the combined dataset (Table 35). The p values for the selected weather variables from the step wise regression of both orchards combined were highly significant and ranged between less than 0.0001 and 0.036. The effect that the tree canopy as potential transpiring area has on ETc was investigated by doing simple linear regressions with fractional light interception and LAI data available for selected dates during the two growing seasons. Table 36 shows the coefficients of determination for simple linear regressions of daily ETc with fractional light interception (FI), CLAI (ceptometer leaf area index), TLAI (Tree canopy area based leaf area index), OLAI (orchard level leaf area index) and selected weather variables for both the young and full-bearing orchards during the 2022/23 and 2023/24 growing seasons. For the young orchard FI was the only canopy variable that related significantly at a 95% confidence level to the ETc (R^2 = 0.806) and only in the second season. The daily ETc rate of the young orchard also related significantly to Rn, Tmax, T_{mean} and ETo, with p-values less than 0.05 and coefficients of determination of 0.852, 0.703, 0.521 and 0.663, respectively. For the full bearing orchard, ETc related significantly to the various LAI variables and Rn, with coefficients of variation of 0.963 and 0.978, respectively. Based on the limited dataset there was no consistent effect of canopy related variables on the ETc if both sites and seasons were considered and further research in this regard is recommended.

5.3.5 Evapotranspiration based water use efficiency and productivity

In 2023/24, ETc from October until May at the young orchard amounted to about 59% of the total effective rainfall and irrigation applied whereas the ETc at the full bearing orchard exceeded it by 75%. The latter was probably possible due to the fact that the orchard depleted almost all the available winter rainfall supplemented water deeper in the soil profile – even beyond 900 mm depth (Figure 46). Irrigation water productivity for the young orchard amounted to 3.464 kg m^{-3} and for Welgemoed, despite the low yield of 2024, to 5.103 kg m^{-3}. Ayars et al. (2017) found irrigation water productivity for four-, five- and six-year-old trees of 5.15, 5.35 and 5.58 kg m^{-3} for surface drip irrigated trees.

Biophysical water productivity for Avontuur based on 4659.1 m^3 ha^{-1} ETc for October 2023 until May 2024 and marketable yield of 27.1 t ha^{-1} equalled 5.819 kg m^{-3}. Biophysical water productivity for Welgemoed based on 8985.5 m^3 ha^{-1} ETc for October 2022 until May 2023 and marketable yield of 33.3 t ha^{-1} equalled 3.705 kg m^{-3}. Due to the lower yield in 2024 though the water productivity based on 8885.5 m^3 ha^{-1} ETc for October 2023 until May 2024 and marketable yield of 16.9 t ha^{-1} dropped by almost 50% compared to the previous season to 1.899 kg m^{-3}. Economic water productivity for the two orchards based on gross farm income and ETc from October 2023 until May 2024 amounted to R75.47 m^{-3} for Avontuur and R20.60 m^{-3} for Welgemoed. Due to the effect of blemishes on the gross farm income economic water productivity was only R 3.66 m^{-3} for Welgemoed in 2022/23 despite the marketable yield of 33.3 t ha^{-1}.

Table 36. Summary of coefficients of determination (R^2) and Pearson p-values(p) for simple linear regressions of crop evapotranspiration versus the fractional light interception, ceptometer modelled leaf area index, tree canopy area based leaf area index, orchard leaf area index and weather variables for the young and full bearing cultivar 'Wonderful' pomegranate orchards during selected dates of the 2022/23 and 2023/24 growing seasons. Bold black text indicates variables which related significantly to crop evapotranspiration at a significance level of 5% (p≤0.05) and increased green colour intensity indicates increasing R^2 values.

Site	Seasons	SI	FI	CLAI	TLAI	OLAI	Rn	T_{max}	T_{min}	RH_{max}	RH_{min}	T_{mean}	Wind speed	VPD	ETo
Young	2022/23	R^2	0.966	0.317	0.317	0.317	0.959	0.954	0.927	0.900	0.848	0.944	0.613	0.978	0.946
	2023/24	R^2	**0.806**	0.140	0.140	0.140	**0.852**	**0.703**	0.249	0.016	0.006	**0.521**	0.208	0.279	**0.663**
Full bearing	2022/23	R^2	0.531	**0.963**	**0.963**	**0.963**	**0.978**	0.704	0.749	0.020	0.410	0.750	0.533	0.675	0.830
	2023/24	R^2	0.115	0.022	0.022	0.022	0.289	0.085	0.130	0.027	0.001	0.139	0.037	0.065	0.105
Young	2022/23	p	0.118	0.619	0.619	0.619	0.129	0.138	0.174	0.205	0.255	0.152	0.427	0.094	0.149
	2023/24	p	**0.002**	0.361	0.361	0.361	**0.001**	**0.009**	0.208	0.767	0.860	**0.043**	0.256	0.178	**0.014**
Full bearing	2022/23	p	0.271	**0.018**	**0.018**	**0.018**	**0.011**	0.161	0.134	0.860	0.359	0.134	0.270	0.178	0.089
	2023/24	p	0.510	0.777	0.777	0.777	0.272	0.576	0.482	0.756	0.946	0.467	0.715	0.626	0.531

SI - Statistical index, FI - fractional light interception, CLAI - ceptometer leaf area index, OLAI - orchard leaf area index, TLAI – Tree canopy area based leaf area index, Rn - Net radiation, T_{max} - Maximum temperature, T_{min} - Minimum temperature, RH_{max} - Maximum relative humidity, RH_{min} - Minimum relative humidity, T_{mean} - Mean temperature, VPD - vapour pressure deficit

If the effect of blemishes were omitted from the market classification, ETc based economic water productivity increased to R93.87 m^{-3} for the young orchard in 2023/24 and for the full bearing orchard in the 2022/23 and 2023/24 seasons to R26.43 m^{-3} and R26.03 m^{-3}, respectively.

The modelled ETc based biophysical water productivity for intermediate bearing apple trees with medium canopy cover in two South African production regions over various seasons ranged between 2 and 8.1 kg m^{-3} (Dzikiti et al., 2018), whereas that for full bearing high canopy cover trees varied between 8.8 and 14.4 kg m^{-3}. The ETc based biophysical water productivity for pomegranate trees of 5.8 kg m^{-3} for the young and 3.7 kg m^{-3} for the full bearing fell within the range of that for the intermediate bearing apples with medium canopy cover. It should be noted though that the full bearing pomegranate orchard was not irrigated optimally. The economic water productivity for the apple trees at the time ranged between R7.8 m^{-3} and R41.6 m^{-3} for the intermediate bearing and between R37.1 and R59.1 m^{-3} for the full bearing apple trees. Based on the data of the young orchard it seems as if economic water productivity could exceed that for apple, with or without blemishes being accounted for in the quality evaluation. Although tempting, direct comparison of data from 2018 to current conditions is not valid due to volatility of the markets and changes in the rand value.

5.4 CONCLUSIONS

The monthly average daily crop evapotranspiration for the young orchard reached maximum values of. 3.5 mm d^{-1} and 2.6 mm d^{-1} in January 2023 and February 2024 for the 2022/23 and 2023/24 seasons, respectively. Maximum evapotranspiration for the full bearing orchard occurred during January in both seasons, reaching 5.4 mm d^{-1} and 5.2 mm d^{-1} in 2022/23 and 2023/24, respectively. The monthly average daily crop evapotranspiration was about 1 mm or less for both research sites during May, June and July.

The seasonal water use for the young orchard based on measured and modelled orchard level ETc data from 1 October until 31 May was 596.7 mm and 465.9 mm for the 2022/23 and 2023/24 growing seasons, respectively. The total ETc for the full bearing orchard, measured and modelled for the same period, amounted to 898.5 mm in the 2022/23 growing season and to 888.6 mm during 2023/24. The young orchard had canola mulch on the tree row with almost no weeds present in the tree or work row, whereas the full bearing orchard did not have a mulch, but weeds contributed to the water use especially at the beginning of the growing season. Evaluation of the effect of selected weather and tree canopy variables on transpiration and ETc indicated that solar radiation was the main factor determining pomegranate orchard water use.

Due to lack of total seasonal irrigation data for 2022/23, water use efficiency data was only available for 2023/24 and ETc amounted for the young orchard to about 59% of the total effective rainfall and irrigation applied. The full bearing orchard, perceived to be underirrigated during the season, made use of winter water supplies in the soil profile as the ETc exceeded the total effective rainfall and irrigation applied by 75%. Irrigation water productivity amounted to 3.464 kg m^{-3} and 5.103 kg m^{-3} for the young and full bearing orchards, respectively, in 2023/24.

Biophysical water productivity for the young orchard amounted to 5.819 kg m^{-3} in 2023/24, total yield data not being available for the 2022/23 season as a result of theft on the farm. Biophysical water productivity for Welgemoed for 2022/23 amounted to 3.705 kg m^{-3}, but dropped due to poor flowering and fruit set and consequently lower yield in 2023/24.by almost 50% (1.899 kg m^{-3}). Economic water productivity for the two orchards based on gross farm income and ETc from October 2023 until May 2024 amounted to R75.47 m^{-3} for Avontuur and R20.60 m^{-3} for Welgemoed. Due to the effect of blemishes on the gross farm income economic water productivity was only R 3.66 m^{-3} for Welgemoed in 2022/23 despite the marketable yield of 33.3 t ha^{-1}. If the effect of blemishes were omitted from the market classification, ETc based economic water productivity increased to R93.87 m^{-3} for the young orchard in 2023/24 and for the full bearing orchard in the 2022/23 and 2023/24 seasons to R26.43 m^{-3} and R26.03 m^{-3}, respectively.

CHAPTER 6: MODELING WATER USE OF POMEGRANATE ORCHARDS VARYING IN CANOPY COVER

6.1 INTRODUCTION

According Jovanovic et al. (2020) the FAO56 approach is the most used and reliable approach to estimate crop evapotranspiration at the field scale through multiplying the grass reference evapotranspiration (ETo) with a crop coefficient (Kc). Although crop coefficients were listed for several crops in FAO56, it contained no data for pomegranate (Allen et al., 1998). There were at the time of inception of the project also no locally developed crop coefficients for pomegranate orchards. The fourth aim of this project, which focusses on water use and water productivity of pomegranate orchards, was therefore to develop a method for practical estimation of crop coefficients for application in a water use model to enable calculation of individual orchard water requirements under local conditions. Such a model could aid producers to schedule irrigation according to tree water requirements and prevent over- or under-irrigation which impacts the environment (leaching of fertilizers and water losses) and fruit tree performance (yield and quality). Rallo et al. (2021) in an update of the FAO56 documentation relatively recently, published indicative standard values for single crop coefficients relative to the mid- and end-season, under temperate climate for - amongst other tree crops - pomegranate. The Kc values reported by the pomegranate research were strongly related with the fraction of ground cover (Rallo et al., 2021 and references therein). According to Pereira et al. (2020), tree canopy properties such as height, fractional light interception (FI) and leaf area index (LAI) can indirectly be related to crop coefficients for purposes of irrigation scheduling. This chapter presents data for a young and a full bearing orchard in different production areas on the seasonal changes in fractional light interception and leaf area index and seasonal variation in transpiration and single crop coefficients. Transpiration coefficients estimated from tree height and fractional light interception are compared to Kt values based on sap flow measurements. The potential of the tree shaded area to estimate difficult to obtain tree properties to derive Kc values indirectly or to estimate Kc values directly is explored. The chapter concludes with research results on the use of satellite based remote sensing to estimate pomegranate water use.

6.2 METHODOLOGY

The research was conducted at a young pomegranate orchard at Avontuur (33°07'29.7"S; 18°56'08.8"E) and at a full bearing pomegranate orchard at Welgemoed (33°35'18.3048"S; 18°59'19.302"E), which covers an area of 6.7 and 4.9 hectares, respectively (Refer to Chapter 3.4). An automatic weather station was installed within 50 m from each orchard to monitor the necessary variables hourly (Refer to Chapter 3.3) to calculate reference evapotranspiration (ETo) for calculation of crop coefficients and rainfall as input for soil water balance calculations. Sap flow derived transpiration (Refer to Chapter 4.2.2) and soil water balance and meteorological system derived ETc (Refer to Chapter 5.2.1 and 5.2.2) was used to calculate transpiration and crop coefficients.

6.2.1 Fractional light interception and leaf area index

Tree height, fractional light interception (FI) and the tree shaded area was monitored at selected dates throughout the season (Refer to Chapter 3.7 for details) to investigate the prospects to directly or indirectly estimate Kc values for pomegranate trees. Fractional light interception was measured approximately monthly in 2022/23 using a LP-80 Accupar ceptometer at two soil water balance trees from September 2022, and from December 2022 when a second ceptometer became available, also at the four sap flow trees. Measurements continued until early July in 2023. In 2023/24, the measurement protocol was adapted to measure fractional light interception at eight trees per site per measurement day using two Accupar LP-80 ceptometers. Measurements were done about monthly at the young and the full bearing orchards from August 2023 until June 2024 on full sun days. Measurements on both sides of the tree row were conducted about one hour before to one hour after solar noon. Refer to Chapter 3.7 for details regarding the measurement protocol.

Fractional light interception was also measured during April 2024 for a range of tree sizes (n=6) at each orchard and leaves were collected during natural leaf fall to calibrate the Accupar LP-80 for actual leaf area index (LAI) estimates. A regression relationship was obtained between Accupar LP-80 ceptometer derived LAI (CP-LAI) and LAI calculated from measured canopy dimensions and actual

leaf area. Leaf area index was expressed per tree canopy area (Tr-LAI) and orchard area allocated per tree (OLAI). In 2023/2024, on the same dates that FI was measured, the shaded tree area was determined for three trees per orchard using a manual method that employed 10 cm x 10 cm demarcated hard boards that covered the full surface allocated per tree. Photos were taken of the shaded area and the number of shaded blocks and their degree of shading (25%,50%, 75% or 100%) in the allocated area was determined and averaged. The shaded area was related by linear regression to FI, Tr-LAI and OLAI and by linear and non-linear regression to orchard level Kc values.

6.2.2 Single and basal (transpiration) crop coefficients

Transpiration coeffcients were calculated as T:ETo (Volschenk et al., 2003). Soil water balance based crop coefficients (Kc) were calculated according to Allen et al. (1998) as the ratio of ETc to ETo for the tree row, work row and fully allocated orchard surface per tree, respectively. For the micrometeorological systems crop coefficients (Kc) for the two research sites were calculated according to Allen et al. (1998) as the ratio of orchard scale measured ETc to ETo.

6.2.3 Allen and Pereira approach

The transpiration crop coefficient (K_t) was estimated based on the latest publication from Pereira et al. (2020), which adds more information to Allen and Pereira (2009). The measured K_t was derived from actual transpiration measurements for the young and full-bearing orchards and ETo during the 2023/24 growing season. In this study, K_t full will be estimated based on the plant height. K_t full was defined as the estimated K_t during the peak growing stages of a crop where full ground cover is achieved or LAI >3 (Pereira et al.., 2020). The density coefficient K_d and the $K_{t\,full}$ are used in Eq, 31.

$$K_t = K_d K_{t\,full} \quad \text{[Eq. 31]}$$

In this study, the K_d was calculated using the fractional light interception, and the K_d relates the increase in K_t with an increase in vegetation. The K_d was calculated as follows:

$$K_d = min(1, MLfc_{eff}, fc_{eff}{}^{(\frac{1}{1+h})}) \quad \text{[Eq. 32]}$$

The K_t full values were estimated as a fraction of the mean plant height (m), and it was adjusted for the specific climate.

$$K_{t\,full} = F_r(\min(1.0 + 0.1h, 1.20) + [0.04(u_2 - 2) - 0.04(RH\ min - 45)](\frac{h}{3})^{0.3}) \quad \text{[Eq. 33]}$$

Where *h* is the maximum pant height in m, u_2 is the mean value of the wind speed at 2 m height during the mid-season in m s^{-1}, RH min is the minimum relative humidity during the mid-season in percentage and Fr [1.0] is an adjustment factor used to adjust $K_{t\,full}$ for crops which shows signs of stomatal control.

$$F_r = \frac{\Delta+\gamma(1+0.34u_2)}{\Delta+\gamma(1+0.3u_2\frac{r_1}{100})} \quad \text{[Eq. 34]}$$

Where Δ is the slope of the saturation vapour pressure vs temperature curve (kPa $^oC^{-1}$), γ is the psychometric constant (kPa $^oC^{-1}$), r_1 is the mean leaf resistance for the vegetation in the question (s m^{-1}) and the value of r_1 is limited to 100 s m^{-1} or more (Pereira et al., 2020). Estimated average plant height and the fractional (fc) interception over the season was calculated from data estimated using a polynomial relationship between the measured plant height and the fractional light interception with the day of season. The estimation of the mean leaf resistance calculations were done based on the method suggested by Taylor et al. (2014) where the values of the mean daily r_l for this study was estimated from inverting Eq. 34. A resistance correction factor (F_r) was calculated by inverting Eq 33 using the daily values of $K_{t\,full}$. The $K_{t\,full}$ values were estimated using the daily K_t and the K_d values, both determined from measured transpiration data and inverting Eq. 31. Mean leaf resistance was derived from fortnightly means of tree height, fractional interception, RH_{min} and wind speed before K_t was estimated.

6.2.4 Estimating evapotranspiration using satellite-based remote sensing data

Eighteen Landsat eight Operational Land Imager (OLI) and Thermal Infrared Sensor (TIRS) images having a cloud cover of less than 50% with path/row 175/083 representing the pomegranate orchard during the period September 2022 to October 2023 (Table 37) were freely accessed and downloaded from https://earthexplorer.usgs.gov/. Various software techniques, such as Quantum Geographical Information Systems (QGIS), were used to generate the raster map for the study area to enable evapotranspiration (ET) processing and evaluation. The availability of satellite observation data plays a crucial role in enhancing surface land monitoring capabilities, where more data availability contributes to more dependable land cover classification and facilitates change detection processes (Li et al., 2020). Data processing requires less cloud cover to avoid errors, distortions, or inaccuracies introduced into data. If clouds dominate the area during the collection dates, it is recommended to wait for the next revisit time to collect data. This approach to collecting data and various operational limitations, such as the data acquisition strategy, payload specifications, station acquisition capability, and instrument-related challenges, also impact data availability (Gascon et al., 2017; Wulder et al., 2016). It is noteworthy that Landsat Eight does not capture observations worldwide. Instead, its coverage includes all sunlit land areas and coastal regions near the shore with a solar elevation exceeding five degrees (°). The use of two remote sensing (RS) models in this study evaluated the accuracy, provided cross-validation, and captured variability in the orchard, as each energy balance (EB) method has its predictions, strengths, and limitations. Therefore, combining them helps address any gaps, improves reliability, and offers more robust insights into water use.

Table 37. Details of Landsat- 8 OLI and TIRS images acquired for a fully mature pomegranate orchard from September 2022 until October 2023

Month	Image Acquisition Dates	Day of the Year
September	6th September 2022	249
	22nd September 2022	265
October	8th October 2022	281
	24th October 2022	297
November	25th November 2022	329
December	27th December 2022	361
January	12th January 2023	12
February	13th February 2023	44
March	1st March 2023	60
April	2nd April 2023	92
	18th April 2023	108
May	4th May 2023	124
	20th May 2023	140
June	21st June 2023	172
July	7th July 2023	188
August	8th August 2023	220
September	9th September 2023	252
October	10th October 2023	283

6.2.4.1 PySEBAL-based evapotranspiration

Remote sensing images were analysed using a Python Program called PySEBAL, a version of SEBAL created by Hessels et al. (2017). The model data were converted into difference indices to estimate RS-based ET using eight Landsat images processed using

PySEBAL (Bastiaanssen et al., 1998; Laipelt et al., 2021). It is an open-source platform that uses semi-automatic processing to execute SEBAL on Landsat satellite imagery, as it allows large data functions, images, and other datasets. It selects cold and hot pixels using an automated anchor pixel approach, which entails creating a collection of predefined criteria and applying computer algorithms to determine the pixels in images that satisfy the requirements (Jaafar and Ahmad, 2019; Xue et al., 2020). In this study, RS-based meteorological data were downloaded from Geospatial Interactive Online Visualization and Analysis Infrastructure (Giovanni), (https://giovanni.gsfc.nasa.gov/giovanni/#service=TmAvMp&starttime=&endtime=), an online tool developed by NASA to access and analyse earth science data, which was further analysed by using Microsoft Excel.

Ranges in the Normalized Difference Vegetation Index (NDVI), land surface temperature (TS), momentum roughness length (z_{om}), and surface albedo (α) are predefined criteria assessed in PySEBAL (Xue et al., 2020). The first step in estimating ET is using SEBAL to determine latent heat flux from remote sensing (Kustas et al., 1994; Boegh et al., 2002). The SEBAL equations used by the model follow the equations published by Allen et al. (2007), and the first step is to allow the algorithm to complete the EB equation to estimate the ET_c. According to Bastiaanssen et al. (1998) and Allen et al. (2007a), the equations to obtain the EB variables are clarified and summarised below.

$$Rn = (1 - \alpha)K(in) + (Lin - Lout) - (1 - \varepsilon\_0)Lin \quad \text{[Eq.35]}$$

The net solar radiation (Rn) flux is computed for each pixel using albedo and transmittances from short-wave bands and long-wave emissions, where K (in) is the incoming short-wave radiation (W m^{-2}), α is the dimensionless surface albedo, Lin is the incoming long-wave radiation (W m^{-2}), Lout the outgoing long-wave radiation (W m^{-2}), and ε_0 the dimensionless surface thermal emissivity. The surface thermal emissivity was estimated using NDVI and an empirically derived method:

$$\varepsilon\_0 = 1.009 + 0.047In\,(NDVI) \quad \text{[Eq. 36]}$$

Where NDVI is greater than zero; otherwise, the emissivity is assumed to be zero. NDVI can be calculated using the following bands:

$$NDVI = \frac{NIR - Red}{NIR + Red} \quad \text{[Eq. 37]}$$

Where NIR is the near-infrared band represented by band five, whereas Red is the red band represented by band four.
The incoming shortwave radiation was predicted assuming cloud-free conditions as follows:

$$K\_in = G\_sc \times cos\ \theta \times d\_r \times \tau\_sw \quad \text{[Eq. 38]}$$

Where G_sc represents the solar constant (1367 W m-2), cos θ is the cosine of the solar zenith angle, d_r is the inverse relative distance between Earth and the Sun, and τ_sw is the one-way transmittance. The overall value for τ_sw can be predicted for clear and relatively dry atmospheric conditions as follows:

$$\tau\_sw = 0.75 \times 2 \times 10^{-5} \times z \quad \text{[Eq. 39]}$$

At an elevation above sea level represented by z (in meters), the long-wave components L(in) and L(out) were calculated using the following equations:

$$L(in) = 1.08 \times (-In\tau_{sw})^{0.265} \times S \times T(ref^4) \quad \text{[Eq. 40]}$$

Where S is the Stefan Boltzmann constant 5·67 × 10^{-8} (W m^{-2} K^4), $T(ref^4)$ is the surface temperature at a reference point, selected to a well-watered pixel.

$$L(out) = \varepsilon\_0 \times s \times T_0^4 \quad \text{[Eq. 41]}$$

Where ε_0 is the dimensionless surface thermal emissivity and T_0^4 is the fourth power of the absolute temperature (T_0), measured using the surface temperature.

The estimations of G were calculated using empirical equations, as they were not directly generated from the RS images. Estimations utilise NDVI and Rn using the following equation:

$$G = 0.30(1 - 0.98(NDVI)^4)Rn \quad \text{[Eq. 42]}$$

H is the rate of heat loss by convection and conduction to the air, which is influenced by variations in temperature. This was calculated using the following equation:

$$H = \frac{\rho \times Cp}{r\_ah(dT)} \quad \text{[Eq. 43]}$$

where ρ is the air density (kg m^{-3}), Cp is the specific heat at constant pressure (1004 J kg^{-1} K^{-1}), dT is the temperature difference (K), and r_ah is the aerodynamic resistance to heat (s m^{-1}). To calculate the aerodynamic resistance to heat (r_ah), the following equation was used:

$$r\_ah = \frac{1}{(k.u)\frac{In\,(\frac{z1}{z2})}{u}} \quad \text{[Eq. 44]}$$

where u is the friction velocity, k is von Karman's constant (0·41), and z1 and z2 are the temperatures at different heights above the ground (K). The model requires one wind speed calculation to classify the rate of u and calculate an independent surface wind speed at a high level above the surface of the Earth, which is applied to all pixels of the image. The wind profile demonstrates the resulting equation:

$$u(z) = \frac{u^*}{k} \cdot ln\,(\frac{z-d}{z0}) \quad \text{[Eq. 45]}$$

where u* is the friction velocity, z-d is the difference between the height above the ground and the displacement height (d), and z0 is the roughness length. The surface roughness length for momentum transport was calculated using the following equation:

$$zom = a \times h \times b \quad \text{[Eq. 46]}$$

a × b are constants, and h is the mean height of the vegetation surrounding the meteorological station. Once u* is determined, the wind velocity at a selected height can be calculated using the H equation (Eq. 3.11). The use of a hot and cold pixel is then deployed to estimate a linear correlation between Ts and dT, where dT is calculated as:

$$dT = aT\_s + b \quad \text{[Eq. 47]}$$

where a and b are determined using Ts and dT estimates of the driest and wettest pixels, which then leads to the final step of selecting the daily ET, estimated by multiplying the value of the Evaporative Fraction (EF) and the daily estimated Rn. This equation is expressed as follows:

$$EF = \frac{\lambda ET}{Rn - G} \quad \text{[Eq. 48]}$$

6.2.4.2 EEFlux-based evapotranspiration.

The METRIC algorithm, fully automated and developed by Allen et al. (2007a, 2007b, and 2012), has been integrated into Google Earth Engine (GEE) as Earth Engine Evapotranspiration Flux (EEFlux). This integrated version was utilised to calculate ET, with the necessary data acquired from the EEFlux website (https://EEFlux-level1.appspot.com). The Landsat OLI and Thermal Infrared Sensor (TIRS) images from 1984 to the present day can cover most parts of the geographical region worldwide (Allen et al., 2015). The images used in this study are presented in Table 3.2. The downloaded data from the platform used NLDAS hourly data and grid MET daily gridded weather data, employing net radiation, wind speed, specific humidity, and T_{air}, engaging the American Society of Civil Engineers (2005) to estimate ET maps with ETo using the Penman-Monteith equation. The METRIC model solves the energy balance (H) from contextual image data and LE by residuals using equations 3.11 to 3.16, as explained in Section 3.2.3.1. The model then incorporates the calculation of a dimensionless parameter called the Bowen ratio (β) by Bowen (1926), which is expressed as:

$$\beta = \frac{H}{\lambda ET} \quad \text{[Eq. 49]}$$

Where H denotes the sensible heat flux, λETa signifies the latent heat flux, and λ representing the latent heat of vapourisation, like the parameters explained in Equation 3.1.

The model, as compared to SEBAL, uses hot and cold pixels, and the criteria for identifying anchor points involve agricultural areas characterised by vigorous and actively transpiring vegetation. They closely resemble reference conditions (cold pixels) as well as surfaces exhibiting minimal or absent vegetation cover (hot pixels), with minimal residual evaporation from the soil (Kjaersgaard et al., 2009), where the SEB computes the cold pixels according to the following equation:

$$Hcold = Rncold - Gcold - \phi \cdot \lambda ETrh \quad \text{[Eq. 50]}$$

H_{cold}, Rn_{cold}, and G_{cold} are the sensible heat, net radiation, and soil heat flux (W m^{-2}) within the image, respectively, during the satellite overpass. ETrh represents the hourly ET_o for cool-season clipped grass (mm h^{-1}), while ϕ signifies the ratio of alfalfa-to-grass-reference ET varying between 1.2 and 1.4 (Tasumi, 2003; Folhes et al., 2009). The hot pixels were estimated using Equation 17, assuming that $\phi \cdot \lambda ETrh$ tends to approach zero during extended periods of drought or absence of irrigation. Alternatively, when rainfall or irrigation occurs, an approximation of the residual ϕ·λETrh is calculated using hourly or daily water balance methods applied to the upper soil profile (Allen et al., 2007a). After obtaining the values of a and b from Equation 3.14, these variables are used in a step-by-step procedure that relies on the Monin-Obukhov similarity theory to calculate H for every pixel. By applying this theory and considering local meteorological conditions and surface characteristics, the H values for individual pixels are gradually refined, resulting in spatially resolved values across the study area (Allen et al., 1998; Anderson et al., 2012). The approach of generating readily available images from EEFlux using the website mentioned above led to easily accessed data that were downloaded and analysed by first using QGIS to clip the images to the vector of the study area. The refined images of the study area were further cleaned and analysed using Microsoft Excel.

6.3 RESULTS AND DISCUSSION

6.3.1 Seasonal variation in basal and single crop coefficients

The T:ETo ratio was calculated for the young and full-bearing orchards during 2022/23 and 2023/24 in Figure 60a and Figure 60b, respectively. The daily T:ETo ratio varied from 0.06 to 0.3 for the young orchard and 0.1 to 0.4 for the full bearing orchard during both growing seasons. It is important to mention that the daily T:ETo ratio curves that were obtained from this study did not clearly resemble any of the typical four stages of the crop coefficient curve proposed by Allen et al. (1998). The ratio for both orchards during the 2022/23 growing season tend to gradually increase from October 2022 to mid-February 2023. The 2023/24 season ratios for both orchards seemed to be lower during summer compared to earlier in the season and in March. Monthly averaged ratios for both sites were shown in Figure 61. During the 2022/23, the highest monthly average ratio for the young orchard was observed during the summer season in December 2022 (0.137) and for the full bearing orchard in March 2023 (0.18) during early autumn. The monthly average ratio agrees with the basal crop coefficient (Kcb) curve (Allen et al.,1998) in 2022/23. The ratio will be higher when the tree canopy has developed fully, which is generally by mid-summer for the pomegranate trees. Contrastingly, the ratio during the 2023/24 season had the highest monthly average ratio during late spring in October 2023 for the young and full bearing orchards. The second season agrees with what was observed for macadamia nuts where the Kcb was observed to be high during late spring and became lower during the growing season (Gush and Taylor, 2014). Gush and Taylor (2014) indicated that this behaviour can be attributed to the transpiration rate not levelling up to the evaporative demand during the summertime.

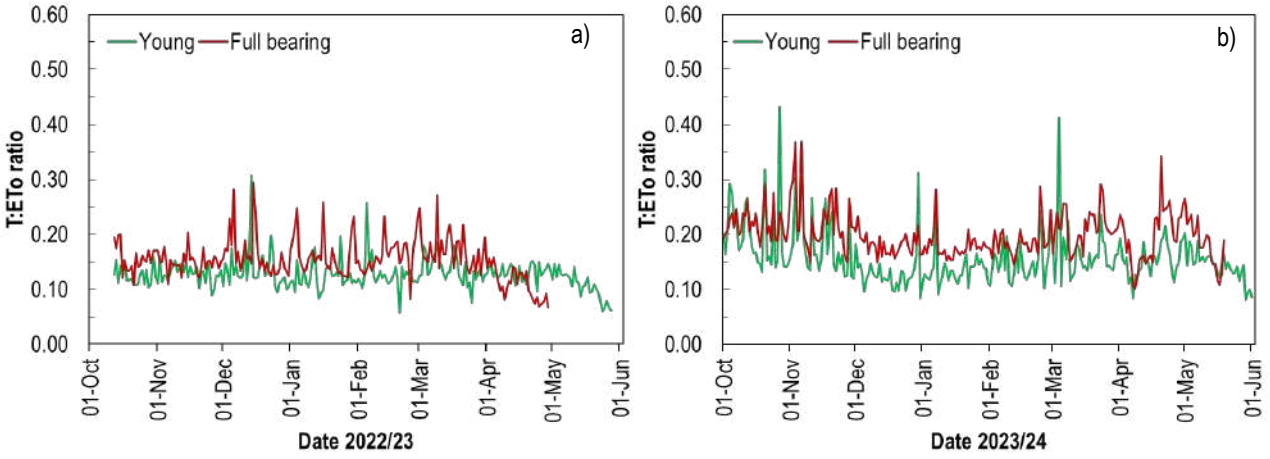

Figure 60. The transpiration to reference transpiration (ETo) ratio trends for the young(a) and full bearing(b) pomegranate orchards measured during the 2022/23 and 2023/24 growing seasons at Avontuur and Welgemoed.

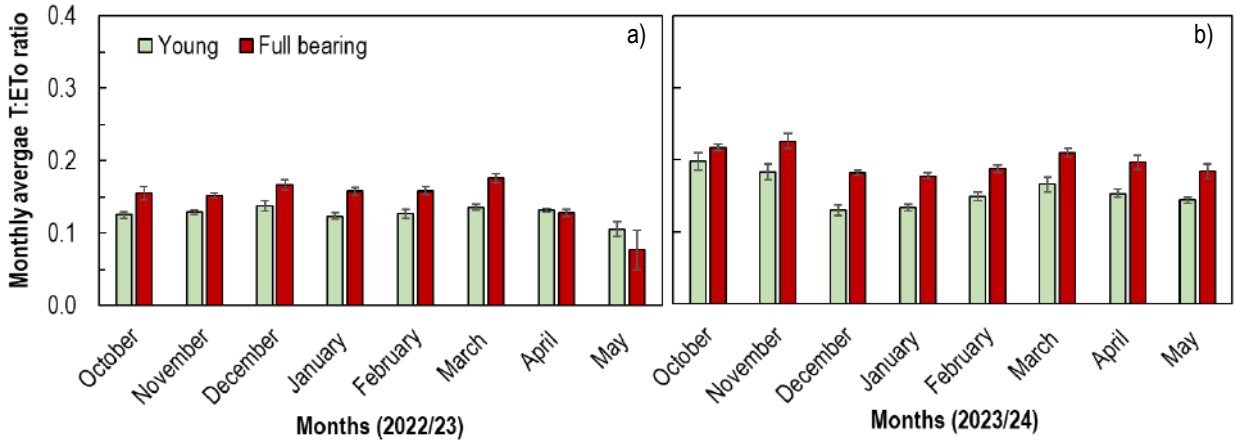

Figure 61. The monthly averaged transpiration to reference transpiration (ETo) ratio trends for the young(a) and full bearing(b) pomegranate orchards measured during the 2022/23 and 2023/24 growing seasons at Avontuur and Welgemoed

The monthly average T:ETo ratios for this study were very low but were comparable to the K_{cb} for peaches (0.05 and 0.27, Gush and Taylor, 2014). However, other crops such as citrus and macadamia nuts reported by Gush and Taylor (2014) had higher ratios ranging between 0.41 and 0.74. The monthly averaged ratio of ETc to ETo is displayed in Figure 62 for the tree row (a, b), work row (c, d) and orchard (e, f) for the young and full bearing orchards. The trends for the tree row over the season followed more the pattern of canopy development over the season than the ETc:ETo ratio for the full surface area allocated per tree (Figure 62a and b).

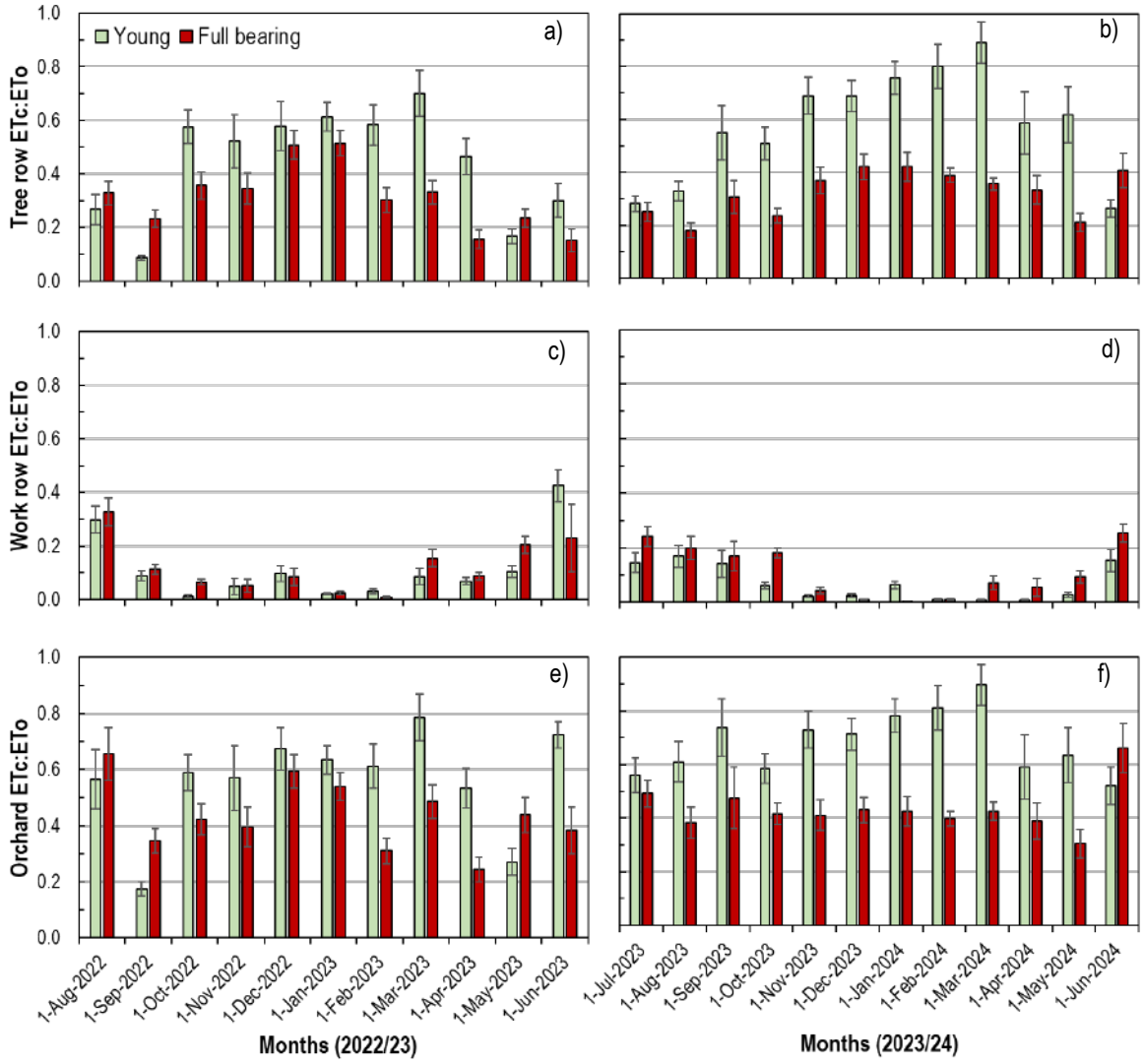

Figure 62. The monthly averaged soil water balance based evapotranspiration to reference transpiration (ETo) ratio trends for the young(a) and full bearing(b) pomegranate orchards measured during the 2022/23 and 2023/24 growing seasons at Avontuur and Welgemoed. Averages were based on available data from two soil water balance installations.

At Avontuur, in the tree row, in August 2023 the ratio amounted to 0.27 and decreased to 0.09 during September 2023 (Figure 62a). It was around 0.59 for October 2022 and December until February 2023, being 0.52 in November 2022. The ETc:ETo ratio increased to 0.7 in March 2023 after which it decreased to 0.46 and 0.17 in April and May 2023. The ratio was 0.3 on average for June until August 2023. From September until March it increased in general from 0.55 to 0.89, with a slight dip in October to 0.51. It decreased to 0.58, 0.62 and 0.26 in April, May and June, respectively. For the full bearing orchard the ETc:ETo ratio tended to be lower or comparable to that for the young orchard in the first season and lower in the second. The ratios for the full bearing orchard seemed lower for the second season compared to the first, but displayed much less variability. At Welgemoed the ratio for the tree row was 0.33 in August 2022 and was slightly lower in September 2022 at 0.23 (Figure 62a). The ratio was 0.36 and 0.34 in October and November and increased, reaching a seasonal maximum of 0.51 during December 2023 and January 2023. Hereafter it decreased to about 0.3 in February and March a gradually to a value of about 0.16 in April and 0.23 in May 2023. The ratio was 0.25 during June

2023 and tended to increase from 0.0.18 August 2023 to a maximum of 0.42 in December 2023 and January 2024. The ratio decreased to 0.39 and 0.36 in February and March 2024 and decreased gradually to 0.21 in May 2024. The ETc:ETo ratio in June 2024 was 0.41.

In the work row of the young orchard, the ETc to ETo ratio remained 0.10 or less during the growing season from September 2022 until May 2023 (Figure 62c). When exceptionally high rainfall occurred during June 2023, the ratio reached 0.42**.** In August 2022 and July until August 2023 the ratio remained between 0.28 and 0.29 and decreased in September 2023 to 0.19 (Figure 62c and d). During October, November and December 2023 when rainfall was 0.4 mm, 9.8 mm and 0.2 mm respectively the ratio was 0.08, 0.04 and 0.02. From December 2023 until May 2024 the ratio for the work row remained 0.03 or less, increasing to 0.26 in June 2024. At the full bearing orchard in the work row the ratio was 0.33 in August 2022, after which it decreased and remained 0.15 or less until April 2023. The ratio changed to 0.2 during May and 0.23 in June 2023. The ratios ranged between 0.17 and 0.24 during July until October 2023. Hereafter it ranged between 0.01 and 0.07 during November until April 2024, increasing to 0.09 in May and 0.25 in June 2024.

For the young orchard the ETc to ETo ratio was 0.57 and 0.17 in August and September and it increased in general from October 2022 from 0.59 to a maximum of 0.79 in March 2023 (Figure 62e). The exceptions were November, January and February which displayed lower ratios of 0.57, 0.63 and 0.61, respectively, compared to a linear trend. After harvest in March it decreased to 0.53 and to 0.27 in April and May 2023, respectively. With exception of a very high ratio in June 2023 (which had a total of 187 mm rainfall) and being lower October, the ratio tended to increase in general during the 2023/2024 season from 0.56 in July to 0.9 in March 2024. The ratio reduced to 0.59, 0.63 and 0.52 in April, May and June 2024, respectively. For the full bearing orchard the ETc to ETo ratio was 0.66 in August 2022. It tended to increase from 0.35 in September to 0.59 in December, but remained more or less similar during October and November. It was slightly lower in January 2023, with a definite decrease in February to 0.31. It was 0.49 in March and decreased again to 0.24 in April, after which it increased to 0.44 in May 2023. The ETc: ETo ratios in June, July, August and September 2023 fluctuated and was 0.38, 0.49, 0.38 and o.48, respectively. The ratio was fairly similar from October until April and on average 0.41. It decreased in May to 0.3 and increased again in June to 0.66, probably due to the water use from the work row area (Figure 62d).

The trends of individual tree soil water balance determined ETc:ETo ratio for the tree row and fully allocated orchard area does not agree with that for the Kt, as it indicated that the coefficients for the young orchard were higher compared to that for the full bearing orchard. The monthly averages of the soil water balance based ETc:ETo ratios was based on data available data for days with ETc:ETo ratios of between zero and 1.2 and does not represent a full dataset for each month per site. This may provide a possible explanation for the difference in trends for the ratios of transpiration and soil water balance based ETc, respectively, to ETo.

Figure 63 (a and b) shows the seasonal dynamics of orchard scale crop coefficients of the young and full bearing orchards during the 2022/23 and 2023/24 growing season. During the first season (Figure 63a), the ETc to ETo ratios trend moved at the same rate from October 2023 to mid-February. The ratio started to be volatile and went on a downward trend from March to June 2024.Figure 63b showed a rapid increase from July to mid-September 2023 and showed a gradual decline from November2023 to March 2024. The daily ETc: ETo ratio varied from 0.004 to 1.185 for the young orchard and 0.029 to 1.315 for the full bearing orchard during both growing seasons (Figure 63a and b). Figure 64 (a and b) shows monthly averaged ETc: ETo ratio where the full bearing orchard had a high ratio as compared to the young orchard for both the growing seasons.

Figure 64 shows monthly ETc: ETo ratio of the young and full bearing orchards which exhibited the same trend during the 2022/23 growing season. The trend during the 2022/23 growing season was constant from October 2022 to March 2023 with little variability between the months however the trend tends to have a rapid decline from April towards June 2023 (Figure 64a). Figure 64b shows a rapid increase from July to September 2023 where it reaches a maximum for the young and full bearing orchards during the 2023/24 growing season. It is important to mention that there was a lot of month-to-month variation from the young orchard as compared to the full bearing orchard (Figure 64b). Both Figure 63b and 62b shows a gradual decline from October to December 2023.

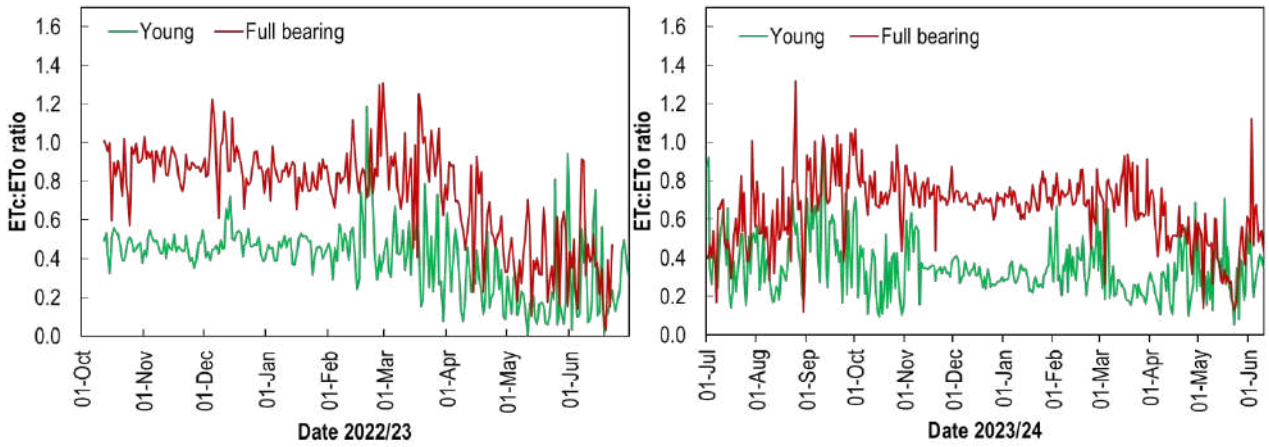

Figure 63. The orchard level crop evapotranspiration (ETc) to reference transpiration (ETo) ratio trends for the young(a) and full bearing(b) pomegranate orchards measured during the 2022/23 and 2023/24 growing seasons at Avontuur and Welgemoed

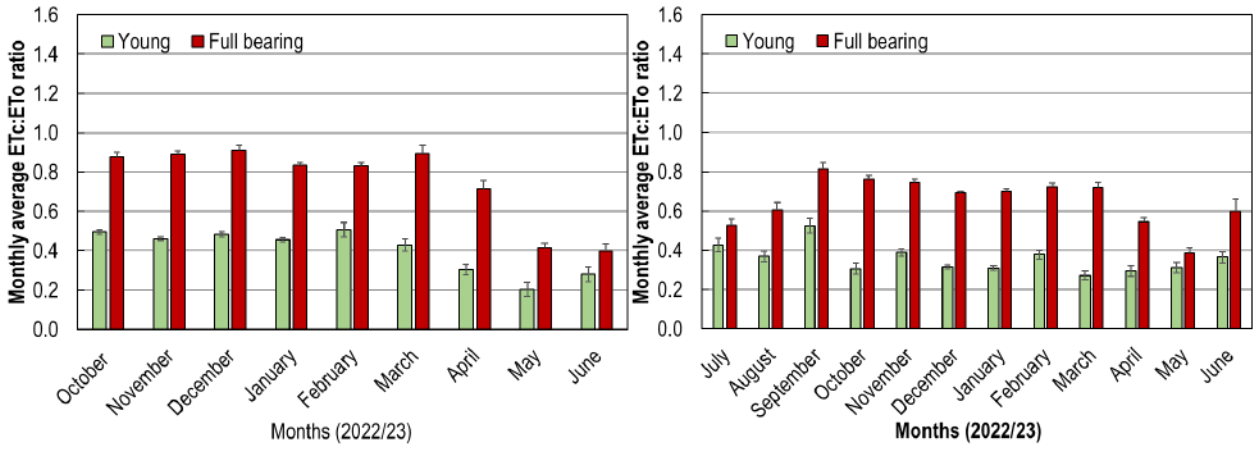

Figure 64.The monthly averaged orchard level evapotranspiration (ETc) to reference transpiration (ETo) ratio trends for the young (a) and full bearing (b) pomegranate orchards measured during the 2022/23 and 2023/24 growing seasons at Avontuur and Welgemoed

6.3.2 Relating crop coefficients to fractional light interception, tree height and shaded area

6.3.2.1 Measured tree height, light interception and tree shaded area

The variability in height for the trees selected for growth (5), soil water balance (2) and sap flow (4) as measured during the two seasons are displayed in Figure 65. The average tree height for the young orchard trees from end September 2022 until June 2024 ranged between 1.9 (±0.1) m and 2.4 (±0.09) m, and for the full bearing orchard between 2.9 (±0.11) m and 3.1 (±0.09) m.

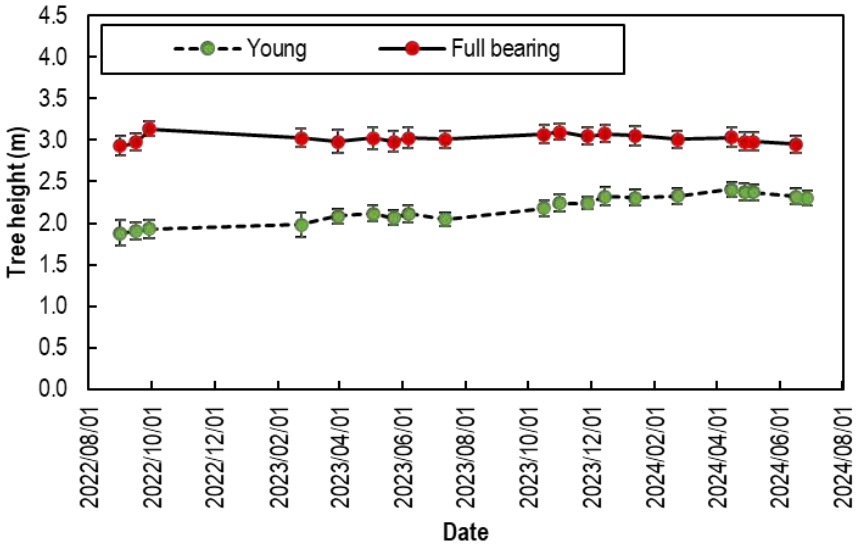

Figure 65. Averaged tree height for trees selected for growth, sap flow and soil water balance measurements (n=11) at the young and full bearing orchards as measured on selected days from August/ September 2023 until June 2024 at Avontuur and Welgemoed, respectively.

Fractional light interception was measured at the soil water balance trees from September 2022, and for the sap flow trees from December 2022 when a second LP-80 Accupar sceptometer became available. Measurements continued until early July 2023. Fractional light interception measured during the 2022/2023 season ranged between 0.13 and 0.33 for Avontuur, and 0.3 and 0.6 for Welgemoed (data not shown). The fractional light interception for the full bearing trees at Welgemoed decreased earlier at the end of the season (i.e. after March) compared to the young orchard. During the 2023/2024 season the fractional light interception were measured for the eight trees and ranged at the young orchard between 0.11 to 0.39, while light intercepted at the full bearing orchard amounted to a minimum of 20% and a maximum of 70% of incoming solar radiation. Average fractional light interception ranged between 0.13 (±0.01) and 0.31 (±0.02) for Avontuur and 0.30 (±0.01) and 0.48 (±0.02) for Welgemoed during the 2023/2024 season (Figure 64a).

The Accupar LP-80 estimated maximum leaf area index for the 2023/2024 season was 0.75 (±0.02) m^2 m^{-2} for the young orchard and 1.3 (±0.04) m^2 m^{-2} for the full bearing orchard (Figure 66b). An excellent linear regression relationship was obtained during April 2024 between leaf area and leaf dry mass for each orchard to allow estimation of the actual leaf area of trees collected during natural leaf fall (R^2 values > 0.99). Calibration of the Accupar LP-80 for actual LAI estimation was thereafter completed for both research sites to enable estimation of leaf area index based on tree canopy area and on the area allocated per tree from ceptometer modelled LAI data (data not shown).

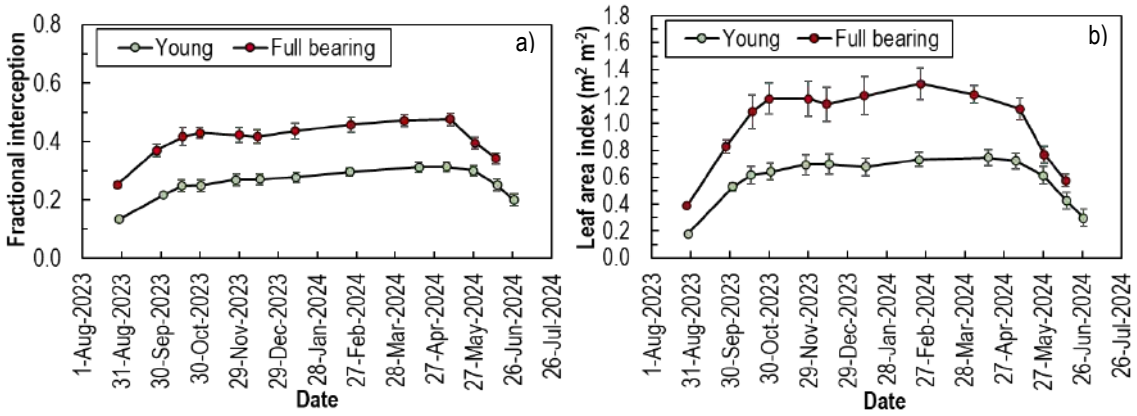

Figure 66. Seasonal trends in average fractional light interception and leaf area index modelled from Accupar LP-80 measurements for eight trees in the young (Avontuur) and full bearing (Welgemoed) orchards from August 2023 until June 2024 (27 September, n = 4 for Welgemoed – poor weather conditions prevented a complete measurement set).

Linear regressions of the averaged FI, tree area based LAI and OLAI, respectively, to the shaded area measured for three trees at selected dates over the 2023/34 season was highly significant ($p<0.0001$) and indicated that the manual method making use of demarcated hardboards can be used to estimate the tree canopy properties indirectly (Figure 67). The error of the estimate though was quite high, being 0.036, 0.262 and 0.159 for FI, tree canopy area based LAI and OLAI, respectively. The mean absolute errors were smaller and amounted to 0.026, 0.174 and 0.093 for the three respective variables. An outlier from the full bearing orchard originating from June 2024 was removed from the dataset as it differed by more than two standard deviations from the trendline. To estimate Kc from the shaded area seems risky although the linear and non-linear regressions where significant at a 95% confidence level (p-values of 0.042 and 0.012, respectively). The coefficients of determination for the linear and non-linear trendlines were 0.423 and 0.568, with standard errors of the estimate being 0.11 and 0.086, respectively (Figure 68). Linear regressions conducted for the orchards separately was not statistically significant.

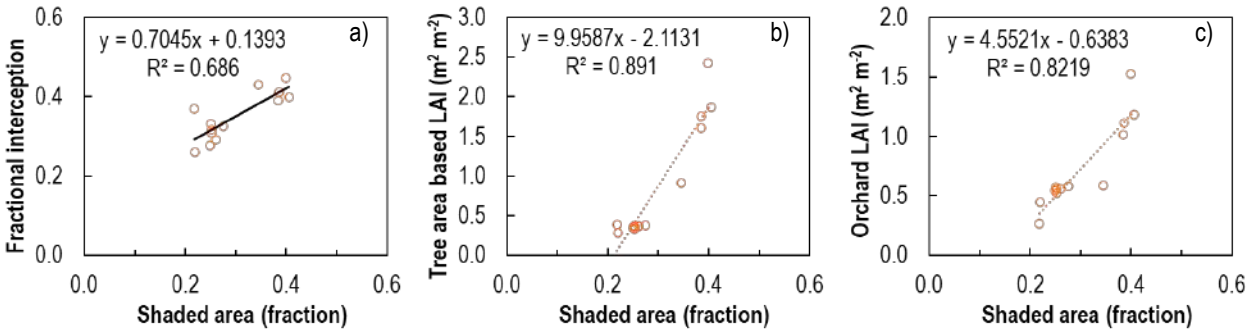

Figure 67. Comparison between Accupar LP-80 ceptometer fractional light interception, tree canopy area based leaf area index (LAI) and orchard LAI to the tree shaded area measured for selected dates at the young (Avontuur) and full bearing (Welgemoed) orchards from August 2023 until June 2024

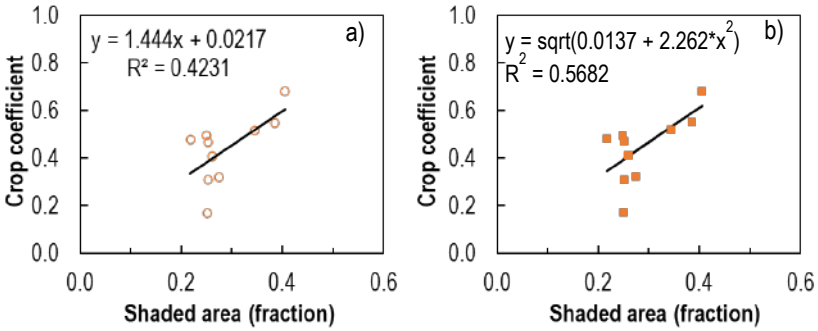

Figure 68. Comparison of the a) linear and b) non-linear regression trends of orchard level crop coefficients to the fractional shaded tree area for the young and full bearing cultivar 'Welgemoed' pomegranate orchards during the 2023/24 season

6.3.2.1 Estimating crop coefficients from fractional light interception and tree height

The mean leaf resistance was calculated during the 2023/24 growing season for the young and the full bearing orchards for each day using fractional light interception and plant height estimated using polynomial regression relationships (data not shown). The mean leaf resistance for the young orchard ranged from 935 to 2963.88 s m^{-1}, and for the full-bearing orchard from 1860.21 to 7134.04 s m^{-1} (Figure 69). The mean leaf resistance (r_l) for the young and full-bearing orchard gradually increased from October to late December 2023 and the r_l reached a plateau around January and February 2024.The r_l rapidly increased from early May to end May reaching maximums for both the young and full bearing orchards. Figure 70 (a and b) depicts the comparison between the actual K_t calculated from transpiration data and the K_t estimated using the Allen and Pereira approach for the young and full-bearing orchards during the 2023/24 growing season. The young orchard estimated K_t and the measured K_t decreased from October to December and had a slight increase from January to March that then had a gradual decrease from mid-May towards early June. The full bearing

orchards exhibited similar general trends from those observed for the young orchard. It is important to mention that the estimated and measured K_t values as well as trends were comparable. Figure 71 showed a very good linear regression relationship between the estimated and the measured K_t with R^2 values of 0.99 and p-values less than 0.0001 for both the young and full bearing orchards. Figure 71 (a and b) showed positive linear regression relationships between the estimated and the measured K_t for the young and full-bearing orchards during the 2023/24 growing season. The regression relationship also had very good R^2 value of 0.994 for data of the two orchards combined (Figure 72). However, the method relies heavily on r_l, which may vary for different orchards. More research in this regard is required before the method can be recommended to estimate K_t values for orchards for which r_l values are not available.

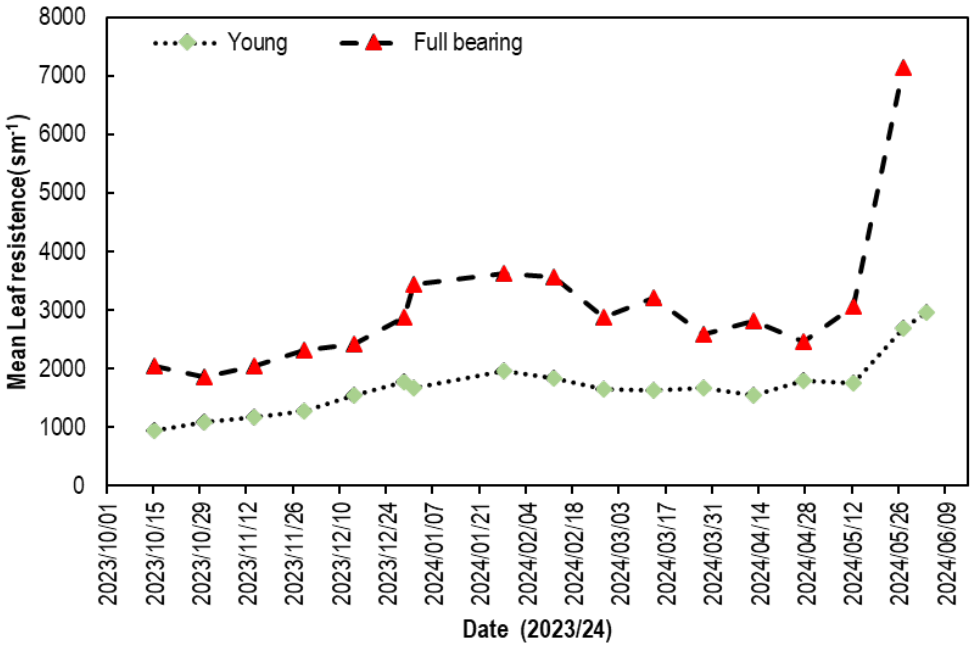

Figure 69. Mean leaf resistance for the young and full bearing pomegranate trees calculated from bi-weekly averaged input data for periods between October 2023 and June 2024 at the Avontuur and Welgemoed farms, respectively

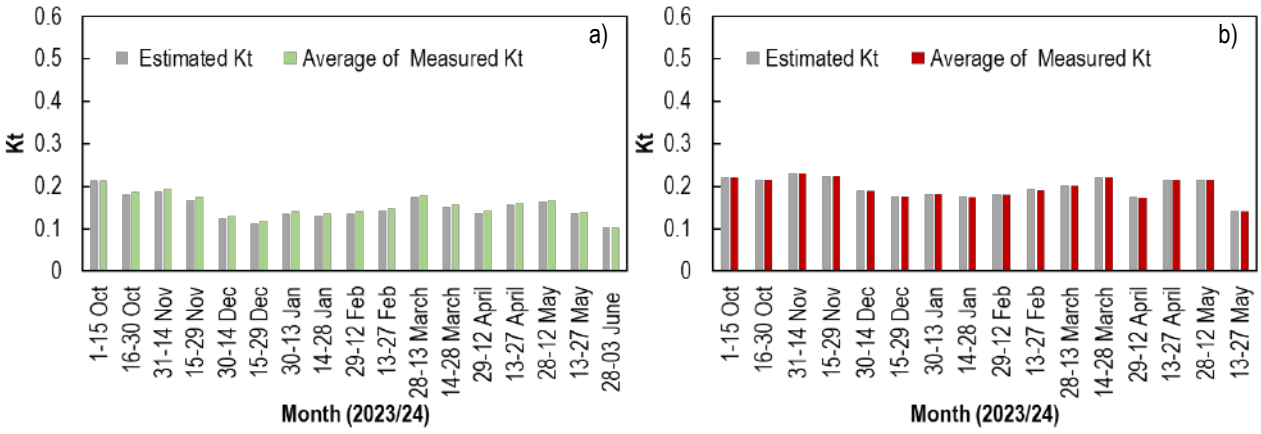

Figure 70. Estimated and measured K_t for the young and full bearing pomegranate trees monitored between October 2023 and June 2024 at the Avontuur and Welgemoed farms, respectively. Estimated K_t values were based on bi-weekly averaged input data whereas measured K_t values were fortnightly averages of daily data.

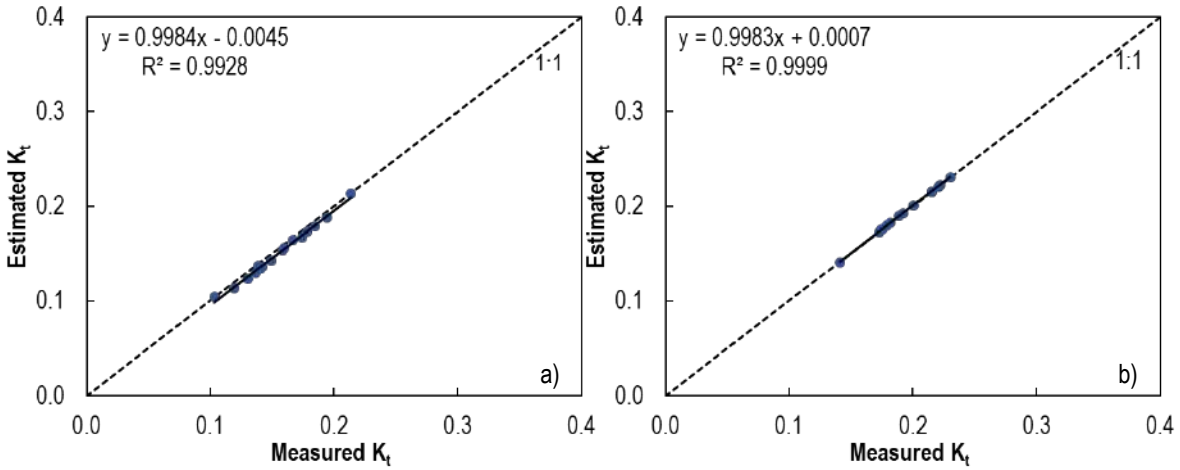

Figure 71. The relationship between estimated K_t and measured K_t of the young pomegranate orchard (a, n = 18) and a full-bearing pomegranate orchard (b, n = 17) during the 2023/24 growing season

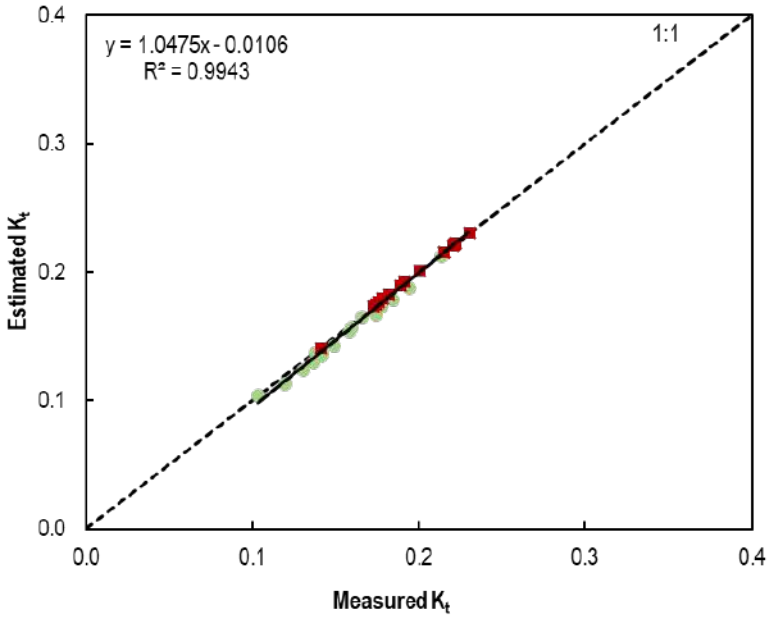

Figure 72. The relationship between estimated K_t and measured K_t data of the young (green dots) and full-bearing (red diamonds) pomegranate orchards combined (n = 35) during the 2023/24 growing season

6.3.3 Use of remote sensing to estimate pomegranate water use

In the following section ground measured and remote sensing model derived orchard ET is compared. To assess the accuracy of the models used to estimate ET in the study area, it is crucial to acknowledge that ground-based measurements inherently carry a margin of error and uncertainties, which should be considered when employing them to validate the precision of satellite-derived assessments (Karimi and Bastiaanssen, 2015). High-quality ground-measured data were used to validate the estimated RS data, where dates were selected based on the image acquisition dates in Table 37. For dates on which errors were detected in ground-based measurements, substitution with other data recorded within the same week as the acquisition dates were used to maintain consistency.

6.3.3.1 Daily reference evapotranspiration.

Daily ETo calculated from AWS data using the P-M equation was compared with RS estimations of ETo from the study area from September 2022 to October 2023. The observed results presented in Figure 73 indicate a moderately strong linear relationship for both RS models, with R^2= 0.6973 ($p<0.0001$) and a slope of 0.832546, with an estimated RMSE = 1.07 for PySEBAL, whereas EEFlux reported an R^2= 0.805 ($p<0.0001$) and a slope of 0.7799 with an estimated RMSE = 0.749. Thus, EEFlux was the most reliable RS model for estimating the ETo during the study period. The PySEBAL model indicated a positive correlation (closest to the 1:1 line) from the data annotated from the image acquisition date of the 1st of March 2023 ($ETo_{PySEBAL}$ at 5.7, ETo_{AWS} at 5.9) and the 09th of September 2023 ($ETo_{PySEBAL}$ at 2.6, and ETo_{AWS} at 2.4). In contrast, EEFlux also indicated a positive correlation annotated on the 06th of September 2022 ($ETo_{EEFluxL}$ at 2.9, ETo_{AWS} at 2.8), the 08th of October 2022 (ETo_{EEFlux} at 5.1, ETo_{AWS} at 4.9), and the 27th of December 2022 (ETo_{EEFlux} at 6.3, ETo_{AWS} at 6.4). The model that reported higher overestimated values in the season was PySEBAL on the 12th of January 2023 ($ETo_{PySEBAL}$ at 6.3, ETo_{AWS} at 4.5) and the 02nd of April 2023 ($ETo_{PySEBAL}$ at 5.4, ETo_{AWS} at 3.6). In contrast, EEFlux moderately overestimated only on the 12th of January 2023. On the other hand, both RS models indicated an underestimation of values, where EEFlux was underestimated on the 02nd of April 2023 (ETo_{EEFlux} at 1.7 and ETo_{AWS} at 3.6) and 18th of April 2023 (ETo_{EEFlux} at 1.8, and ETo_{AWS} at 4.4), and PySEBAL was underestimated on the 08th of October 2022 (ETo_{EEFlux} at 2.8, and ETo_{AWS} at 4.9).

The Penman-Monteith equation method, which the FAO recommends, is the most accurate method for estimating reference crop evapotranspiration, as evidenced by the literature. However, this method needs a large amount of weather data. The linear regression of values of reference evapotranspiration that were calculated by the ground-based method to that calculated by the RS models indicated that the remote sensing models used resulted in a moderate to high positive correlation when compared to the ground-based estimated ETo. The coefficients of determination for EEFlux and PySEBAL was 0. 83 and 0. 68, respectively (Figure 73). To estimate evaporative demand to manage irrigation efficiently using remote sensing, the EEFlux indicated to be the better model to be employed.

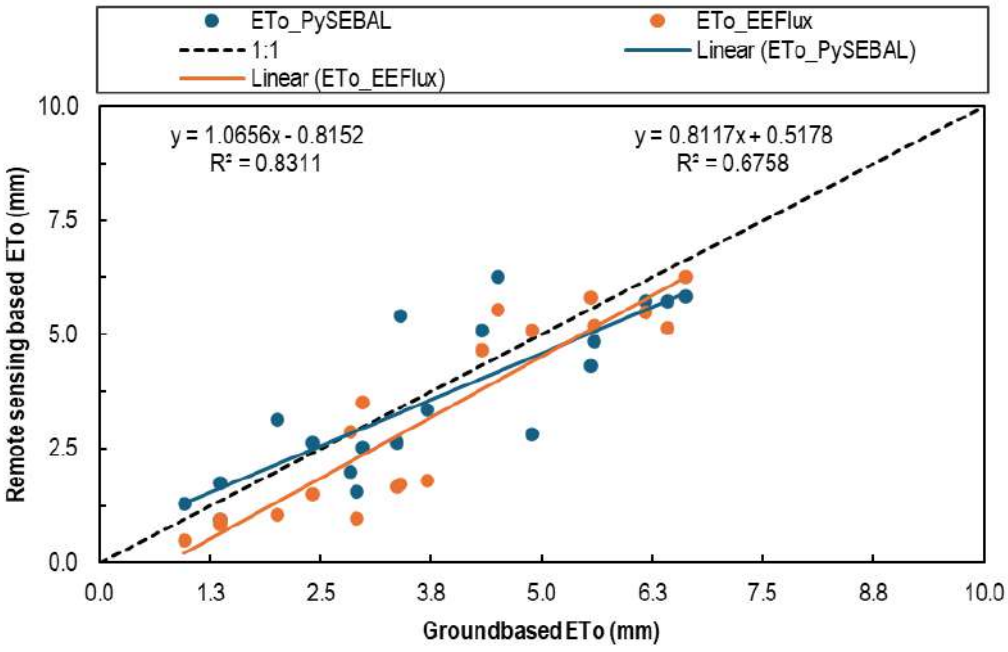

Figure 73. Comparison of remote sensing estimated reference evapotranspiration, ETo (PYSEBAL, EEFLUX) to ground-based ETo calculated from automatic weather station data at the Welgemoed pomegranate orchard near Wellington for the period September 2022 until October 2023

6.3.3.2 Seasonal dynamics of orchard evapotranspiration.

The available ET values of each ground-based and RS technique were compared from September 2022 to October 2023, indicating significant spatiotemporal variations (Figure 74).

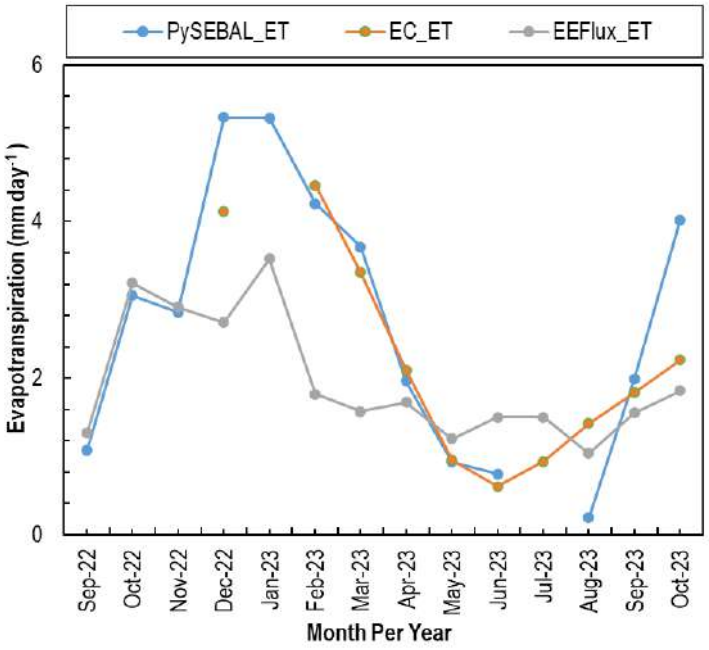

Figure 74. Crop evapotranspiration (ET) data derived from a ground-based measurements (EC) technique and two remote sensing techniques (PySEBAL and EEFlux) for selected dates from September 2022 to October 2023

The ET derived by EC indicated higher values and variations in patterns for most of the months as compared to the RS models, starting at 5.6 mm day^{-1} during the fruit growth stage in December 2022 and increasing to 6.9 mm day^{-1} at the fruit ripening stage in February 2023, which was the highest ET estimation in the season. A decrease was observed from February to the harvest stage in March 2023, recording 3.2 mm day^{-1}, and it consistently decreased between April and May 2023, going forth until reaching a minimum of 1.1 mm day^{-1} in the dormancy stage in June 2023. A gradual increase was observed from July (1.9 mm day^{-1}) to September 2023 (3.5 mm day^{-1}), representing the transition from winter dormancy (bud stage) to the sprouting of the first leaves. In October 2023, an increase to 4.3 mm day^{-1} was estimated, representing the appearance of the flower bud stage and flower buds.

6.3.3.3 Daily evapotranspiration.

The EC data were used to calculate ET for comparison with the RS estimates of ET from September 2022 to October 2023. The annotated results in Figure 75 indicate a strong and moderate relationship with a statistically significant relationship compared with both RS models, with R^2= 0.6733 ($p < 0.05$) for $ET_{PySEBAL}$ and R^2=0.4131 ($p < 0.05$) for ET_{EEFlux}. The EEFlux model indicated a positive correlation (closest to the 1:1 line) from April 18, 2023 (ET_{EEFlux} at 1.7 and ET_{EC} at 1.6), May 4, 2023 (ET_{EEFlux} at 1.4 and ET_{EC} at 1.6), May 20, 2023 (ET_{EEFlux} at 0.8 and ET_{EC} at 0.7), June 21, 2023 (ET_{EEFlux} at 1.3 and ET_{EC} at 1.5), August 8, 2023 (ET_{EEFlux} at 1.0 and ET_{EC} at 1.1), and September 9, 2023 (ET_{EEFlux} at 1.5 and ET_{EC} at 1.6). In contrast, the PySEBAL model reported ET values within the acceptable range for most dates, resulting in a stronger overall correlation. The $ET_{PySEBAL}$ reported a positive correlation only on one date, on May 4, 2023 ($ET_{PySEBAL}$ at 1.5 and ET_{EC} at 1.4). Both models indicated underestimated and overestimated ET values, with EEFLux reporting the most overestimated ET values compared to PySEBAL. Alternatively, PySEBAL indicated values that were underestimated more than those of EEFlux.

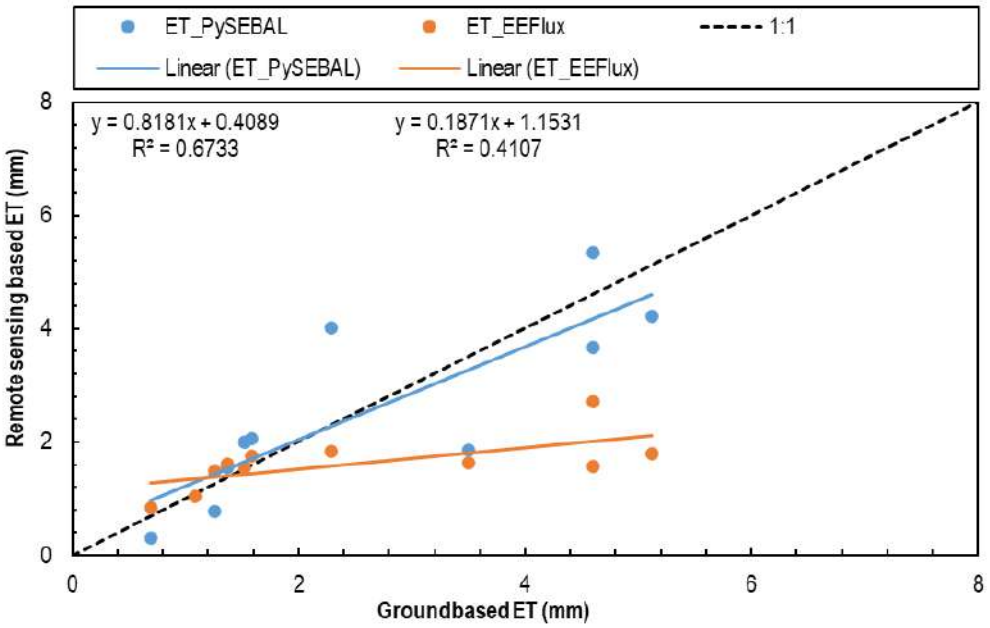

Figure 75. Comparison of estimated crop evapotranspiration (ET) using Remote sensing (PySEBAL, EEFLUX) to ground-based ET (Eddy Covariance) at the Welgemoed pomegranate orchard near Wellington for the period September 2022 until October 2023

Water use estimations indicated variation between RS models. The PySEBAL model ETc had a moderate positive correlation with R^2 of 0. 69 to the ground-based ETc indicated as compared to EEFlux, which indicated a moderate positive correlation resulting in an R^2 of 0. 41. Although Bastiaanssen et al. (2005) demonstrated that the average accuracy of SEBAL is 85 %, models are prone to uncertainties. This is because the accuracy of ground-based reference maps depends on errors obtained in field measurements and uncertainties of satellite data and samples of spatiotemporal errors (Weiss et al, 2004). As both models indicated underestimated and overestimated ET values, PySEBAL overestimated the crop evapotranspiration in the orchard from November 2022 to January 2023 (reporting an average of 5 mm day^{-1}). However, EEFLux reported the most overestimated ET values. Alternatively, PySEBAL indicated values that were underestimated more than those of EEFlux. Variations and more reasons for the uncertainty of using Landsat images for estimations as models in this study used Landsat 8 images, were reported by Senay et al. (2016), which impact data alongside the identification of pixels used by various models using satellite imagery.

6.3.3.4 Crop coefficients

The crop coefficient was estimated using three different systems. Ground-based crop coefficients (Kc) were calculated according to Allen et al. (1998) as the ratio of ETc (Eddy covariance) to ETo (Automated weather station) for the full orchard surface. The remote sensing-based Kc was estimated based on the empirical equations used in PySEBAL and EEFlux, which also follows the Allen et al. (1998) approach of estimating reference evapotranspiration. PySEBAL provides Kc estimated images as an output from running the model using the surface energy balance algorithm, as it uses Python for scripting. In contrast, EEFLux does not and must calculate the ratio of the measured ETc to ETo annually.

The seasonal pattern of Kc obtained using the ground-based techniques varied significantly from the two RS techniques presented in Figure 76. Simple linear regression between the ground-based and RS-based techniques $Kc_{PySEBAL}$ and Kc_{EEFLux} (Figure 77) resulted in a relatively weak relationship with coefficient of determination (R^2) of 0.0099 (p-value = 0.7799) and R^2 of 0.0776 (p-value = 0.4356), respectively. A positive correlation (closer to the 1:1 line) was observed when validating $Kc_{PySEBAL}$ to Kc_{ground} on February 13, 2023 ($Kc_{PySEBAL}$ at 0.7 and Kc_{ground} at 0.8). In contrast, a positive correlation was observed when validating Kc_{EEFlux} to Kcground on April 2, 2023 (Kc_{EEFlux} at 0.9 and Kc_{ground} at 1.0).

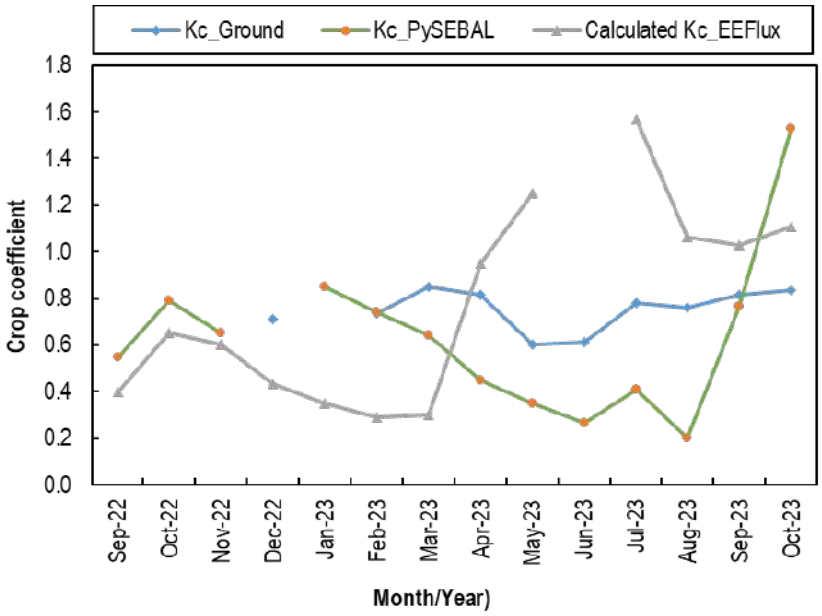

Figure 76. Crop coefficient (Kc) data derived from ground-based measurements (ratio of eddy covariance evapotranspiration to automatic weather station reference evapotranspiration) and two remote sensing techniques (PySEBAL and EEFlux) from September 2022 to October 2023

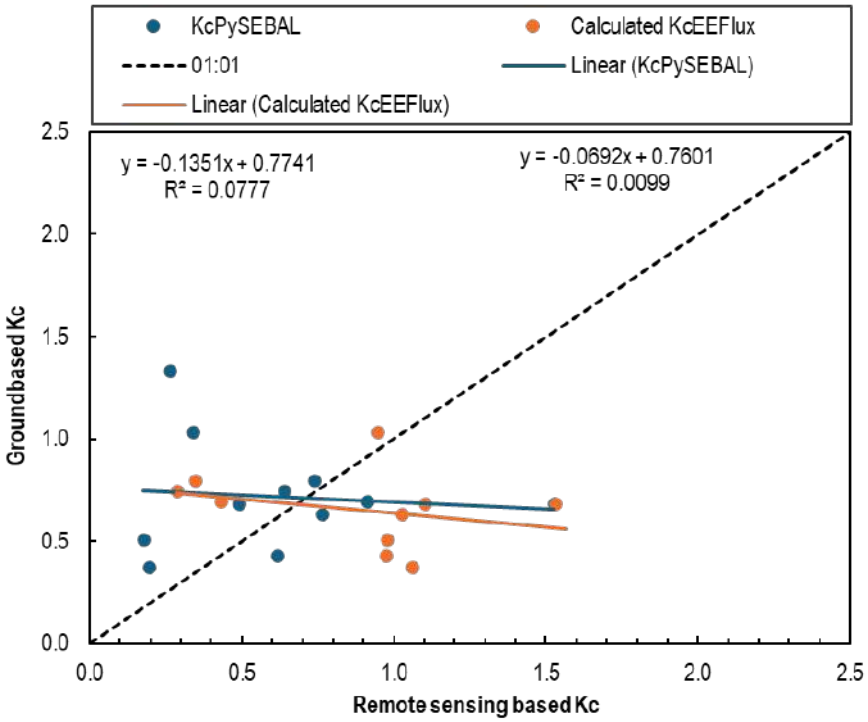

Figure 77. Comparison of remote sensing (PySEBAL, EEFLUX) estimated crop coefficients (Kc) to ground-based Kc calculated from eddy covariance evapotranspiration and weather station derived reference evapotranspiration at the Welgemoed pomegranate orchard near Wellington for the period September 2022 until October 2023

Based on the reference and actual evapotranspiration correlation results, it is advised to use the PySEBAL model to estimate ET as it has a higher positive correlation when validated against ground-based ET than when using EEFLUX. It is essential to obtain as

accurate as possible water use estimations in an orchard to assist in aiding irrigation decisions that can ultimately positively affect the water needs. The crop coefficients derived from the ratio of ET and ETo resulted in a poor correlation due to the overestimations and underestimations of ET and ETo, as previously discussed. Williams and Fidelibus (2016) and Blatchford et al. (2019) reported that Kc values may vary with agricultural practices as there are variances in many parameters, including climate, cultivar, soil type, and agronomic techniques, resulting in values not being universal, therefore, presented data in this study may differ with that of different authors. Pereira et al. (2021a) reported that values should be at most 1.2 with advection for trees and vines, as they do not obtain full crop development due to training and pruning. However, Rallo et al. (2021) reported that much larger Kc values were also reported without signalling the presence of advection due to the complexities in orchard systems. In this study, values that exceeded 1.2 were estimated by RS models used, which resulted in a drastic spike for EEFLux-generated data in the winter months (Refer to Figure 76).

6.4 CONCLUSIONS

The monthly average T:ETo ratio for the young orchard ranged from 0.13 to 0.20 for the 2022/23 season and ranged from 0.11 to 0.14 during the 2023/24 growing season. For the full bearing orchard it ranged from 0.08 to 0.20 for the 2022/23 season and from 0.18 to 0.23 during the 2023/24 growing season. The monthly average T:ETo ratio for the young orchard were generally higher during the 2022/23 season as compared to the 2023/24 season. The monthly average T:ETo ratios for this study were very low, but comparable to that of peaches. However, other crops such as citrus and macadamia nuts reported by Gush and Taylor (2014) had higher ratios. The T:ETo ratio was higher during the 2023/24 as compared to the 2022/23 growing season for both orchards.

The ETc:ETo ratios based on the soil water balance gave seasonal trends that were not comparable to the T:ETo ratio and ETc:ETo ratios based on the surface renewal and the eddy covariance systems. This anomaly was attributed to monthly averages which were based on incomplete soil water balance datasets per month. The ETc:ETo ratios based on the micro meteorological systems were higher for the full bearing orchard as compared to the young orchards for both growing seasons. The monthly average ETc: ETo ratio for the young orchard ranged from 0.23 to 0.506 for the 2022/23 season and from 0.310 to 0.525 during 2023/24. The monthly average ETc: ETo ratio for the full bearing orchard ranged from 0.397 to 0.911 for the 2022/23 season and varied between 0.386 and 0.816 during the 2023/24 growing season.

The estimated K_t based on the Allen and Pereira approach was comparable to the measured K_t for both the young and the full bearing orchards. However, the method relies heavily on rl, which may vary for different orchards. More research in this regard is required before the method can be recommended to estimate K_t values for orchards for which r_l values are not known. Tree canopy properties can be estimated from the tree shaded area manual method making use of demarcated hardboards although the error of the estimate can be considered high, being 0.036, 0.262 and 0.159 for FI, tree canopy area based LAI and OLAI, respectively. Although the regression relationship between orchard level Kc and tree shaded area was significant at a 95% confidence level, the coefficients of determination was low (R^2 = 0.42 for linear and 0.57 for non-linear trends) and it seems risky to estimate crop coefficients for irrigation scheduling using this method without further refinement.

To estimate reference evapotranspiration to manage irrigation efficiently using remote sensing, the EEFlux indicated to be the better model to be employed. It is, based on actual evapotranspiration correlation results, advised to use the PySEBAL model to estimate ET as it has a higher positive correlation when compared to ground-based ET than when using EEFLUX. There was not a significant linear regression relationship between Kc values determined from eddy covariance ETc and weather station derived ETo and the ones determined from ETc and ETo calculated using the two remote sensing products, EEFLUX and PYSEBAL and further data collections and research is required in this regard.

CHAPTER 7: CONCLUSIONS AND RECOMMENDATIONS

7.1 CONCLUSIONS

- Water use of pomegranate orchards, in terms of monthly average daily crop evapotranspiration, reached maximum values of. 3.5 mm d^{-1} and 5.4 mm d^{-1} for the young and full bearing orchards, respectively, in mid-summer, with values of 1 mm or less presiding during late fall until mid-winter during the 2022/23 and 2023/24 seasons. Orchard upscaled daily transpiration rates were low compared to evapotranspiration and monthly averages from October to May reached a maximum of 1 mm d^{-1} for both orchards in the 2022/23 season, and maxima of 1.1- and 1.3-mm d^{-1} for the young and full bearing orchards, respectively, in 2023/24.

- The seasonal total transpiration and evapotranspiration of the orchards can with proper interpretation be used for water management purposes. It is important to note that canola mulch covering a double drip line may have reduced evaporative losses for the young orchard and water use may have been affected by advective conditions at times after harvesting of surrounding winter wheat fields. There were almost no weeds present during the growing season in the young orchard. The full bearing orchard did not have a mulch, but a dense weed stand at the beginning of the season until end October after which chemical control was applied.

- Seasonal transpiration from 1 October 2022 until 31 May for the two respective seasons amounted to 28.5% and 47% of orchard evapotranspiration for the young, and 18% and 28% of orchard evapotranspiration for the full bearing orchard. This indicates that there is scope to decrease non-productive water losses from these orchards through irrigation and orchard management in support of sustainable water management.

- The maximum seasonal evapotranspiration over the two seasons approached 600 mm for the young orchard and it was against expectations, lower for the second compared to the first season. Seasonal water use may have been affected by rainfall, which was more prevalent in the first summer compared to the second, adding to evaporative losses.

- Although the perception is that the full bearing orchard was underirrigated, it made extensively use of winter rainfall water supplies in the soil which allowed seasonal evapotranspiration to approach 900 mm during the two seasons. These values can possibly be considered as a lower benchmark for seasonal water use of full bearing pomegranate orchards since the trees were not optimally irrigated. The weed stand though was quite dense at the beginning of the season, but after chemical control soil in the work row remained bare for the majority of the growing season until April. Interestingly, the water use was fairly similar during the two seasons despite vastly different crop loads (i.e. c. 50% lower in the second compared to the first).

- With regard to water use efficiency of the young orchard, transpiration from October until May equalled 26.9% and ETc about 59% of of the total effective rainfall and irrigation applied in 2023/24. For the full bearing orchard transpiration amounted to 56.92% of the total effective rainfall and irrigation applied in 2023/24, whereas the ETc exceeded the total effective rainfall and irrigation applied. Water use efficiency can be improved by precision irrigation and timeous weed management.

- Irrigation water productivity amounted to 3.464 kg m^{-3} and 5.103 kg m^{-3} for the young and full bearing orchards, respectively, in 2023/24. For the young orchard it is substantially less (>50%) compared to irrigation water productivity of surface drip-irrigated pomegranate orchards of similar cultivar and age in California. If the good yield of the orchard is taken into account, the irrigation water productivity could be improved by precision irrigation that minimises leaching beyond the major root zone. Irrigation water productivity of the full bearing orchard, which was about 9.3% less compared to that of their counterparts in California, may be increased by applying orchard management practices that could improve yield.

- Biophysical water productivity for the young orchard amounted to 5.819 kg m^{-3} in its fifth year after planting (2023/24) and for the full bearing orchard during a normal bearing year with yield amounting to 33.3 t ha^{-1}, to 3.705 kg m^{-3} (2022/23). The ETc based biophysical water productivity for pomegranate trees fell within the range of that reported for the intermediate

bearing apple trees with medium canopy cover (i.e. between 2 and 8.1 kg m^{-3}), and it was lower compared to that modelled for full bearing apples. It should be noted though that the full bearing pomegranate orchard was not irrigated optimally.

- Economic water productivity for the two orchards based on gross farm income and ETc from October 2023 until May 2024 with the effect of blemishes omitted from the market classification amounted to R93.87 m^{-3} for the young orchard in 2023/24 and for the full bearing orchard in the 2022/23 and 2023/24 seasons to R26.43 m^{-3} and R26.03 m^{-3}, respectively. Apart from the effect of total ETc on the indicator, the economic water productivity was sensitive especially to fruit weight, sunburn colour and degree, which determines amongst other factors, the marketable classes for fruit. These quality parameters, can within limits, be improved through precision irrigation management.

- Seasonal transpiration and crop coefficients were determined for two cultivar 'Wonderful' orchards varying in canopy cover, which can aid in irrigation scheduling of the specific orchards. It should though be kept in mind that the full bearing orchard was not optimally irrigated. The Allen and Pereira approach estimated Kt for both the young and the full bearing orchards succesfully. However, the method relies heavily on measured transpiration inferred mean leaf resistance, which may vary for different orchards. Additional research regarding a practical method to determine mean leaf resistance for orchards is required before the method can be recommended to estimate Kt values for orchards for which mean leaf resistance values are unknown.

- It seems feasible to estimate tree canopy properties such as fractional light interception, tree canopy area based leaf area index and orchard leaf area index from the manually measured tree shaded area, but in contrast to other research published for pomegranate, there was not a highly significant regression relationship between the crop coefficients and the tree shaded area.

- Evaluation of the capability of remote sensing models to estimate reference evapotranspiration and actual evapotranspiration for purposes of irrigation management indicated that EEFlux was the better model to estimate reference evapotranspiration, whereas the PySEBAL model worked better to estimate ET for the full bearing pomegranate orchard. Ground based crop coefficients did not relate significantly to crop coefficients derived using either remote sensing model and more research is required in this regard.

7.2 RECOMMENDATIONS

Further research with better populated datasets is necessary to establish how crop coefficients can be estimated reliably for pomegranate orchards with a range of canopy sizes and to explore the full potential of remote sensing to estimate water use. Producers, the South African Pomegranate Producers' Association, the Water Research Commission, the Western Cape Department of Agriculture, National Department of Agriculture and Science councils can make use of the knowledge generated to improve irrigation scheduling, to perform on-farm and catchment water management and to inform decision making regarding water productivity in the agricultural sector, mindful of limitations outlined in the report.

REFERENCES

ABOU EL-WAFA M (2015) Effect of some treatments on reducing sunburn in 'Wonderful' pomegranate fruit trees. Egypt J Hortic **42 (2)** 795-806.

ABOUKHALED A, ALFARO A and SMITH M (1982) Lysimeters, FAO irrigation and drainage, FAO- Food and agriculture organization of the United Nations **14647** 25-39. Rome, Italy.

ALLEN RG AND PEREIRA LS (2009) Estimating crop coefficients from fraction of ground cover and height. Irrigation Science **28** 17-34.

ALLEN RG, MORTON C, KAMBLE B, KILIC A, HUNTINGTON J, THAU D, GORELICK N, ERICKSON T, MOORE R, TREZZA R AND RATCLIFFE I (2015). EEFlux: A Landsat-based evapotranspiration mapping tool on the Google Earth Engine. In 2015 ASABE/IA Irrigation Symposium: Emerging Technologies for Sustainable Irrigation-A Tribute to the Career of Terry Howell, Sr. Conference Proceedings (1-11). American Society of Agricultural and Biological Engineers.

ALLEN RG, PEREIRA LS, HOWELL TA and JENSEN ME (2011) Evapotranspiration information reporting: I. Factors governing measurement accuracy. Agricultural Water Management 98(6) 899-920.

ALLEN RG, PEREIRA LS, RAES D and SMITH M (1998) *Crop evapotranspiration. Guidelines for computing crop water requirements.* FAO Irrigation and Drainage Paper No. 56. FAO, Rome, Italy.

ALLEN RG, TASUMI M AND TREZZA R (2007) Satellite-based energy balance for mapping evapotranspiration with internalised calibration (METRIC)—Model. Journal of Irrigation and Drainage Engineering **133 (4)** 380-394.

AL-SHAMMARY AAG, KOUZANI AZ, KAYNAK A, KHOO SY, NORTON M and GATES W. 2018. Soil Bulk Density Estimation Methods: A Review. Pedosphere **28(4)**: 581–596.

ANDERSON MC, ALLEN RG, MORSE A AND KUSTAS WP (2012). Use of Landsat thermal imagery in monitoring evapotranspiration and managing water resources. Remote sensing of environment **122** 50-65.

ARENDSE E, FAWOLE OA and OPARA UL (2015) Discrimination of pomegranate fruit quality by instrumental and sensory measurements during storage at three temperature regimes. Journal of Food Processing and Preservation **39(6)** 1867-1877.

AYARS JE, PHENE CJ, PHENE RC, GAO S, WANG D, DAY KR and MAKUS DJ (2017) Determining pomegranate water and nitrogen requirements with drip irrigation. Agriculture Water Management **187** 11–23.

BADRAN MA (2015) Benefits of calcium carbonate sprays on yield and fruit quality of samany and zaghloul date palm under new reclaimed soils. Assiut Journal of Agricultural **46 (5)** 48-57.

BALBONTÍN C, CAMPOS I, ODI-LARA M, IBACACHE A and CALERA A (2017) Irrigation performance assessment in Table grape using the reflectance-based crop coefficient. Remote Sensing **9 (12)** 1276.

BARBEDO JGA (2019) A Review on the Use of Unmanned Aerial Vehicles and Imaging Sensors for Monitoring and Assessing Plant Stresses. Drones **3(40)** 1-27.

BARRET DJ, HATTON TJ ASH JE and BALL MC (1995) Evaluation of the heat pulse velocity technique for measurement of sap flow in rainforest and eucalypt forest species of south-eastern Australia. Plant, Cell and Environment 18(4) 463-469

BASTIAANSSEN WG, MENENTI M, FEDDES RA AND HOLTSLAG AAM (1998). A remote sensing surface energy balance algorithm for land (SEBAL). 1. Formulation. Journal of Hydrology **212** 198-212.

BASTIAANSSEN WGM, CHEEMA MJM, IMMERZEEL WW, MILTENBURG IJ and PELGRUM H (2012) Surface energy balance and actual evapotranspiration of the transboundary Indus Basin estimated from satellite measurements and the ETLook model. Water Resources Research **48(11)**.

BASTIAANSSEN WGM, NOORDMAN EJM, PELGRUM H, DAVIDS G, THORESON BP AND ALLEN RG (2005). SEBAL model with remotely sensed data to improve water-resources management under actual field conditions. Journal of Irrigation and Drainage Engineering **131(1)** 85-93.

BELLVERT J, ZARCO-TEJADA PJ, GIRONA J and FERERES EJPA (2014) Mapping crop water stress index in a 'Pinot-noir vineyard: comparing ground measurements with thermal remote sensing imagery from an unmanned aerial vehicle. Precision Agriculture 15 (4) 361-376.

BERDANIER AB, MINIAT CF and CLARK JS (2016) Predictive models for radial sap flux variation in coniferous, diffuse-porous and ring-porous temperate trees. Tree physiology **36 (8)** 932-941.

BERGH O (1990) Effect of time of hand-thinning on apple fruit size. South African Journal of Plant and Soil **7(1)** 1-10.

BHANTANA P and LAZAROVITCH N (2010) Evapotranspiration, crop coefficient and growth of two young pomegranate (Punica granatum L.) varieties under salt stress. Agricultural water management **97(5)** 715-722.

BLAKE GR and HARTGE KH (1986) Bulk density. In: Klute, A., Ed., Methods of Soil Analysis, Part 1—Physical and Mineralogical Methods, 2nd Edition, Agronomy Monograph 9, American Society of Agronomy—Soil Science Society of America, Madison, 363-382.

BOEGH E, SOEGAARD H AND THOMSEN A (2002) Evaluating evapotranspiration rates and surface conditions using Landsat TM to estimate atmospheric and surface resistance. Remote Sensing of Environment **79 (2-3**) 329-343.

BOWEN IS (1926). The ratio of heat losses by conduction and evaporation from any water surface. Physical Review **27(6)** 779–787.

BOTAI CM, BOTAI JO, DE WIT JP, NCONGWANE KP AND ADEOLA AM (2017). Drought Characteristics over the Western Cape Province, South Africa. Water **9**:876.Paarl.

BRINGHENTI T, MORIONDO M, ABDULAI I, JOUBERT E, ROETTER RP, TAYLOR PJ, HOFFMANN MP (2025) Adopting and evaluating a simple model for macadamia tree transpiration in periodically water-scarce subtropical regions. Scientia Horticulturae **341** (113970) 1-10.

BULANON DM, LONAI J, SKOVGARD H and FALLAHI E (2016) Evaluation of different irrigation methods for an apple orchard using an aerial imaging system. ISPRS International Journal of Geo-Information **5(6)** 79.

BURGESS SS, ADAMS MA, TURNER NC, BEVERLY CR, ONG CK, KHAN AA and BLEBY TM (2001) An improved heat pulse method to measure low and reverse rates of sap flow in woody plants. Tree physiology, **21(9)** 589-598.

BURLS NJ, BLAMEY RC, CASH BA, SWENSON, ET, AL FAHAD A, BOPAPE M-JM, STRAUS DM AND REASON CJC (2019). The Cape Town "Day Zero" drought and Hadley cell expansion. Climate and Atmospheric Science **27**.

BURNETT B, ALLEN RG, ROBISON CW, TASUMI M and LORITE I (2008) Estimating the soil surface evaporation and transpiration components from satellite images in the absence of a thermal band. In World Environmental and Water Resources Congress Ahupua'A 1-18.

GALINDO A, COLLADO-GONZÁLEZ J, GRIÑÁN I, CORELL M, CENTENO A, MARTÍN-PALOMO MJ, GIRÓN IF, RODRÍGUEZ P, CRUZ ZN, MEMMI H, CARBONELL-BARRACHINA AA, HERNÁNDEZ F, TORRECILLAS A, MORIANA A, AND LÓPEZ-PÉREZ D (2018). Deficit irrigation and emerging fruit crops as a strategy to save water in Mediterranean semiarid agrosystems. Agric. Water Manag. **202** 311-324.

CHAKMA J (2014) Effect of different orchard management practices on the growth, productivity and rejuvenation of declining trees of pomegranate (Punica granatum L cv. Kandhari Kabuli). MSc Thesis. Yashwant Singh Parmar University of Horticulture & Forestry, Sola.

CHANDRA R, BABU KD, JADHAV VT and TEIXEIRA DA SILVA JA (2010) Origin, history and domestication of pomegranate. Fruit, Vegetable and Cereal Science and Biotechnology **2** 1-6.

CHATER JM and GARNER LC (2018) Foliar nutrient applications to 'Wonderful' pomegranate (Punica granatum L.). II. Effects on leaf nutrient status and fruit split, yield and size. Scientia Horticulturae **242** 207-213.

CHOUDHURY BJ, AHMED NU, IDSO SB, REGINATO RJ and DAUGHTRY CS (1994) Relations between evaporation coefficients and vegetation indices studied by model simulations. Remote sensing of environment **50(1)** 1-17.

CLULOW AD, EVERSON CS, MENGISTU MG, JARMAIN C, JEWITT GPW, PRICE JS AND GRUNDLING, PL (2012) Measurement and modelling of evaporation from a coastal wetland in Maputaland, South Africa. Hydrology and Earth System Sciences **16(9)** 3233-3247.

COHEN Y, FUCHS M and GREEN GC (1981) Improvement of the heat pulse method for determining sap flow in trees. Plant, Cell & Environment **4(5)** 391-397.

DAY KR and WILKINS ED (2011) Commercial pomegranate (Punica granatum L.) production in California. Acta Horticulturae **890** 275-286.

DEA 2016. South Africa National Adaptation Strategy. Draft for comments. URL: https://www.environment.gov.za/sites/default/files/docs/nas2016.pdf. (Accessed 02/05/2018).

DELAVARPOUR N, KOPARAN C, NOWATZKI J, BAJWA S and SUN X (2021) A Technical Study on UAV Characteristics for Precision Agriculture Applications and Associated Practical Challenges. Remote Sensing **13(6)** 1204.

DINC N, AYDINSAKIR K, ISIK M, BASTUG R, ARI N, SAHIN A, BUYUKTAS D (2018) Assessment of different irrigation strategies on yield and quality characteristics of drip irrigated pomegranate under mediterranean conditions. *Irrig Sci* **36** 97-96.

DZIKITI S, VOLSCHENK T, MIDGLEY S, GUSH M, TAYLOR N, LÖTZE E, ZIREBWA S, NTSHIDI Z., MOBE N, SCHMEISSER M AND DOKO Q (2018) *Quantifying water use and water productivity of high performing apple orchards of different canopy sizes in winter rainfall areas of South Africa*. Research report no. TT 751-2018, Water Research Commission, Pretoria, South Africa.

ESPINOZA CZ, KHOT LR, SANKARAN S and JACOBY PW (2017) High resolution multispectral and thermal remote sensing-based water stress assessment in subsurface irrigated grapevines. Remote Sensing **9(9)** 961.

evapotranspiration algorithm. IAHS-AISH Publ **352** 120-123.

FATTAHI E, JAFARI A and FALLAHI E (2020) Hand Thinning Influence on Fruit Quality Attributes of Pomegranate (Punica granatum L. cv. 'Malase Yazdi'). International Journal of Fruit Science 20(sup2) S377-S386.

FERNÁNDEZ JE, ALCON F, DIAZ-ESPEJOA, A, HERNANDEZ-SANTANAA, V, CUEVASA MV (2020). Water use indicators and economic analysis for on-farm irrigation decision: A case study of a super high density olive tree orchard. Agric. Water Manag. **237**: 1-13 (106074).

FERNÁNDEZ JE, DURÁN PJ, PALOMO MJ, DIAZ-ESPEJO A, CHAMORRO V and GIRÓN IF (2006) Calibration of sap flow estimated by the compensation heat pulse method in olive, plum and orange trees: relationships with xylem anatomy. Tree Physiology **26(6)** 719-728.

FERNÁNDEZ JE, PALOMO MJ, DÍAZ-ESPEJO A, CLOTHIER BE, GREEN SR, GIRÓN IF and MORENO F (2001) Heat-pulse measurements of sap flow in olives for automating irrigation: tests, root flow and diagnostics of water stress. Agricultural Water Management **51** 99–123.

FERRARA G, PALASCIANO M, COSSIO F, BABU KD and MAZZEO A (2021) Orchard establishment and tree management. In: The Pomegranate: Botany, Production and Uses. SARKHOSH A, YAVARI AM and ZAMANI Z. CABI, Boston, USA.

FLUMIGNAN DL, DE FARIA RT and PRETE CEC (2011) Evapotranspiration components and dual crop coefficients of coffee trees during crop production. Agricultural Water Management **98(5)** 791-800.

FOLHES MT, RENNÓ CD AND SOARES JV (2009). Remote sensing for irrigation water management in the semi-arid Northeast of Brazil. Agricultural Water Management **96(10)** 1398-1408.

FRENCH AN, HUNSAKER DJ, SANCHEZ CA, SABER M, GONZALEZ JR and ANDERSON R (2020) Satellite-based NDVI crop coefficients and evapotranspiration with eddy covariance validation for multiple durum wheat fields in the US Southwest. Agric. Water Manag. **239** (106226).

FUCHS S, LEUSCHNER C, LINK R, CONERS H and SCHULDT B (2017) Calibration and comparison of thermal dissipation, heat ratio and heat field deformation sap flow probes for diffuse-porous trees. Agricultural and Forest Meteorology **244** 151-161.

GARCIA J and BARBEDO A (2019) A Review on the Use of Unmanned Aerial Vehicles and Imaging Sensors for Monitoring and Assessing Plant Stresses Drones **3**(2), 40.

GASCON F, BOUZINAC C, THÉPAUT O, JUNG M, FRANCESCONI B, LOUIS J, LONJOU V, LAFRANCE B, MASSERA S, GAUDEL-VACARESSE A AND LANGUILLE F (2017) Copernicus Sentinel-2A calibration and products validation status. Remote Sensing 9 (6).

GAVILAN P, BERENGENA J and ALLEN RG (2007) Measuring versus estimating net radiation and soil heat flux: Impact on Penman–Monteith reference ET estimates in semiarid regions. Agricultural water management **89(3)** 275-286.

GHOSH SN, BERA B, ROY S and KUNDU A (2012) Integrated nutrient management in pomegranate grown in laterite soil. *Indian* Journal of Horticulture **69(3)** 333-337.

GONZÁLEZ-ALTOZANO P, PAVEL EW, ONCINS JA, DOLTRA J, COHEN M, PAÇO T, MASSAI R and CASTEL JR (2008) Comparative assessment of five methods of determining sap flow in peach trees. Agricultural water management **95(5)** 503-515.

GONZALEZ-DUGO V, ZARCO-TEJADA P, NICOLÁS E, NORTES PA, ALARCÓN JJ, INTRIGLIOLO DS and FERERES EJPA (2013) Using high resolution UAV thermal imagery to assess the variability in the water status of five fruit tree species within a commercial orchard. Precision Agriculture **14(6**) 660-678.

GRANIER A (1985) Une nouvelle méthode pour la mesure du flux de sève brute dans le tronc des arbres. Annales des Sciences. Forestieres **42** 193–200.

GRANIER A, ANFODILLO T, SABATTI M, COCHARD H, DREYER E, TOMASI M, VALENTINI R and BRÉDA N (1994) Axial and radial water flow in the trunks of oak trees: a quantitative and qualitative analysis. Tree physiology **14(12)** 1383-1396.

GREEN S (1998) Measurements of sap flow by the heat-pulse method. HortResearch, Palmerston North.

GREEN S, CLOTHIER B and JARDINE B (2003) Theory and practical application of heat pulse to measure sap flow. Agronomy Journal **95(6)** 1371-1379.

GUSH MB and TAYLOR NJ (2014) The water use of selected fruit tree orchards (Volume 2): Technical report on measurements and modelling. Water Research Commission report, **2(1770)** 1-146.

HALL RL, ALLEN SJ, ROSIER PT and HOPKINS R (1998) Transpiration from coppiced poplar and willow measured using sap-flow methods. Agricultural and Forest Meteorology **90(4)** 275-290.

HESSELS T, VAN OPSTAL J, TRAMBAUER P, BASTIAANSSEN WGM, FAOUZI M, MOHAMED Y AND ER-RAJI A (2017) pySEBAL Version 3.3. 7 [online]

HOLLAND D, HATIB K and BAR-YA'AKOV I (2009) 2 Pomegranate: botany, Horticulture, Breeding. Horticultural reviews **35(2)** 127-191.

HUNSAKER DJ, PINTER PJ, BARNES EM and KIMBALL BA (2003) Estimating cotton evapotranspiration crop coefficients with a multispectral vegetation index. Irrigation science **22(2)** 95-104.

IBRAIMO NA (2018). Water use of deciduous and evergreen tree nut crops: a case study using pecans and macadamias. Thesis submitted in partial fulfilment of the requirements for the degree Ph.D. Agronomy, University of Pretoria.

ICT INTERNATIONAl Pty Ltd, 2014. Comparison of HRM and TDP Methods of Sap Flow Measurement. https://au.ictinternational.com/content/uploads/2014/03/HRM-TDP-compare-alt2.pdf. Visited on 03 August 2021.

INTRIGLIOLO DS, BONET L, NORTES PA, PUERTO H, NICOLAS E, BARTUAL J. (2013) Pomegranate trees performance under sustained and regulated deficit irrigation. *Irrigation Science* **31(5)** 959-970.

INTRIGLIOLO DS, NICOLAS E, BONET L, FERRER P, ALARCÓN JJ and BARTUAL J (2011) Water relations of field grown Pomegranate trees (*Punica granatum*) under different drip irrigation regimes. Agricultural Water Management **98** 691–696.

INTRIGLIOLO DS, WANG D, PÉREZ-GAGO MB, PALOU L, AYARS J, PUERTO H and BARTUAL J (2023) Water Requirements and Responses to Irrigation Restrictions, In: *The Pomegranate BOTANY, PRODUCTION AND USES,* SARKOSH A, YAVARRI A, ZAMANI Z, CAB International Boston, USA.

ISARANGKOOL NA AYUTTHAYA S, DO FC, PANNENGPETCH K, JUNJITTAKARN J, MAEGHT JL, ROCHETEAU A and COCHARD H (2010) Transient thermal dissipation method of xylem sap flow measurement: multi-species calibration and field evaluation. Tree Physiology **30(1)** 139-148.

JAAFAR HH AND AHMAD FA (2020) Time series trends of Landsat-based ET using automated calibration in METRIC and SEBAL: The Bekaa Valley, Lebanon. Remote Sensing of Environment **238**.

JOVANOVIC N, PEREIRA LS, PAREDES P, PÔÇAS I, CANTORE V and TODOROVIC M (2020) A review of strategies, methods and technologies to reduce non-beneficial consumptive water use on farms considering the FAO56 methods. Agricultural water management, 239 106267.

KAHRAMANOGLU I, USANMAZ S and ALAS T (2018) Effects of fruit thinning on the quality and size of Wonderful pomegranate fruits. Advanced Food Science **40(4)** 114-119.

KANGUEEHI GN (2018) Water footprint analysis to improve water use efficiency in Table grape (Vitis vinifera L. cv. Crimson Seedless) production. A South African case study (Doctoral dissertation, Stellenbosch: Stellenbosch University).

KARIMI P AND BASTIAANSSEN WG (2015) Spatial evapotranspiration, rainfall, and land use data in water accounting–Part 1: Review of the accuracy of the remote sensing data. Hydrology and Earth System Sciences **19 (1**) 507-532.

KJAERSGAARD JH, CUENCA RH, MARTÍNEZ-COB A, GAVILÁN P, PLAUBORG F, MOLLERUP M AND HANSEN S (2009). Comparison of the performance of net radiation calculation models. Theoretical and applied climatology **98** 57-66

KNIGHT DH, FAHEY TJ, RUNNING SW HARRISON AT and WALLACE LL (1981) Transpiration from 100-yr-old Lodgepole pine forests estimated with whole-tree Potometers. Ecology **62(3)** 717-726.

KOKKOTOS E, ZOTOS A and PATAKAS A (2020) Evaluation of Water Stress Coefficient Ks in Different Olive Orchards. Agronomy **10(10)** 1594.

Kustas WP, Perry EM, Doraiswamy PC, and Moran MS (1994). Using satellite remote sensing to extrapolate evapotranspiration estimates in time and space over a semiarid rangeland basin. Remote sensing of environment **49(3)** 275-286.

LAIPELT L, KAYSER, RHB, FLEISCHMANN, AS, RUHOFF A, BASTIAANSSEN W, ERICKSON TA AND MELTON F (2021). Long-term monitoring of evapotranspiration using the SEBAL algorithm and Google Earth Engine cloud computing. ISPRS Journal of Photogrammetry and Remote Sensing **178** 81-96.

LARIBI AI, PALOU L, INTRIGLIOLO DS, NORTES PA, ROJAS-ARGUDO C, TABERNER V, BARTUAL J and PÉREZ-GAGO MB (2013) Effect of sustained and regulated deficit irrigation on fruit quality of pomegranate 'Mollar de Elche' at harvest and during cold storage. Agricultural Water Management **125** 61-70.

LARUE JH (1980) Growing pomegranates in California. Univ. The University of California's Division of Agriculture and Natural Resources. Leaflet 2459.

LEE TW (1994) Using PAWS and AgriMet for irrigation scheduling. In: *Tree Fruit IRRIGATION*. EDITORS WILLIAMS KM, LEY TW, Good Fruit grower, Yakima, Washington.

LEVIN GM (2006) Pomegranate Roads: A Soviet Botanist's Exile from Eden, 1st edn. Floreant Press, Forestville, California. 15–183.

LI X, CHEN D, DUAN Y, JI H, ZHANG L, CHAI Q AND HU X (2020) Understanding Land use/Land cover dynamics and impacts of human activities in the Mekong Delta over the last 40 years. Global Ecology and Conservation **22**.

LIU C, SUN G, MCNULTY SG and KANG S (2015) An improved evapotranspiration model for an apple orchard in northwestern China. Transactions of the ASABE **58(5)** 1253-1264.

LOPEZ-BERNAL Á, ALCÁNTARA E and VILLALOBOS FJ (2014) Thermal properties of sapwood of fruit trees as affected by anatomy and water potential: errors in sap flux density measurements based on heat pulse methods. Trees **28(6)** 1623-1634.

LÓPEZ-URREA R, SÁNCHEZ JM, DE LA CRUZ F, GONZÁLEZ-PIQUERAS J and CHÁVEZ JL (2020) Evapotranspiration and crop coefficients from lysimeter measurements for sprinkler-irrigated canola. Agricultural Water Management 239 106260.

MAHOHOMA W (2016) Measurement and modelling of water use of citrus orchards (Doctoral dissertation, University of Pretoria).

MAPETO T, LOUW J, GUSH M and PAUW J (2018) Whole-tree sap flow responses to soil water and weather variables for Pinus radiata and three indigenous species in a southern afrotemperate forest region. Southern Forests: a Journal of Forest Science, **80(4)** 329-339.

MARSHALL DC (1958) Measurement of sap flow in conifers by heat transport. Plant physiology **33(6)** 385.

MASHABATU M, MOTSEI N, JOVANOVIC N AND NHAMO L (2025) A validation of Fruitlook data using eddy covariance in a fully mature and high-density Japanese Plum Orchard in the Western Cape, South Africa. Water **17(3)** 324

MASHAVHATHSKHA KL (2014) Yield and Quality Pomegranate on Selected Geographical Areas in Western Cape Province, South Africa (Masters of Science thesis, University of South Africa).

MAZHAWU E, CLULOW AD TAYLOR, NJ AND SAVAGE MJ (2020). Water use of an intermediate and a mature avocado orchard. Acta Hortic. **1281**, 555-562.

MCCULLOH K, SPERRY JS, LACHENBRUCH B, MEINZER FC, REICH PB and VOELKER S (2010) Moving water well: comparing hydraulic efficiency in twigs and trunks of coniferous, ring-porous, and diffuse-porous saplings from temperate and tropical forests. New Phytologist **186(2)** 439-450.

MCKINSEY AND COMPANY (2010) Confronting South Africa's water challenge https://www.mckinsey.com/~/media/McKinsey/Business%20Functions/Sustainability/Our%20Insights/Confronting%20South%20Africas%20water%20challenge/Confronting%20South%20Africas%20water%20challenge.pdf (Accessed 10 April 2025).

MESHRAM DT, MITTAL HK, PUROHIT RC AND GORANTIWAR SD (2011). Water Requirement of Pomegranate (Punica granatum L.) for Solapur District of Maharashtra State. Acta Hort **890** 311-321.

MESHRAM DT, GORANTIWAR SD, MITTAL HK, SINGH NV and LOHKARE AS (2012) Water requirement of pomegranate (Punica granatum L.) plants up to five year age. Journal of Applied Horticulture **14(1)** 47-50.

MINHAS PS, RAMOS TB, BEN_GAL A,and PEREIRA LS (2020) Coping with salinity in irrigated agriculture: Crop evapotranspiration and water management issues. Agric Water Manag. **227** (105832).

MOBE, NT, DZIKITI, S, VOLSCHENK, T, ZIREBWA, SF, NTSHIDI, Z, MIDGLEY, SJE, STEYN, WJ, LÖTZE, E, MPANDELI, S and MAZVIMAVI, D (2020) Using sap flow data to assess variations in water use and water status of apple orchards of varying age groups in the Western Cape Province of South Africa. Water SA, **46(2)** 213-224.

NOLZ R, CEPUDER P and EITZINGER J (2016) Comparison of lysimeter based and calculated ASCE reference evapotranspiration in a subhumid climate. Theoretical and applied climatology **124(1-2)** 315-324.

NTSHIDI Z, DZIKITI S and MAZVIMAVI, D (2018) Water use dynamics of young and mature apple trees planted in South African orchards: a case study of the Golden Delicious and Cripps' Pink cultivars. Proceedings of the International Association of Hydrological Sciences, **378** 79-83.

OTTO FEL, WOLSKI P, LEHNER F, TEBALDI C, VAN OLDENBORGH GJ, HOGESTEEGER S, SINGH R, HOLDEN P, FUČKAR NS, ODOULAMI RC AND NEW, M (2018) Anthropogenic influence on the drivers of the Western Cape drought 2015–2017. Environ. Res. Lett. **13**:124010.

PARK S, RYU D, FUENTES S, CHUNG H, O'CONNELL M and KIM J (2021) Mapping Very-High-Resolution Evapotranspiration from Unmanned Aerial Vehicle (UAV) Imagery. ISPRS International Journal of Geo-Information **10(4)** 211.

PARVIZI H, SEPASKHAH AR, AHMADI SH. (2014) Effect of drip irrigation and fertilizer regimes on fruit yields and water productivity of a pomegranate (*Punica granatum* (L.) cv. Rabab) orchard. *Agricultural Water Management* **146** 45-56.

PAUDEL I, KANETY T and COHEN S (2013) Inactive xylem can explain differences in calibration factors for thermal dissipation probe sap flow measurements. Tree physiology **33(9)** 986-1001.

PELGRUM H, MILTENBURG IJ, CHEEMA MJM, KLAASSE A and BASTIAANSSEN WGM (2010) ET Look: A novel continental evapotranspiration algorithm. Remote Sensing and Hydrology 2010 Proceedings of a symposium held at Jackson Hole,Wyoming, USA, September 2010. (IAHS Publ. 3XX, 2011)

PEREIRA LS, PAREDES P, LÓPEZ-URREA R, HUNSAKER DJ, MOTA M and SHAD ZM (2021) Standard single and basal crop coefficients for vegetable crops, an update of FAO56 crop water requirements approach. Agricultural Water Management **243** 106196.

PEREIRA LS, PAREDES P, MELTON F, JOHNSON L, WANG T, LÓPEZ-URREA R, CANCELA JJ AND ALLEN RG, (2020) Prediction of crop coefficients from fraction of ground cover and height. Background and validation using ground and remote sensing data. Agricultural Water Management, **241** 106197.

PIENAAR L (2021) The Economic Contribution of South Africa's Pomegranate Industry. Western Cape Department of Agriculture (WCDoA) Division for Macro & Resource Economics and Pomegranate Producers Association of South Africa (POMASA).

POMEGRANATE ASSOCIATION OF SOUTH AFRICA (POMASA). (2013) Pomegranate production guidelines. https://www.sapomegranate.co.za/statistics-and-information/technical-information/. Visited on 09 July 2021.

PRASAD RN, BANKAR GJ and VASHISHTHA BB (2003) Effect of drip irrigation on growth, yield and quality of pomegranate in arid region. Indian journal of horticulture **60(2)** 140-142.

RAJAEI H and YAZDANPANAH P (2015) Buds and leaves in pomegranate (Punica granatum L.): Phenology in relation to structure and development. Flora-morphology, distribution, functional ecology of plants **214** 61-69.

RALLO G, PAÇO TA, PAREDES P, PUIG-SIRERA À, MASSAI R, PROVENZANO G and PEREIRA LS (2021) Updated single and dual crop coefficients for tree and vine fruit crops. Agricultural Water Management **250** 106645.

RANA G, DE LORENZI F, PALATELLA L, MARTINELLI N and FERRARA RM (2019) Field scale recalibration of the sap flow thermal dissipation method in a Mediterranean vineyard. Agricultural and Forest Meteorology **269** 169-179.

RANA G, KATERJI N AND DE LORENZI F (2005) Measurement and modelling of evapotranspiration of irrigated citrus orchard under Mediterranean conditions. Agricultural and Forest Meteorology **128 (3-4)** 199-209.

RYUGO K (1988) *Fruit culture: Its Science and Art*. New York: John Wiley.

SAITTA D, VANELLA D, RAMÍREZ-CUESTA JM, LONGO-MINNOLO G, FERLITO F and CONSOLI S (2020) Comparison of orange orchard evapotranspiration by eddy covariance, sap flow, and FAO-56 methods under different irrigation strategies. Journal of Irrigation and Drainage Engineering **146(7)** 05020002.

SAM MC (2016) Calibration of sap flow techniques in citrus using the stem perfusion method (Doctoral dissertation, University of Pretoria).

SARKHOSH A, ZAMANI Z, FATAHI R and EBADI A (2006) RAPD markers reveal polymorphism among some Iranian pomegranate (Punica granatum L.). Genotypes Scientia Horticulturae **111** 24–29.

SEERAM NP, ZHANG Y, REED JD, KRUEGER CG and VAYA J (2006) Pomegranate phytochemicals. In: Ancient Roots to Modern Medicine. Seeram NP, Schulman RN and Heber D. Boca Raton, Florida: Taylor & Francis Group. 3–29.

SELAHVARZI Y, ZAMANI Z, FATAHI R, TALAEI AR. (2017) Effect of deficit irrigation on flowering and fruit properties of pomegranate (*Punica granatum* cv. Shahvar). *Agricultural Water Management* **192** 189–197.

SENAY GB, FRIEDRICHS M, SINGH RK AND VELPURI NM (2016) Evaluating Landsat 8 evapotranspiration for water use mapping in the Colorado River Basin. Remote Sensing of Environment **185** 171-185.

SENAY GB, FRIEDRICHS M, SINGH RK AND VELPURI NM (2016). Evaluating Landsat 8 evapotranspiration for water use mapping in the Colorado River Basin. Remote Sensing of Environment **185** 171-185.

SHACKEL KA, JOHNSON RS, MEDAWAR CK and PHENE CJ (1992) Substantial errors in estimates of sap flow using the heat balance technique on woody stems under field conditions. Journal of the American Society for Horticultural Science **117(2)** 351-356.

SHAILENDRA A and NARENDRA A (2005) The effect of trickle irrigation on growth, yield and quality of pomegranate (Punica granatum L.) cv. Ganesh in Chhattisgarh region. Mysure Journal of Agricultural Science **39** 175 – 181

SHULMAN Y, FAINBERSTEIN L and LAVEE S (1984) Pomegranate fruit development and maturation. Journal of Horticultural Science **59(2)** 265-274.

SIDHU HS, DÍAZ-PÉREZ JC and MACLEAN D (2019) Controlled Atmosphere Storage for Pomegranates (Punica granatum L.): Benefits over Regular Air Storage. HortScience **54(6)** 1061-1066.

SMITH DM and ALLEN SJ (1996) Measurement of sap flow in plant stems. Journal of Experimental Botany **47(12)** 1833-1844.

STEINBERG S, VAN BAVEL CH and McFARLAND, MJ (1989) A gauge to measure mass flow rate of sap in stems and trunks of woody plants. Journal of the American Society for Horticultural Science **114(3)** 466-472.

STEPPE K, DE PAUW DJ, DOODY TM and TESKEY RO (2010) A comparison of sap flux density using thermal dissipation, heat pulse velocity and heat field deformation methods. Agricultural and Forest Meteorology **150(7-8)** 1046-1056.

SULOCHANAMMA BN, YELLAMANDA REDDY T and SUBBI REDDY R (2005) Effect of basin and drip irrigation on growth, yield and water use efficiency in pomegranate cv. Ganesh. Acta Horticulturae **696** 277 – 279.

TASUMI M (2003). Progress in operational estimation of regional evapotranspiration using satellite imagery. University of Idaho.

TAYLOR NJ, MAHOHOMA W, VAHRMEIJER JT, GUSH MB, ALLEN RG, ANNANDALE JG (2015) Crop coefficient approaches based on fixed estimates of leaf resistance are not appropriate for estimating water use of citrus. Irrig. Sci. **33** 153–166. https://doi.org/10.1007/s00271-014-0455-z.

TIE Q, HU H, TIAN F, GUAN H and LIN H (2017) Environmental and physiological controls on sap flow in a subhumid mountainous catchment in North China. Agricultural and Forest Meteorology **240** 46-57.

TWINE TE, KUSTAS WP, NORMAN JM, COOK DR, HOUSER P, MEYERS TP, PRUEGER JH, STARKS PJ AND WESELY ML (2000) Correcting eddy-covariance flux underestimates over a grassland. Agricultural and forest meteorology 103(3) 279-300.

VERTESSY RA, HATTON TJ, REECE P, O'SULLIVAN SK and BENYON RG (1997) Estimating stand water use of large mountain ash trees and validation of the sap flow measurement technique. Tree Physiology **17(12)** 747-756.

VAHRMEIJER JT, ANNANDALE JG, GUSH MB AND TAYLOR NJ (2015). Citrus water use in South Africa. Acta Horticulturae **1065** 1719-1724.

VILJOEN N (2020b) Pomegranate Production Costs 2020. https://www.sapomegranate.co.za/statistics-and-information/pomegranate-industry-overview/. Accessed on 07 October 2021.

VILJOEN N (2022) Pomegranate Production Costs. https://www.sapomegranate.co.za/statistics-and-information/productions-costs/ Accessed on 08 April 2025.

VILJOEN N and HURTER T (2024) POMASA Industry Overview. https://www.sapomegranate.co.za/statistics-and-information/pomegranate-industry-overview/. Accessed on 19 January 2025.

VILJOEN N. (2020a) Pomegranate Industry Overview. https://www.sapomegranate.co.za/statistics-and-information/pomegranate-industry-overview/. Accessed on 07 October 2021.

VILLALOBOS FJ, TESTI L, ORGAZ F, GARCÍA-TEJERA O, LOPEZ-BERNAL A, GONZÁLEZ-DUGO MV, BALLESTER-LURBE C, CASTEL JR, ALARCÓN-CABAÑERO JJ, NICOLÁS-NICOLÁS E, GIRONA J, MARSAL J, FERERES E (2013) Modelling canopy conductance and transpiration of fruit trees in Mediterranean areas: a simplified approach. Agric For Meteorol **171–172**:93–103

VOLSCHENK T (2020) Water use and irrigation management of pomegranate trees - A review. Agricultural Water Management **241** 106375.

VOLSCHENK T and MULIDZI AR (2020) Scoping study and a baseline understanding of pomegranate orchard water use in selected production areas. WRC Report No. 2958/1/20 132.

VOLSCHENK T, DE VILLIERS JF and BEUKES O. 2003. *The selection and calibration of a model for irrigation scheduling of deciduous fruit orchards*. Research report no. 892/1/03, Water Research Commission, Pretoria, South Africa.

WALTER IA, ALLEN RG., ELLIOTT R, JENSEN ME, ITENFISU D, MECHAM B, HOWELL TA, SNYDER R, BROWN P, ECHINGS S and SPOFFORD T (2000) ASCE's standardized reference evapotranspiration equation. Watershed management and operations management 1-11.

WANG T, MELTON FS, PÔÇAS I, JOHNSON LF, THAO T, POST K and CASSEL-SHARMA F (2021) Evaluation of crop coefficient and evapotranspiration data for sugar beets from Landsat surface reflectances using micrometeorological measurements and weighing lysimetry. Agricultural Water Management, **244** 106533.

WCDEA and DP (2018a) Western Cape Department of Environmental Affairs and Development Planning: State of Environment Outlook Report for the Western Cape Province 2014 – 2017. February 2018. https://www.westerncape.gov.za/eadp/files/atoms/files/00_Executive%20Summary.pdf. (Accessed 25 July 2021).

WCDEA and DP (2018b) Western Cape Department of Environmental Affairs and Development Planning: Western Cape Sustainable Water Management Plan 2017 – 2022. Towards a new norm for water resilience. March 2018. https://www.westerncape.gov.za/eadp/files/atoms/files/WC%20Sustainable%20Water%20Management%20Plan%202018_1.pdf. (Accessed 13 July 2021).

WCDOA & WCDEA and DP (2016). Western Cape Department of Agriculture and the Western Cape Department of Environmental Affairs & Development Planning. Cape Town: A status quo review of climate change and the agriculture sector of the Western Cape Province.. https://docslib.org/doc/10776655/smart-agri-status-quo-review-2016 (Accessed 10 April 2025).

WEISS M, BARET F, SMITH GJ, JONCKHEERE I AND COPPIN P (2004) Review of methods for in situ leaf area index (LAI) determination. Agricultural and Forest Meteorology **121** 37-53.

WETZSTEIN HY, ZHANG Z, RAVID N and WETZSTEIN ME (2011) Characterization of attributes related to fruit size in pomegranate. HortScience, **46(6)** 908-912.

WHITLEY R, ZEPPEL M, ARMSTRONG N, MACINNIS-NG C, YUNUSA I and EAMUS, D (2008) A modified Jarvis-Stewart model for predicting stand-scale transpiration of an Australian native forest. *Plant and Soil*, **305**, 35-47.

WILLIAMS DG, CABLE W, HULTINE K, HOEDJES JCB, YEPEZ EA, SIMONNEAUX V, ER-RAKI S, BOULET G, DE BRUIN HAR, CHEHBOUNI A and HARTOGENSIS OK (2004) Evapotranspiration components determined by stable isotope, sap flow and eddy covariance techniques. Agricultural and forest meteorology **125(3-4)** 241-258.

WILLIAMS LE and AYARS JE (2005) Grapevine water use and the crop coefficient are linear functions of the shaded area measured beneath the canopy. Agricultural and Forest Meteorology **132(3-4)** 201-211.

WRIGHT JL (1982) New evapotranspiration crop coefficients. Journal of the Irrigation and Drainage Division **108(1)** 57-74.

WULDER MA, WHITE JC, LOVELAND TR, WOODCOCK CE, BELWAR AS, COHEN WB, FOSNIGHT EA, SHAW J, MASEK JG AND ROY DP (2016) The global Landsat archive: Status, consolidation, and direction. Remote Sensing of Environment **185** 271–283.

XUE J, BALI KM, LIGHT S, HESSELS T AND KISEKKA I (2020). Evaluation of remote sensing-based evapotranspiration models against surface renewal in almonds, tomatoes, and maize. Agricultural Water Management **238**.

ZHANG H, WANG D, AYARS JE and PHENE CJ (2017) Biophysical response of young pomegranate trees to surface and sub-surface drip irrigation and deficit irrigation. Irrigation Science **35(5)** 425-435.

ZHANG Y, SHEN Y, XU X, SUN H, LI F and WANG Q (2013) Characteristics of the water–energy–carbon fluxes of irrigated pear (Pyrus bretschneideri Rehd) orchards in the North China Plain. Agricultural water management **128** 140-148.

ZHAO N, LIU Y, CAI J, PAREDES P, ROSA RD and PEREIRA LS (2013) Dual crop coefficient modelling applied to the winter wheat–summer maize crop sequence in North China Plain: Basal crop coefficients and soil evaporation component. Agricultural water management **117** 93-105.

APPENDIX A: SOIL PHYSICAL PROPERTIES AND WATER CONTENT SENSOR RELATED INFORMATION

Table 38. Soil particle size analysis (five fraction) of soil sampled at the soil water balance (SWB1-4) sites at the young (SWB1 and 2) and full bearing (SWB3 and 4) pomegranate orchards at Avontuur and Welgemoed, respectively

SWB	Depth (cm)	Clay (%)	Silt (%)	Sand (%)	Sand Fine (%)	Sand Medium (%)	Sand Course (%)	Stone %(v/v)	10 kPa (%)	100 kPa (%)	WHC (mm m^{-1})
SWB1	0-19	0	4	96	20	30	46	10	15	8	64
	19-50	4	4	92	9	24	60	8	16	11	55
	50-75	0	4	96	12	25	59	9	15	9	57
	75-104	4	4	92	10	23	59	30	13	8	44
SWB2	0-20	0	0	100	9	25	66	8	14	9	52
	20-60	0	4	96	15	29	51	13	14	8	56
	60-90	4	4	92	13	24	55	30	13	8	46
	90-120	4	4	92	9	21	62	32	13	8	43
SWB3	0-30	4	8	88	30	23	36	13	18	10	80
	30-60	4	8	88	29	18	42	16	19	11	80
	60-90	4	4	92	22	19	52	26	15	9	61
	90-115	4	8	88	18	16	55	33	15	9	55
SWB4	0-10	4	8	88	21	15	52	12	20	12	78
	10-40	4	8	88	24	17	47	14	19	11	77
	40-70	4	8	88	29	21	38	13	19	11	81
	70-100	0	4	96	22	14	59	18	17	10	71
	100-125	4	4	92	17	10	65	23	17	10	64

WHC - Water holding capacity

Table 39. Bulk density of soils sampled for various soil layers at the soil water balance (SWB) sites for the young and full bearing pomegranate orchards at Avontuur (SWB1 and 2) and Welgemoed (SWB3 and 4), respectively

Orchard	SWB	Soil layer (cm)	Bulk density (g cm^{-3})			
			Tree Row		Work row	
			Mean	STDev	Mean	STDev
Avontuur	SWB1	0-20	1.394	0.084	1.419	0.040
		20-50	1.424	0.038	1.555	0.114
		50-90	1.453	0.134	1.392	0.130
		90-105	1.390	0.210	1.371	0.083
	SWB2	0-20	1.528	0.009	1.488	0.034
		20-60	1.547	0.095	1.477	0.050
		60-90	1.491	0.103	1.528	0.169
		90-120	1.510	0.170	1.501	0.094
Welgemoed	SWB3	0-30	1.484	0.080	1.590	0.070
		30-60	1.735	0.009	1.702	0.026
		60-90	1.697	0.017	1.923	0.033
		90-115	1.925	0.020	1.604	0.018
	SWB4	0-40	1.538	0.074	1.641	0.033
		40-70	1.638	0.007	1.687	0.023
		70-100	1.635	0.008	1.703	0.024
		100-125*	-	-	-	-

STDev – Standard deviation, *Water table present

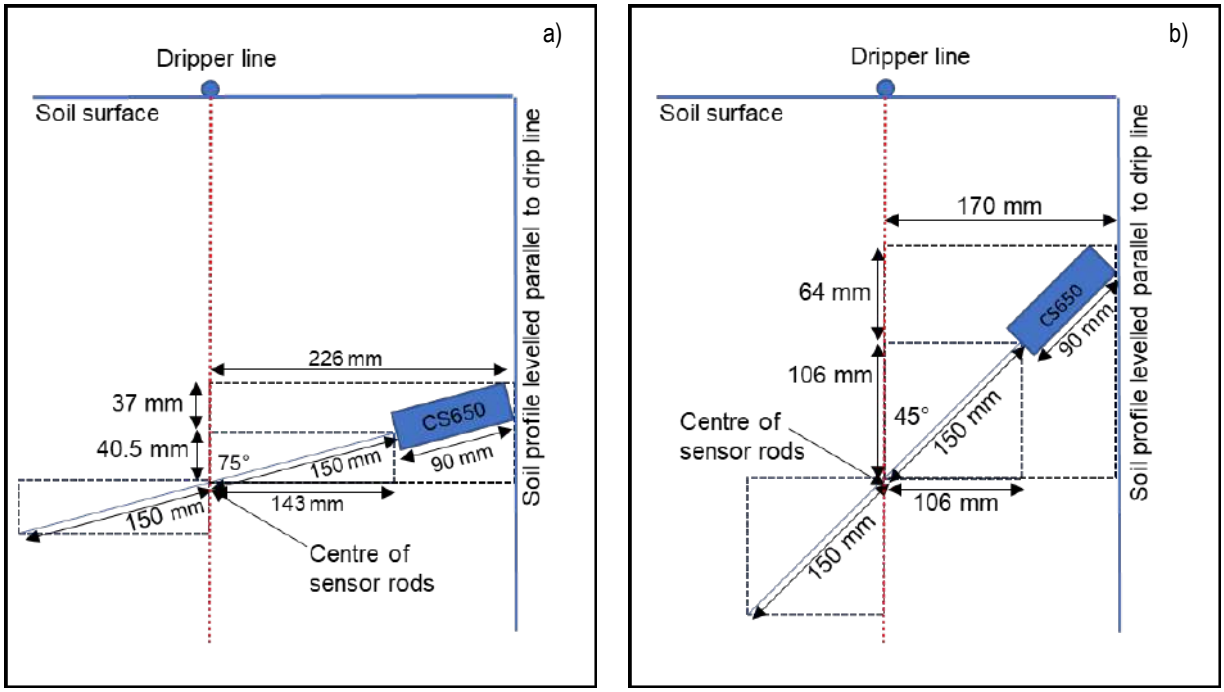

Figure 78. Installation diagram for a CS650 sensor indicating the positioning relative to the dripper line and levelled soil profile to monitor soil water content for any selected soil depth increment at a) Avontuur and b) Welgemoed. Installation depths from the soil surface will differ for different soil depth increments.

Table 40. CS650 soil water content sensor *in situ* calibration equations for the top soil at Avontuur and all soil layers at Welgemoed. Data for SWB3 and 4 has been combined for Welgemoed.

SWB	Soil layer	Layer ID	R^2	p-value	SE of estimate	MAE	Model equation
SWB1	0-200	L1	92.9	0.000	0.007	0.006	VSWC_L1 = -0.0324183 + 0.02368*Ka_L1
SWB1	200-500	L2	85.0	0.000	0.013	0.011	VSWC_L2 = -0.0357025 + 0.0229494*Ka_L2
SWB2	0-200	L1	92.0	0.000	0.008	0.005	VSWC_L1 = -0.0388143 + 0.0253356*Ka_L1
SWB2	200-600	L2	83.8	0.000	0.013	0.010	VSWC_L2 = -0.0277347 + 0.0212824*Ka_L2
SWB3&4	0-300/0-330	L1	76.0	<0.0001	0.004	0.003	VSWC_L1 = sqrt(-0.000231865 + 0.000506095*Ka_L1^2)
SWB3&4	300-600/ 330-660	L2	37.4	0.003	0.014	0.012	VSWC_L2 = 0.0152453 + 0.0133054*Ka_L2
SWB3&4	600-900/ 660-1050	L3	76.5	<0.0001	0.016	0.013	VSWC_L3 = 0.000882135 + 0.0171283*Ka_L3
SWB3&4	900-1150/ 1050-1250	L4	66.0	<0.0001	0.262	0.201	VSWC_L4 = exp(-0.971899 - 8.20365/Ka_L4)

Ka - Bulk dielectrical permittivity, MAE – Mean absolute error, SE – standard error

APPENDIX B: SAP FLOW SCOPING STUDY

Before onset of the research the suitability of the sap flow technique to estimate transpiration for pomegranate trees was determined. Factors that were considered included the tree structure, tree wood anatomy, calibration and field data quality aspects of the methodology.

B1. Tree structure

Pomegranate trees can be either single or multistemmed. To install sap flow equipment to measure the transpiration of multi-stemmed bushy trees requires a lot of equipment and becomes costly especially for young trees where between four and six stems protrude from the soil surface. Prevalence of many watershoots at the origin of the stem is also typical of pomegranate trees, but it can be contained if managed correctly early in the season. For young single stemmed trees with stem diameter less than 40 mm stem heat balance could work, but equipment should be at least 1.0 m above the ground to get good quality data. Tree structure will have to allow installation of this equipment. In the mature orchard at Welgemoed (Block W43) the tree stem split into between two to five branches at about 286±46 mm from the ground. In the young orchard at Avontuur it could in exceptional cases reach 400 mm from the ground. The heat pulse velocity heat ratio method can be applied for single stemmed trees with diameter exceeding 40 mm. In the case where the tree stem split into two distinct branches the branches can be instrumented separately to ensure the total sap flow for the tree is measured. However, as soon as the tree become multi-stemmed, it becomes too costly to measure representatively for an orchard.

B2. Wood anatomy

The wood sections from the young trees did not always show a distinct difference between summer and spring flush wood. The distance from the bark to the cambium of the stems for the young and mature trees was on average c.1060 µm. The xylem diameter for the young trees did not differ between summer and spring wood and averaged 33.8 µm. For the mature tree branches the xylem diameter of the spring wood (c. 43 µm) was larger compared to that of the summer wood (c. 34 µm). The distance between the xylem vessels for the young and mature branches did not differ for spring and summer wood, averaging 85.8 and 60.6 µm, respectively. The distance between the xylem vessels for the young trees for summer wood was almost double that for spring wood, whereas there was no significant difference between the spacing of the xylem vessels for the spring and summer wood for the mature tree branches. Thermally homogeneous wood suitable for sap flow measurements should have a distance less than 400 µm between the vessels and the lumen diameter should be less than 100µm. According to the data obtained from these wood sections the 'Wonderful' pomegranate tree wood anatomy is suitable for the heat pulse velocity heat ratio sap flow method.

Table 41. Wood anatomy characteristics (±standard deviation or SD) of young (YP) and mature (MP) 'Wonderful' pomegranate tree branches sampled January 2022

Sample	Bark to cambium		Xylem diameter (lumen)				Distance between xylem vessels			
	Distance (µm)	SD	Spring wood (µm)	SD	Summer wood (µm)	SD	Spring wood (µm)	SD	Summer wood (µm)	SD
YP1	770	152.2	41.3	5.6	35.7	10.3	59.6	30.1	113.1	44.0
YP2	1246	20.8	36.4	4.6	28.5	5.8	57.0	30.2	87.8	58.7
YP3	1012	46.2	30.2	6.7	30.5	7.9	39.1	20.7	94.6	58.4
MP1	857	106.9	41.6	7.1	31.5	9.6	74.5	45.7	85.5	46.7
MP2	1313	45.6	42.5	7.9	35.9	4.5	78.8	39.7	75.0	33.9
MP3	1166	62.4	43.8	7.3	33.5	7.4	55.0	23.3	58.6	31.1
Young	1009	237.7	36.0	5.5	31.5	3.7	51.9	11.2	98.5	13.1
Mature	1112	232.4	42.6	1.1	33.6	2.2	69.4	12.7	73.1	13.6

B3. Field-data quality evaluation

The sap flow scoping study selected the heat ratio method (HRM) of monitoring sap flow (Burgess et al., 2001) amongst others as the most suitable to determine transpiration for pomegranate trees. The method can only measure transpiration for tree stems >40 mm, which means that the transpiration represented by c. 7% of the young trees at Avontuur cannot be determined. In the full bearing orchard less than 0.5% of the trees had stem diameters smaller than 40 mm. In-field measurements to determine if the HRM renders sap flow data of acceptable quality were completed in block W43 at the farm Welgemoed in Drakenstein district. Four sets of thermocouples and heaters were installed at depths representing sap flow for one single-stemmed tree (Figure 79). The preliminary data obtained for the period 18 February until 11 May 2022 appears to be of satisfactory quality except for a few days at the beginning of March during which the thermocouples at the 13 mm installation depth were misaligned (Figure 80).

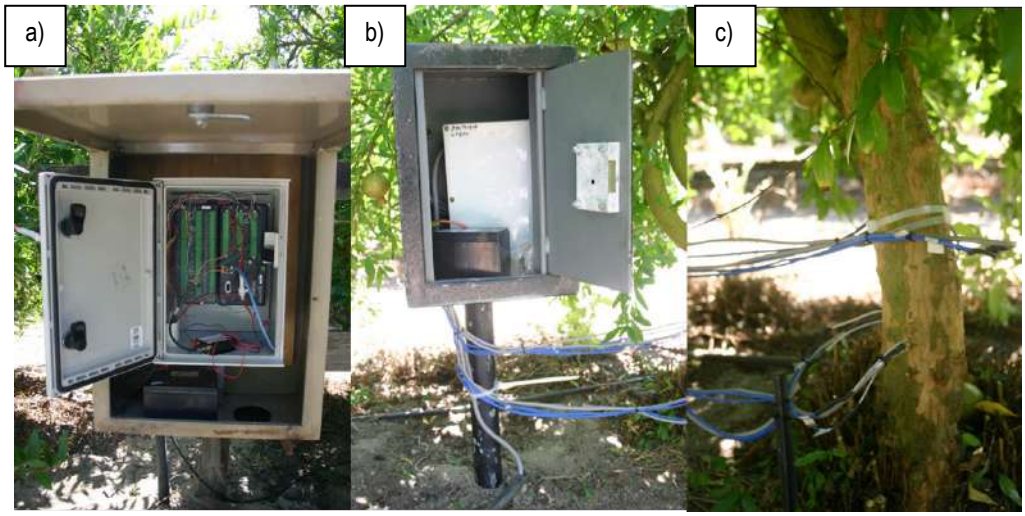

Figure 79. Heat pulse velocity heat ratio equipment installed in a single tree at block W43 on the farm Welgemoed in Drakenstein district during January 2022. Equipment includes a) a logger box, b) tree box and 3) a set of two thermocouples and one heater installed at c. 13-, 23-, 33- and 43-mm depths each in the tree stem.

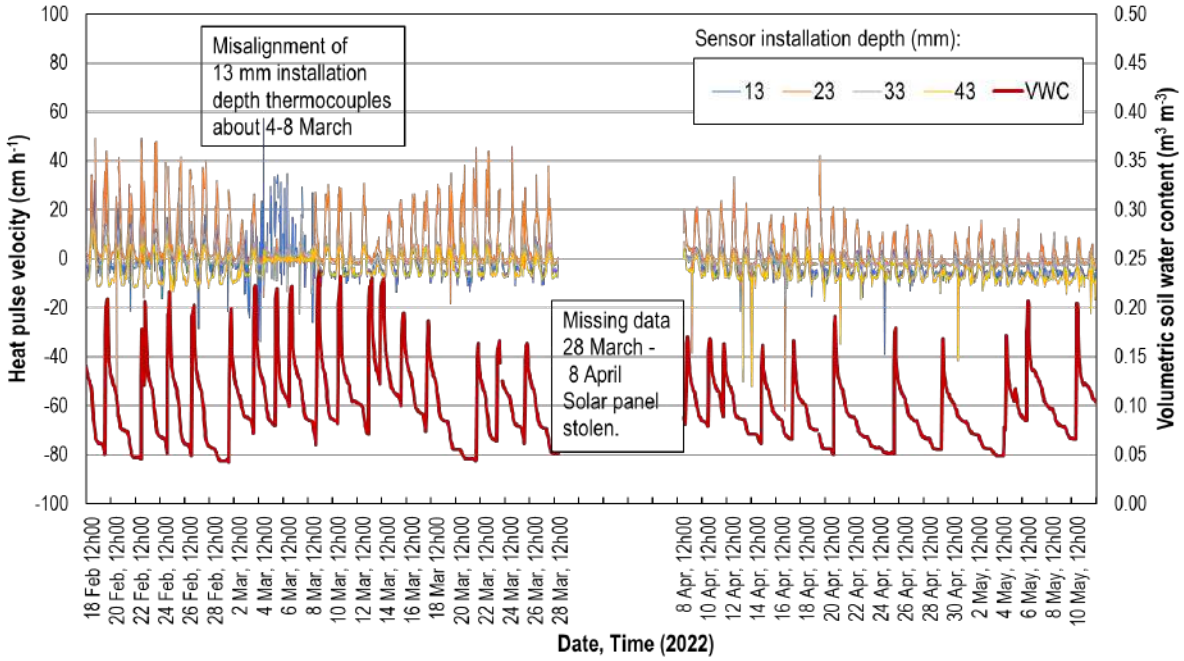

Figure 80. Preliminary heat pulse velocity data for a cv. 'Wonderful' pomegranate tree measured at four different depths in the stem from 18 February until 11 May 2022 using the heat ratio method. The volumetric soil water content (VWC) measured by a CS616 soil water content reflectometer installed in the top 300 mm soil depth increment is also displayed.

B4. Calibration of the heat ratio method in potted pomegranate trees

Pomegranate (cultivar 'Wonderful') trees were obtained from a nursery in May 2022 and were potted in 80 ℓ plastic containers in a 1:2 (v/v) mixture of compost to sand in August 2023. These trees were grown in a glasshouse on the University of Pretoria's Innovation Africa@UP (25° 44‟ 58.66"" S, 28° 15‟ 31.65"" E) platform. The trees had attained a suitable stem diameter in December 2024 for the start of calibration experiments. The heat ratio method was used to estimate transpiration (Burgess et al., 2001). One heat pulse probe set was used for each tree (each consisting of a heater probe inserted into a 2.5 mm brass collar and two type-T copper-constantan thermocouples embedded in 2 mm outside-diameter PTFE tubing, placed equidistantly up and down stream of the heater probe at a distance of 0.475 cm). Equipment was locally manufactured by Aquamet (Pietermaritzburg, South Africa). The heat pulse velocity (V_h) in cm h^{-1} for each probe set was calculated following Marshall (1958) as:

$$V_h = \frac{k_w}{x} \ln\left(\frac{v_1}{v_2}\right) * 3600 \qquad \text{[Eq. 48]}$$

where k_w is the thermal diffusivity of green (fresh) wood (assigned a value of 2.5 x 10^{-3} cm^2 s^{-1} (Marshall 1958)), x is distance in cm between the heater and either the upper or lower thermocouple, v_1 and v_2 are the maximum increases in temperature after the heat pulse is released (from initial temperatures) as measured by the upstream and downstream thermocouples and 3600 converts seconds to hours. Heat pulse velocities were measured and logged every 15 minutes using a CR1000 data logger and an AM16/32B multiplexer (Campbell Scientific Ltd, Logan, Utah, USA). Wounding was determined at the end of measurements by cutting the tree down and excising the part of the stem where the probe was inserted. Wound width was determined to be 0.33 for Tree 1 and 0.29 for Tree 2 (**Error! Reference source not found.**A and B).

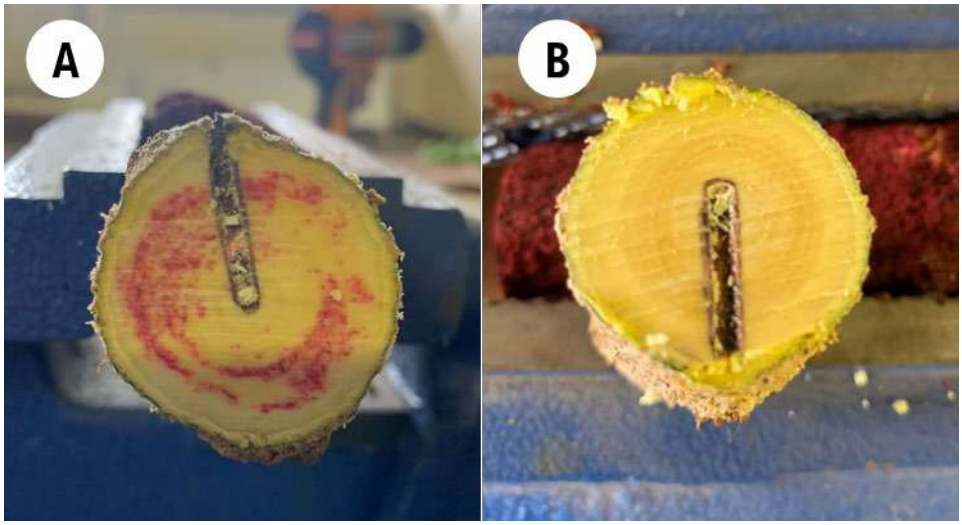

Figure 81. Wounding of the pomegranate trees as a result of probe insertion. A and B refers to Tree 1 and 2, respectively

B4.1 Description and measurement protocol

A cantilever weighing lysimeter was used for the calibration of the sap flow system. The design of the lysimeters is given in Figure 82**Error! Reference source not found.**. The load cells used in the system have a range of 0 - 500 N which is equal to 0 - 51 kg with a sensitivity of 3.20789 mV V^{-1} (LC serial # 703370). Power was provided to the load cell via a 12 V battery and a voltage regulator to ensure a constant 12 V supply. The output signal from the two load cells was measured over a differential channel to increase the sensitivity of measurements on a CR1000 data logger (Campbell Scientific Inc.) at a 1 s interval and then averaged over 15 min.

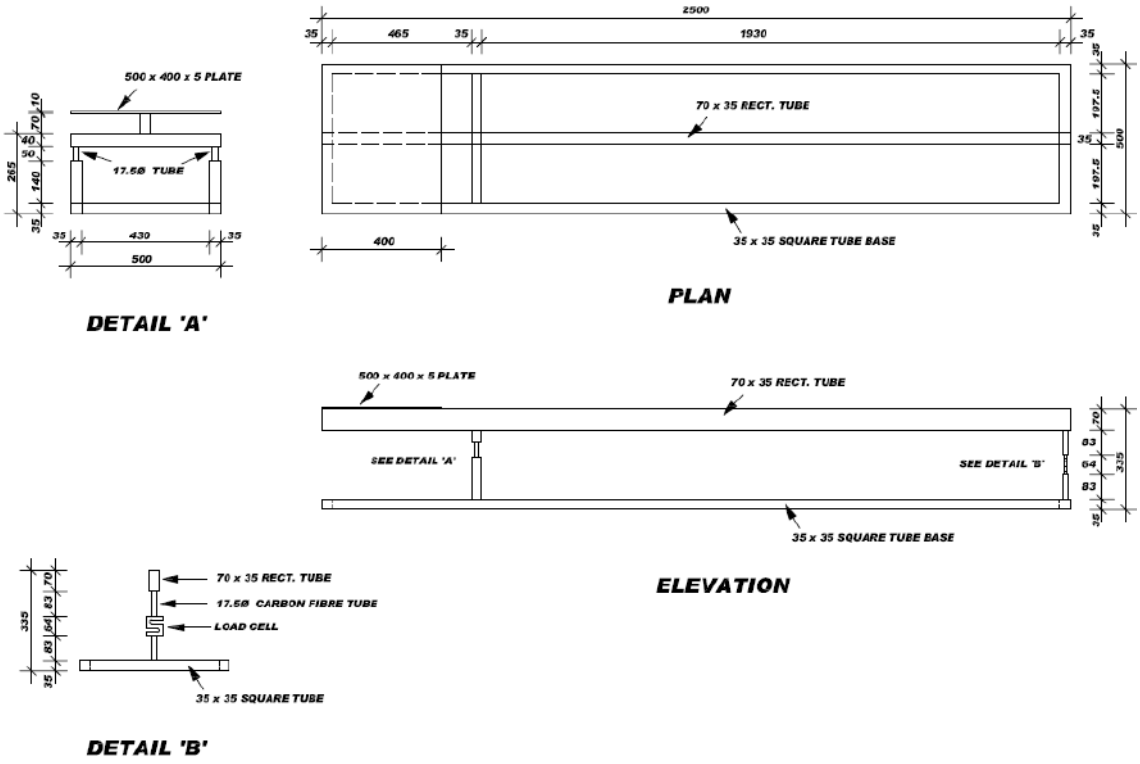

Figure 82. Detailed sketch of the cantilever weighing lysimeters

B4.1.1 Calibration of the load cell on the weighing lysimeter

In order to determine the resolution of the load cell and convert the signal (mV^{-}) data into actual load or mass, calibration of the weighing lysimeters was required. The two weighing lysimeters were calibrated by adding various known masses on the lysimeter, using a set of 11 loads 0.5 kg, whilst the tree was on the lysimeter. It was reasoned that this would be the range in which measurements would be made. The two weighing lysimeter were calibrated by adding and removing the same mass to test for any hysteresis in the measurement. The calibration results of lysimeter 1 and lysimeter 2 are shown in **Error! Reference source not found.**. There was a strong linear relationship between the load cell output (mv) and the calibration mass (kg), with a 0.994 to 0.995 determination coefficient for both lysimeters. There was no evidence of hysteresis which would impact results.

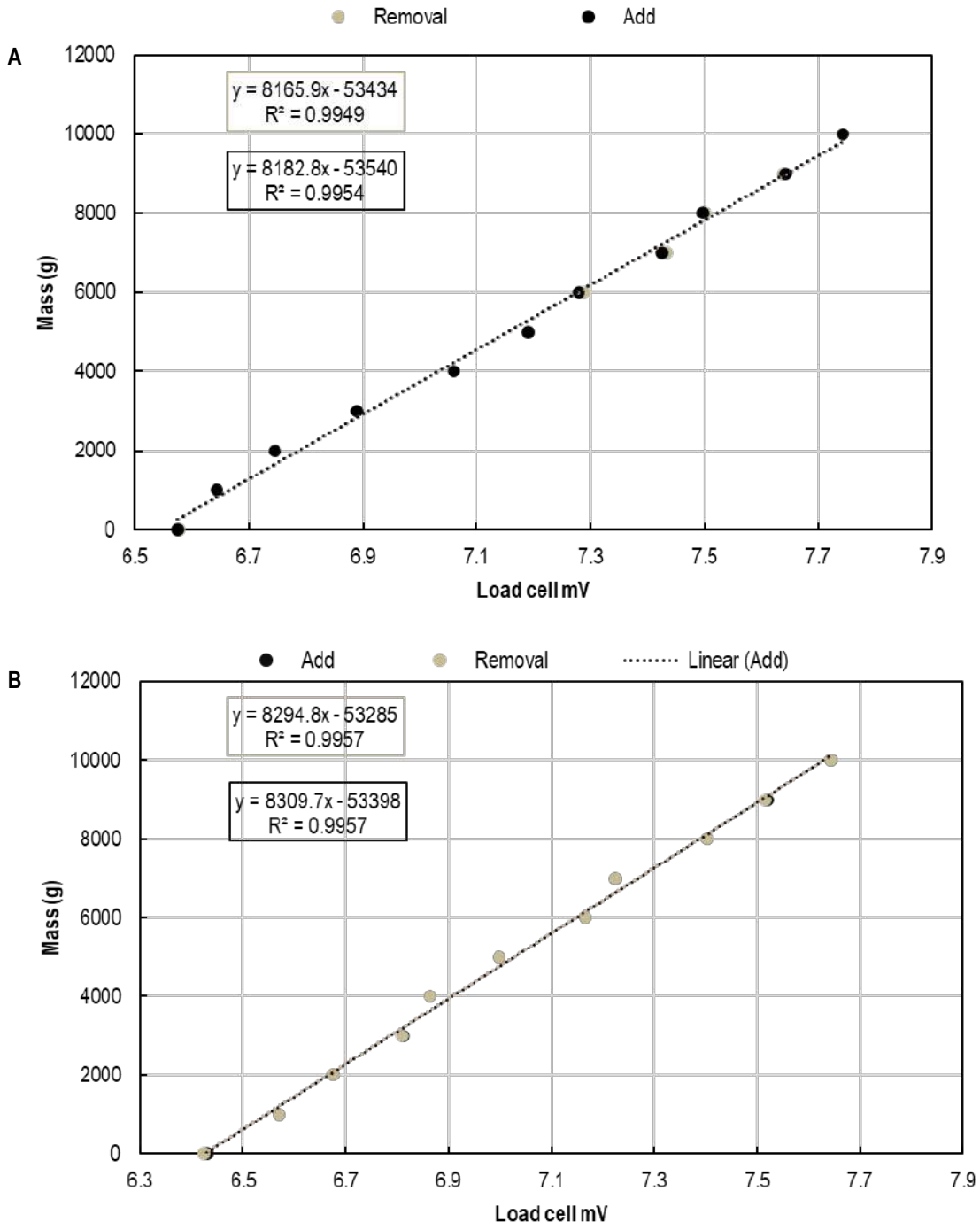

Figure 83. Calibration of load cells for the small cantilever style weighing lysimeters. A) Lysimeter 1 and B) Lysimeter 2. To check for hysteresis mass was added to the lysimeter and then removed.

B4.1.2 Calibration of the sap flow techniques

Each pot was covered with clear plastic to eliminate loss of water from the soil through evaporation and drainage of water from the bottom of the pot (**Error! Reference source not found.**). Trees were irrigated three times during the night for 4 min, which equated to 1.6 ℓ during each night in order to ensure that the trees were not water stressed.

Figure 84. A) Pomegranate trees on the weighing lysimeters, with the pots covered in clear plastic. B) Insertion of heat pulse probe in the stem of a pomegranate tree.

Two pomegranate trees were used to calibrate sap flow (tree 1 circumference = 9.8 cm and tree 2 circumference = 10.7 cm). Tree 1 was calibrated on lysimeter 2 and tree 2 on lysimeter 1. Due to the irrigation of trees at night, calibration was performed between 7:00 and 18:00, when the trees were actively transpiring. **Error! Reference source not found.** illustrates the hourly comparison between transpiration of the two pomegranate trees, with a comparison of daily totals in **Error! Reference source not found.**. Tree 1 had higher hourly and daily transpiration than tree 2. However, the trend in water use was very similar.

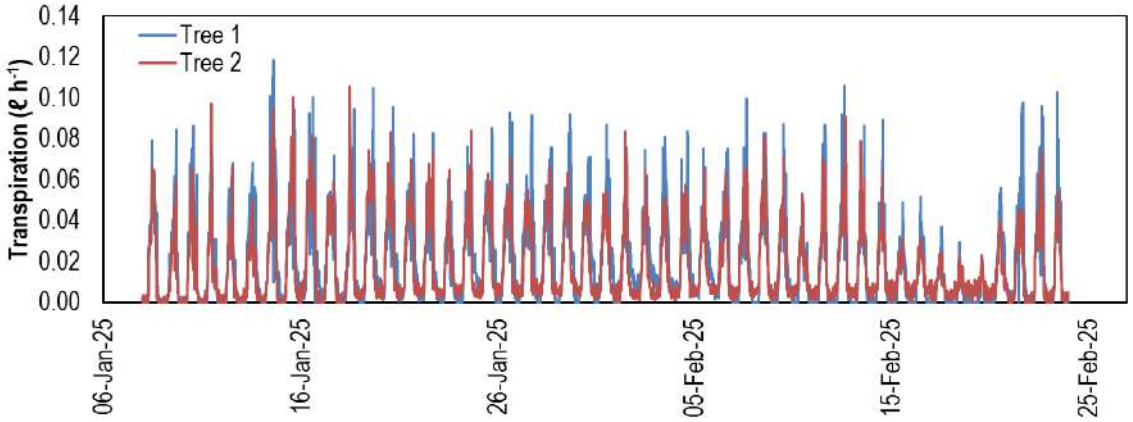

Figure 85. Comparison of hourly transpiration of the two pomegranate trees determined using the heat ratio method

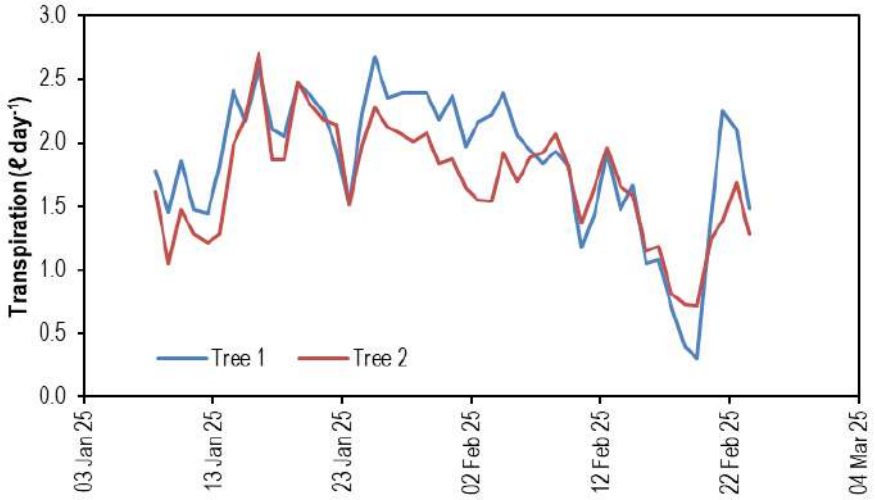

Figure 86. Comparison of daily transpiration of the two pomegranate trees determined using the heat ratio method

The comparison of hourly transpiration determined using the weighing lysimeter and the heat ratio method is shown in **Error! Reference source not found.** for the two trees. Once again, the trend in transpiration was similar for the sap flow method and the lysimeter. Importantly calibration was conducted during daylight hours.

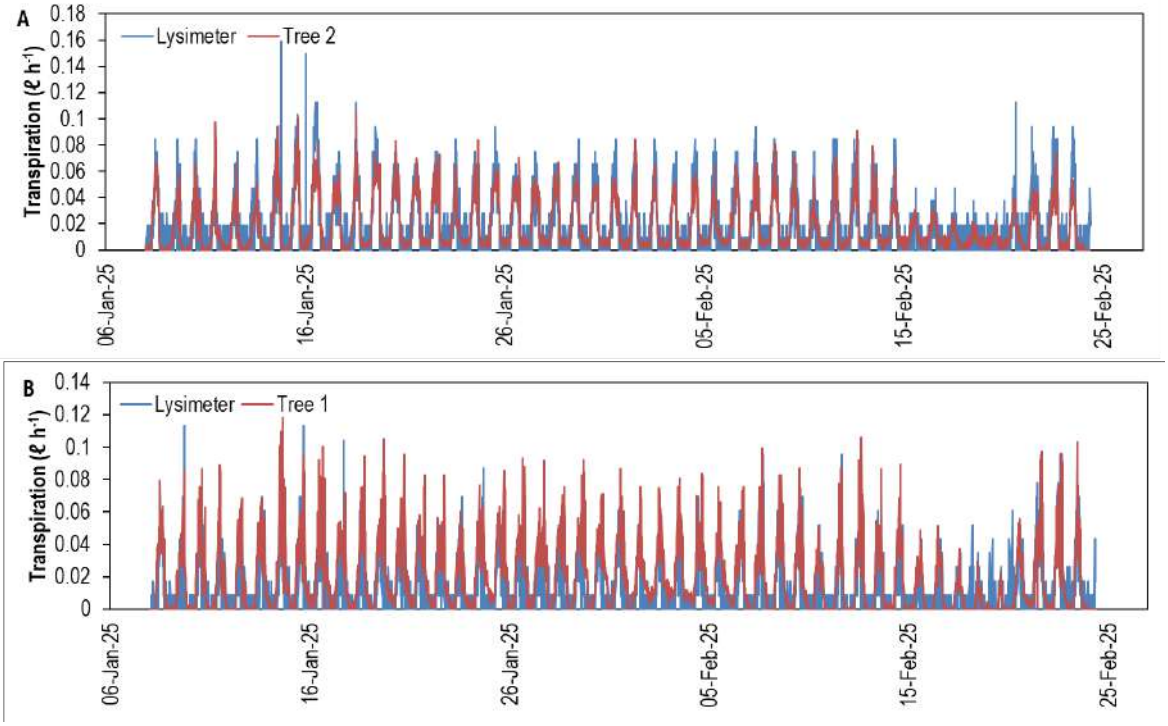

Figure 87. Comparison of hourly transpiration determined using the heat ratio method and the lysimeter for A) tree 2 and B) tree 1

Due to potential issues with lags between transpiration and sap flow, calibration was performed by totalling values between 7:00 and 18:00 (**Error! Reference source not found.**). In addition, as zero mass loss from the lysimeter had to correlate with zero sap flow from the HRM system, the linear regression was forced through 0. The relationship between transpiration determined using the HRM system and that determined by the weighing lysimeter was fairly good for both trees with an R^2 value of 0.9933 for tree 2 and 0.9764 for tree 1. However, the slope of the relationship between the two measurements was poor for Tree 1 with a value of 1.4311, indicating that in this tree transpiration was overestimated by the HRM measurement. In contrast, transpiration in tree 1 was well estimated with a slope of 1.0718, which is close to a 1:1 relationship. The heat pulse velocity data from tree 1 showed more variation than tree 2 and

this could have contributed to the poor relationship with the lysimeter measurements. At such low transpiration measurements (<3 L day^{-1}) small errors in measurement can lead to large errors between the two methods.

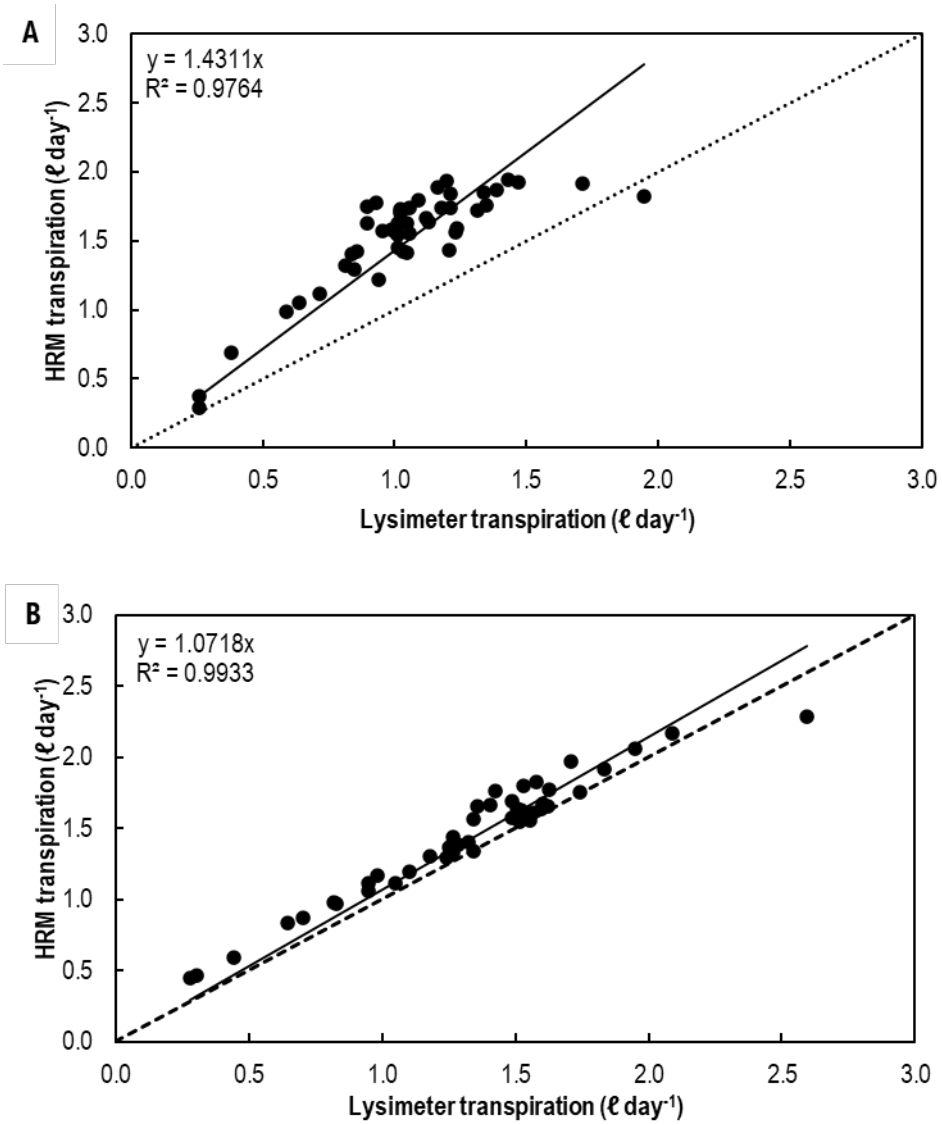

Figure 88. Calibration of transpiration determined by the heat ratio method with transpiration determined using a weighing lysimeter for A) Tree 1 and B) Tree 2. The 1:1 line is indicated by the dotted line.

Conclusion

Transpiration of pomegranate trees can be well estimated using the heat ratio method without the need for adjustment. There is no requirement for a calibration factor.

APPENDIX C: CAPACITY BUILDING

1. **Students**

The project has one PhD and two MSc students who registered to complete their studies in 2025.

Mr Muthianzhele Ravuluma (Student number: 2012066870) registered at the University Free State Doctor of Philosophy in Agriculture, majoring in Agrometeorology in June 2021 with Dr Tharaga as main supervisor. His thesis title is “Current and future water use of pomegranate orchards in the Western Cape of South Africa". Mr Ravuluma attended a UNESCO training workshop (ICT-IAEA) on Open Hardware and Open Software solutions for sustainable development, 13 – 17 May 2024 in Cape Town. South Africa.

Ms. Raesibe Kgaphola (Student number 2015162072) registered for an MSc in Agriculture, majoring in Agrometeorology, in February 2022, with Dr. Tharaga as supervisor at the University of the Free State. The title of Ms. Kgaphola’s thesis is “Determination of Pomegranate orchard water use using eddy covariance and remote sensing.”

After two failed attempts to get potential students admitted at Stellenbosch University, Mr Daniel Havenga (Student number 21898138) registered in February 2023 for an MSc in Horticulture at Stellenbosch University with Dr Dzikiti as supervisor. The title of his thesis is “Water use efficiency of pomegranate”.

2. **Institutional capacity building**

Mr Muthianzhele Ravuluma was appointed as Junior Researcher at the Soil and Water Science Department at ARC Infruitec-Nietvoorbij.

APPENDIX D: KNOWLEDGE DISSEMINATION

Knowledge transfer for this project and publishing of articles were limited since data collection continued until June 2024 and finally processed water use data from the water use and water productivity project became only available later.

Two manuscripts were published:

Kgaphola, R.L., Tharaga, P.C., Volschenk, T, Dzikiti, S. 2024. Using remote sensing models to determine evapotranspiration of a pomegranate Orchard in a Mediterranean climate. Proc. II International Symposium on Precision Management of Orchards and Vineyards. Acta Hortic. 1395:45-52

Ravuluma, M., Tharaga, P., Volschenk, T., Dzikiti, S. Walker, S. 2025. Sap flow dynamics of young and mature pomegranate (Punica granatum L.) orchards under semi-arid conditions. Proc. XII International Workshop on Sap Flow. Acta Hortic. 1419:19-26

A combined information day for the pomegranate industry is planned for 29 May 2025 where data from the pomegranate water use and water productivity project as well as from the refinement of irrigation management of pomegranate orchards using drone technology project (C2020/2021-00943) will be conveyed to producers.

If sufficient funding is obtained it is planned to do an oral presentation of the research conducted at the ISHS VIth International Symposium on Pomegranate and Minor Mediterranean Fruit in Italy, 22-24 September 2025.

Other potential publications will be identified with input from senior project team collaborators, the PhD and MSc students.

APPENDIX E: ABSTRACTS FOR STUDENTS

1. PhD student

Mr Muthianzhele Ravuluma registered at the University Free State Doctor of Philosophy in Agriculture, majoring in Agrometeorology in June 2021 (Student number: 2012066870) with Dr Tharaga as main supervisor. His thesis title is “Current and future water use of pomegranate orchards in the Western Cape of South Africa". The department of Soil, Crop and Climate of the University of the Free State accepted Mr Ravuluma's proposal on 5 December 2022. The study aims to determine the current and modelled future water use of selected pomegranate orchards under irrigation in the Western Cape. The specific objectives align with Aims 1, 2 and 4 of the research project and are as follows: 1. To determine transpiration rates of individual pomegranate trees using the sap flow method and scale them to orchard level. 2. To estimate the ET on pomegranate orchards using the eddy covariance for the mature orchard and surface renewal for the young orchard. 3. To model the water use of a young and mature pomegranate orchard under future climate change. Mr Ravuluma has with assistance of the project team completed relevant field data collection and data processing for the project. Mr Ravuluma was actively involved in writing of the final report and reregistered to complete his studies in 2025.

2. MSc students:

2.1 Ms Raesibe Kgaphola

Ms. Kgaphola (Student number 2015162072) registered for an MSc in Agriculture, majoring in Agrometeorology, in February 2022, with Dr. Tharaga as supervisor at the University of the Free State. Ms. Kgaphola presented a proposal on the 5th of December 2022 regarding “Estimation of net ecosystem exchange, water use and biomass production of a pomegranate orchard using remote sensing.” She was requested by the university to amend the objectives for the study since validating biomass estimated from remote sensing images using ground measurements was problematic. The title of Ms. Kgaphola’s thesis changed to “Determination of Pomegranate orchard water use using eddy covariance and remote sensing.” She presented the proposal on 5 May 2023, which the Department of Soil, Crop, and Climate of the University of the Free State accepted. The objective of the study is to determine the water use of a full-bearing pomegranate orchard under irrigation using micrometeorological and remote sensing techniques. Specific objectives included: 1) to quantify water use (ET) of a pomegranate orchard at different growth stages during the season; 2) to calculate crop coefficients using ground-based measurements and satellite data; 3) to determine the Normalized Difference Vegetation Index (NDVI) at selected growth stages during the season using satellite images and 4) to verify and validate remote sensing derived ETo, ET, and Kc using ground-based measurements. These objectives link closely with Aims 1 and 4 of the water use and water productivity project which intended to determine water use of pomegranate orchards and to develop a method for practical estimation of crop coefficients to enable calculation of individual orchard water requirements. She contributed to the contents of the final report and registered for 2025 in order to complete her thesis.

2.2 Mr Daniel Havenga

Mr Havenga registered in February 2023 for an MSc in Horticulture at Stellenbosch University with Dr Dzikiti as supervisor. The title of his thesis is “Water use efficiency of pomegranate”. The overall aim is to investigate variations in the water use efficiency of young and mature pomegranate orchards. Specific aims include to 1) Quantify the seasonal changes in tree water status and growth of irrigated pomegranate trees; 2) Estimate the water use and water use efficiency of pomegranate orchards; and 3) Quantify the partitioning of water use in pomegranate orchards using a dual source evapotranspiration model. His specific aims align with project aims 1-3. Mr Havenga presented his thesis proposal to the university on 25 April 2023 and it was accepted. He contributed to the contents of the final report and registered in 2025 to complete his thesis.

APPENDIX F: CONFERENCE PRESENTATIONS

Mr Muthianzhele Ravuluma (PhD student) presented a poster in Zealand at the ISHS XIIth International Workshop on Sap Flow 2023 which was held from 30 October until 3 November 2023. Poster title: “Sap flow dynamics of young and mature pomegranate (Punica granatum L.) orchards under semi-arid conditions.” Poster authors: M. Ravuluma, P.C. Tharaga, T. Volschenk, S. Dzikiti and S. Walker. Mr Ravuluma received the ISHS Young Minds Award for the best poster presentation at this 12th International ISHS workshop for sap flow.

Ms Raesibe Kgaphola (MSc student) delivered an oral presentation at the 2nd International Symposium on Precision Management of Orchards and Vineyards in Tatura, Australia held from 3-8 December 2023. Presentation title: “The use of NDVI to manage water stress of a pomegranate orchard in a Mediterranean climate using remote sensing.”

Mr Lester Sassman, Research Technician, attended the 38th South African Society for Agricultural Technologists on the 22-25 October 2024. He presented a poster titled: “An Accurate Method of Measuring Light Interception for Pomegranate Orchards” and won the “Most Applicable Presentation” award.